ESRDC SEMI-ANNUAL REPORT

Reporting Period: August 2016 - March 2018

Submitted to:
The Office of Naval Research

Grant Number: N00014-16-1-2956

Submitted by:
Florida State University

June 2018

This is the third semi-annual report submitted under this grant.
Research results from the most recent six month reporting period are highlighted red.

This page intentionally left blank

ELECTRIC SHIP RESEARCH

ESRDC

AND DEVELOPMENT CONSORTIUM

MISSION STATEMENT

The Electric Ship Research and Development Consortium brings together, in a single entity, the combined programs and resources of leading electric power research institutions to advance near- to mid-term electric ship concepts. The consortium is supported through a grant from the United States Office of Naval Research.

This page intentionally left blank

Executive Summary

The Electric Ship Research and Development Consortium consists of universities dedicated to helping enable affordable, effective, sustainable future electric ships. It does this primarily in four ways:

1. Conducting relevant engineering research to provide understanding and data needed for new ship design
2. Working with Navy organizations for bilateral technology transfer
3. Working with relevant partners to help assure the technology advances are available to the Navy
4. Providing graduates skilled in the field to help achieve a world leading domestic infrastructure for electric ship design and construction

This report summarizes the progress on each research project for the period from August 2016 to March 2018. Research results for the most recent six month period from October 2017 to March 2018 have been highlighted red in this report. Even though this is a multiyear research program, this report includes several important findings.

The first thrust is Combat Power and Energy Systems Design Methodologies. This thrust advances the state-of-the-art in design and analysis methods for combat power and energy systems in future surface combatants. The development uses a tool-independent environment to ensure broad applicability for any design process. When mature, the information will be implemented into the Smart Ship Systems Design (S3D) environment to facilitate inclusion in future preliminary design exercises. Significant advances include:

- A method to get new technology and designs into FOCUS-compliant, LEAPS-integrated software was demonstrated. This is an important software step to convert the activities of the ESRDC and Navy personnel into a format that is useful in the Navy's ship design process.
- A warship is a classic example of an attractive application of risk-sensitive control. Classical techniques in optimal control, where one aims to optimize the step-by-step performance fail to capture the effect of extreme fluctuations, or mitigate these fluctuations. On the other hand, the traditional min-max approach is ultraconservative. The advance here was to develop a mathematical approach to demonstrate that risk-sensitive control may be sufficiently general to be applicable to practical systems like warships.
- A framework was developed that allows for systematic evaluation of networked control systems, of a meaningful scale, with respect to the all-electric ship platform.

The second thrust is High Power Dense Component Development and Characterization. Researchers in this thrust plan to achieve heretofore impossible performance from key power system components. This is intended to provide a smaller, lighter power system with capability beyond what is currently achievable. Significant advances include:

- Simulations of forced/convective heat transfer of 120 power cables under different boundary conditions demonstrated the best location to place the cooling equipment, namely at the top wall of the cable cabinet.
- Provided engineering data that suggests that electrically, dc cables may be smaller than ac cables for the same load. This promising result makes it prudent to look in more detail at the thermal and mechanical performance.
- The development of a technique for enhancing the stability and reliability of superconducting cable systems by incorporating a small volume of solid nitrogen in superconducting terminations.

The third thrust is System Management and Control Technologies. This research provides engineering information needed for well-designed and tested system-level control approaches. Recognizing the limitation imposed by communication latency, power system control approaches are focusing on coordinated local control to react to changes on the appropriate time scale. Significant advances include:

- Researchers developed models of high temperature superconducting components and incorporated these models into the smart ship system design (S3D) environment. This permits an assessment of the impact of superconductivity on power system performance, weight, and volume.

- Engineering data has been developed to permit the design of stable robust dc power systems. Technically, a developed model provided information on the stability of designs for dc power systems.

- Research evidence was gathered that further emphasizes the importance and necessity of adopting a distributed control design structure for zonal distribution systems.

The fourth thrust is Developing New Design Functionalities. Researchers in this thrust expect to preserve and expand the Navy's investment in S3D as an agile, rapid, tool-development test bed to enable Navy engineers to develop better and more capable ships. Significant advances include:

- The team achieved a significant improvement in the accessibility of S3D. Through this advance, users can query the corpus using a natural language expression. This makes the system more useful to less specialized users.

- A key attribute of the S3D is that all disciplines, e.g., naval architects, power engineers, control engineers, and mechanical engineers, see a visualization of the same design, but they see it in a form that is useful for them. The system developers added valuable capability to the time-domain thermal simulation tool. The improvement was to enhance the user interface of vemESRDC to improve accessibility by S3D users, permitting them to explore various thermal system configurations and run test cases with ease. This is critical, as thermal management can be a significant factor in determining the final size and weight of a ship's plant.

- S3D version 2.0 was released in in June 2017, followed by extensive testing and upgrading of both the user experience and FOCUS compliance.

The fifth thrust is System Level Experimentation. One of the important attributes of the ESRDC is that the member universities have world-class capabilities for testing at the kilowatt to megawatt power scale incorporating, as appropriate, hardware-in-the-loop technology. The testing provides a cost effective link between analytical assessments and the full scale testing that is in the purview of the Navy. This will explore the full functionality, including system-level control, of the components, models, and subsystems developed including MVDC system protection and the effect of various control strategies to maximize system performance. Significant advances include:

- Since this thrust focuses on testing to support development, researchers conducted significant preliminary investigations during the early stages of this multiyear research program. However, specific accomplishments will become more numerous as the individual development projects mature and need experimental feedback.

- Experimental results from the recently enhanced dc testbed at UT, with expected commissioning of updated hardware to follow.

Contents

Thrust 1: Combat Power and Energy System Design Methodologies

Technical Objectives

Advance the state of the art design and analysis methodologies for combat power and energy systems in future surface combatants. The methodologies will be developed in a tool-independent environment to ensure broad applicability for any design process. Applicable methodologies will be implemented in the Smart Ship Systems Design (S3D) environment once they are sufficiently developed.

The goals of this thrust are to integrate and analyze the effects of technological advances to achieve affordable superiority, and to improve Navy's capabilities in the design of complex systems.

Technical Approach

Conduct research in four major areas:

- Set-based design capabilities and metrics.
- Advanced risk-averse design, risk analysis, and risk mitigation approaches.
- Incorporating controls in the design cycle.
- Incorporating higher fidelity and real-time simulation in the design cycle.

Progress Statement Summary

Current work reported herein includes:
1.1.1 Develop methods and metrics to characterize systems and automated generation of templates for facilitating SBD
1.2.1 Develop stochastic response generation framework to facilitate risk-averse designs
1.2.2 Quantify the effects of system/subsystem failures and mitigation approaches to assess and perform de-risking procedures within the DDC
1.3.1 Develop methodologies to determine control fidelity requirement throughout the DDC
1.3.2 Develop sizing of energy storage for shipboard power systems and its impact on EPLA
1.3.3 Develop data communication architecture to support control systems
1.4.1 Develop guidelines for model fidelity requirement for off-line and real-time analyses of emerging technologies applied to shipboard power systems
1.4.2 Investigate performance modeling and cyber physical protection of the control communication network in electrical ship systems
1.4.4 Interfacing guidelines to support control system evaluation and development
1.4.5 HIL resource partitioning for controls evaluation

The following projects are planned for future work:
1.1.2 Develop flexible power quality requirements and its impact on electric power (plant) load analysis (EPLA)
1.3.4 Partition control functions and data communications
1.4.3 Approaches to facilitate CHIL simulations with WBG converters
1.4.6 Theoretical foundation for effective linkage of external time domain simulation capabilities with a design framework like S3D

1.1.1 Develop methods and metrics to characterize systems and automated generation of templates for facilitating SBD

Task: Multi-fidelity modeling

Technical Objectives

Develop a methodology that fuses diverse information sources, e.g. experimental data and simulation outputs of variable fidelity/resolution, using only a few high-fidelity samples to construct a response surface and its uncertainty. This methodology-provides huge computational speed increases due to incorporation of inexpensive low-fidelity predictions. Using some high-fidelity data, it safeguards against erroneous low-fidelity predictions.

Technical Approach

Some of the methods being considered include:

- Gaussian process regression/kriging [1] [2].
- Linear and nonlinear autoregressive algorithms (e.g. co-kriging/deep Gaussian processes) [2].
- Exploit correlations between high- and low-fidelity via machine-learning tools [3].
- Recursive co-kriging for computational efficiency.
- Active learning based on acquisition functions for optimization/design problems.

Progress Statement Summary

We have developed linear and non-linear multi-fidelity algorithms that can be used in design but also in extracting useful correlations using just a few high-fidelity data points and several low-fidelity data points [3] [4]. To illustrate the cross-cutting applicability of the new algorithms and codes we have developed, we include here a pedagogical example of how to discover an unknown functional relationship between input and output with the blue curve, shown in Figure 1. We assume that we only know four high-fidelity points, and based on this information, the best estimator using Gaussian Process Regression (GPR) is shown with the red-dot line on the left panel. However, sampling a low-fidelity model shown on the right with the pink line and using only seven points we can reduce the uncertainty and obtain a very good estimation of the unknown functional relationship. In fact, if we sample the low-fidelity model, we eliminate the uncertainty and we 'discover' the relationship exactly! The key here is that the low-fidelity model (pink curve), although not accurate, has a high degree of correlations, in terms of the slope, with the high-fidelity model. In addition, the Bayesian framework allows us to infer also the uncertainty, and therefore we know when our measurements are adequate.

We have extended the multifidelity information fusion method so that we can deal effectively with the problem of 'hidden' cross-correlations. Specifically, we introduce higher-dimensional embeddings of the data (based on 'embedology' techniques from topology and dynamical systems [5]), in which the high- and low-fidelity cross-correlations become more pronounced and hence they can be better exploited. The embedding theorems guarantee the one-to-oneness (via homeomorphisms, diffeomorphisms or even isometries) between the two data set embeddings. Through this correspondence, the high-fidelity model turns into a function of the low-fidelity model on the appropriate manifold, which drastically enables established information fusion schemes such as a nonlinear auto-regressive GP [2]. We have demonstrated its effectiveness through some benchmark problems, including functions with discontinuities. The work establishes a useful synergy between theoretical concepts (observability, embedding theorems) and data-driven applications of machine learning.

We have continued our work on multi-fidelity modeling for non-stationary processes [6]. In particular, we have linked Gaussian Process Regression with data-driven manifold embedding for robust nonlinear

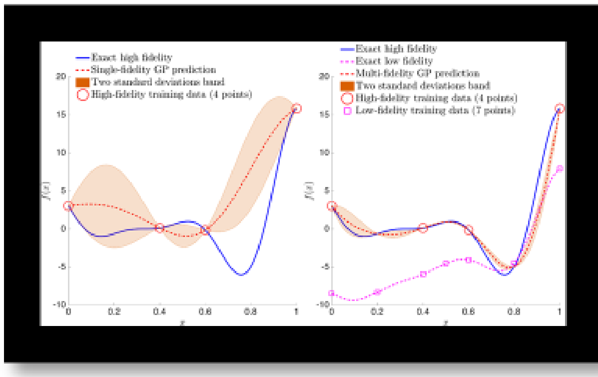

Figure 1: Discovering nonlinear functional relationships from data and models. On the left, we only have four high-fidelity data points. On the right, we use these points and in addition, we sample a low-fidelity model (and therefore inexpensive pink curve) at 7.

information fusion. The motivation of this work comes from several factors. Sometimes, Gaussian Process Regression (or any regression methods) fails to estimate true value with the highest fidelity model. The reason may be that we have **too few data** to determine the right kernel, or that there is partial input information, and hence there are latent dimensions (gaps). To address this issue we can increase the number of data points; this is the very first remedy but it is very expensive. Another possibility is to expand dimensions (features) of data, but in this case we have to guarantee that dimension expansion makes the result more accurate, and, most importantly, we have to tackle the open issue of the curse of dimensionality.

Next, we give an example of dimension expansion. The highest fidelity data (y) are given by the following equation with $dt = 0.002$.

$$y = 0.1t + sin(2\pi t) \quad t \in [0, 20] \tag{1}$$

Now, the question is how many data points do we need for estimating this function? We can use in this case a composite kernel, e.g. combine a linear kernel with a periodic kernel, but here we demonstrate with this simple pedagogical example how to 'expand dimensions'. Let the following x be the low fidelity function of y. Then, the highest fidelity function (y) can be rewritten as a two-dimensional function.

$$x = sin(2\pi t) \tag{2}$$

The highest fidelity function (y) becomes a plane on the (t, x)-dimensional space as follow:

$$y = 0.1t + x \tag{3}$$

Now, we can easily estimate how many points we need for estimating the two-dimensional plane. In fact, using only 6 data points, we can estimate all true values accurately, as seen in Figure 2 below.

Dimension expansion is a trade-off between additional cost from the '***curse of dimensionality***' on one hand and cost reduction since we are now dealing with "'***a smooth manifold***' on the other hand. In future work, we will further exploit this powerful idea for modeling more complex high-dimensional surfaces and synamic electrical and mechanical systems of interest to multiple disciplines of ESRDC design.

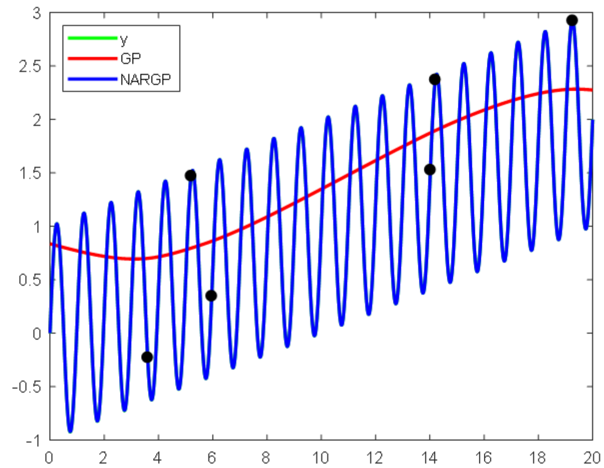

Figure 2: Representing the non-stationary periodic signal with a Gaussian Process fails, but using dimension expansion leads to the correct answer given only six points in the new coordinate system.

Task: Development of methods and metrics to characterize and analyze ship systems and to facilitate SBD

Technical Objectives

Investigate systems engineering tools that aid in narrowing down the design space, thereby helping facilitate the set-based-design (SBD) paradigm. Additionally, to explore validated metrics to evaluate candidate designs followed by efforts to incorporate SBD functionality into S3D.

Technical Approach

This task proposes exploring well-established tools under the umbrella of systems engineering used typically in the consumer products industry to focus on pertinent client requirements (CR) and link them to relevant engineering characteristics (EC) capable of fulfilling them. Part of quality function deployment, the house of quality (HOQ) is a tool commonly used to integrate the "layman's" CR to EC. Further, to better understand interactions between pertinent parameters and design factors, the Taguchi Method (TM) is proposed. The work done here benchmarks the modular multilevel converter- (MMC) based system, and a combination of mentioned tools could provide a means to meticulously filter the complex design space to emphasize the most important and relevant design parameters through the following rigorous tasks:

- Expert knowledge elicitation — This first step gathering subject specific data forms the input to the HOQ. Surveys aimed at power electronics experts to obtain information that sheds light on the various MMC-related design aspects will be used.
- HOQ — Data from the customer (in this case naval shipboard compatibility guidelines from IEEE and MIL standards, etc.) and subject matter experts (obtained from step 1) form the inputs. HOQ combines the customer needs with technical aspects to help rank and filter pertinent EC.
- TM — Highlighted EC from the HOQ form a basis to build a Taguchi orthogonal array. This process helps better understand the various combinations of design factors and their interactive impacts on the desired output, and to eventually obtain the most optimal or robust' design.

Progress Statement Summary

Current work has resulted in a preliminary HOQ that identifies the power converter-related heat-sink as a pertinent aspect to fulfill the customer requirement of high power density via the MW/m3 metric. The contribution of heat sinks toward an overall converter volume along with a related TM analysis that helps narrow down robust designs and best candidate design factors (such as submodule voltages). Important design guidelines have been used and documented in the MMC designs compatible for naval shipboard power systems from work done previously.

An investigation of product development tools to aid real-time design exercises has been done in [7]. This focuses on collecting expert knowledge and performing a QFD to rank pertinent metrics. The developed tools have been applied to a set-based design exercise for an MMC converter in [8]. This methodology employs TM for set evaluation and narrows down the sets through iterations. An example of applying FFM can be found in [9] where the overall design space has been explored to make the design robust and comprehensive. Current work focuses on developing a reliability metric for MMC converter employing the same strategies developed in [7–9].

Two major advances occurred during this performance period:

First, the software was applied to a real use case outside of the development arena. Specifically, during the creation of a baseline ship design in S3D version 2.0 to support the HTS project, this software was used to merge two databases created by two separate engineers. One database held the electrical system design, and the second database held the thermal system design. This test example performed a deep copy of components, connections, nodes, systems and diagrams from one database into the other. Identical items were flagged and relevant connections and system notations were transferred to the respective components rather than duplicating components. Bounding box geometry was created as needed to facilitate visualization in the LEAPS editor. The resultant design contains over a thousand components, five thousand nodes, and five thousand connections in three disciplines, all stored in a LEAPS database and complying with the FOCUS Product Meta-model. This robust test case is a significant step toward production-ready software.

Second, an algorithm for a rapid linear system solver was developed, coded in *MATLAB*, and tested on several simple systems using a limited set of component types. More advanced system testing is in progress, along with automatic extraction of the data required for the analysis from the LEAPS database. The algorithm will need to be expanded to accommodate additional component types such as switches and energy storage. Following proof of concept, coding in C++ is planned for future incorporation in the S3D software.

In the course of the above two efforts, many incremental advances were achieved. For example, the templating software was revised to allow affine scaling of the equipment locations to correspond with the dimensions of the ship into which the template is copied. Code was streamlined to prepare for clear transfer and integration with the S3D software. Recognition of items by global unique identifier (GUID) was implemented.

Task: Stochastic analysis

Technical Objectives

Define stochastic simulation and scripting capability that can be used for design purposes, and in particular for Electric Power Load Analysis (EPLA).

Technical Approach

This task will explore:

- Generalized Polynomial Chaos (gPC) theory for uncertainty quantification.
- Inverse simulation to propagate design requirements to decision variables.

Progress Statement Summary

Combining generalized Polynomial Chaos (gPC) theory with an overloading and object-oriented programming approach, we developed a scripting and simulation tool that, while it is based on a fully analytical approach to uncertainty quantification, does not require formulating the problem in the gPC variables. Thanks to object-oriented implementation, it is possible to use a standard simulation model and to smoothly alternate deterministic and stochastic analysis. Changing the variable declaration changes the nature of the model, while the code stays the same. As a result, a model can be written in this new domain without considering the presence of uncertainty.

We tested the tools performing sensitivity analysis on a small ship power system. We then started using the tool to solve inverse simulation problems in the presence of uncertainty. Through the use of gPC, we intend to create a framework for a direct solution to the inverse problem under uncertainty. The benefits of a stochastic approach to inverse simulation are not limited to applying inverse simulation to stochastic systems. Instead, we intend to develop methods to define the desired outputs as probability density functions (PDF). This application will allow imposition soft constraints on the desired outputs and to evaluate how tolerance ranges propagate to control quantities.

This task was suspended due to lack of funding. Expect this work to recommence in March 2018.

Task: Implementation of templates for semi-automated design of ship systems

Technical Objectives

Explore methodologies to accomplish distributed system design and analysis in a set-based design paradigm such as the Navy's Rapid Ship Design Environment (RSDE) process. Specific goals include the production of distributed system designs in a semi-automated manner based on a small amount of input provided in template format; these distributed system designs will be responsive to the overall ship design.

The goal of this task is to develop a semi-automated design methodology and tool that can be applied to any distributed system such as electrical power, chilled water, seawater, fire main, data, or communications. This methodology provides a distributed system design that connects sources to sinks based on rules defined by templates chosen by the designer. The results are then available to any other LEAPS-integrated software, (e.g. S3D for analysis, ASSET for weight evaluation, etc.).

Technical Approach

Develop template implementation software that is directly integrated with the LEAPS data repository using the FOCUS product meta-model.

- This software begins with a ship design, synthesized using ASSET 7.0 and stored in a LEAPS database.
- A second database is populated with system template sections that can be created within S3D.
- The system routing tool constructs and electrical power corridor that collects power from onboard generators and distributes power to all loads.
- Relevant components are placed in 3D space in the proper zone and logically connected, and the associated S3D simulation models are linked as well.

Continued work will accomplish sizing and positioning of the components.

Progress Statement Summary

The methodology for linking template segments into a cohesive whole was developed and implemented in FOCUS-compliant, LEAPS-integrated software. Fully developed and properly connected segments of a bus are created and stored in a LEAPS database. Each segment includes dummy components, denoted ‘plugs’, which are used to connect to the next segment. When the bus is assembled, the plugs are removed and the system connectivity elements (nodes and linkages) associated with them are connected to the adjacent template segment. Since the complexity of the system exists within the templates and not in the connectivity process, this methodology is applicable to essentially any type of system backbone.

The output of this process is a fully-connected, FOCUS-compliant electrical distribution system with established systems and common views that are properly populated.

During this reporting period, we finalized the methodology for extracting adjacency matrices and adjacency lists from a LEAPS database. We then began development of an algorithm for sizing of components and began exploring the use of clustering algorithms in segregating the distribution systems, as described in [10, 11].

This work has also benefited from collaboration with a NICOP project on network theory applications in early-stage ship design, generating ongoing work in conjunction with Virginia Tech.

Two papers were presented during ESTS 2017 detailing progress in this area [10, 11].

Two major advances occurred during this performance period: First, the software was applied to a real use case outside of the development arena. Specifically, during the creation of a baseline ship design in S3D version 2.0 to support the HTS project, this software was used to merge two databases created by two separate engineers. One database held the electrical system design, and the second database held the thermal system design. This test example performed a deep copy of components, connections, nodes, systems and diagrams from one database into the other. Identical items were flagged and relevant connections and system notations were transferred to the respective components rather than duplicating components. Bounding box geometry was created as needed to facilitate visualization in the LEAPS editor. The resultant design contains over a thousand components, five thousand nodes, and five thousand connections in three disciplines, all stored in a LEAPS database and complying with the FOCUS Product Meta-model. This robust test case is a significant step toward production-ready software.

Second, an algorithm for a rapid linear system solver was developed, coded in *MATLAB*, and tested on several simple systems using a limited set of component types. More advanced system testing is in progress, along with automatic extraction of the data required for the analysis from the LEAPS database. The algorithm will need to be expanded to accommodate additional component types such as switches and energy storage. Following proof of concept, coding in C++ is planned for future incorporation in the S3D software.

In the course of the above two efforts, many incremental advances were achieved. For example, the templating software was revised to allow affine scaling of the equipment locations to correspond with the dimensions of the ship into which the template is copied. Code was streamlined to prepare for clear transfer and integration with the S3D software. Recognition of items by global unique identifier (GUID) was implemented.

1.1.2 Develop flexible power quality requirements and its impact on electric power (plant) load analysis (EPLA)

The work planned for this project is anticipated to begin mid to late 2018.

1.2.1 Develop stochastic response generation framework to facilitate risk-averse designs

Task: Risk-sensitive optimization

Technical Objectives

Develop risk-sensitive control methodologies aimed at optimizing operational performance, which are also robust and reduce extreme fluctuations. Classical techniques in optimal control, where one aims to optimize the step-by-step performance over a given time-horizon, or in the average, fail to capture the effect of extreme fluctuations, or mitigate these fluctuations. On the other hand, the traditional min-max approach is ultraconservative. In taking this approach, the minimizing controller is guarding against all possible uncertainties, which are considered 'equally likely.' As a result, such an approach may indicate that the performance goals can never be met. A less conservative approach is to introduce in the model a 'function' that measures the likelihood of the uncertainty. This is basically the difference in approach between classical robust control theory, where disturbances are modeled deterministically, and stochastic control, where disturbances are modeled as stochastic processes. Risk-sensitive optimal control provides the crucial link between stochastic and deterministic approaches by providing controls that have excellent average performance, while at the same time heavily penalizing large fluctuations.

Technical Approach

Develop risk-sensitive control using a novel study of Dirichlet or Neumann eigenvalues on the entire space.

- In [12] we consider the infinite horizon risk-sensitive problem for nondegenerate diffusions, (i.e. dynamical systems described by stochastic differential equations, with a compact action space, and controlled through the drift).
- We only impose a structural assumption on the running cost function, namely near-monotonicity, and show that there always exists a solution to the risk-sensitive Hamilton-Jacobi-Bellman (HJB) equation, and that any minimizer in the Hamiltonian is optimal in the class of stationary Markov controls.
- Under the additional hypothesis that the coefficients of the diffusion are bounded, and satisfy a condition that limits (even though it still allows) transient behavior, we show that any minimizer in the Hamiltonian is optimal in the class of all admissible controls.
- In addition, we present a sufficient condition, under which the solution of the HJB is unique (up to a multiplicative constant), and establish the usual verification result.
- We also present some new results concernin the multiplicative Poisson equation for the elliptic operators on the whole space.

In [13] we study the eigenvalue problem on the whole space for a class of second order, elliptic operators of the form associated with nondegenerate diffusions.

- The potential, or running cost is not assumed to be near-monotone as done in [12], and the results are much more general. We present various results that relate the strict monotonicity of the principal eigenvalue of the operator, with respect to the potential function, to the ergodic properties of the corresponding 'twisted' diffusion, and provide sufficient conditions for this monotonicity property to hold.
- Based on these characterizations, we extend or strengthen various results in the literature for a class of viscous Hamilton-Jacobi equations of ergodic type to equations with measurable drift and potential.

- In addition, we establish the strong duality for the equivalent infinite dimensional linear programming formulation of these ergodic control problems. We also apply these results to the study of the infinite horizon risk-sensitive control problem for diffusions.

- We establish existence of optimal Markov controls, verification of optimality results, and the continuity of the controlled principal eigenvalue with respect to stationary Markov controls.

Progress Statement Summary

Past work supported by ONR on this topic was reported in [14]. The main results of the recent work in [12] can be divided into two groups. Those concerning the risk-sensitive control problem, and those concerning the multiplicative Poisson equation (MPE) for (uncontrolled) diffusions. For the risk-sensitive control problem, there are two sets of results. First, under the hypothesis that the running cost is near-monotone relative to the optimal value, and an assumption on the drift that limits but not precludes transience of the controlled process, we establish existence of a solution to the risk-sensitive HJB equation, and also existence of a stationary Markov control, which is optimal over the class of all admissible controls. We wish to point out the optimality over nonstationary controls is very hard to obtain for the risk-sensitive problem without blanket geometric ergodicity hypotheses. For this reason, the optimal control problem is often restricted to stationary Markov controls, and in this paper, we have managed to overcome this limitation. The second set of results, which comprises a significant portion of the paper, concerns the MPE.

Here, the running cost takes the role of a potential, which satisfies the near-monotonicity hypothesis relative to the principal eigenvalue of the operator. We present a comprehensive study of the relationship between the solutions of the MPE and their stochastic representations, and the recurrence properties of the so-called 'twisted process,' which is associated with eigenfunctions of the principal eigenvalue. In the quantum mechanics literature, this eigenfunction is called the ground state, and the twisted process is described by a diffusion, which we refer to as the ground state diffusion. The important contribution of this paper is the sharp characterization of the recurrence properties of the ground state diffusion in terms of the monotonicity of the principal eigenvalue as a function of the potential.

Summarizing the main contributions in [13], we have: (a) established several characterizations of the property of strict monotonicity of the principal eigenvalue, (b) extended several results in the literature on viscous HJB equations with potentials vanishing at infinity to measurable potentials and measurable drift, (c) studied a general class of risk-sensitive control problems under a uniform ergodicity hypothesis, and established uniqueness of a solution to the HJB equation and verification of optimality results, and (d) established continuity results of the controlled principal eigenvalue with respect to stationary Markov controls.

In [15] we continue the work previously published in [13]. Here, we present some Liouville-type results for eigenfunctions of second-order elliptic operators with real coefficients. Second, we prove a lower bound on the decay of positive supersolutions of general second-order elliptic operators in any dimension, and discuss its implications to the Landis conjecture. Our approach is based on stochastic representations of positive solutions, and criticality theory of second-order elliptic operators.

Another recent paper [16] studies a class of multidimensional piecewise Ornstein-Uhlenbeck processes with jumps, which contains the limit processes arising in multiclass many-server queueing models with bursty arrivals and/or asymptotically negligible service interruptions in the Halfin-Whitt regime as special cases. We provide quantitative rates of convergence with respect to the total variation norm as well as the Wasserstein metric. In the case of exponential ergodicity, we also prove contractivity under the Wasserstein metric, by establishing an asymptotic flatness property of the process. The results in this paper provide crucial foundations for the study of risk sensitive control systems. This study is currently under way.

During this period, several important results were obtained. These appear in the following publication.

The first publication [17] is studying the ergodic control problem for a class of jump diffusions in the d-dimensional Euclidean space, which are controlled through the drift with bounded controls. The Levy measure is finite, but has no particular structure; it can be anisotropic and singular. Moreover, there is no blanket ergodicity assumption for the controlled process. Unstable behavior is 'discouraged' by the running cost which satisfies a mild coercive hypothesis (i.e., is near-monotone). We first study the problem in its weak formulation as an optimization problem on the space of infinitesimal ergodic occupation measures, and derive the Hamilton-Jacobi-Bellman equation under minimal assumptions on the parameters, including verification of optimality results, using only analytical arguments. We also examine the regularity of invariant measures. Then, we address the jump diffusion model, and obtain a complete characterization of optimality.

The second publication [18] is studying the $c\mu$ rule for multi-class queueing systems. When the service rates μ are known, the $c\mu$ rule is guaranteed to minimize the expected holding-cost over any fixed time horizon in the single server setting. But for a general parallel-server network, we show that the $c\mu$ rule does not ensure stability. We present sufficient conditions for the stability of the $c\mu$ rule for a general parallel-server network and also necessary and sufficient conditions for a special class of parallel-server networks where the rule has a hierarchical structure. We next consider learning-based variants of the $c\mu$ rule when the service rates μ are unknown and analyze their performance based on the holding-cost *regret*. In the single server setting, we establish that scheduling according to the $c\mu$ rule using empirically learned service rates achieves a holding-cost regret that does not depend on the time horizon. The single-server network allows for *explore-free* scheduling — it is sufficient to 'exploit' at all times using the empirically learned service rates. We demonstrate that this is not true in a general parallel-server network and propose a scheduling algorithm which is tuned to dynamically explore server rates but in such a manner that it eventually satisfies an explore-free condition. We also prove that this algorithm achieves a regret that scales as a constant with the time horizon.

Lastly, [19] presents a simple counterexample to a nonlinear version of the Krein-Rutman theorem reported in [20]. Correct versions of this theorem, and related results for superadditive maps are also presented.

Task: Risk-averse design

Planned future work.

1.2.2 Quantify the effects of system/subsystem failures and mitigation approaches to assess and perform de-risking procedures within the DDC

Task: Resilient topology design for shipboard power system

Technical Objectives

Design new SPS networks that exhibit very high capability to withstand external attacks compared to nominal topologies [21].

Technical Approach

Design new primary distribution network topologies that are tolerant to external attacks.

- Firstly, resiliency of nominal SPS topologies such as ring bus, double-bus double-breaker (DBDB), breaker-and-a-half topologies (BAAH) will be studied.
- Resiliency of the topologies will be quantified in terms of total load shed experienced following a worst-case attack on the network [22]. An attack that causes maximum disruption in a network is referred to as the worst-case instance. Such attacks can be identified by using an optimization framework that considers power flow components in a network.
- The framework will be developed based on bi-level programming that has inner and outer levels of problem, where the solution to one level of problem is nested in the other. For our formulation, the outer level problem will be an attacker's problem while the inner level problem will be a network operator's problem.
- Objectives of both the problems are different. An attacker problem's objective will be to identify network elements that maximize load shed, while that of an operator will be to minimize the impact of the attack, by appropriate generation scheduling.
- Using the framework, resiliency of nominal SPS topologies will be analyzed and based on the study new resilient SPS topologies will be designed.

Progress Statement Summary

Work done so far has been focused on formulating a problem statement and summarizing relevant literature in the field. Additionally, an optimization formulation that can be considered as the inner level problem of the proposed framework has been derived. It is a network operator's problem or a power flow formulation for an MVDC ship network. The objective of the formulation is to minimize total load shed in a network. The variables of the framework are generator's power output, power flow in lines and load served at each node of the network. An outer level problem will be formulated next to form a bi-level problem.

Work done so far focuses on formulating a problem statement and summarizing relevant literature in the field. Additionally, an optimal power flow formulation (4) – (10) for an MVDC ship network is derived. It takes into account line and bus disruptions during an attack on the network. The line disruptions in the network are modeled as integer variables. The developed framework is a mixed integer non-linear programming problem (MINLP). The objective of the formulation is to minimize the total load shed in a network during an attack. The variables of MINLP include generator's power output (P^{gen}), power flow in lines (P^L), bus voltage (V), and the load served (D_i) at each node of the network. For any given attack, the formulation shown below determines the disruption and minimizes the load shed in the network:

$$\min_{P^L, P^{gen}, S, V} \quad \sum_i S_i \tag{4}$$

$$s.t. \quad P_i^{gen} - \sum_{l/o(l)=i} P_l^L + \sum_{l/e(l)=i} P_l^L = D_i - S_i \quad \forall i \in \nu \tag{5}$$

$$P_l^L - G_l(V_{o(l)} - V_{e(l)})(V_{o(l)})(1 - d_l) = 0, \quad \forall l \in \varepsilon \tag{6}$$

$$0 \leq P_i^{gen} \leq \overline{P}_i^{gen}, \quad \forall i \in \nu \tag{7}$$

$$0 \leq S_i \leq D_i, \quad \forall i \in \nu \tag{8}$$

$$\underline{P}_l^L(1 - d_l) \leq P_l \leq \overline{P}_l^L(1 - d_l), \quad \forall l \in \varepsilon \tag{9}$$

$$(1 - d_l) = (1 - x_l)(1 - y_{o(l)})(1 - y_{e(l)}), \quad \forall l \in \varepsilon \tag{10}$$

where S_i is the load shed at node i. The variables x and y are binary line and bus attack variables, respectively. A value of '1' for the variables means that the corresponding line or bus is interdicted and vice versa. d is a binary line interdiction variable that represents the lines that are affected by bus interdiction variable (x) and line interdiction variable (y). The set of all buses is ν and the set of all lines is ε. The indices *o(l)* and *e(l)* refer to the origin and destination of a line l, respectively.

Nominal MVDC electric ship architectures are based on ring bus, breaker-and-a-half (BAAH) and double-bus-double-breaker (DBDB). For this study, three different SPS topologies based on the nominal architectures are designed. The topologies are similarly sized with the same number and ratings of generators and loads and have about 30 buses and 40 DC lines. The total generation in the topologies is assumed to 25% more than the corresponding load demand. The resiliency of the developed topologies will be studied in future work.

An attacker-defender based optimization framework is proposed for analyzing the resiliency of electric ship topologies. First, the nominal electric ship topologies such as the ring bus, double bus double breaker (DBDB) and breaker and a half (BAAH) topologies are studied using the proposed approach. The analysis provided some insights on further improving the resiliency. The worst case attacks are closer to the load and generator locations and the equipment have at most 2 out-feeds or in-feeds connecting them to the network. Therefore, new electric ship topologies (hexagonal and rhomboid topologies) are designed that have higher generator out-feeds. Hexagonal topology is one of the new topologies which is shown in Figure 3. It can be observed that the main generator 2 has 6 out-feeds and the other generators have about 3 out-feeds.

Resiliency analysis results for the nominal and new electric ship topologies are presented in Figure 4. For a fair comparison, all the topologies are similarly sized with the same number and ratings of generators and loads. To generalize, the ratings are normalized to total load demand in the network. Thus, the net load demand in all the topologies is 1:0 p.u. Normalized load shed for increasing orders of contingency is depicted in Figure 4. It can be observed that there is complete or 1.0 p.u load shed at the 8^{th} order contingency for BAAH and ring bus topology. On the other hand, the complete load shed occurs at 14^{th} order contingency in the new topologies. In addition, the slope of the resiliency curve is about half of that of the nominal topologies. Thus it can inferred that the new electric ship topologies exhibit very high resiliency over the nominal topologies [23].

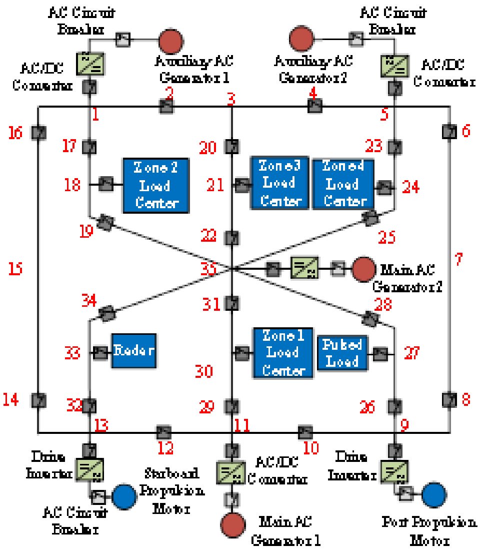

Figure 3: Hexagonal topology with increased generator in-feeds and load out-feeds.

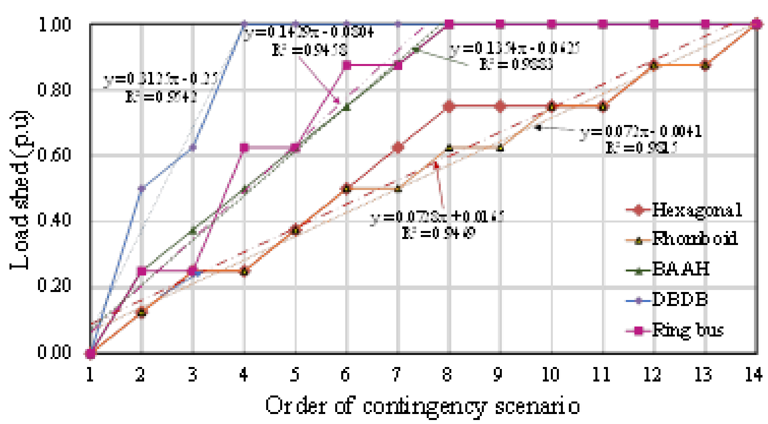

Figure 4: Resiliency curves for nominal and new SPS topologies.

1.3.1 Develop methodologies to determine control fidelity requirement throughout the DDC

Task: Standardized control system representation

Technical Objectives

Develop a standardized way to represent control and its effects on system behavior throughout the entire design process, and particularly in the early design stages. The challenge in meeting this objective is that in different stages of the control cycle only partial information on the system is available, because the design process is still progressing.

A general approach to incorporating controls in the full design development cycle will be introduced. The approach will improve fidelity of early-stage design, potentially shortening the design cycle. It will develop a control representation strategy that is compatible with and evolves together with the design cycle. This will help to accomplish set-based design under the "Rapid Ship Design Environment (RSDE)" paradigm [24], which requires the ability to represent the effects of control within the context of the early-stage design of an entire ship.

Technical Approach

- Classify types of analysis important in different phases of the design cycle.
- Determine required control characteristics to support the controls design cycle.
- Develop a family of control system representations providing optimal trade-off between fidelity and modeling efforts throughout the design cycle. The appropriate level of modeling granularity will be defined for different stages of the design process and for different analysis types. In particular, methods to track power and energy in early design stages will be developed. The concept of quasi-steady state will be introduced.
- Test early-stage control system representation in S3D.

Progress Statement Summary

Current work is focusing on control for early ship design. The objective is to incorporate controls in early stage conceptual ship design, automating the process of setting up the ship configuration for a given mission segment. For each mission segment, ship behavior must be established across all major disciplines, such as electrical, mechanical, HVAC and so on, so that proposed design performance can be evaluated. The problem can be framed as a constrained static optimization problem. An appropriate cost function is minimized to provide a semi-optimal control solution. The optimization process will be developed in collaboration with the S3D team at USC. The progress is described in [25].

Incorporation of a control layer in early stage conceptual ship design has been analyzed in collaboration with the S3D team at USC. The purpose of Early Control is to compare all possible steady-state operating points given a ship design and a particular mission segment, and to select the optimal ship configuration. This Early Control problem has been addressed as a constrained static optimization problem. A categorization of optimization methods that can be used to solve this problem is shown in Figure 5.

A sample design problem has been studied to evaluate two different solution methods [25]. The problem was set to minimize fuel consumption while satisfying a specific load demand for a particular mission segment. The Lagrange multiplier method (calculus-based method) and a mixed integer enumerative method were applied to solve the problem. S3D was used to evaluate all possible operating points for the second method and to validate the mathematical result from the Lagrange multiplier method.

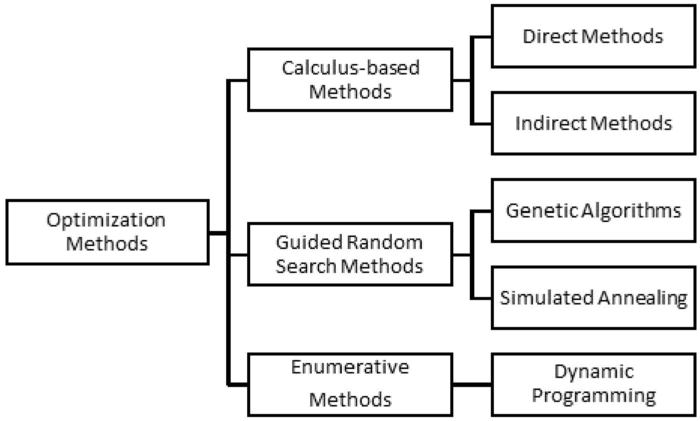

Figure 5: Optimization methods.

Each method has its advantages and disadvantages. The use of a calculus-based method requires the development of a cost function that needs to be minimized, which in many cases may not be straightforward. On the other hand, the enumerative technique is not based on a cost function but requires more computational effort to evaluate all possible solutions and the solution is sensitive to discretization of the search space.

As future work, other optimization techniques and more complex mission scenarios will be studied. Since different approaches may be better suited for different missions depending on the objective and complexity of the problem, a comparative study is planned to be performed.

The problem of early stage ship design evaluation has been framed as a constrained optimization problem. A certain scenario determines a set of constraints on ship operation. The ship has a set control variables that determine system behavior. The goal is to determine optimal values for the control variable set that provide optimal performance for the ship that is being analyzed while satisfying the set of constraints.

Current work focuses on the optimization problem for the electrical and the cooling systems. In the electrical system, the control variables are mainly the amount of power that each generation unit supplies to loads for a specific mission segment. The electrical system operating point determines the thermal loads on the system. The cooling system must be configured to provide adequate cooling and maintain acceptable operating temperatures. The set of control variables for the thermal system includes valve settings and pump coolant flow.

In the previous work, the optimization problem was formulated and solved for a notional design in the electrical domain. In that study, the problem was solved using two methods: the Lagrange multiplier method (calculus-based method) and the mixed integer enumerative method. Although this study provides a general platform for problem formulation, the applied methods to solve the problem can become impractical for a larger scale problem. The Lagrange multiplier method requires a complete mathematical formulation of the problem, which tends to be a manual time-consuming task. On the other hand, the mixed integer enumerative method requires a significant amount of computational resources which grows quickly for large scale problems.

To minimize the computational requirements, the application of guided random search methods such as Genetic or Particle Swarm optimization algorithms is under study. These methods can provide results of high accuracy in a computationally efficient manner.

Task: Digital observers and surrogates

Technical Objectives

- Develop and demonstrate observers to detect system dynamics that signal abnormal behavior of the system in an all-electric ship, indicating such incidents as power failure or malicious cyber attacks.

- Use observers within a model-based compensator control scheme to affect rapid system reconfiguration and control dictated by the system response, providing advanced capability for rapid system control.
- Extend observer use to protect system integrity.

Technical Approach

- Upgrade and bring up to date a previously constructed model of an all-electric ship, providing sufficient flexibility to include the latest decisions on design parameters.
- Assess model fidelity versus required accuracy and running speed to construct effective observers.
- Demonstrate in simulation the effectiveness of power failure and abnormal behavior detection, as well as fast load reduction response.
- Demonstrate unusual system behavior detection to protect against external attack.

Progress Statement Summary

Current work is concentrated on updating models of the all-electric ship operating in a seaway (Figure 6). In addition, a preliminary assessment has begun on developments in failure detection for commercial applications to determine effectiveness and relevance for military applications.

We are progressing on time with the scheduled tasks:

- The first task, updating the model of the all-electric ship (Figure 6) has been completed, upgrading modular subsystem models and parametrizing the equations in terms of parameters to be detected. Existing models of failure detection in offshore systems have been studied in order to draw parallels to naval ship system detection and determine their relevance and effectiveness in military applications.
- Currently we are studying the connection of detection systems to sensors on naval ships as a critical component of the detection scheme and as a potential area for cybersecurity improvements.
- We have implemented the first observer models using unscented Kalman filters, which can handle effectively the inherent nonlinearities of the models of the electric ship.

After updating models used for simulation of the all-electric ship operating in a seaway, several test cases have been run and analyzed.

The test cases we have run so far include:

- Startup to a speed of 25 knots in calm seas.
- Acceleration from 25 knots to 30.5 knots in calm seas.
- AC braking in calm seas.
- 45° and 90° heading changes in calm seas.
- 45° turn at 25 knots with second-order wave forces.
- 25 knots in head seas, at sea state 6.
- 360° turn at 25 knots in sea state 6.

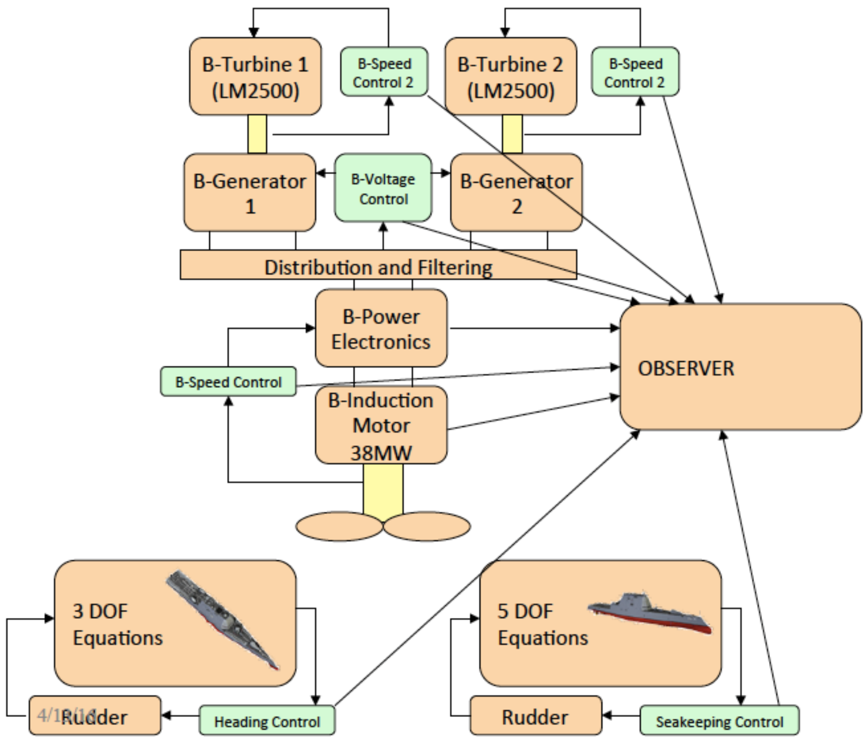

Figure 6: Observer-based model of electric ship in a seaway.

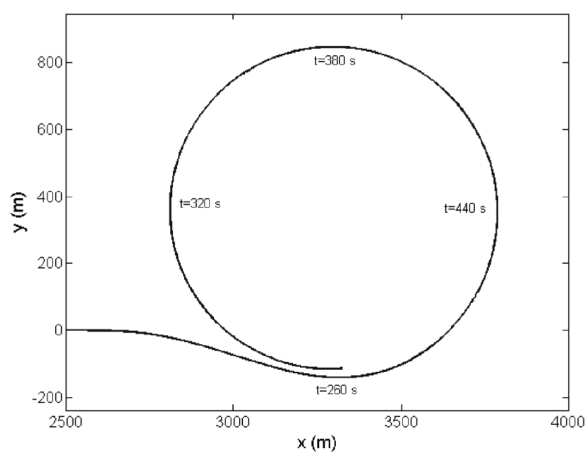

Figure 7: Circle maneuver with a 360 deg turn of the AES in a sea state 6 seaway; see Figure 8 for speed and propeller responses.

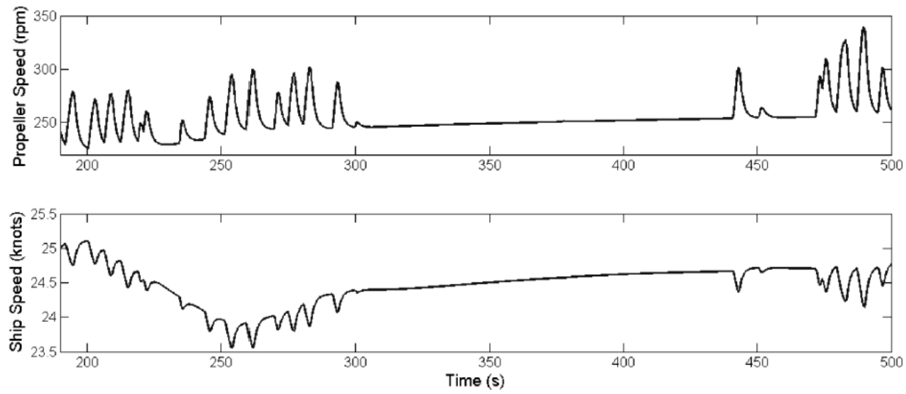

Figure 8: Propeller speed and ship speed during a 360 deg turn in sea state 6 (see Figure 7).

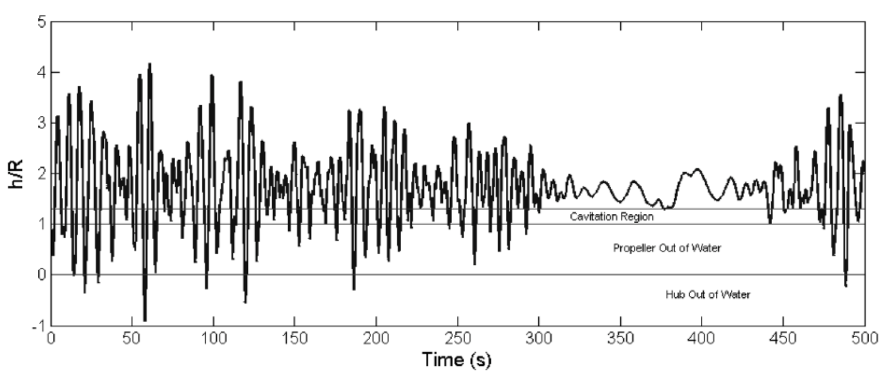

Figure 9: Propeller submergence to radius during the 360 deg turn of the AES in a sea state 6 seaway (see Figure 7).

1.3.2 Develop sizing of energy storage for shipboard power systems and its impact on EPLA

Technical Objectives

Develop a comprehensive solution to sizing energy storage simultaneously considering individual priorities such as fuel cost, survivability and reliability of ship, and mission load requirement.

Technical Approach

Develop a framework allowing existing solutions to be integrated.

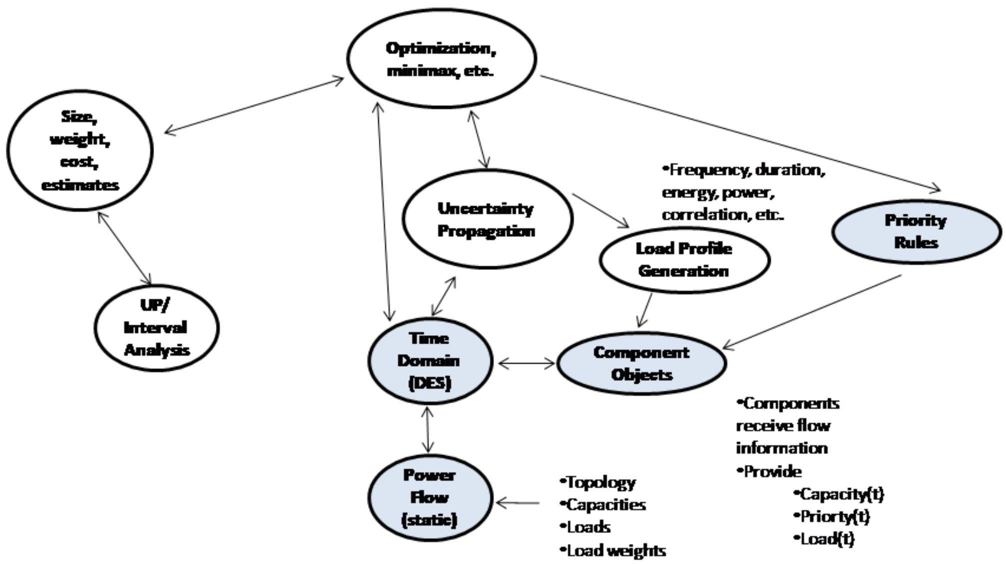

Figure 10: Energy storage sizing framework.

Progress Statement Summary

Development on the framework, illustrated in Figure 10, continued with additional refinements on an earlier developed algorithm for computing values of performance metrics (e.g., operability) with an optimal energy scheduling algorithm. Optimal in this context loosely means that no scheduling algorithm can perform better. The intent is to include energy storage in early stages of design where the energy allocation scheduling is not necessarily known. Therefore, considering optimal performance for a given size and configuration of energy storage gives confidence in identifying only infeasible solutions, which is useful and lends itself to set-based design practices. A description of this algorithm [26] was published at ESTS 2017.

Energy storage sizing and operational characteristics were investigated to find solutions to smooth power demand pulses with complementing storage technologies. By combining larger sized but slower responding with faster but small units, trade-offs in technologies were explored. Experiments using PHIL were used to link the two technologies to a flywheel and capacitors, both with power electronics interfaces, with a simulated rest-of-system. The experimental results showed that the advanced controls, taking full benefit of the converter interfaces, allows for improved utilization of available resources [27]. The project was performed in collaboration with the JHU Applied Physics Laboratory.

1.3.3 Develop data communication architecture to support control systems

Task: Methodology for designing SPS communication architectures

Technical Objectives

Develop a means of systematically and methodology characterize options and explore the solution space are needed. Data communication timing requirements from next-generation control and automation systems are insufficiently defined and categorized in order to effectively design SPS (Shipboard Power System) communication architectures. Further, the timing characteristics of many existing communications equipment and corresponding best-network designs with respect to SPS communications are not well understood.

Due to the many options with fundamentally different underlying communication schemes and capabilities, CAN, for example, is typically a serial fieldbus technology with a linear bus structure, while EtherCat is frame-based and possibly based on a dual-ring physical network. Both are industrial-strength technology options and enable automation and real-time operation. All available communication and networking options have bitrate and distance limitations that vary widely and choosing appropriate technologies in the context of next-generation controls is not clear.

The envisioned outcomes/objectives from this task are:

- Identification and categorization of timing and latency requirements on the communication platform for next-generation control and automation systems.
- An open architecture with reference offline (non-real-time) implementation for a communication platform, including secure communication protocols, with packet formats for the control of power devices in different operation modes.
- A prototype implementation (architecture and controls) with a real-time network simulator (developed in collaboration with Project 1.4.2) that is used to demonstrate the proposed methodology.

Technical Approach

- Gather a set of representative controls in collaboration with Thrust 3 and control system baselines in Thrust 1.
- Compare and contrast timings against current standards including 1676-2010 – IEEE Guide for Control Architecture for High Power Electronics (1 MW and Greater) Used in Electric Power Transmission and Distribution Systems.
- Consider options in control partitioning for feasibility of data communications and trade-offs with respect to data rate, bus utilization, responsiveness, security, openness and availability of control-communication APIs that facilitate implementations in controller hardware-in-the-loop (CHIL) experiments.

Progress Statement Summary

Applicable standards were reviewed [28] with respect to control architectures for power electronics-based building blocks (PEBB) and systems. The PEBB are envisioned to be the major base components in a more agile next generation of SPS.

OPNET installed license renewed and demo cases of routing Ethernet messages and interfering with timing and package losses complete. As a lightweight, open-source alternative to OPNET, Linux NetEm [29] was configured, installed, and tested with a simple CHIL setup. Rudimentary data communication perturbations including network delays and dropping packets was applied to a simple control setup, which was connected to a power system simulation.

Worked with Thrust 3 to build a set of representative controls and implementations. This set will be used better understanding data communication requirements and develop data communication architectures that are relevant to SPSs.

Collaboration with Thrust 3 began to build a set of representative controls and implementations.

The existing communication architectures for shipboard systems have been reviewed. The identification and categorization of the timing and latency requirements on the communication architecture from the control systems is in progress. The major communication protocols that must be supported by the architecture have been identified. The design of the experimental studies including simulations is in progress.

The majority of this period focused on published-subscribe-based messaging for controller-controller communication. In particular, Data Distribution Service (DDS) and Message Queuing Telemetry Transport (MQTT) were explored as well as specific implementations including Mosquitto, Open DDS, and RTI DDS. The RTI-based DDS implementation was leveraged in CHIL experiments for distributed control-to-control messaging on NI platforms [30]. Experiments for determining communication latencies using DDS and other related protocols were performed in order to gauge typical latencies. The observed latencies varied significantly depending on the specific implementation, computing hardware, and operating system configuration. As such, additional investigations are planned to decouple the hardware from the software and configuration latencies.

Initial investigation of wireless architectures and protocols began this period. On the implementation side, experiments were setup to better understand latencies and gain experience using Zigbee devices and associated protocols.

1.3.4 Partition control functions and data communications

Planned future work

1.4.1 Develop guidelines for model fidelity requirement for off-line and real-time analyses of emerging technologies applied to shipboard power systems

Task: CPU/FPGA and HIL co-simulation

Technical Objectives

Test and validate new solutions and technologies for Medium Voltage Direct Current (MVDC) systems. The real-time hardware-in-the-loop (HIL) simulator is an effective tool to use to conduct such tests and validations. A critical challenge is that the emerging power electronics are fast compared to the 'real-time' capabilities of traditional simulators. The UT-CEM hardware-in-the-loop system mitigates that challenge by using both CPU and FPGA for a power system model. To efficiently simulate a complex power system model using a real-time simulator, special skills and expertise are required. The CPU-based simulation solution allows us to simulate a power network with 30-50 μs time step; the FPGA-based solution allows us to simulate a power electronics system with less than 500 ns time step. The challenge addressed in this research is how to effectively perform a multi-domain real-time simulation with both detailed power electronics switching devices and a system network model.

Another objective of this work is to interface the real-time digital simulator with the UT-CEM microgrid. The digital simulator will be used to simulate missing components in the real microgrid to support the anticipated experiments. Subscale ADM experiments conducted on the UT-CEM microgrid can be an important step in the realization of a full-voltage full-power ADM three-zone demonstrator, providing a testbed for components, subsystems, controls, and the overall performance of the MVDC ship architecture.

Technical Approach

- Develop a versatile capability using existing Opal-RT CPU-based and NI FPGA-based co-simulation platforms for a shipboard MVDC system.
  - Study partitioning strategy for the MVDC network model to perform efficient simulation.
  - Implement a MVDC system network model on Opal-RT simulator.
  - Implement high-fidelity power converter models on NI FPGA simulator.
  - Configure the communication interface of the two simulators to perform effective multi-domain simulation study.
- Implement flexible interfaces for hardware controller and power equipment for hardware dc microgrid test.
  - Develop interfaces for hardware controllers to conduct real-time controller hardware-in-the-loop (CHIL) tests; expected real-time CHIL tests may include:
    - MVDC shipboard power system reconfiguration method test.
    - MVDC system protection algorithm validation.
    - Advanced control algorithm tests for MVDC system.
  - Develop interfaces to integrate real-time digital simulator with hardware DC microgrid; detailed approaches include:
    - Design and develop a power amplifier to interface the digital simulator with hardware power system.
    - Implement appropriate power equipment model or network circuit model on digital simulator to perform power hardware-in-the-loop (PHIL) test.

Progress Statement Summary

UT-CEM team will closely collaborate with other ESRDC researchers (i.e. FSU, USC, etc.) in this area to develop the multi-domain real-time simulation platform. Current progress includes preliminary testing for an energy management system approach for a small-scale power system and the test results will be presented in a smart grid conference. Currently, the co-simulation approach using the Opal-RT and FPGA simulators are exercised. Preliminary CHIL tests for DC protection algorithms [31,32] are also conducted in the simulation platform. The next step will focus on developing a suitable MVDC shipboard power system model in the real-time digital simulator to perform DC power network reconfiguration algorithm tests (a collaborating effort with ISSAC Corporation under a SBIR program).

Current progress includes preliminary testing for an energy management system approach for a small-scale power system and the test results will be presented in a smart grid conference. The co-simulation approach using the Opal-RT and FPGA simulator has been exercised. Preliminary CHIL tests for DC protection algorithms [31,32] were conducted in the HIL simulation platform.

During May–September 2017, the research team utilized the Opal-RT simulator to model a simplified MVDC system with two Power Generation Modules (PGMs), one main dc bus, dc isolation devices, and two constant loads. The simplified MVDC system is simulated with 50 μs time step and the switching frequency of the power electronics devices is chosen as 2 kHz. Some numerical errors were observed in the numerical simulation due to the relatively large simulation time step. The numerical simulation error is reduced when the interleaved control method is used for converters. Various fault cases are simulated to test the developed dc protection methods. The improved local measurement-based dc short-circuit fault detection and location method was tested in this HIL simulation environment.

In order to improve the numerical simulation accuracy, the converter switching model is being implemented in the NI PXIe FPGA real-time simulator. The simulation time step for power converters was reduced to 250–500 ns. The power electronic device switching frequency was increased to 5 kHz to emulate the actual switching frequency of IGBT devices. The preliminary simulation results indicated that the numerical simulation error was significantly reduced. In addition, the converter controller with fault detection and current limitation function is being implemented and tested in NI-sbRIO controller. Preliminary results are being generated to validate the performance of the developed dc protection strategy.

Some relevant research results regarding HIL simulation test results for fault protection and system control have been published [33, 34]. An additional book chapter is being prepared [35] summarizing preliminary microgrid control HIL test results.

In this reporting period, the research team has finished the dc-dc converter modeling in the NI PXIe FPGA real-time simulator and finished the control-HIL simulation test for both dc-dc converter interleaving control and fault protection control. The control is implemented in a National Instrument (NI) single board reconfigurable I/O platform (sbRio-9606) and a NI general-purpose inverter controller. The control system has been transferred to a low-voltage dc hardware test-bed. The control and protection algorithm has been successful tested and demonstrated in this environment. One related research paper on the subject matter has been published [36]. This is a collaborative work with researchers at Aalto University in Finland. In this work, a look-ahead model predictive control approach is developed to control the optimal operation for dc microgrids with renewable sources, energy storage systems, and flexible loads. Control-HIL tests were conducted to illustrate the effectiveness of the proposed approach. In addition, the book chapter with control-HIL test results has been accepted for publication [35].

Task: Impedance measurements using PHIL

Technical Objectives

The importance of impedance measurements with respect to stability analysis of systems has long been recognized. With the development of PHIL capabilities, impedance characteristics become also useful in determining stability and accuracy properties of PHIL experiments, which inherently involve evaluation of integrated systems. Therefore, accurate and quick assessments of impedances of Devices Under Test (DUT) are desirable. Currently, impedance measurements at CAPS are only based on a single tone approach, i.e. injecting a single frequency sine wave at a time and sweeping over a selected frequency range. Although reliable, this approach is often inefficient, hence the motivation to implement other impedance measurement techniques that are suitable in medium voltage PHIL experiments.

Another motivation is the possible change in upstream or downstream impedance when changing a source or load of a system. An example of this is looking at a system comprising a source, a Power Conversion Module (PCM), and a load. Changing the source, for example, can have consequences during early stage testing of systems as connections to grid power rather than PHIL-simulated shipboard turbine-generator behavior may yield impedance characteristics that stable in one case but unstable in the other.

This task aims at extending HIL simulation capabilities to take full advantage of available modeling, simulation, and PHIL interactive operation up to medium voltage and megawatt-range power level.

Technical Approach

The current approach being used for impedance measurements at CAPS is the single tone method. This method is accurate, however highly time consuming. Three other methods are being researched to determine their viability in medium voltage noisy PHIL experiments:

- Multi-tone
  - A single signal made up by the superposition of sine waves with different frequencies. This allows one injection signal to perturb several frequencies at the same time, drastically reducing measurement time.
- Chirp
  - A continuous sweeping wave over a given frequency range. This method is short and measures a seemingly continuous band of frequencies rather than a discrete set of points like the single tone and multi-tone.
- Pseudorandom binary sequence (PRBS)
  - A PRBS based off of a maximum length sequence has properties similar to white noise, therefore it is able to excite all frequencies within its excitation bandwidth at once.

Progress Statement Summary

A thorough comparison between the four previously mentioned impedance techniques in regards to PHIL applications is currently being performed at CAPS. The different methods are being assessed based on their accuracy, resolution, experimental time required, and other key parameters for the optimization of future experiments. Figure 11 shows the results of the successful implementation of each technique in a real-time simulation. It is important to note that this preliminary data does not represent a direct comparison between the methods, as further testing still needs to be completed.

Impedance measurements in medium voltage megawatt range PHIL measurements have successfully been done at CAPS [37]. This study showed AC and DC measurements of a PCM as the DUT connected to a simulated Rest of System (ROS). This research used the single tone method for perturbing the DUT to gather impedance information.

Furthermore, simulations are being performed using the four techniques mentioned with simulated noise to determine their viability in medium voltage megawatt PHIL experiments [38]. We are using these techniques to probe a modeled PCM for the IPES model. The purpose of this is to determine the upstream or downstream impedance effects from changing a source or load in the system.

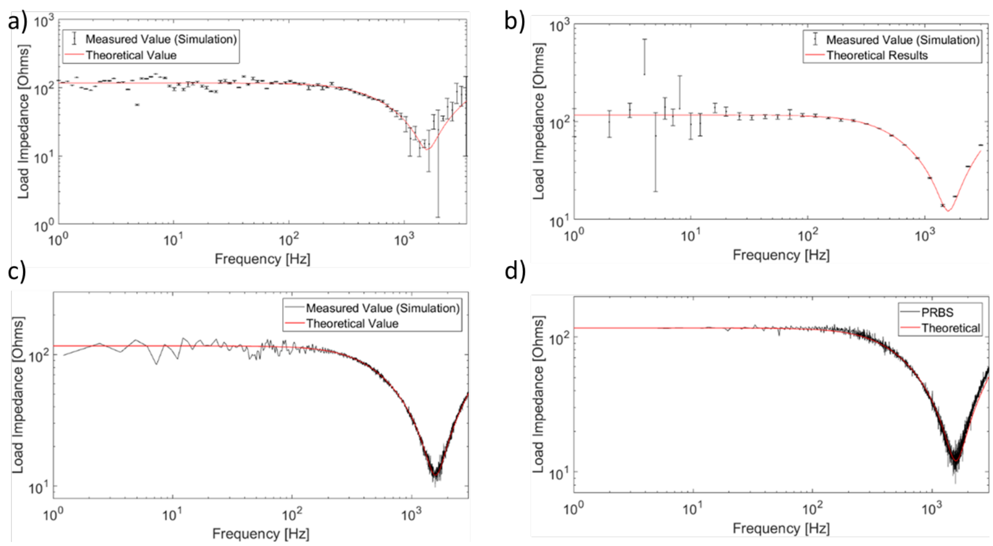

Figure 11: Successful implementation of different PHIL impedance measuring techniques in a noisy medium-voltage environment. The four techniques of interest are: (a) Single tone, (b) multi-tone, (c) chirp, and (d) PRBS.

1.4.2 Investigate performance modeling and cyber physical protection of the control communication network in electrical ship systems

Task: Performance modeling and cyber physical protection of the control area networks in electrical ship systems

Technical Objectives

Identify the requirement and develop models of the communication latencies of the CAN from typical power system devices that are spread in many different time granularities in electrical ships. Our focus is to model the communication response time, the decision time of the protection systems without considering the impact of cyber threats.

Investigate the impact of the possible cyber-attacks on the fast resilience or protection of such a communication network, that is, the ability of the network to withstand and recover rapidly from various network disruptions, particularly for the cyber-attacks that must be considered in an electrical ship system. Our focus is to identify the possible attacks to the major CAN protocols that are widely deployed in the control system networks and investigate the protection measures with revised models on the communication performances.

Technical Approach

- Develop theoretical performance models on the communication response time and protection decision time of the control area networks without considering the impact of the cyber attacks.
- For the major communication protocols of the control area networks in electrical ship systems, investigate the security issues and possible defense strategies of the major communication protocols that are used in the control area networks of the ship systems.
- Revise the performance models with added cyber-physical protection measures for the control area networks in electrical ship systems.
- Validate the performance models by the testbed with Beckhoff's EtherCAT platform and OPNET computer simulations.

Progress Statement Summary

By reviewing the literature, the team has identified five major communication protocols for CANs: DNP3, Modbus TCP/ICC Master tools, EtherCAT/Beckhoff, Profinet, and CANopen/CAN. The theoretical work in modeling the communication response time, decision time, synchronization, etc., has been started and is in progress. The team has also worked on the identification of the possible cyber-attacks against the communication protocols.

The performances of the commonly used protocols listed above have been compared. Depending on the protocol, observed latencies vary from tens of microseconds to hundreds of milliseconds. The typical applications are general purpose computers (DNP3), in-vehicle networks (CANopen/CAN), industrial device's application layer (Profinet), and communications among many industrial (electronic) devices within the same networks (Modbus, EtherCAT) and across different networks (Modbus TCP). Based on the literature review and time-scale requirements from the control system of electrical ships, we have initial real-time characteristics of the control area networks that can be used for electrical ship systems.

According to the protocol performance and our real-time requirement, we have decided to use the EtherCAT protocol with Beckhoff implementation as the communication protocol for the control area networks. The analysis of the protocol with different topologies and configurations is in progress. The simulation platform with the network emulator OPNET is in progress.

In addition, the team has started work to identify possible cyber-attacks against the communication protocols. Further, a grouping protocol was developed [39].

- Different network topologies, such as the star network, and technologies, such as the EtherCAT technology have been explored. Their latency properties have been modeled.
  - EtherCAT
    Total communication cycle time [40]:

$$T_C = 2(T_M + n * T_S + T_C^P) + T_{idle} \tag{11}$$

  - Star structure
    Total communication cycle time:

$$T_C = 2(T_M + n * T_S + 2m * T_J + T_C^P) + T_{idle} \tag{12}$$

- Identified possible types of threats in a CAN network, such as data and control information tampering, Byzantine attacks, and collusions.
- Different types of communications techniques have been explored:
  - UDP
  - TCP
  - OpenDDS
- Different security schemes have been explored, such as encryption and decryption: for messages in application layer, transport layer security (TLS), network layer security (IPsec), link layer encryption and authentication (LLEA), and physical layer security.
- Test plans have been propounded: the securities will be implemented in OPNET interfacing with the 4-zone ship model case of RTDS [41] or OPAT-RT.
- The security functions for 4-zone ship communications are implemented outside of the RTDS by techniques in item 4 (listed below) using the device in Figure 12 outside of the RSCAD module. They depend on further experiments.

Explanations for technology terms used in Figure 12:

1. RTDS is power electronics simulation hardware by RTDS Technologies, Inc.
2. RSCAD is power electronics simulation design software for RTDS by RTDS Technologies, Inc.
3. OPNET is a network simulation software by OPNET Technologies, Inc.
4. Mamba is a Single Board Computer by VersaLogic Corp. running Linux.
5. Dell server is a Dell EMC PowerEdge R230 rack server by Dell Inc. running Linux.
6. Items 4 and 5 serve the same function as a part of the simulation communications paths. In the Simulation Lab at CAPS, the Dell servers are replacing the Mambas gradually.
7. The GTFPGA server is a Linux computer with an RTDS specific communication interface card connected with optical fiber to item 1, and serves as a data switch platform between RTDS and external simulation software or power hardware-in-the-loop (PHIL) device.
8. Python hub is a Python program which runs on item 7 and provides the data switch function between items 1 and 3.

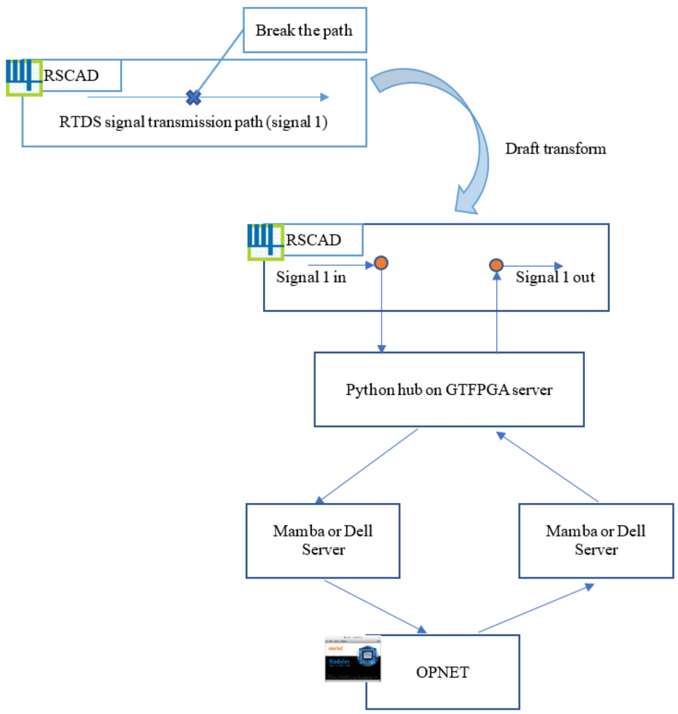

Figure 12: Test setup for security communication on RTDS 4-zone model.

1.4.3 Approaches to facilitate CHIL simulations with WBG converters

Planned future work

1.4.4 Interfacing guidelines to support control system evaluation and development

Task: Interfacing guidelines to support control system evaluation and development

Technical Objectives

Define interfaces between testbeds and control systems. The outcomes of this task will determine to what extent existing interoperability standards can be leveraged and developing guidelines for testbed and control system component interfaces to allow efficient development and evaluation of SPS control systems. The interfacing objectives include the capabilities to exchange increased amounts of information and individual signals at every simulation/execution time step, which typically is in the range of 2–50 microseconds, for two reasons: parts of the shipboard power systems of interest require control- and observability in this time range and, while evaluating system designs, a larger signal count than strictly necessary for final implementations is required to allow detailed analysis of processes and events. The experience gained will also be provided in collaboration with IEEE standards working groups on best practices for hardware-in-the-loop simulations [42] to accelerate the development cycle and applicability.

Technical Approach

Investigate separation and interconnection of different controls and automation functionalities that allow defining effective implementations of the controls to be evaluated.

- Using control designs to provide underlying requirements including signal count, fidelity and resolution, update rates, and priorities.
- Conducting simulation of the networked controls and control layers will expand on current practice of directly linked simulation signals, and make use of communications network models and simulators.
- Target co-simulation and surrogate controls to extend the capabilities to a wider set of applications, tools, and platforms.

Progress Statement Summary

Digital and analog interfaces are common practice but cumbersome and insufficient for automation in both practice and experimentation beyond small-scale systems. The inherent limitations in signal count and associated brittleness of installations must be overcome. To this extent, our first efforts focused on evaluating the feasibility of digital interfaces to a real-time simulator that allows logging of a larger number of signals (currently 64 per interface) at simulation time steps of about 50 microseconds. The difficulties in implementing such features are partly due to the lack of standards with respect to high-bandwidth interfaces to real-time and large-scale simulators. While building on off-the-shelf networking components and Ethernet communication, custom but open-source programming is used to implement solutions.

The data capturing design and implementation specifically targeted for RTDS real-time simulations was presented at the North American RTDS Applications & Technology Conference [43].

Collaboration with the Time Domain Electric System Model Working Group in Project 1.4.5 resulted in initial discussions and preliminary definitions for characteristics that a model implementation should define. The goal is to create more standard terms used for characterizing model implementation specifics. By doing so, the control evaluation framework can more precisely and efficiently determine the appropriateness of a given model implementation for a given experiment.

Collaboration with Thrust 3 resulted in an initial demonstration of a power sharing implementation for exercising and better understanding the controls evaluation and partitioning framework. A description of the control evaluation framework [44] was published at ESTS 2017 and a presentation of the implementation [45]

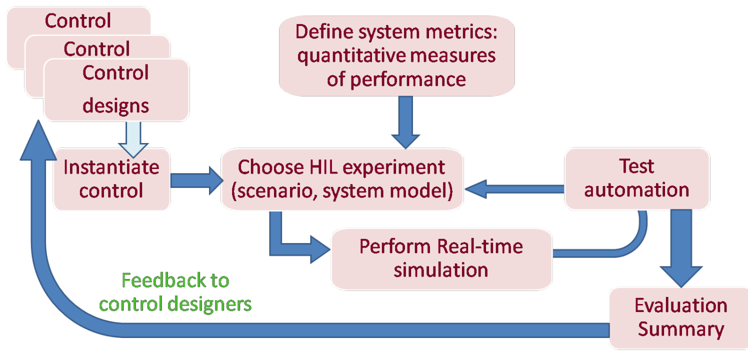

Figure 13: Controls evaluation framework and process.

was presented at the ONR Controls Workshop in August. Figure 13 illustrates the controls evaluation framework and process.

Further development of the key controls evaluation framework (CEF) components continued. As illustrated in Figure 14, the key components that were the focus of this update include power system models (specially designed for real-time execution), load profiles, metrics, and partitioning.

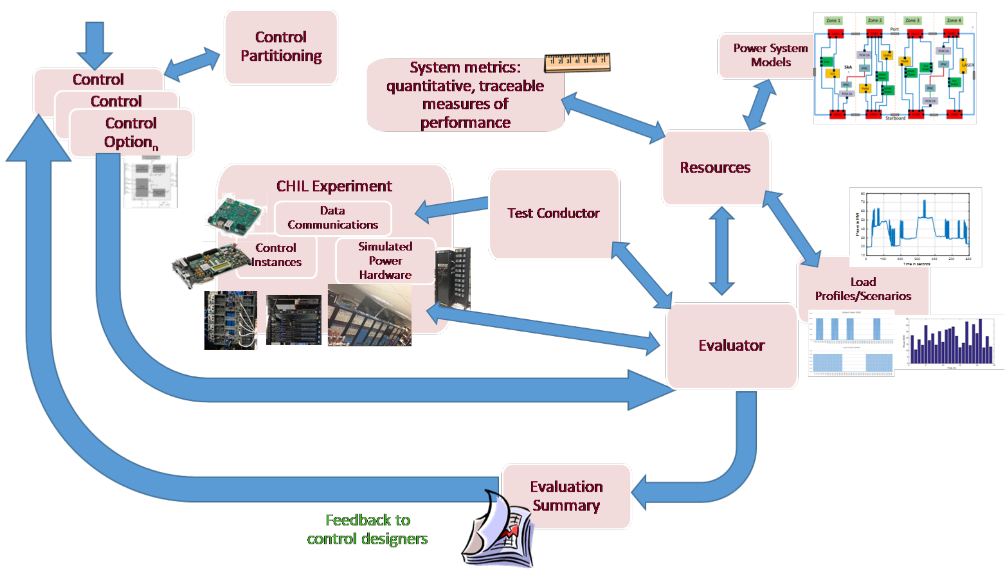

Figure 14: Controls evaluation framework overview.

During this period, the CEF teamed up with CDR Stevens of US Naval Academy to incorporate more meaningful load profiles. The power system load demands on Naval ship are generally unique and existing load profiles are insufficient to provide traceability to meaningful performance metrics. CDR Stevens generated a set of load profiles that are used as load parameter values in the real-time simulation.

A presentation [46] and discussion session was organized at the ONR Controls Workshop, which resulted in valuable feedback [47] from industry and academia. Additional details were published in an ASNE AMTS conference publication [48]. The intent of the afternoon session was to help direct development of the CEF towards a useful platform.

Additional interfaces were added to the controller hardware-in-the-loop (CHIL) testbed including Data

Distribution Service (DDS) and an alternative UDP-based interface for interfacing with power system simulation hardware. Traditional CHIL experiments typically insert a combined hardware and software solution into a real-time simulated power system environment; however, the CEF is designed to allow control software solutions to be inserted. The flexibility of software interfaces for hosting externally-developed controls allows for significant flexibility but can be problematic for CHIL experimentation if the software interface is not well-defined and robust. Therefore, a subset of typically used control software interfaces are being explored and tested within the context of the CEF.

1.4.5 HIL resource partitioning for controls evaluation

Task: HIL resource partitioning for controls evaluation

Technical Objectives

Develop a methodology for determining sufficient power system testbed resources (e.g. Digital Real-Time Simulators, controller hardware) to realize environments for evaluating controls. The type and quantity of resources needed for an appropriate HIL setup depends on many factors including: the desired accuracy/quality of the results, the available models, and what aspect of a given control is being evaluated while determining the resources and how to maximize the results.

Technical Approach

- Define and categorize/partition/separate the different aspects of 'control' that will be evaluated. Many terms are used with respect to controls. Terms such as controller, control algorithm, and control approach have a variety of different meanings. Further, the representation of controls generally evolves throughout the design development cycle (DDC). For instance, one may want to evaluate the control function in early design stages, whereas later in the design stages, a controller including both hardware and software may be the evaluation focus.
- Evaluate a set of 'surrogate' hardware platforms for hosting controls. This task is closely related to Project 1.4.4. Loosely speaking, this task is concerned with the allocation of an HIL testbed resource, whereas Project 1.4.4 focuses on appropriate interfaces and guidelines for improving the ability to instantiate controls for HIL-based evaluation. Obviously, there will likely be some overlap between this task and Project 1.4.4.
- Develop benchmarks for gauging hardware applicability.

Progress Statement Summary

Efforts were made to experiment with capabilities of hardware from the recent DURIP award [49]. These capabilities include the range of software (e.g. Simulink RT targets and desktops) and data communications with DRTSs (i.e. RTDS, Opal-RT).

Efforts were also made to develop a set of benchmarks for gauging the suitability of surrogate control hardware for hosting and evaluating controls. Specifically, initial specifications and considerations were developed.

A model working group within the ESRDC team members titled, 'Time Domain Electric System Model Working Group (TDESMWG)' was initiated. The goal is to develop a companion dynamic simulation model for the 10kT ship model available in S3D and to provide coherency in modeling development between various ESRDC entities. A model description document (MDD) that entails the salient features of the shipboard power system (SPS) model by detailing the module and component characteristics and requirements is in progress. The SPS model will also be used for controller hardware-in-the-loop (CHIL) based control evaluation experiments. Implementation of the SPS model will be undertaken on several digital real-time simulation (DRTS) platforms while adhering to real-time constraints.

The SPS MVDC distribution will be of 12 kV class with a 100 MW power system rating. Figure 15 below shows a block diagram of a notional four zone MVDC SPS. The system will be comprised of multiple power generation modules that are of dual output feed type. Load modules such as power conversion modules (PCM-1A) and propulsion motor motors (PMM) will be implemented. Special modules such as energy storage, rail gun, laser, and radar will be modeled in the SPS. The power model, as well as supporting control systems, are open models developed under the ESRDC initiative. The model will support cross-zone interconnection of modules and host energy storage modules (ESM) for increased survivability and serviceability of vital un-interruptible loads. Module controls will be defined and made available so as to allow for internal or external control of the system for CHIL based studies.

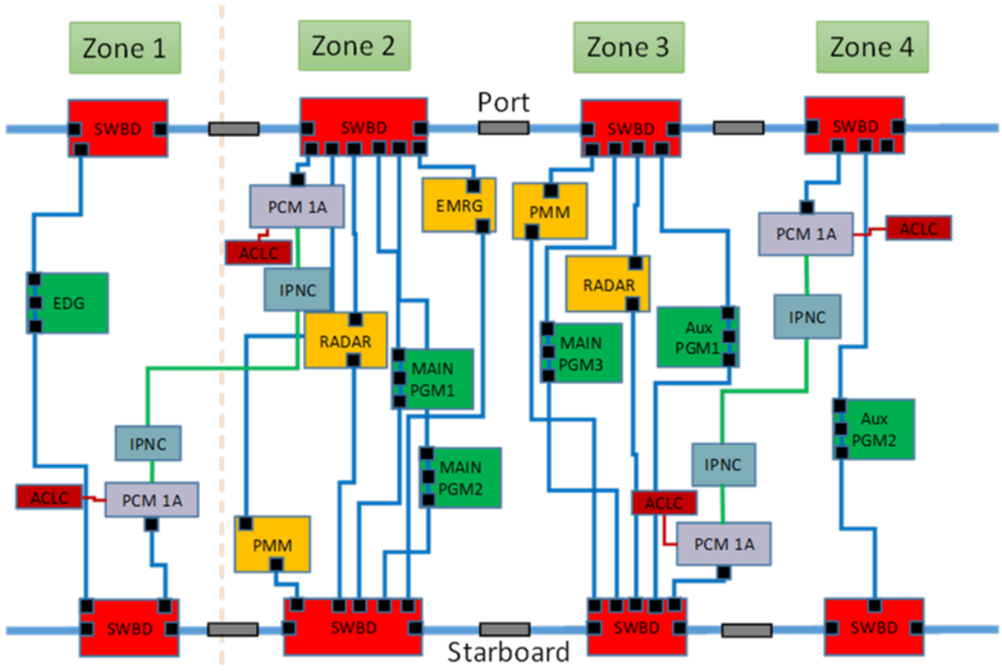

Figure 15: Block diagram of notional four zone MVDC SPS.

Implementation of the real-time shipboard power system models progressed by refining modules of the MVDC-based architecture, and extending the model to incorporate four zones illustrated in Figure 15. Interfaces have been added to allow a more detailed monitoring (i.e., with time steps in the microsecond-range as executed by the simulator) and agile controller interface. Further expansion is now better supported through common naming conventions. The developed component and system models have been tested through software, real-time simulator control instantiations as well as CHIL-based controls for power management. The efforts and salient aspects are presented in [47, 50].

1.4.6 Theoretical foundation for effective linkage of external time domain simulation capabilities with a design framework like S3D

Planned future work

This page intentionally left blank

Thrust 2: High Power Dense Component Development and Characterization

Technical Objectives

Advance technology developments in power electronics and controls to achieve heretofore impossible performance from a doubly-fed induction motor; combination of a pulsed alternator, storage, and power electronics and controls to power an electromagnetic launcher or laser, or to enhance power quality when neither weapon system was needed; and the use of storage, power electronics, and controls to develop a power node that provides power routing and protection. The anticipated advances are expected to lead to smaller, more capable warships. Under this approach, future ships become smaller and lighter by reducing the size of power modules, by increasing the functionality of power modules so that fewer are required, and by reducing the size of the interconnecting power and heat transfer corridors (e.g. cabling).

Significant technical progress has been made leading to smaller lighter warships. The primary areas of emphasis include power electronics, rotating machines, cables, and thermal management systems. It is critical that these be considered together if true high performance at small system size is to be achieved. The advances included design optimization of high speed rotating machines, the thermal, electrical, and mechanical testing of power cables to assure long life at reduced size, the exploration of new models to design storage systems based on the functionality required rather than on limited figures of merit, and in the conceptual design of heat transfer corridors.

Technical Approach

Conduct research in five major areas:

- Power elecronic converters.
- Energy storage.
- Rotating machines.
- Cables.
- Thermal and power corridors.

Progress Statement Summary

Current work reported herein includes:

2.1.1 Develop high power density WBG modular converters
2.1.2 Develop high-frequency magnetic component design methodology
2.1.4 Explore thermal energy storage in ship systems
2.1.5 Performance-based design criteria for storage systems
2.2.1 Develop concepts for shipboard heat-transfer corridors
2.2.2 Design considerations for MVDC cables
2.2.3 Develop requirements for power dense superconducting cables for MVDC systems
2.2.4 Develop integrated thermal and electrical power corridor concepts

The following projects are planned for future work:

2.1.3 Develop emergency power operating characteristics of WBG converters

2.1.1 Develop high power density WBG modular converters

Task: Develop high power density WBG modular converters

Technical Objectives

Research high efficiency and high power density BESS. Currently, Si IGBT is applied to power electronics converters interfacing with battery storage for electric ship application. These Si IGBT has the 'current tailing' problem, which will affect efficiency and lead to slower switching frequency resulting in large-size passive components; thereby the power density is degraded.

WBG technology will allow SiC MOSFETs to be applied to a BESS. SiC MOSFET does not have tailing current issue, switching frequency can be increased to reduce passive component size and weight. The good thermal capability will also benefit power density and reliability further. However, although SiC MOSFET has lower switching loss due to fast switching speed, fast switching speed will result in more serious EMI issues. This task focused on researching a novel converter that can take advantage of WBG devices without degrading EMI. In addition, this new BESS is preferred to achieve fault ride-through capability, which will benefit a breakerless MVDC system operation.

Technical Approach

- Develop a soft-switching current-fed isolated DC/DC converter for BESS application that can achieve higher switching frequency and a smaller dv/dt.
- Develop the dynamic models for proposed BESS under normal conditions and fault conditions.
- Develop the corresponding control systems under both normal and fault conditions to achieve fault ride-through capability.
- Verify the proposed technology using simulation results and a downscaled testbed using Si MOSFETs.

Progress Statement Summary

Previous ESRDC research on BESS converters is focused on the multi-function implementations and fault ride-through capability [51,52]. The current ESRDC progress including developing a topology that can achieve soft-switching capability and use MOSFET device interfacing with battery storage.

The proposed topology is shown in Figure 16, which can achieve soft-switching capability. Figure 17 illustrates the zero-voltage switching (ZVS) boundaries for all the switches. At battery side low voltage side (LVS), the ZVS boundary of upper switches under different d, which are symmetric to the point $(D, \phi) = (0.5, 0)$. A larger d will extend the ZVS area, and when $d > 1$, ZVS can be always achieved for LVS arm. For HVS arms, the arm current comprises both the ac and dc currents, making the ZVS conditions more complicated. The ZVS boundaries of S_m and S_a are also symmetrical with respect to $\phi = 0$, the ZVS boundaries for S_m under different d and m are plotted in Figure 17, where m is the ratio of dc inductance and ac inductance, i.e., $m = L_{dc}/L_s$. The ZVS area will be extended with a smaller d; when $d < 1$, ZVS can be always maintained for $D < 0.5$. However, $d < 1$ will reduce the ZVS area of LVS arm. Therefore, $d = 1$ is preferred. The ZVS area will also increase when m decreases. Nevertheless, the smaller dc inductance may result in larger dc current ripple. Fortunately, the dc current ripple will not increase much for small dc inductor in MVDC application where D is around 0.5. $d = 1$ and $D_h, D_l < 0.5$ will ensure ZVS for switches of both side arms.

The proposed converter can be considered as a boost converter cascaded with a dual-active-bridge (DAB) converter. The corresponding averaged circuit model for dc grid integration is developed in Figure 18, where the boost converter with equivalent capacitance and dc inductance features the current-fed port, and the idab determined by power equations represents the output current of DAB stage. To verify the developed averaged circuit model, both the circuit-based model and averaged circuit model are simulated in $MATLAB$/Simulink for a 3 kW converter. The step response results of the two models are compared in Figure 19. The averaged model matches very well with the circuit-based model, demonstrating the validity of the derived model. Based on the developed averaged circuit model, the small-signal state-space equations can be derived.

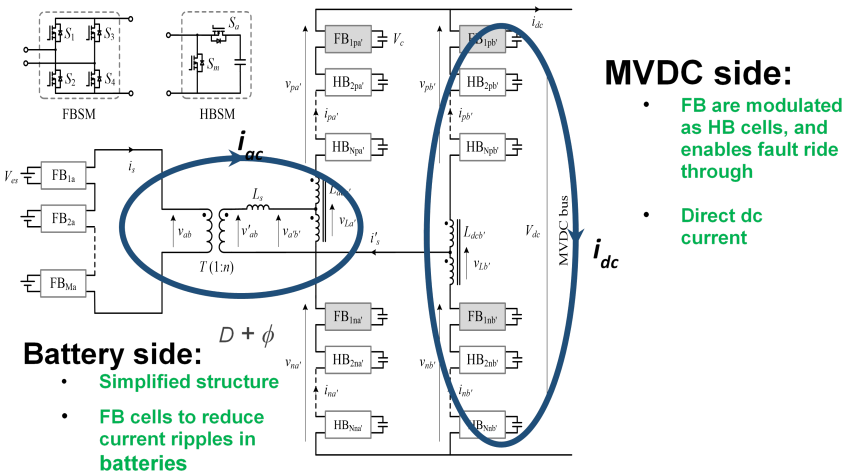

Figure 16: Proposed CF-MDAB BESS converter.

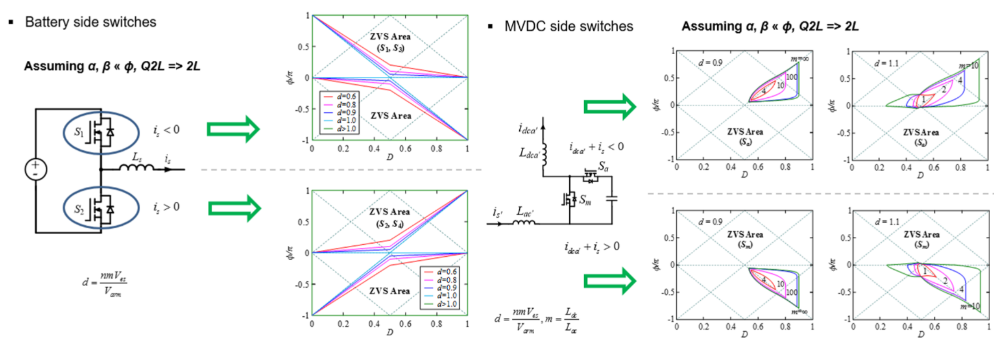

Figure 17: Soft-switching conditions derived for all switches.

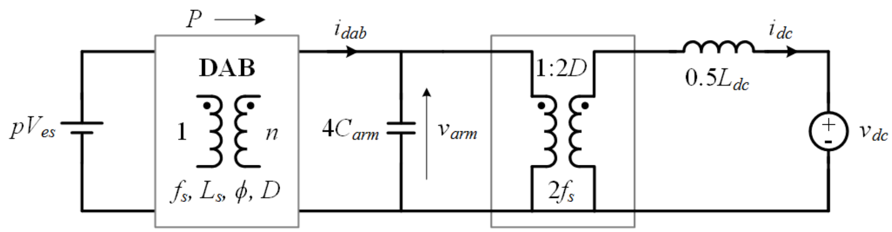

Figure 18: Averaged circuit model of CF-MDAB BESS converter.

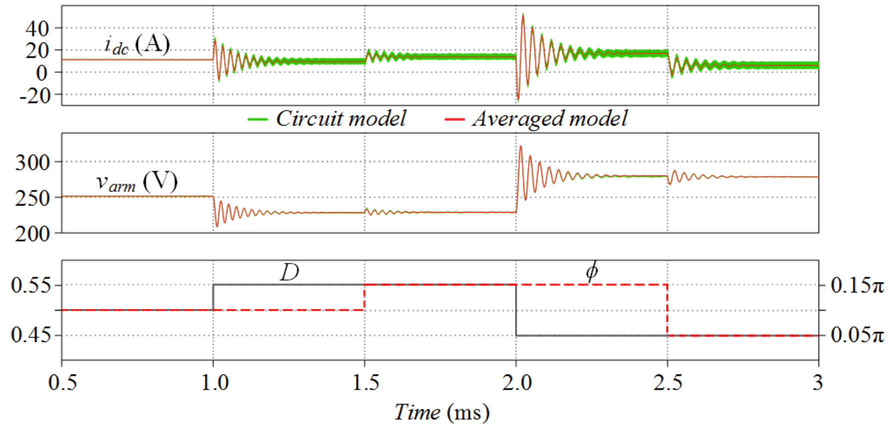

Figure 19: Simulation waveforms of CF-MDAB dynamics.

Task: PEBB 1000 based power conversion system design and demonstration

Technical Objectives

The 100 kW SiC-based Power Electronics Building Block — PEBB 1000 [53] enables high scalability and modularity allowing numerous power conversion topologies to be implemented by series and parallel connection of PEBBs. Practically any required current and voltage level (consequently power level) of power converters comprising numerous PEBBs can be achieved. SiC-PEBBs 1000 truly enable, for the first time, the notion of a high power density PEBB-only integrated power systems for future Navy ships, benefitting from system and commercial advantages featured by the PEBB modular concept, and from the exceptional power processing capabilities offered by SiC semiconductors.

The PEBB 1000 version 1.0 prototype had been designed, built, and tested in CPES labs under ONR project award N000141410408 that was completed in the third quarter of 2016. Research effort under this ESRDC will be focused on hardware and software improvements of the PEBB 1000 v1.0 in order to achieve a successful demonstration of a modular multi-PEBB power converter. Redesign, construction and testing of improved PEBB 1000 prototype (version 2.0) will be accomplished, followed by construction of several PEBB units.

In this task, the construction of multiple PEBB 1000 units is proposed to demonstrate the operation of a modular power converter (multi-function capability) and power conversion system (two to three converters), which will have as fundamental challenges:

1. The very design and operation of a high power density SiC-PEBB based modular power converter, as well as that of a PEBB-based power conversion system;

2. The harsh dv/dt environment resultant from the use of SiC devices;
3. The thermal management system of the PEBB;
4. The shaping and containment of electric and magnetic fields within the PEBB structure;
5. The EMI containment and filtering strategy;
6. The PEBB control system.

Technical Approach

One of the important technical objectives towards the achievement of high-density PEBB-based converters is a volume reduction of passive components that comprise each PEBB, and consequently PEBB-based converter. This particular task proposes switching-cycle control (SCC) to modulate the converter arm current to switching frequency, and thus balance the capacitor voltage every switching cycle [54]. The polarity change of the arm current every switching cycle also enables zero-voltage switching (ZVS) behavior of all the SiC MOSFETs, which nearly eliminate the turn-on losses.

Using SCC described above, capacitor voltages in each converter cell are balanced every switching cycle. The polarity change of the arm current every switching cycle enables zero-voltage switching (ZVS) behavior of all SiC MOSFETs, which nearly eliminate the turn-on losses. In order to realize closed-loop SCC, the hybrid-current-mode switching cycle control (HCM-SCC) has been proposed that directly regulates the load current and capacitor voltages. The HCM-SCC relies on high-amplitude, high-bandwidth, and high-accuracy switch current sensors. This is realized by a proposed embedded Rogowski switch-current sensor (RSCS) developed by CPES for SiC MOSFET modules [53]. In addition to the current monitoring and control, the RSCS can also be used for a short-circuit protection of SiC MOSFETs. This control method was verified experimentally using PEBB 1000 prototypes.

Particularly important task related to PEBB-based power electronic converter operation is the development of hierarchical control structure featuring a decentralized control [55] where each PEBB 1000 comprises its own digital controller (local controller), while high-level controller oversees the operation of the whole PEBB-based converter. Achieving proper synchronization between these controllers is one of the key research points allowing for ultra-high scalability of more than 1000 PEBB nodes per converter [56–60]. A new distributed control and communication architecture is proposed for communication system between central and PEBB controllers [55, 61, 62], and one of the important requirements for modular converter system is precise synchronization [56] for gating signals in all PEBBs. Another requirement is communication topology, which determines the propagation latency performance and limits the maximum operating switching frequency.

Progress Statement Summary

The single-module-per-arm Multi-Modular Converter (MMC) is shown in Figure 20, where module model in the dashed blue box is simplified into three elements, a capacitor represents the DC-link capacitor bank C, an SPDT switch $S_U(S_L)$ that reflects the half-bridge configuration, and a lumped inductor L represents the total differential-mode and cable inductance. The upper module and the lower module are connected jointly at 'PH' to form an MMC phase leg. 'PH' is then connected to a large phase inductor L_O, a voltage source v_s, and then the middle point of the DC source voltage 'm'. This is a very basic single-phase MMC topology with only one module on the MMC arm.

To decouple the capacitor voltages from the fundamental frequency and its harmonics, the extreme approach is to balance them at one switching period, named switching-cycle control (SCC) [54]. In order to resolve these issues, a new control approach named switching-cycle control (SCC) has been proposed. The concept is to take a full advantage of the State III and IV from Figure 20, that has been neglected in conventional control methods. The operation waveform is shown in the same figure where small total arm inductance is needed for fast control of iMEAN. Between State I and State II, State IV is inserted, when $-V_{DC}/(2L)$ leads to a quick drop of the i_{MEAN}. i_U and i_L also drop accordingly until i_L reaches a negative peak value. The negative part of i_L discharges v_{CL_AC} to the initial value at the beginning of the switching period.

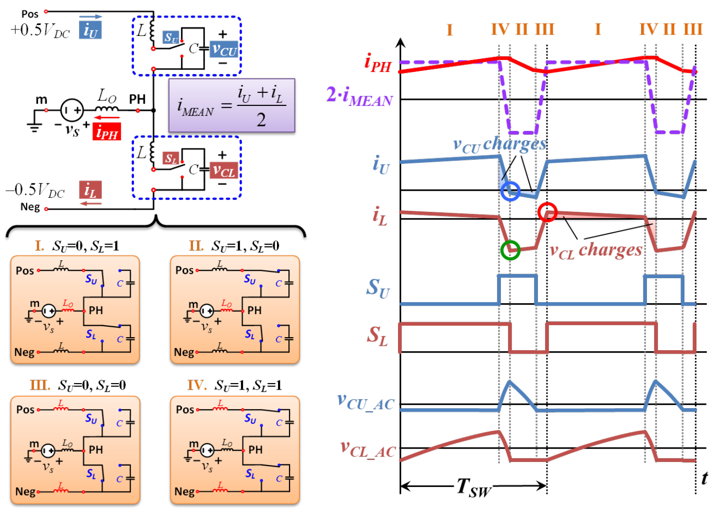

Figure 20: Fundamentals of single-PEBB MMC, by switching-cycle control.

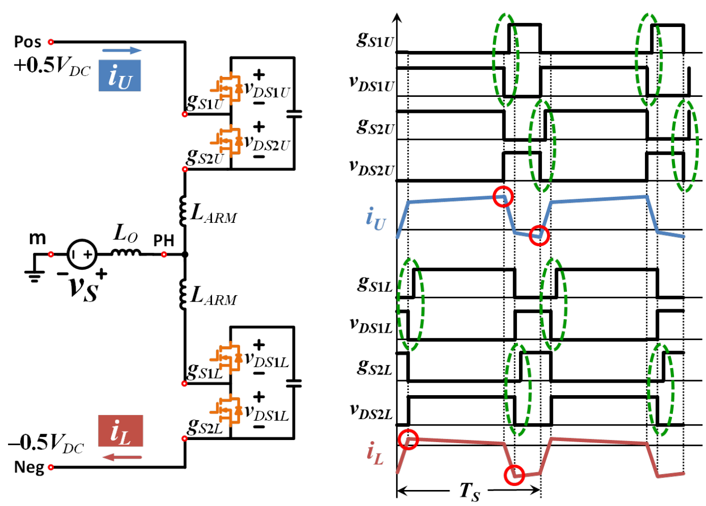

Figure 21: ZVS turn-on of all the four SiC MOSFETs in SCC.

On the other hand, v_{CU_AC} is charged by i_U during State IV where i_U is positive, and then discharged to the initial value by i_U during State II where i_U is negative. Finally, at State III the i_{MEAN} rises quickly by the effect of $V_{DC}/(2L)$, and i_U and i_L are reset back to the initial value. The phase current i_{PH} is still controlled to make sure its switching-cycle average value follows the load demand, despite that a small portion of the effective control time has been taken by State and IV and III.

As the polarity of the arm currents i_U and i_L are changing every switching cycle, zero-voltage switching (ZVS) turn-on of every SiC MOSFET is realized. Figure 21 shows the single-phase MMC with upper MOSFET S_{1U} and S_{2U}, and lower MOSFET S_{1L} and S_{2L}. Their drain-source voltage V_{DS1U}, V_{DS2U},

V_{DS1L}, and V_{DS2L} have been discharged to zero by the two arm currents before the rising edge of their gate command g_{S1U}, g_{S1U}, g_{S1L} and g_{S1L}. Therefore, zero turn-on losses are expected, which is very desirable for SiC MOSFETs.

Proposed control method The SCC offers an impressive cut of passive components in the MMC cell, reducing capacitors by 93%, inductors by 97%, and eliminating the turn-on loss offering semiconductor loss reduction by additional 10%.

Based on the SCC behaviors, when the rising and falling edge of S_U is pre-set, it is common to use the turning points encircled in green and red in Figure 22 to determine the falling and rising edge of S_L, respectively. Furthermore, the duty cycle of S_U controls the switching-cycle average value of phase current i_{PH}. Longer 'low' time of S_U increases the average i_{PH}, and longer 'high' time decrease the average i_{PH}. Accordingly, the block diagram of a closed-loop SCC realization is proposed in Figure 22. Two controller units are applied for the upper and lower module, respectively.

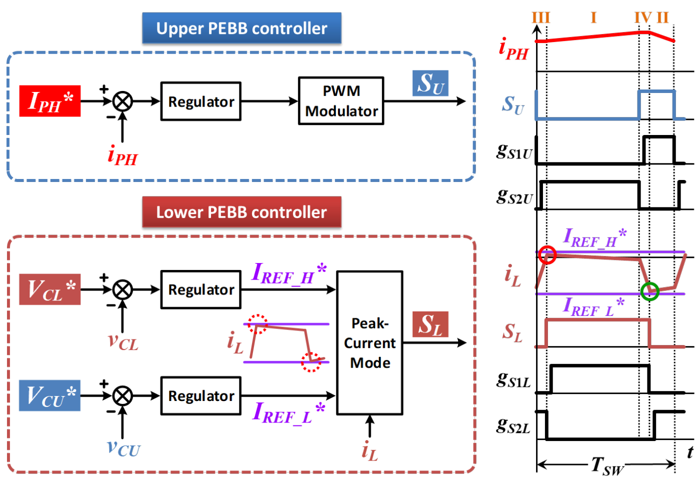

Figure 22: Control block diagram of the closed-loop HCM-SCC.

The upper module is responsible for regulating the average phase current. The phase current error $I^\star_{PH} - i_{PH}$ signal is fed to a regulator that generates a modulation reference. The reference is given to a pulse-width modulator that generates S_U. After a logic inverter and dead-time generators, the gate signals g_{S1U} and g_{S2U} are generated and sent to the half-bridge gate driver board. This mechanism is the conventional average-current-mode (ACM) control.

The lower module is responsible for regulating the upper and lower average capacitor voltages. The average voltage error $V^\star_{CL} - v_{CL}$ of the lower capacitor at the outer loop is fed to a regulator that generates a high reference current $I^\star_{REF\_}$ for the inner loop. The average voltage error $V^\star_{CU} - v_{CU}$ of the upper capacitor at the outer loop is fed to a regulator that generates a low reference current $I^\star_{REF\_L}$ for the inner loop. The two current boundaries define a band area that limits the lower arm current i_L. As soon as i_L touches $I^\star_{REF\_H}$, S_L generates a rising edge to transit the switching states from III to I with a turning point, which is realized by giving g_{S2L} a 'turn-off' command. As soon as i_L touches $I^\star_{REF\_L}$, S_L generates a falling edge to transit the switching states from IV to II with a turning point, which is realized by giving g_{S1L} a 'turn-off' command. The rising edges g_{S1L} and g_{S2L} are produced by dead-time generators. This 'compare and turn-off' mechanism of the inner current loop is conventionally named peak-current-mode (PCM) control.

As this closed-loop SCC realization combines the conventional ACM and PCM controls for the upper and lower arms, respectively, it is named hybrid-current-mode switching-cycle control (HCM-SCC). Three strong correlations build the foundation of HCM-SCC. First, the average phase current i_{PH} has a strong negative correlation with the upper duty cycle d_U (average value of S_U). Second, the average lower capacitor voltage v_{CL} has a strong positive correlation with the high reference current $I^\star_{REF\_H}$. The third one is that average voltage v_{CU} of the upper capacitor has a strong positive correlation with the low reference current $I^{\star}_{REF\_L}$. However, some weak coupling between the two voltage loops may have potential influence on the control performance.

The biggest challenge in the HCM-SCC is the accurate high-BW sensing of the high-amplitude lower arm current i_L. The amplitude of i_L can be very high, and contains components of DC, fundamental frequency, switching frequency, and other higher frequencies. Commercially available sensors (e.g. the high-power coaxial shunt resistor) have a large size, weight, and high cost, so the embedded Rogowski current sensors here present obvious available resource. The sensed two switch-current signals $-i_{S1L}$ and i_{S2L} are directly given back to the PEBB controller. Figure 23 shows hardware implementation/structure for HCM-SCC. The Rogowski coil board was assembled on top of the SiC MOSFET module. Signals are transmitted to the signal processing board via two coaxial cables. The signal processing board is directly plugged into the analog sockets on the PEBB control board. A precharge switch and a resistor are mounted on the positive DC bus. Figure 23 shows the test waveforms obtained in the given setup. It can be noticed that capacitor voltages v_{CU} and v_{CL} are controlled steadily at 500 V, with excellent balancing at every switching cycle without drifting. The switching-frequency ripple is minimal, with only 40 V peak-to-peak parasitic ringing observed at around 5 MHz due to the ESL and bus-bar inductance of the series DC-link capacitors. The phase current i_{PH} has about 8 A switching frequency ripple, and four switching states on it are observed. The two arm currents i_U and i_L and mean current i_{MEAN} are operating at the SCC mode, whose dominant frequency component is at 40 kHz.

The bottom waveforms in Figure 23 show switch currents i_{S1L} and i_{S2L} from the RSCS. These two are added to produce i_{L_SEN}.

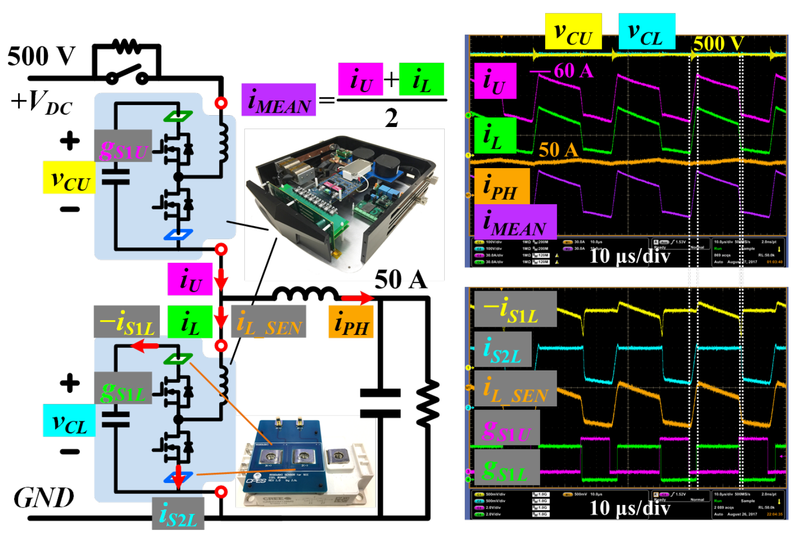

Figure 23: Experimental results of HCM-SCC.

Figure 24 shows the ZVS turn-on behavior of all the four switches. The signal signals g_{S1U}, g_{S2U}, g_{S1L} and g_{S2L} are the gate commands sent from the main controller FPGA, rather than the real gate terminals on the gate driver board. There is about 200 ns total delays between the FPGA commands and the gate-source voltages. Therefore, all the actual gate-source voltages are fired after the drain-source voltage V_{DS1U}, V_{DS2U}, V_{DS1L} and V_{DS2L} are discharged by the arm currents. No device turn-on voltage ringing is observed in the waveforms.

<u>*Decentralized control*</u>

Figure 25 illustrates proposed distributed control and communication network. In order to make the interface between modulator and PEBB gate drivers, we distribute the modulator and PEBB sorting algo-

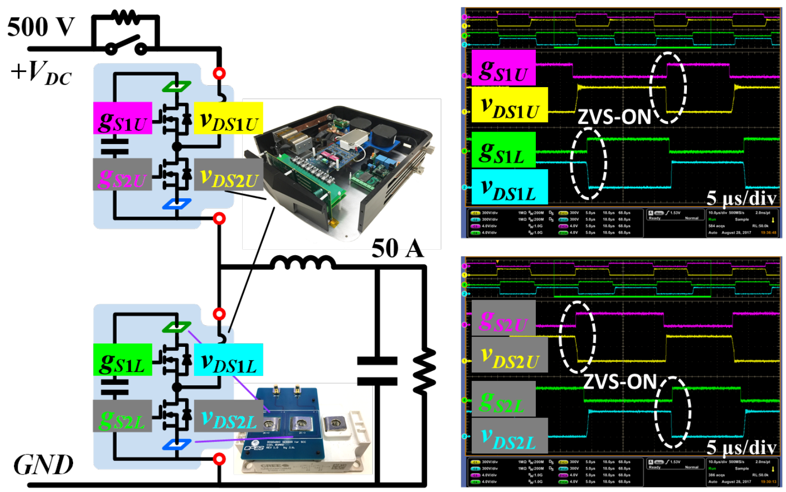

Figure 24: ZVS behavior of HCM-SCC.

rithms to each PEBB (PEBB controller). This way, there are only 2 (for half-bridge) or 4 (for full-bridge) interface IOs between PEBB controller and PEBB gate drivers. In order to make the interface between central controller and PEBB controller modular, we make all the controllers two interface IOs and use TDM (Time Division Multiplexing) communication to transmit the information of the PWM references, sensing voltages and currents, etc. With a good communication network, we can distribute control algorithms as desired, as long as all the necessary information can be correctly transmitted. For example, we can distribute central control algorithm to each PEBB, and hence increase redundancy and reliability of the control system.

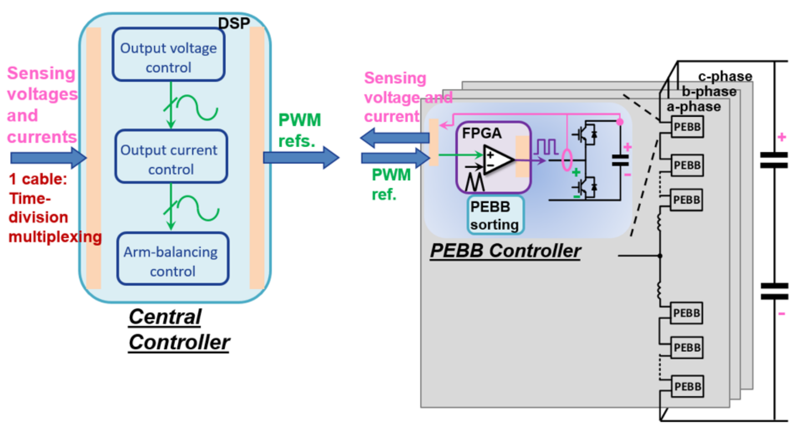

Figure 25: Fully distributed control and communication network.

Synchronization realization between one master and two slaves controllers is achieved with the synchronization accuracy of ±5 ns, as well as synchronization with 5 times oversampling based clock and data recovery, expected to significantly save communication bandwidth. Simple structure in Figure 26 illustrates this.

Considering synchronization specifications, the synchronization methods are the syntonization based on CDR (Clock and Data Recovery) to get a constant offset between two nodes and the synchronization based on PTP (Precision Time Protocol) to compensate the constant offset.

Preliminary synchronization specifications are:

- The switching frequency is 1-100 kHz.
- The communication frequency is the same as switching frequency.
- The offset compensation frequency is several times per second.
- The synchronization accuracy is ± 5 ns jitter per node.
- The node forward delay is 1 word (8 bits) per node.

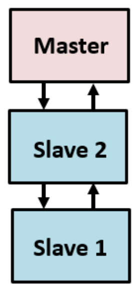

Figure 26: A simple distributed communication network — two PEBBs and a master controller

For each node in the communication system, there is a receiver at the input and a transmitter at the output. The receiver shown in Figure 27 contains four blocks, clock and data recovery & NRZI (NRZI Non-Return to Zero, Inverted) decoder block, bit to byte block, 4B/5B decoder block and byte to packet block. The transmitter shown in Figure 28 contains three blocks, packet to byte block, 4B/5B encoder block and byte to bit & NRZI encoder block.

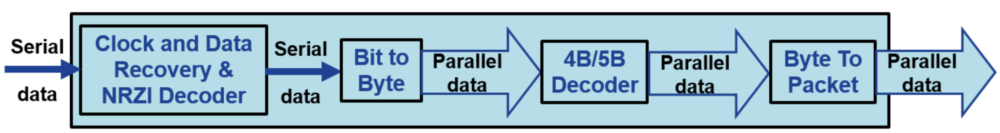

Figure 27: Receiver block.

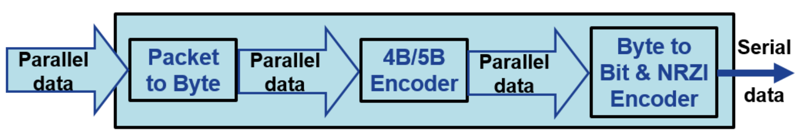

Figure 28: Transmitter block.

For clock and data recovery block, the oversampling method is used to make the offset between nodes constant. The frequency of local clock is five times the frequency of input data. Each bit of input data is sampled five times. The clock and data recovery block adjusts the local time counter base on the input data transition. For 4B/5B encoding, the input is a 4-bit character and the output is a 5-bit character based on a data encoding and a command encoding table. This 4B/5B encoding method is used to guarantee enough '1' of the serial data and a command table for the command transmission.

For NRZI encoding, the input and output are both serial data. The input '1' is represent by a transition of the physical level at the output, and the input '0' is represent by no transition of the physical level at the output. This NRZI encoding method is used to guarantee enough data edges for CDR to detect.

The clock and data recovery block makes the offset between two nodes constant, then the next step is to compensate the offset and realize the final synchronization based on PTP method. The synchronization principle is shown in Figure 29.

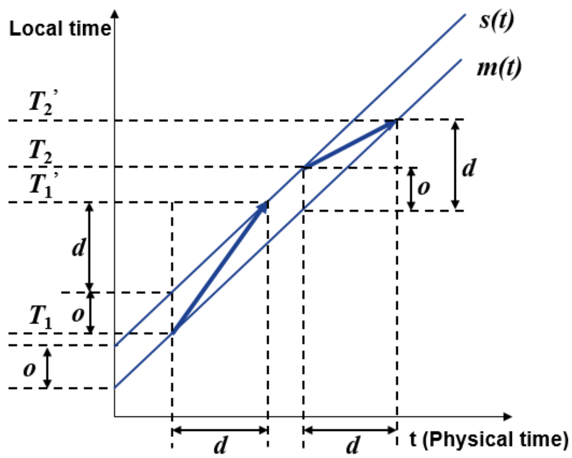

Figure 29: Synchronization based on PTP.

In summary, in order to get a good synchronization performance among all the controllers, a new synchronization method is proposed combining the syntonization based on CDR (Clock and Data Recovery) to get a constant offset between two nodes and the synchronization based on PTP (Precision Time Protocol) to compensate the constant offset.

An experiment with three FPGA boards (Altera MAX 10 10M08SAE144C8G), one as a master and the other two as slaves (as shown in Figure 30), is done to verify the synchronization design.

The PWM output of master, slave 2 and slave 1 are shown as channel 1, channel 2 and channel 3 respectively on Figure 30 below illustrating good synchronization among three FPGAs. Zooming in, the jitter of slave 2 shown in right figure is 4.9 ns (less than ±5 ns - period of the local clock).

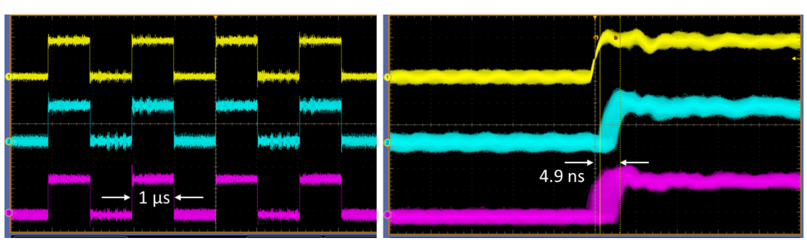

Figure 30: (left) PWM test with CDR and PTP synchronization, and (right) clock jitter measurement (slave 2).

2.1.2 Develop high-frequency magnetic component design methodology

Task: Advanced passives for WBG converters

Technical Objectives

Design MMCs using WBG semiconductor switches. Wide bandgap (WBG) semiconductor switches are being widely considered for medium- to high-voltage DC applications, which allow higher switching frequency operation with lower switching losses compared to existing switch topologies. In particular, for considered applications, Modular Multilevel Converters offer an excellent approach due to their inherent modularity, scalability, and highly efficient performance [63]. Designing such converters through multi-objective optimization is of interest, because such an approach allows the trade-off between competing objectives (for example, mass and loss) to be explicitly and quantitatively identified.

In this work, designing and sizing of MVDC power electronic converter is studied. Specifically, MMCs with WBG devices and advanced materials for passive design are considered, and their effect on system sizing vs loss trade-offs of the system is studied. Of particular interest in this effort will be the use of advanced passives in the design of the MMC, such as the use of coupled symmetrical three phase inductors or permanent magnet inductors in the MMC legs.

Technical Approach

- Develop computationally efficient high-speed simulation model of the MMC.
- Develop mass and loss models of the active and passive components.
- Develop a multi-objective optimization problem for system design.
- Develop sizing model of the system.

Progress Statement Summary

The first step in this effort is the development of a high-speed simulation model for the MMC. This is necessary because the use of multi-objective optimization-based design will require millions of time-domain simulations. An initial version of this model is complete. The considered permanent magnet AC machine MMC system is shown in Figure 31.

A comparison between high-speed simulation and detailed waveform-level simulation model is shown in Figure 32. Parameters used for the simulation are presented in Table 1. For the system considered, the high-speed simulation is almost 2000 times faster than the detailed model. Details are set forth in [64].

Table 1: System parameters.

Permanent Magnet AC Machine		
Rated speed: 3000 rpm	P: 16	$L_a = L_d$: 0.6 mH
Rated Power: 120 kW	λ_m: 0.23	Machine resistance: 20 $m\Omega$
Modular Multilevel Converter		
Number of submodules: 4	DC bus voltage: 2 kV	C_{in}: 2 mF
Switching frequency: 13.6 kHz	Load: 100 kW	L_l: 0.36 mH
Submodule Capacitance: 1.36 mF	L_f: 0.34 mH	

To illustrate the use of high-speed simulation, an optimization study was formulated for the MMC design. This study uses same machine and MMC parameters shown in Table 1, except the leg inductance, submodule capacitance and switching frequency which are kept variable. In this initial study, conventional passives are used. The Pareto-optimal front showing trade-off between mass and loss is shown in Figure 33.

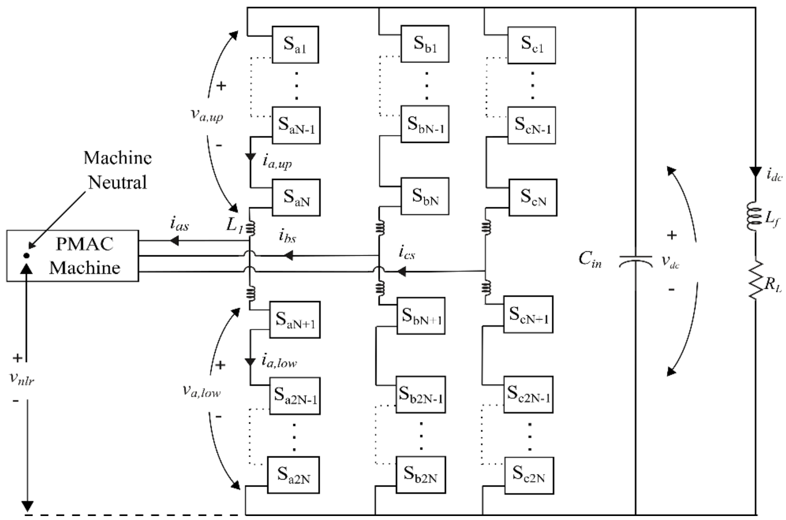

Figure 31: Considered MMC system structure.

Current progress includes development of accurate loss models of the system and inclusion of newly developed symmetrical three-phase inductor.

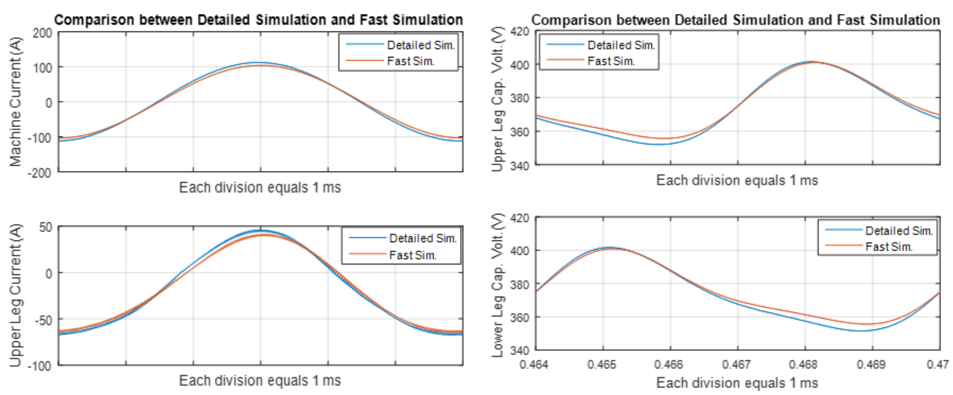

Figure 32: Comparison between high-speed simulation and detailed waveform-level simulation.

The development of a high-simulation model of an MMC based generator rectifier system has been completed and has been published in [64]. The objective of the high-speed simulation is to rapidly calculate steady-state waveforms. These steady-state waveforms will be used for calculation of mass and loss, and impose system constraints on the optimization design.

In order to illustrate the simulation consider a permanent magnet AC machine generation with an MMC active rectifier shown in Figure 31 and with parameters listed in Table 1. A comparison between high-speed simulation and detailed waveform level simulation is shown in Figure 32. The high-speed simulation is approximately 577 times faster than the detailed simulation model. Details of the work are set forth in [64].

Based on the high-speed simulation, the MMC design process has been formulated as an optimization problem. In the optimization study, leg inductance, submodule capacitance, the number of submodules, and the switching frequency are picked using a multi-objective optimization which minimizes converter loss and mass. Converter loss includes conduction and switching losses in submodules, and resistive losses in leg

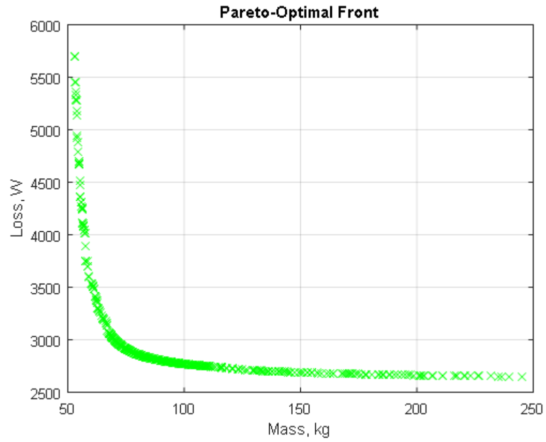

Figure 33: Loss vs. mass Pareto-front of the MMC design.

inductor. Work on switching loss calculation in submodules is in progress, however, an estimated value is calculated in the current optimization problem. Eddy current or hysteresis losses in inductor have not been included.

Converter mass includes mass of the inductor and capacitors which are calculated using a metamodel. Constraints imposed on the system design optimization are: (1) the analysis converges, (2) the DC power requirement is satisfied, (3) the capacitor voltage ripple is within specified limits, (4) the system never operates over-modulated region, (5) the maximum limit on pk-pk leg current amplitude is satisfied, (6) the maximum limit on inductor current density is satisfied, (7) the life expectancy of the submodule capacitor is higher than specified, and (8) the worst case DC fault current is under specified limits.

To demonstrate the design optimization, a 100 kW 4 kV MVDC system is optimized with the same machine parameters as in Table 1 except P = 16, rated speed = 1250 rpm, and rated power = 100 kW. The parameter distribution is shown in Figure 34. Based on the system designer's requirement, a design can be picked.

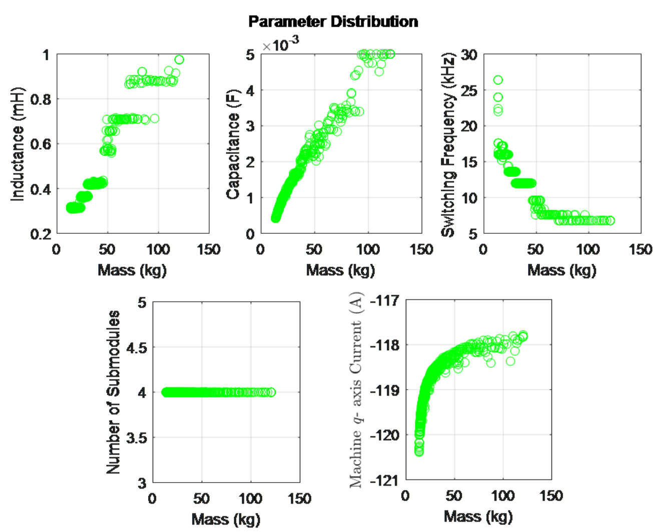

Figure 34: Parameter distributions.

Presently, inclusion of detailed inductor loss models and newly developed symmetrical three-phase inductor as part of the MMC is being considered. To incorporate variations in machine sizing, a newly developed machine metamodel is also considered to be added in the formulation of the optimization problem. Inclusion of thermal models will be undertaken to accurately impose constraints on thermal design of the system. Additional improvements considered in the design optimization include using improved capacitor models to include frequency effects, improved semiconductor loss models, and the consideration of multiple operating points for the system design.

Task: High-speed machines

Technical Objectives

The objective of this task is to develop an optimization-based design process for high-speed electric machines. High-speed electric machines significantly contribute to improved power density, and in specific applications may increases the overall system efficiency. However, the design of such machines is challenging, with regard to mechanical stresses, thermal management, and high-frequency loss mechanisms [65, 66]. This task will address these issues. However, effort thus far has focused on the first of these issues, in which an alternative analytical formulation has been derived for the structural analysis of high-speed rotor. Specifically, this work aims to incorporate the structural analysis of high-speed surface-mounted permanent magnet machines (HS-SMPM) into an optimization-based design process. Consequently, computational efficiency and accuracy are priorities. Due to the high rotor speeds, the permanent magnets are subject to critical centrifugal forces, which are typically contained by nonmagnetic sleeves made of carbon fiber, glass fiber, or titanium alloys. Figure 35 depicts a typical configuration of a HS-SMPM rotor.

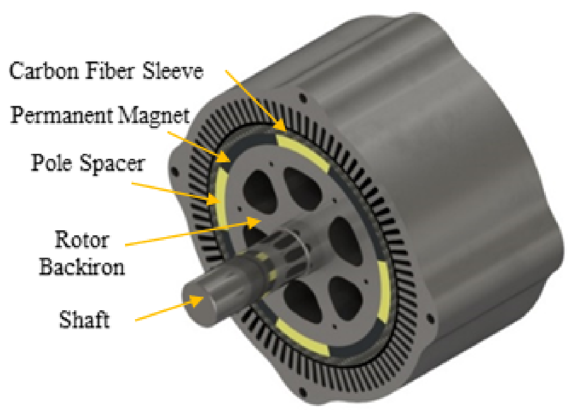

Figure 35: Typical configuration of HS-SMPM.

Previous published work does not consider design geometries with gaps between one rotor pole and the next, making the entire circumference between the rotor backiron and the retention sleeve covered by the magnets [67–69]. This restriction simplifies the analysis, but it compromises the minimization of mass and cost during the machine optimization. The model introduced by this task allows the estimation of stresses (radial, tangential, axial, and Von-Mises) and deformation in retention sleeves when pole gaps exist in the rotor. The results were validated through finite element analysis.

Technical Approach

- Compute stresses and deformation on the retention sleeve created by the centrifugal forces of the permanent magnets, considering orthotropic materials such as carbon fiber.

- Include the body forces in the solution of radial stress differential equation.
- Predict the stresses and deformations across the rotor resulting from the press fit during assembly, and from thermal expansion during operation.
- Develop an electromagnetic model for high frequency losses in the windings, permanent magnets, retention sleeve, and stator and rotor core.
- Develop a thermal model for the additional heat sources from high frequency losses, and account for the deteriorated convection due to the retention sleeve.

Progress Statement Summary

The proposed model has been able to accurately predict the stresses and deformation in the retention sleeve, considering the centrifugal force produced by the permanent magnets, body forces, and press fit. The results were validated with a commercial software based on Finite Element Analysis (FEA), and are depicted in Figure 36 and Figure 37.

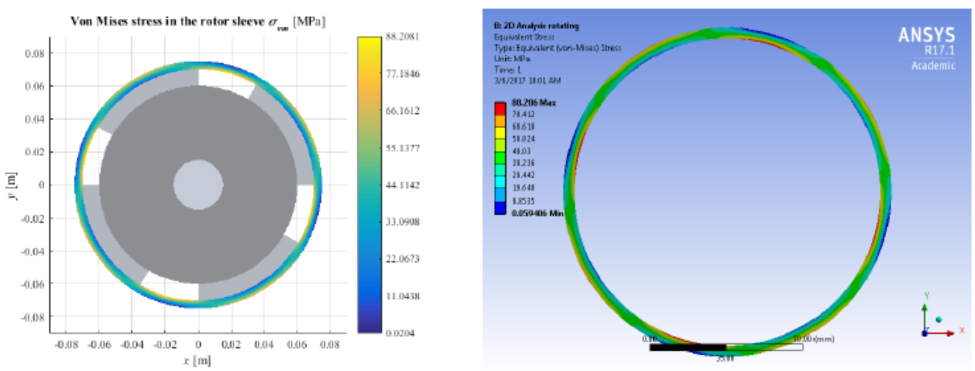

(a) (b)

Figure 36: Von-Mises (equivalent) stress (used as failure criteria): (a) results from the proposed model; (b) results from FEA used for validation of the proposed model.

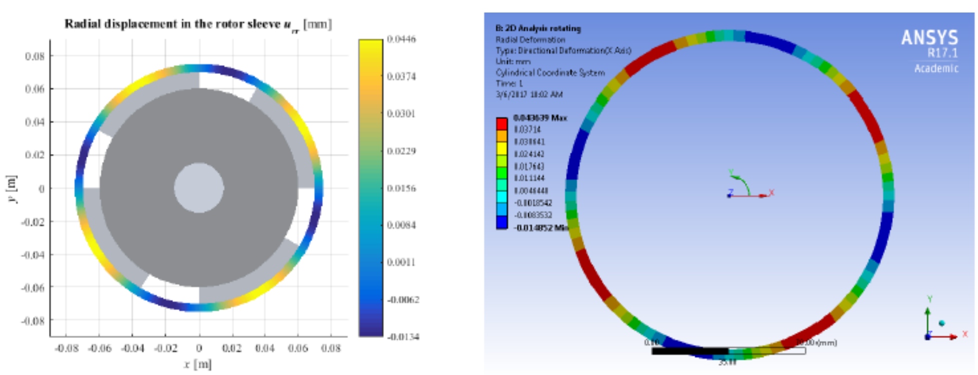

(a) (b)

Figure 37: Radial displacement: (a) results from the proposed model; (b) results from FEA used for validation of the proposed model.

As discussed previously, a model to predict the retention sleeve stresses from centrifugal forces and body forces had been developed and produced excellent results. Recent work undertook thermoelastic stresses modeling, the third point discussed in the Task: High-speed machines Technical Approach. Using unidirectional carbon fiber reinforced material is highly advantageous from the strength, weight, and electromagnetic loss perspectives. However, such composite material sleeve typically has a small or even negative coefficient of expansion in the fiber's direction, squeezing the rotor while the steel expands. This configuration results in significant stresses for certain geometries.

The retention sleeve is mounted around interleaved surface mounted magnets and poles spacers. This means that the interference fit has multiple interfaces among parts of dissimilar materials. The resulting stress fields in the rotor of a given geometry are shown in Figure 38 below.

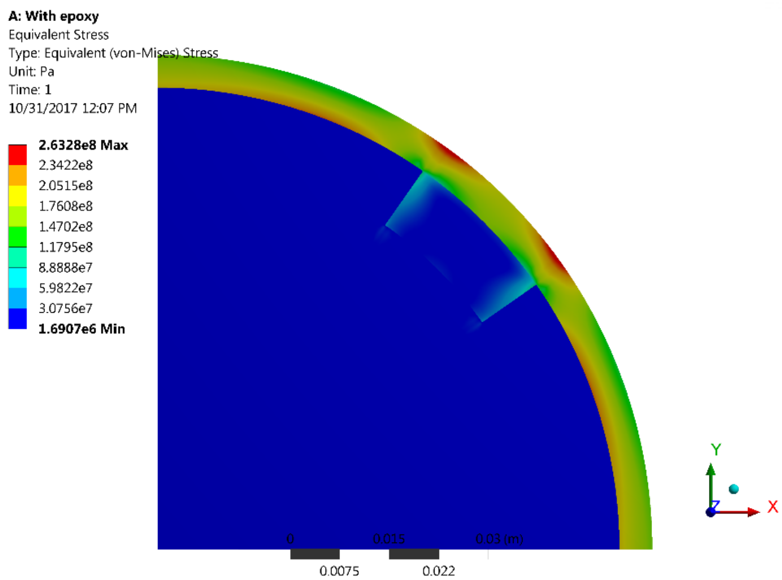

Figure 38: FEA results for Von-Mises stress fields across the rotor of a SMPM for 1 pole.

Recent developments from this task resulted in a fast-analytical model. The proposed model was tested against a Finite Element Analysis based model. This model was validated in the search space of an optimization problem to ensure that the error is bounded across the search space. Figure 39 illustrates the error for maximum Von-Mises stress between the proposed model and FEA.

As previously stated in the Task: High-speed machines Technical Objectives, the validation of proposed models is accomplished by comparing predictions of stress fields and peak stress values to those obtained from FEA based numerical simulations. The complete structural analysis can be summarized in three main loading conditions: surface forces exerted by the magnets into the inner diameter of the sleeve (first point in the Task: High-speed machines Technical Approach); body forces of the sleeve itself (second point in the Task: High-speed machines Technical Approach); and interference stresses induced by the differential thermal expansion among composite sleeve, magnets and epoxy fillers (third point in the Task: High-speed machines Technical Approach). These three effects are illustrated in Figure 40. Previous work under this effort had achieved good agreement for stress fields associated with the first two points in the Task: High-speed machines Technical Approach. The third point in the Task: High-speed machines Technical Approach, interference fit, requires a more convoluted formulation, since it involves the equalization of the deformation among three different bordering materials.

The previous semi-annual report described the proposal of an approximation that only aimed to predict the peak stress, under a bounded maximum error. Subsequently, the model had to be integrated into a

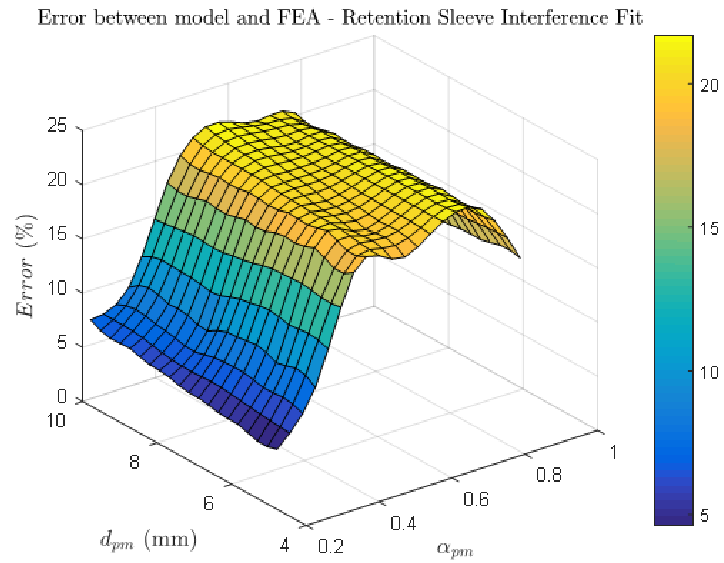

Figure 39: Error between proposed model and FEA for maximum Von-Mises stress, for different values of angular fraction of permanent magnet α_{pm} and depth of permanent magnet.

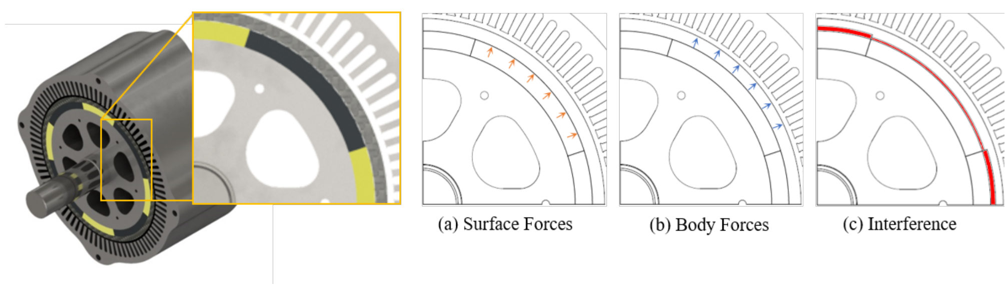

Figure 40: Stress conditions modeled in the structural analysis of the rotor retention sleeve.

machine optimization process. Since composite materials are of interest for the sleeve, Tsai-Wu failure criteria was implemented as the most appropriate to predict failure of the sleeve. This criterion is an empirical model that combines biaxial stresses and the orthotropic nature of the material. Nevertheless, the approximation in the interference model only estimated peak stress, disregarding location and the two orthogonal stress components. Recent work revisited the underlying formulation for the structural analysis of the overall model. Another general solution was proposed to the problem's differential equations, addressing anisotropic materials in non-axisymmetric loading conditions.

The proposed model captures the stress fields observed in FEA for all three stress conditions discussed above. The analytical solution provides all stress components (radial, hoop, shear, and axial if plane strain formulation is selected). In order to illustrate the results obtained, consider the radial stress component as depicted in Figure 41, for each stress condition. Subsequently, all three conditions are combined and verified against the Tsai-Wu failure criteria. Hence, no single condition alone defines if and where the rotor retention sleeve will fail. Furthermore, the interference stress produces a corresponding stress field in the magnet, which is combined to the boundary conditions of the centrifugal forces to determine if the magnets fail under compression. This implies that the machine geometry must be optimized not only to ensure the sleeve's structural integrity, but also the permanent magnet's.

The proposed model can be incorporated to the machine optimization as a structural constraint. However, this approach does not ensure an optimal sleeve thickness. It only guarantees a viable solution. In order to ensure cost minimization, a thickness optimization is proposed. Note that this entails three nested optimizations: (i) find maximum stress $\rightarrow$ (ii) find optimal sleeve thickness $\rightarrow$ (iii) find optimal machine design. Then, the next step is the formulation and implementation of this optimization problem to design a Navy relevant generator.

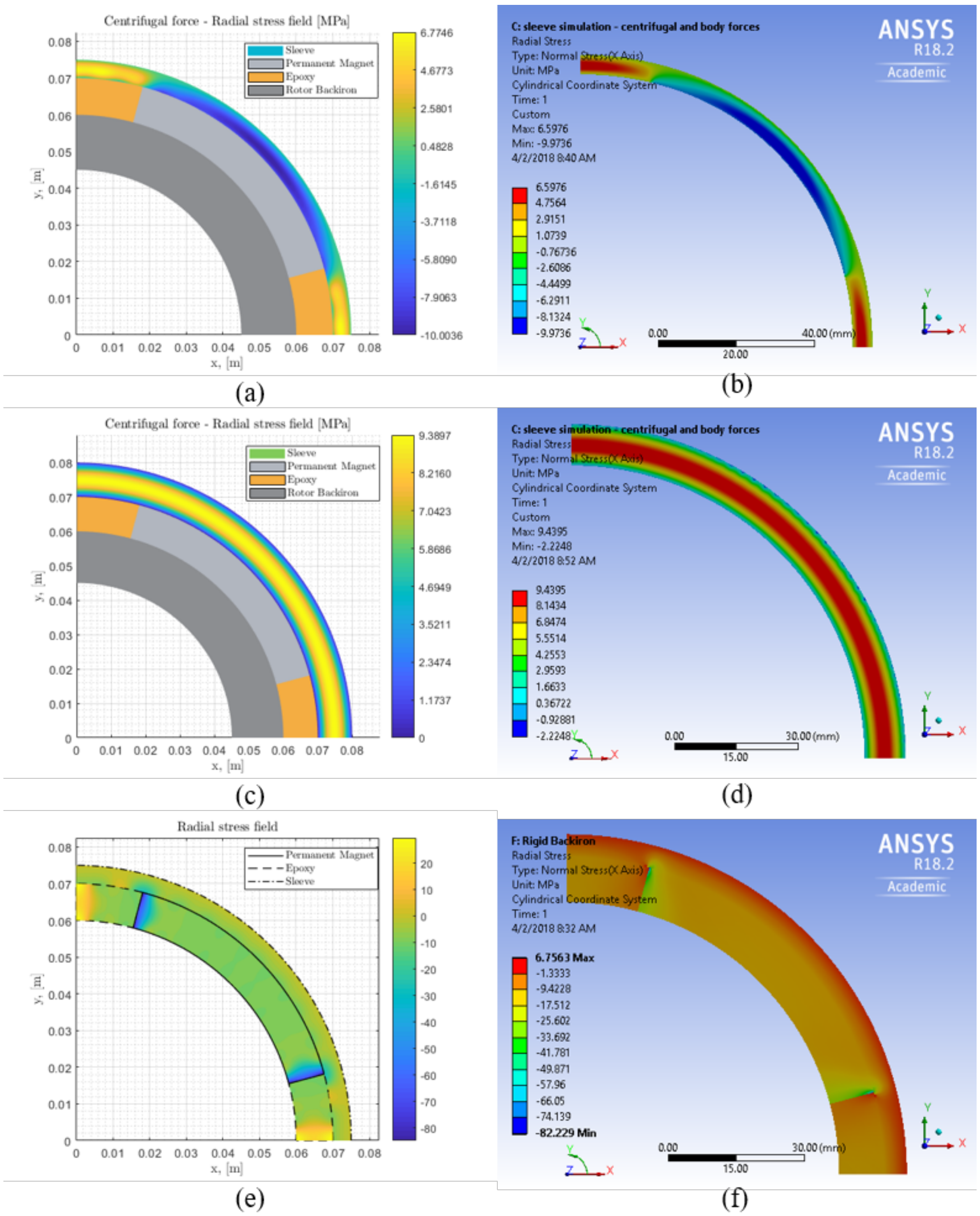

Figure 41: Proposed model validation against FEA based simulation, comparing the radial stress component: (a) analytical model radial stress field for surface forces (magnet pressure); (b) FEA radial stress field for surface forces (magnet pressure); (c) analytical model radial stress field for sleeve body forces; (d) FEA radial stress field for sleeve body forces; (e) analytical model radial stress field induced from interference due to thermal expansion; (f) FEA radial stress field induced from interference due to thermal expansion.

Task: High-frequency transformers for WBG power electronics

Technical Objectives

The technical objective of this task is to develop a high-frequency transformer design model for WBG semiconductor-based isolating power converter. With the advancements in wide-bandgap (WBG) semiconductor devices, there has been an increase in the operating frequency of power converters. Consequently, the reduction in the size of magnetic components is possible enabling increased power density. Although the size reduction in the magnetic components is significant, the high-frequency effects such as skin effect, proximity effect, and parasitic capacitances become very important, increasing the challenge in the design of the magnetic components.

The objective of this task is to develop a high-frequency transformer design model for WBG semiconductor-based isolating power converter. This includes accurately estimating the high-frequency losses and parasitic capacitance in the transformer and incorporating their effect at the design level itself.

Technical Approach

- A multi-objective optimization process is used for the transformer design.
- A variety of analyses such as electric, magnetic and thermal are developed to determine the transformer performance.
- For the purposes of multi-objective design optimization, these analyses are incorporated into a fitness function, which is based on metrics of interest such as mass, loss, as well as the satisfaction of the various geometric and operating constraints.

As this approach involves evaluating thousands of designs for optimization, the analysis methods developed are required to be computationally efficient.

Progress Statement Summary

A prototype high-frequency core-type transformer is built as an application for an isolating DC/DC converter shown in Figure 42.

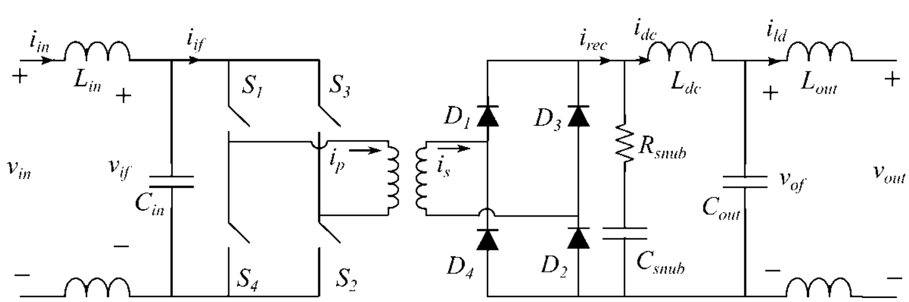

Figure 42: Isolating DC/DC converter.

A computationally efficient and accurate method is used to estimate leakage inductance of the transformer [70]. The estimated leakage inductance is useful in modeling the transformer. The proposed method is validated using 3-dimensional Finite Element Analysis (FEA) and experimental results. The total leakage inductance of the prototype transformer as referred to primary is estimated by the proposed method to be 32.1 μH. This stands in close agreement with the experimentally measured value of 30.7 μH and that estimated by FEA is 28.4 μH.

Time domain modeling of the isolating DC/DC converter is used to estimate the high frequency harmonics of the transformer winding currents, necessary for high-frequency loss estimation. The waveform-level simulation of the DC/DC converter is simplified to reduce the computational time. This is further validated by the laboratory experiments. The comparison of the high-frequency transformer primary current as estimated by the simplified waveform-level simulation to waveform level simulation (WLM) and experimental data is shown in Figure 43.

A method to estimate proximity effect loss in a core-type transformer has been established. It will be validated for the case of prototype high-frequency transformer using a high-frequency power source.

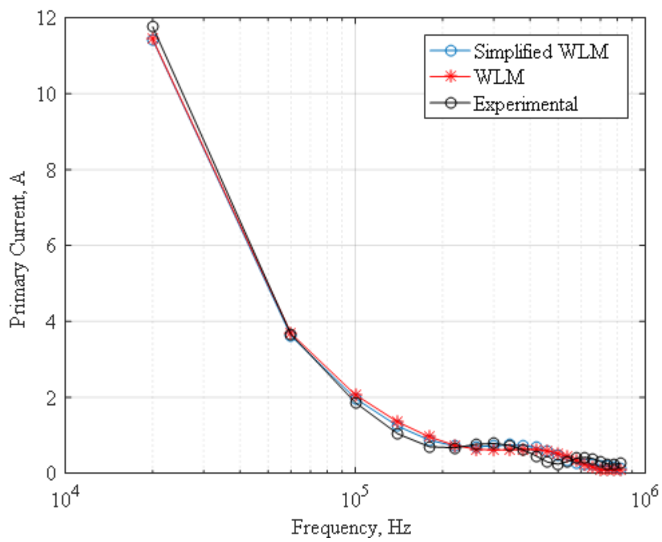

Figure 43: High-frequency harmonics in transformer currents.

During this reporting period, a method to estimate proximity effect loss in a core-type transformer has been established. The proximity effect loss model uses normalized mean squared flux densities in the coil regions [70]. These values are determined using the same transformer magnetic analysis used for leakage inductance estimation. In addition to the proximity effect loss, the transformer loss model includes DC conductor loss, skin effect loss, and core loss. The Modified Steinmetz Equation is used to estimate core loss. Using the proposed approach, the total transformer loss estimated for a test transformer with a 7.5 A, 20 kHz sinusoidal primary current and 10 Ω resistive load on secondary side is 26.6 W. The experimentally measured value is 23.4 W, so the loss prediction was off by 11.8%. The performance of the proposed proximity effect loss model is being further explored using ANSYS Maxwell eddy current analysis.

Effort has also gone into thermal modeling of the transformer. The core-type transformer thermal analysis was performed using a Thermal-equivalent circuit approach. The thermal equivalent circuit of one-eighth of the core-type geometry is shown in Figure 44. Blocks A–D represent the core regions and the winding regions are represented by blocks G–N. The transformer thermal analysis is intended to estimate the temperature rise due to the losses in the core and windings as well as the peak temperature locations while considering the temperature effects on the material properties. This is useful in transformer design process to limit the transformer loss and the resulting temperature rise to a reasonable value.

A multi-objective design optimization of a core-type transformer using computationally efficient magnetic, time domain, and thermal analyses will be set forth in the next reporting period.

During this reporting period, the magnetic analysis used to estimate the transformer leakage inductance has been improved to include frequency dependence. At high frequencies, the time varying magnetic leakage fields generate eddy-currents in the windings that in turn affects the magnetic field distribution. As a result,

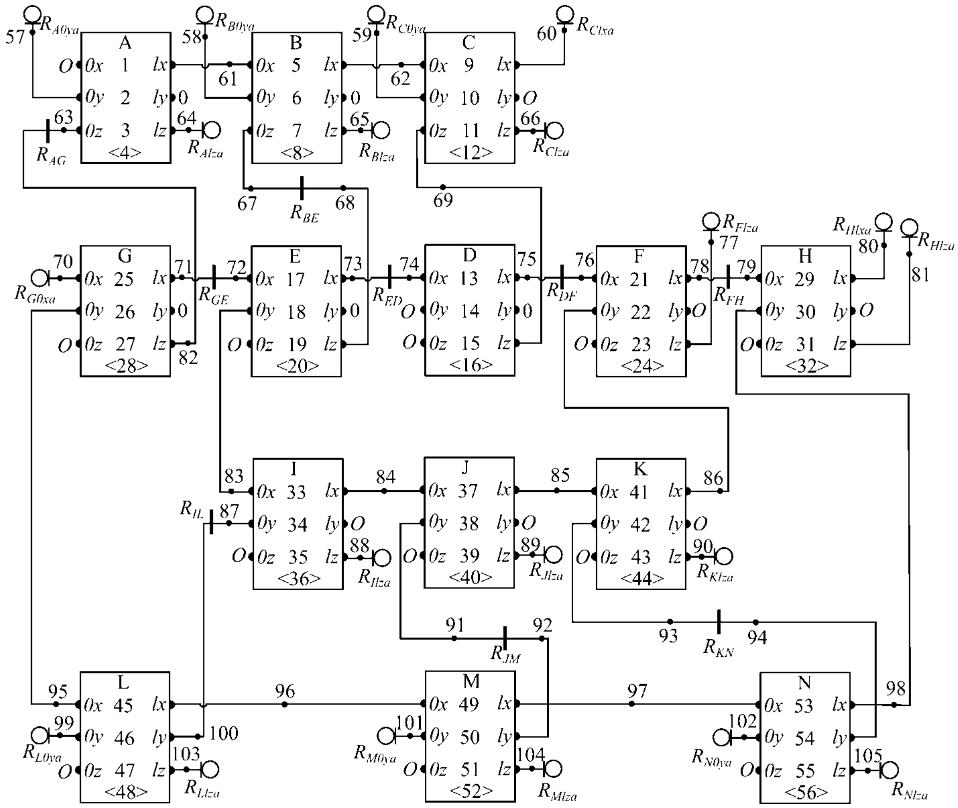

Figure 44: Core-type transformer TEC.

the effective value of transformer leakage inductance is dependent on frequency. The analytically calculated fields using static and harmonic (frequency dependent) analysis are compared to the fields obtained using 2D FEA simulation in case of a prototype high-frequency transformer. The decrease in the magnetic field intensity magnitude within each layer is observed to be pronounced at 20 kHz as shown in Figure 45. The reduction of leakage inductance with frequency is important because the leakage inductance is the main source of impedance in the transformer, and largely governs the resulting current waveforms. It is particularly critical in resonant converters, though a hard-switched converter is considered here.

In addition to the effort to capture the impact of frequency dependent leakage inductance, expressions for the transformer parasitic capacitances have been derived using analytical methods. The effect of transformer parasitic capacitances is analyzed by deriving the high-frequency transformer common-mode (CM) and differential-mode (DM) equivalent circuits.

Finally, a multi-objective design optimization of core-type transformer using the magnetic, time domain, and thermal analyses has been completed during this reporting period. Effort has gone into understanding the effect of inclusion of these analyses in the high-frequency transformer design using four case studies as described in Table 2. In Study 1, a relatively simple design code is which does not consider thermal effects or high-frequency effect. In Study 2, the thermal impact is considered. Study 3 includes high-frequency loss model. Finally, Study 4 is a complete design model. The Pareto-optimal fronts obtained in each of these case studies are as shown in Figure 46. The designs form these four fronts have been compared at the same mass, same loss and same weighted fitness value to understand correlation between parameters like leakage inductance and CM capacitance, aspect ratio, etc. It was found that the inclusion of thermal effects and capacitance constraints have a similar impact to the design resulting in increased use of core material and less conductor. They also tend to favor designs with thin (few layers) with increased winding spacing.

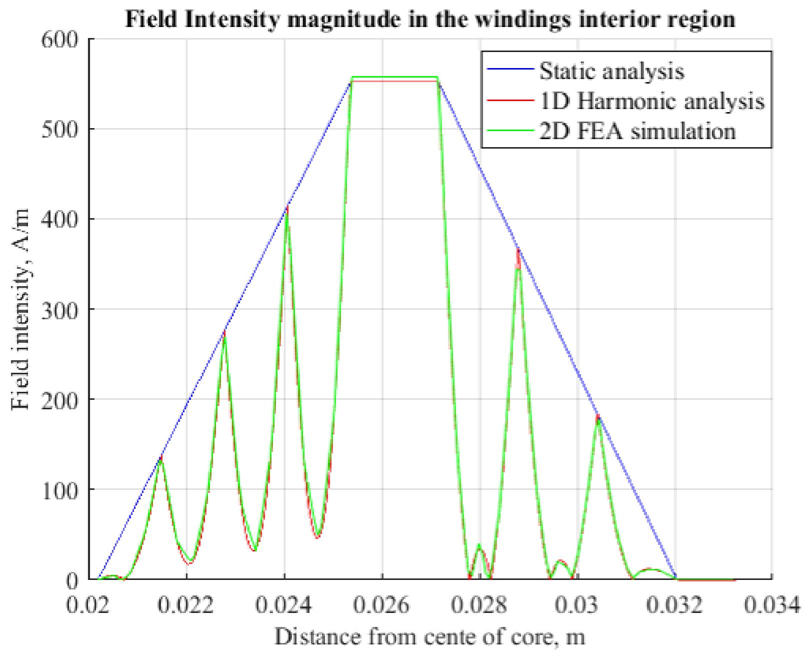

Figure 45: Peak temporal field magnitude along coil regions in transformer core-interior.

Table 2: Case studies implemented.

Analysis	Study 1	Study 2	Study 3	Study 4
Thermal Analysis	✗	✓	✓	✓
Winding Loss due to Skin and Proximity effects	✗	✗	✓	✓
Parasitic Capacitances	✗	✗	✗	✓

The detailed analyses and the complete design methodology for the high-frequency transformer can be found in the dissertation titled ‘Design methodology for a high-frequency transformer in an isolating DC-DC converter’. The dissertation author, Veda Samhitha Duppalli, graduated from Purdue University in May 2018 and has joined Cummins Inc, in Minneapolis, MN.

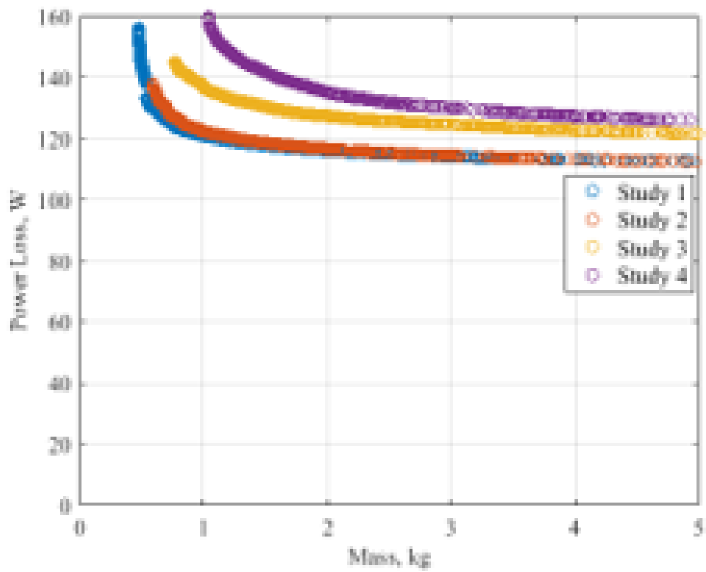

Figure 46: Pareto-optimal fronts comparison for case study 1-4.

Task: High-speed IPM machines

Technical Objectives

The objective of this task is to develop a rigorous design method of V-shaped IPMs, wherein electromagnetic and structural analyses are incorporated in a multi-objective optimization environment. Interior Permanent-magnet Machines (IPMs) have seen wide usage in the industry due to its robustness, high efficiency, and low manufacturing cost [71]. Among many existing IPM topologies, V-shape IPMs have been shown in literature to exhibit higher power density compared to other commonly used IPM topologies [72]. However, the design of V-shaped IPMs is a challenging task due to the complexity of the rotor structure and magnetic saturation. Hence, the electromagnetic analysis of IPMs is commonly done using FEA, which can become cumbersome as the design space becomes large.

The structural analysis is also an important part of the IPM design process, as high stresses often develop in the thin rotor bridges, rendering the rotor prone to mechanical failure. In high-speed applications, the structural integrity of the machine becomes especially concerning. Hence, a method is desired to incorporate both electromagnetic and structural analyses in the design process.

The objective of this task is to set forth a rigorous design method of V-shaped IPMs, wherein electromagnetic and structural analyses are incorporated in a multi-objective optimization environment. To this end, an electromagnetic analysis and a structural analysis suitable for use in a multi-objective optimization environment are proposed. Both analyses are based on analytical methods to reduce computational cost, while preserving a reasonable degree of accuracy compared to conventional finite-element methods. A design study will be conducted using the proposed design method to compare the performance of V-shaped IPMs and surface-mount PM machines (SPMs) for a high-speed generator application.

Technical Approach

- Develop a computationally efficient electromagnetic analysis to compute the air gap flux density in a V-shaped IPM.

- Develop a structural analysis to predict the peak stresses developed within the rotor bridges under centrifugal force.
- Develop a design paradigm based on multi-objective optimization incorporating the electromagnetic and structural analyses, as well as relevant design constraints.
- Conduct a design study of V-shaped IPMs and compare the performance of the machine with surface-mount PM machines (SPMs) for a high-speed generator application.

Progress Statement Summary

An electromagnetic analysis to compute the air gap flux density is proposed [73]. The proposed model is a hybrid approach that combines the computational efficiency of an analytical field solution and the ability to address magnetic saturation of a magnetic-equivalent-circuit (MEC) approach. The proposed model is validated using FEA and is shown to yield accurate predictions while saving computational cost.

A structural analysis is also proposed to analytically determine the mechanical stresses developed within the bridges [74]. In the proposed method, static stress/strain analysis is applied to obtain a linear system of equations where the mechanical loads exerted upon the rotor bridges can be simultaneously solved. The predictions of stresses made by the proposed analysis are compared with those obtained from FEA and they are shown to be in agreement.

With the electromagnetic and structural analyses established, a multi-objective design method is set forth for the design of V-shaped IPMs. As a preliminary study, a design comparison between the IPMs and the SPMs is conducted for a 2.5-hp motor application with 5:1 constant-power speed ratio. The resulted Pareto-optimal fronts of the IPMs and the SPMs are shown in Figure 47. The total cost of the magnetically active materials and the total loss of the machines are the design objectives to be minimized in this study. It can be observed that, for the considered application, the IPMs appear to have an advantage over the SPMs. For a similar material cost, the IPM yields considerable loss reduction compared to the SPM. The cross-sectional view of an IPM yielded by the proposed design paradigm is shown in Figure 51.

The next step will be to determine appropriate specifications for a Navy relevant generator design and to perform a study comparing the IPM and SPM machines in that context.

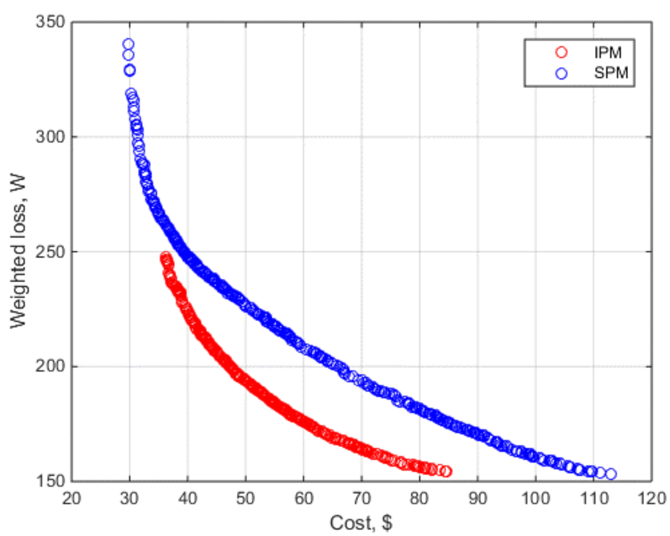

Figure 47: Pareto-optimal fronts.

In previous work, a hybrid approach combining analytical field solution with a magnetic-equivalent-circuit was proposed, and validated to compute the air gap flux density [73]. Also, a structural analysis model was proposed to analytically determine the mechanical stresses developed within the bridges [74]. With the electromagnetic and structural analyses established, a multi-objective design method was set forth for the design of V-shaped IPMs.

Recent work explored the multi-objective optimization of a 20 MW generator, where the total mass of the machine and the aggregate loss are the objectives to be minimized. Two studies were performed. The first study sets the rotor speed fixed as design specification at 3600 rpm, with three operating points of interest: 1/3, 2/3 and full power output, weighted at 0.45, 0.45 and 0.1, respectively. The resulting Pareto-optimal front and a sample design are shown in Figure 48 and Figure 49, respectively. In this case, the combination of low radius and substantial length may be problematic from a mechanical shock point of view. In the second study, the generator speed be a free parameter in the range from 1800 to 3600 rpm. Figure 50 (a) shows the Pareto-optimal front; Figure 50 (b) depicts the chosen operating speed versus mass. Interestingly, the maximum speed stayed below 3300 rpm.

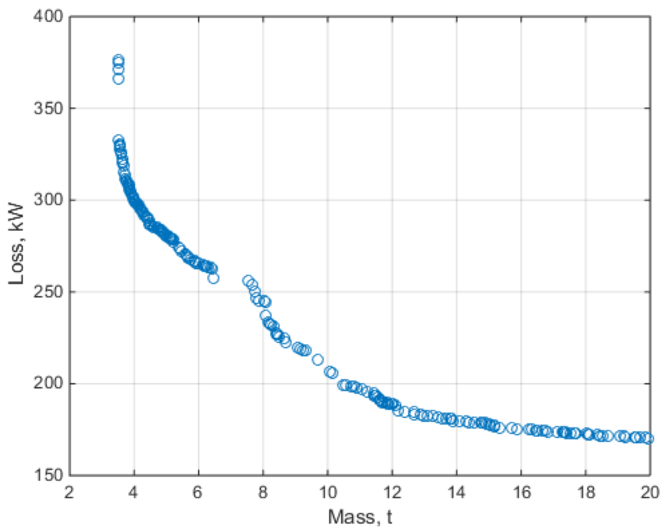

Figure 48: Pareto-optimal front with design speed at 3600 rpm.

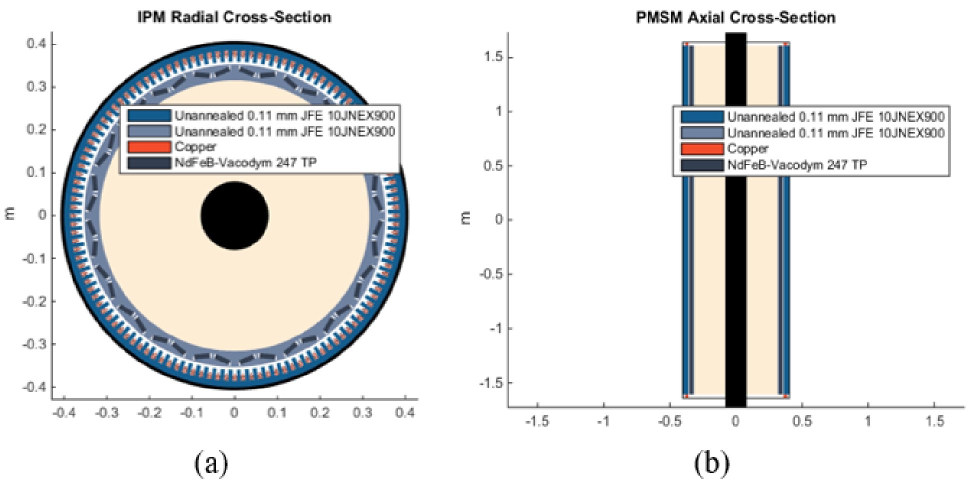

Figure 49: Representative IPM design cross-section from 3600 rpm fixed design speed Pareto-optimal front: (a) radial cross-section; (b) axial cross-section.

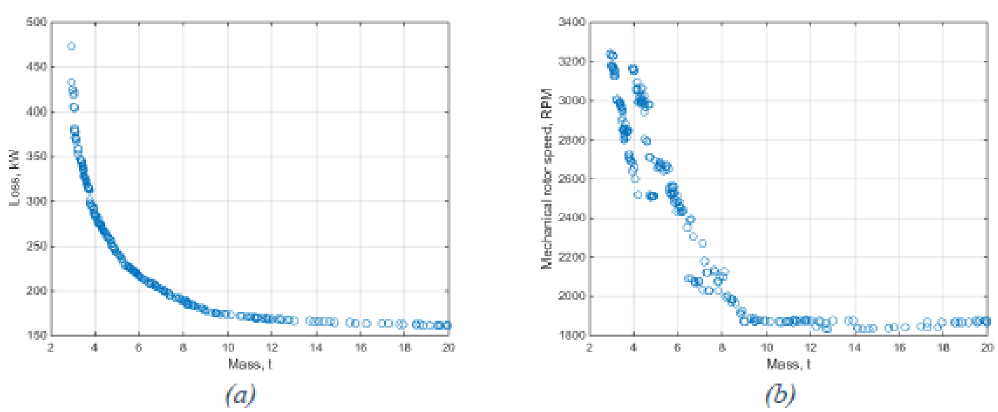

Figure 50: (a) Pareto-optimal front with optimized rotor speed; (b) optimized rotor speed for each optimal design.

As a continuation of the previous work on the structural analysis of IPMs, the proposed analytical model is validated using FEA on an IPM shown in Figure 51. An FEA simulation is conducted at 5000 RPM to obtain the peak stresses developed in the inner and outer bridges of the machine. The comparison between the FEA and model predictions are shown in Table 3. It can be seen that proposed analytical model is reasonably accurate compared to FEA, while being much more computationally efficient.

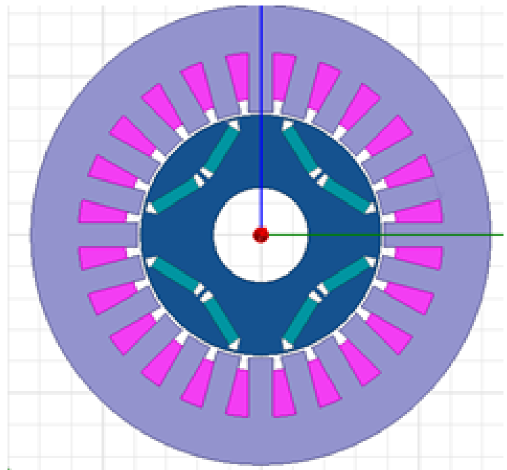

Figure 51: IPM cross-section.

Table 3: Peak stress at 5000 RPM computed using FEA and proposed model.

	FEA	Model	Relative Error
Inner bridge	35.83 MPa	39.03 MPa	8.93%
Outer bridge	31.38 MPa	30.92 MPa	1.46%

2.1.3 Develop emergency power operating characteristics of WBG converters

Planned future work

2.1.4 Explore thermal energy storage in ship systems

Task: Realize integrated two-phase cooling to enable compact, reliable, and high-performance power electronic converters

Technical Objectives

Scale and integrate two-phase cooling on the substrate of power electronic converters and develop models for co-design of electronic-thermal system.

Technical Approach

Integrate highly efficient two-phase cooling in microchannel onto the substrate of power electronic converters.

- Enable rapid and effective cooling.
- Improve the converter power density and performance.

Progress Statement Summary

An initial thermal model has been established to predict the temperature response of converters with varying heat transfer coefficients. Early results are shown in Figure 52.

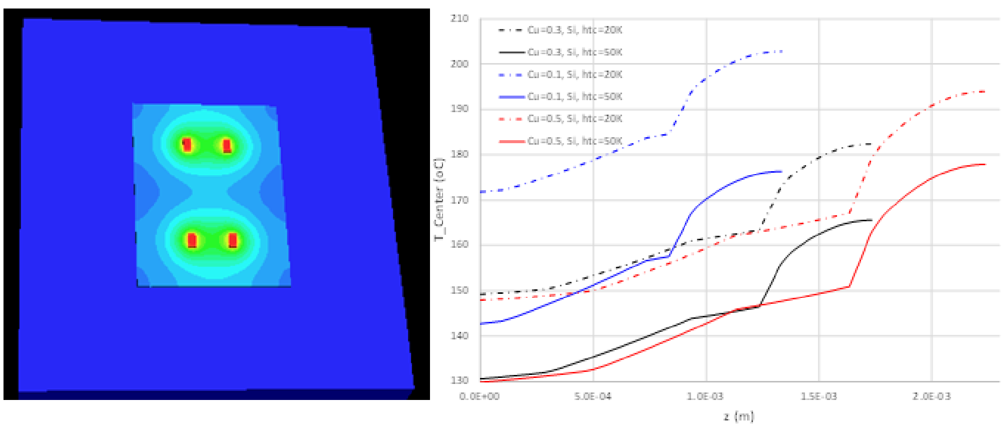

(a) (b)

Figure 52: Early results of temperature distribution on a 100 MW converter; (a) contours of surface temperature; (b) temperature distribution.

In addition to demonstrating these concepts on 1 cm long samples of Si substrate, the interconnected microchannel concept is being developed using 2.6 cm copper samples (shown in Figure 53). This move would allow us to develop scaling laws and thermal/fluids models.

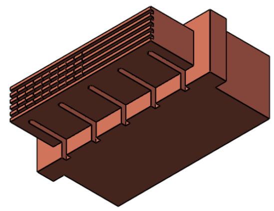

Figure 53: Cu microchannels.

Task: Thermal energy storage

Technical Objectives

Device thermodynamically optimal, thermal energy storage solutions targeting the specific needs of all-electric ship and evaluate their system level impact on ship temperature distribution, the potential for reduction of installed cooling systems requirements and enhanced ability to manage large heat fluxes. This effort will lead to improved thermal management and overall fuel savings.

Technical Approach

- Integrate thermal storage models into ship level thermal models.
- Optimize sensible and phase change thermal storage units for ship relevant operating condition, and in this way, identify optimal charging/discharging cycles, sizing and placing of storage units.

Progress Statement Summary

The development of condensation and evaporation models has started; phase-field and level-set methods are currently under consideration for two-phase modeling. A thermodynamic model for a sensible thermal storage unit, driven by a hot stream has started.

A dimensionless model of a notional all-electric ship integrated energy system constituted of three loads (i.e., two pulsating and one fixed), heat exchanger, chilled water unit, and sensible thermal energy storage has been formulated. The thermal energy storage in the considered system can be used for high-heat flux removal as well as an emergency cooling load to increase the ship survivability. The developed model will be used to determine the optimal thermal mass allocation based on entropy generation minimization.

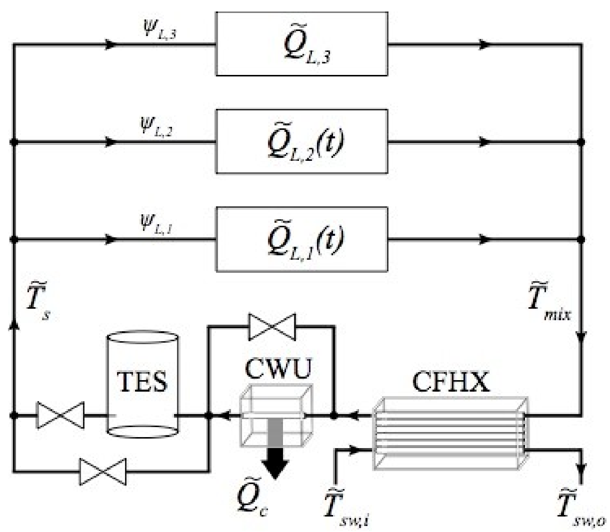

Figure 54: Schematic diagram of a notional all-electric ship integrated energy system cooling network.

2.1.5 Performance-based design criteria for storage systems

Technical Objectives

Conduct an updated comparative study of the characteristics of various energy storage devices (chemical, mechanical, electromagnetic, thermal) to support design of a 12 kV DC 100 MW ship power system, taking into account the latest technology developments and matching the performance of each energy storage solution to the expected load scenarios.

Another critical question that one must consider in the transition to a 12 kV DC system is the relative roles of generation and storage. Thus, this project focuses also on the engineering data to support the trades in DC systems required among generation, storage, speed of control, and load and/or source ramp rates. While there are some general established relationships for ac systems, there is little relevant information for DC systems.

The Navy will obtain less costly and more effective ships by having the engineering data to assess the storage technology, size, and location, as well as the proper coordination with generating units needed for its suite of ship missions.

Technical Approach

Study important issues connected with energy storage systems in shipboard DC power system, specifically the following:

- Quantify the optimal performance space of each storage technology and provide engineering data for its design and procurement.
- Determine the optimal amount of energy storage in a 12 kV DC 100 MW power system based on effectiveness sensitivity curves with regard to size, cost, etc., including the possibility that in some cases no energy storage is the best solution.
- Define whether the best solution is one type of storage technology or a combination of energy storage technologies.
- Determine the optimal granularity and topographical distribution of the energy storage modules in the shipŠs power grid, developing notional effectiveness curves for key mission loads for a 12 kV DC distribution system.
- Determine the proper coordination between the potential insertion in the grid of power from energy storage on one hand and the system's response to a fault on the other.

The development of appropriate models and simulations will be the key to evaluating the optimum capacity and distribution of energy storage and special purpose power generation/conditioning elements. The investigation will balance both information-rich models, such as highly detailed physics-based models, as well as decision-making models that can take advantage of partial information from early-stage design results. Both models developed from existing (legacy) equipment (e.g. drawn from ASSET) as well as models for new proposed technology solutions, for which legacy data may not be available, will be integrated.

This model-based approach will be conducted within the *Matlab*/Simulink platform. It will provide support from design through operation and could incorporate also optimization tools. By its own nature, this project will coordinate with and profit from related thrusts, and in turn will also benefit and inform other efforts within ESRDC. This approach is expected to be useful not only for ships but also for bases, governmental and civilian land facilities, satellites, vehicles, aircrafts, and possibly the larger terrestrial power grids.

Progress Statement Summary

With the growth of intermittent sources of electric power, of time dependent loads, and of the electrification of transportation, system designers are increasingly turning to storage to provide for system stability and effectiveness. This is an expected outcome, as storage is a way to match generators, which have longer life when operated at approximately constant rotational velocity, to variable loads. A simple analogy is that storage is to an electromechanical system as a transmission is to a purely mechanical system (Figure 55).

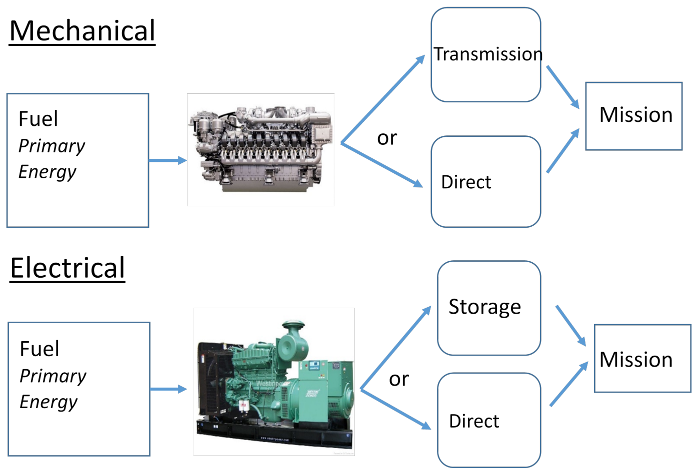

Figure 55: Storage can play an analogous role in an electrical system as a transmission plays in a mechanical system.

This use of storage has prompted the development of a range of storage technologies ranging from batteries to capacitors, to inductors, to flywheels, to fuel cells, to compressed gas, to pumped liquids. The diversity of storage technologies has led to the need to assess a range of technologies for specific applications. An important step in the assessment process occurred in 1968 when D. V. Ragone published a paper [75] highlighting for automotive engineers that batteries had differing power and energy capabilities depending on the battery chemistry. In a mobility application, power is important for acceleration and energy is important for range. This is important because there is a fundamental link between power and energy in a battery and it is determined, as Ragone highlighted, by the particular battery chemistry. Over time, the comparison made by Ragone of power and energy from batteries has been extended to other technologies and that extension is conventionally called a Ragone plot. An example is shown in Figure 56.

This highlights that, consistent with Ragone's paper, different battery chemistries lead to different relationships between power and energy. The major shortcoming of this chart is that there is not fundamental way to specify the boundaries of each of the ellipses. For example, Figure 57 adds flywheel point designs to a typical Ragone plot.

This shows that the simplistic chart shown in Figure 56 with clear boundaries between the various technologies is misleading. It should be noted that there is no reason to assume that the flywheel ellipse in Figure 57 is correct. It was simply expanded to cover a finite number of applications for which it is known that flywheels are competitive solutions.

Efforts have been made to try to set fundamental limits on the technologies [76, 77]. In [76], analysis suggested that that lithium ion batteries, fuel cells, and flywheels have about the same maximum energy density using today's technology. This implies that, in Figure 56, the lithium ion and flywheel ellipses should be expanded upward to the fuel cell level.

But the fields are not static. Emerging technologies, particularly nanotechnology, are showing excellent promise increase the energy density of all of the technologies [78]. In this environment, it should be recognized

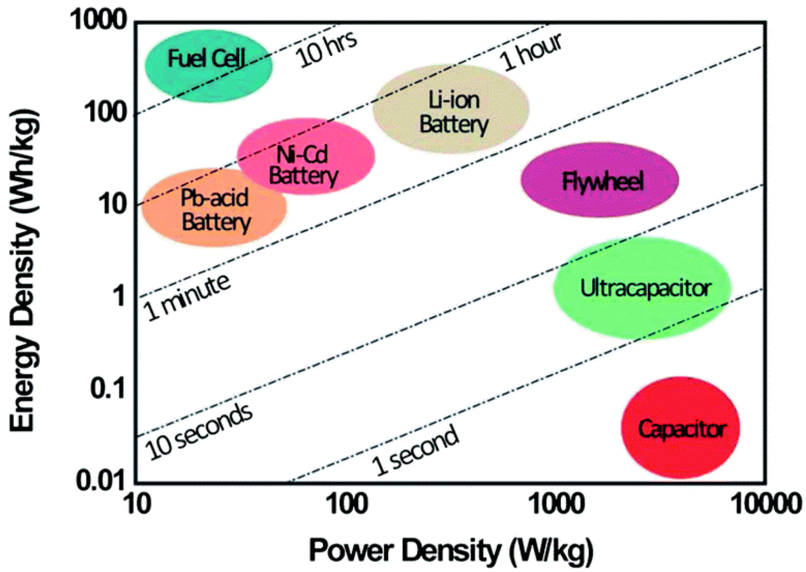

Figure 56: A conventional Ragone plot comparing various battery chemistries with other storage technologies.

that Ragone plots tend to be backward looking characterizations of technology that has been developed rather than predictors of the limits to future storage technology.

Included in [77] is the fact that internal dissipation and leakage losses result in reduced energy availability at high and low powers. This is a factor that is not incorporated in the basic Ragone chart. In [77], the Ragone plot is modeled as a source of information about the available energy while driving a constant power load. This research used constant loads, modified to avoid system instabilities, and idealized components that permitted analytical solutions. While this provided excellent insight into some of the basic processes, it too has its limitations. For example, [76, 77] both addressed superconducting magnetic energy storage (SMES). In [76] it is pointed out that quenching constraints and shielding requirements reduced the energy density of a SMES system significantly, these factors were not modeled in [77].

The effects of losses in storage systems were highlighted in [76] and were addressed in a different way in [79]. This approach to storage characterization recognized that all storage systems have a turnaround efficiency and a loss rate while charged. These are important parameters as the flywheel can have a better turnaround efficiency than a battery system, but the flywheel also has a higher loss rate when charged. So the flywheel wins when the hold time is measured in hours while the battery is better for longer storage times. In [79], a procedure was developed to calculate the conditions under which it was more cost effective to generate electricity from the prime energy source rather than to store energy.

This same approach was applied on a wider scale in [80]. That research concluded that over a significant range of situations, electricity-to-electricity storage is the most expensive and least efficient solution available. There are applications, e.g. pulse shaping, in which storage is likely the most cost effective approach. Consequently, electricity storage should be used sparingly and only when it is the best option. This situation arises because liquid fuels have such high power and energy densities compared to most other technologies. They are always a default when they can be made to work. Because hydrocarbon fuels have CO_2 emissions challenges, there is a global research effort to drive down the cost of hydrogen [81].

A conclusion from this summary is that the selection of an appropriate storage technology, when one is needed, is not a simple choice. The answer depends on the input constraints, the turnaround efficiency of the storage medium, the storage losses, the time over which storage is needed, the power and energy requirements of the output from the storage system, and the physics and chemistry within the storage technologies themselves.

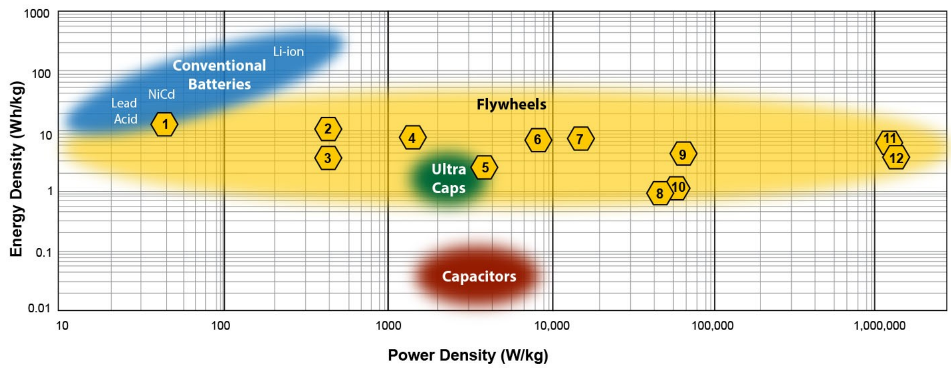

Storage Type Batteries (Conventional Batteries)	Specific Power (W/kg)	Specific Energy (Whr/kg)
Lead-acid	75 - 300	30 - 170
Ni-Cad	50 - 315	150 - 300
NaS	150 - 230	150 - 755
NaNiCl2	150 - 200	100 - 790
Li-ion	150 - 335	75 - 560

#	Machine	Pulse Width (s)	Energy Density (Whr/kg)	Power Density (W/kg)
1	FESS	1800	18.30	25.00
2	ALPS	120	11.82	272.73
3	HVHP	0.01	4.33	300.00
4	Transit Bus	60	8.89	1333.33
5	EMALS	3	1.43	2608.70
6	CHPS	0.01	7.00	10000.00
7	Ignitex	10	5.83	15625.00
8	Iron Core	0.01	1.05	80000.00
9	AIR	0.35	3.00	80000.00
10	Small Cal	0.01	2.89	768518.52
11	Cannon Cal	0.01	5.50	1200000.00
12	Sub Scale	0.01	2.67	1250000.00

Figure 57: A nominal Ragone chart with 12 examples of flywheel point designs highlighted.

This situation has led one research team to solve the full system performance to screen various storage technologies rather than to propose solutions based on approximations [82]. The project showed that such an approach was possible, but time consuming, costly, and depends on the researchers making reasonable choices early in the research. For example, the flywheel assumptions were inappropriate in [82] leading to a possible erroneous conclusion that the technology is not appropriate. There was not time or funding to run multiple iterations that would be needed to achieve optimal configurations of each of the technologies examined.

This past research highlights the importance of having an accurate and appropriate technology screening tool to design energy storage systems. Even with a screening tool, it is possible that suboptimal decisions will be reached due to the complex number of variables that need to be considered.

This past research highlights the importance of having an accurate and appropriate technology screening tool to design energy storage systems. Even with a screening tool, it is possible that suboptimal decisions will be reached due to the complex number of variables that need to be considered. This paper describes an approach to filter the variables appropriately to achieve a good answer in a much shorter time.

In order to accomplish the task of the optimal choice of energy storage technology mix for a given application, an energy storage selection tool was developed. This tool is described macroscopically in Figure 58.

The tool made use of an extensive amount of data based primarily on the research done at the University of Edinburgh, UK, [83] and on internal data generated at CEM over several decades of R&D work performed there.

The storage technologies examined are listed below:

- Pumped Hydro.

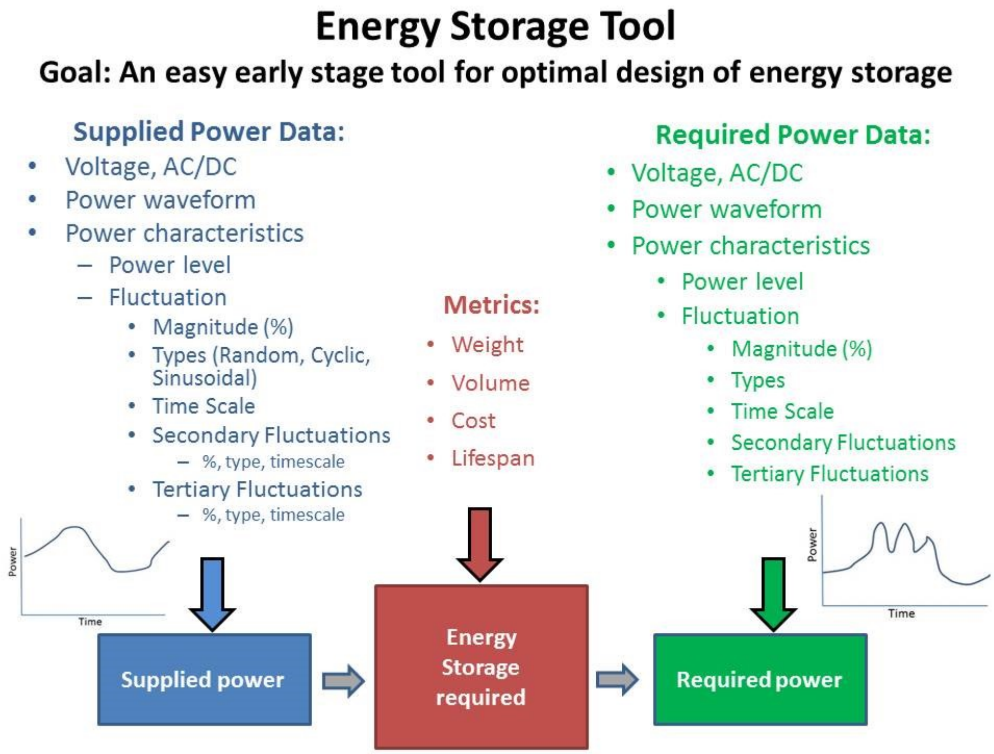

Figure 58: General description of the goal and functionality of the energy storage tool developed at CEM.

- Compressed Air
- Flywheel
- Zinc Silver Oxide
- Alkaline
- Lead Acid
- Lithium Ion
- Nickel Metal Hydride
- Nickel Cadmium
- Nickel Iron
- Nickel Zinc
- Sodium Sulphur
- Sodium Nickel Chloride
- Zinc Air
- Iron Air
- Polymer Exchange Mem.

- Direct Methanol
- Molten Carbonate
- Solid Oxide
- Vanadium Redox
- Zinc Bromine
- Polysulphide Bromine
- Superconducting
- Supercapacitor
- Sensible Heat
- Latent Heat
- Reaction Heat

The criteria used in the evaluation of the technologies are also listed below:

- Specific Energy [Wh/Kg]
- Energy Density [KWh/m^3]
- Specific Power [W/Kg]
- Power Density [KW/m^3]
- Efficiency [%]
- Lifespan [yr]
- Cycle Life [cycles]
- Self-Discharge Rate [%/day]
- Scale [MW]
- Energy Capital Cost [US$/KWh]
- Power Capital Cost [US$/KW]
- Technical Maturity
- Environmental Impact

The tool has been developed on the *MATLAB* platform. After the energy storage options suitable for the system under consideration are selected, the user can choose the ranking of the criteria whereby the various technologies will be evaluated. The technologies are then scored accordingly and a total composite score is generated. Modeling and simulation of the selected technology mix will then have to follow to validate the selection and explore further areas of opportunities within the design space.

2.2.1 Develop concepts for shipboard heat-transfer corridors

Technical Objectives

Develop heat-transfer corridors for next-generation all-electric ships' power and weapons systems that will handle increased power density and increased waste heat and high-heat flux sources dispersed throughout the entire ship.

Technical Approach

Study new levels of heat generation, pulsation rates and distribution will present great challenges to the capabilities of conventional cooling systems. This project will investigate and develop heat-transfer corridors both independently from cables (pure heat-transfer corridor), and in connection with cables (hybrid corridors). These heat-transfer corridors will play the role of a 'thermal bus' similarly to an electrical bus.

- The thermal bus will serve as the main corridors (paths) for transport of thermal energy.
- It is envisioned that a hierarchy of core and branch (distribute) will be established, in a way that the core thermal bus structure will be flexible to adapt to mission changes and upgrades in electrical and electronic components and the branch buses will integrate to the core bus and serve specific needs of devices. This effort will lead to a robust ship thermal infrastructure, to deal with all-electric ship thermal management needs, which is flexible and adaptable to future requirements as technology progresses.
- HTS thermal aspects will be explored in connection with the hybrid corridors.

Progress Statement Summary

Progress has been made in the development of flexible heat-transfer corridors that address ship zonal load requirements. Initial development of a mathematical framework that will allow the exploration of system level configurations of heat transfer corridors has initiated. At the equipment level, flexible heat-transfer corridors for Power Electronic Building Blocks are being explored. Quantification of HTS thermal needs that will be leveraged in a ship solution hybrid heat-transfer corridor is underway.

A process to lay piping networks within the ship is being tailored to group sets of pipes into corridors (analogous to the power corridor concept). The proposed concept is currently being assessed numerically using a computational tool that is capable of generating a layout for a given set of loads that need to be cooled. Ongoing efforts include the study of a heat transfer corridor in which the thermal conduits (buses) are enclosed in a corridor and exposed to natural convection. Figure 59 illustrates two configurations under consideration.

A study of cooling corridors that serve enclosures (e.g. ship compartments, power corridors) is ongoing. The initial effort has been to focus on model development and the exploration of cooling corridors placement within an enclosure. The current study has covered up to 5 cooling corridors/channels per enclosure. A parametric study varying the area allocated to the corridors/channels has also been conducted.

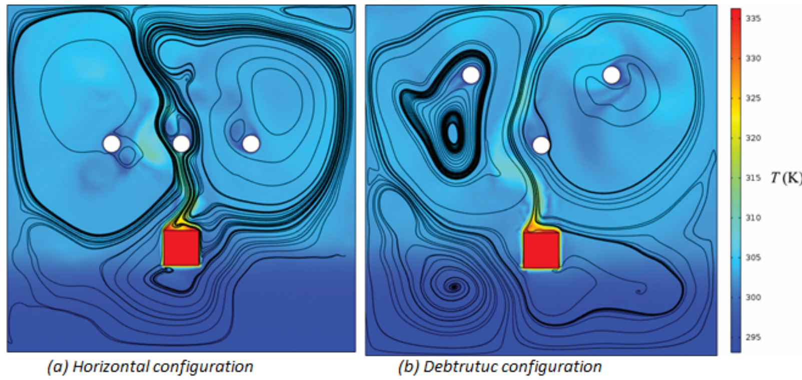

Figure 59: Cross-sectional temperature field of a notional heat transfer corridor with (a) horizontal and (b) dendrittic piping configuration.

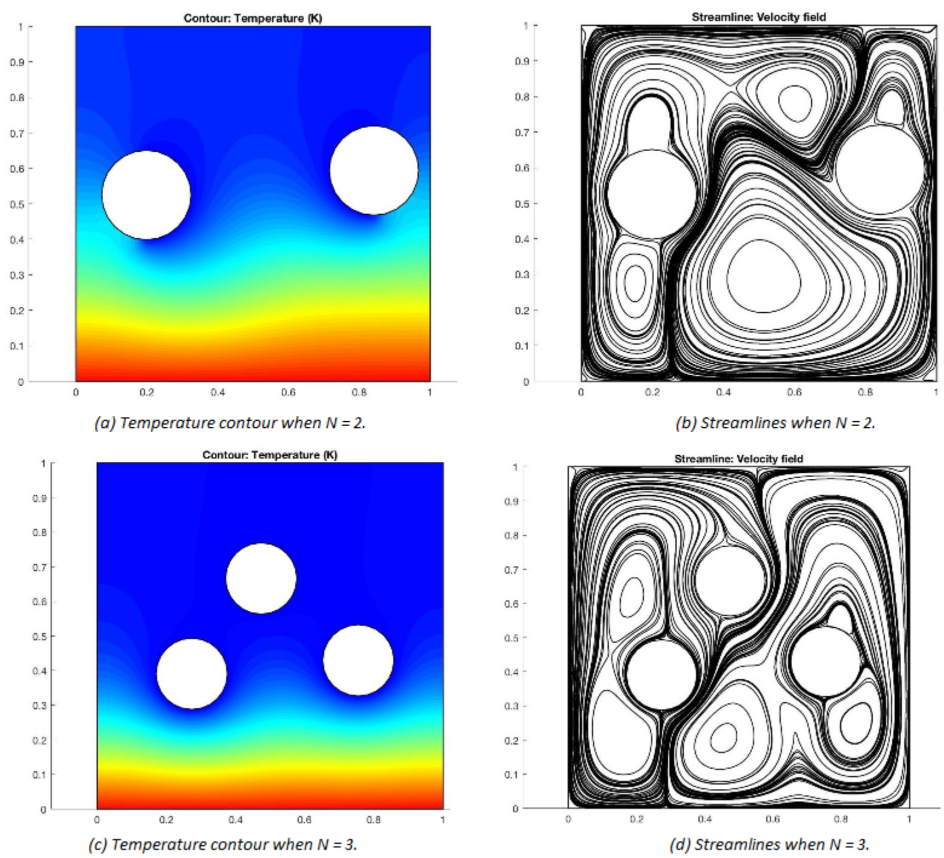

Figure 60: Temperature contours and streamlines in the enclosure with two and three cooling channels.

Task: Thermal modeling of power cables

Technical Objectives

Determine local temperature fields to enable cable layout and cooling system requirements. High-current power cables generate substantial heat during operation time, and in some extreme cases when the thermal loads continue to accumulate, the surface temperature of the cables could potentially exceed the allowable temperature beyond melting of the insulation layer. Therefore, accurate prediction of the local temperature field of the power cables as well as their surroundings is crucial to the layout of the cable cabinet and the design of cooling system. High-fidelity modeling of forced/natural convective heat transfer and heat generation/conduction inside solid cable arrays simultaneously is complicated because of the complex geometry and the conjugate heat-transfer modes. To this end, we have employed the Smoothed Profile Method (SPM) in the context of spectral/hp element method [84, 85], which is highly accurate and flexible to accommodate to very complex geometry boundary and conjugate heat transfer.

Technical Approach

- Upgrade and speed up our thermal fluid modeling software, by taking advantage of the fast solver based on Fourier method.
- Re-design the interface of the thermal fluid modeling software, and make it be compatible with some popular and free open-sourced pre-process and post-process software, such as Gmsh and Paraview.
- Predict the temperature field and evaluate the performance of 3 different arrangements of cooling devices, based on 120 power cables, each carrying 80 A current, with a 1 inch diameter.

Progress Statement Summary

Our research focused on the simulations of forced/convective heat transfer of 120 power cables under different boundary conditions. Current progress includes identifying the best location to place the cooling equipment, namely at the top wall of the cable cabinet. Figure 61 shows the local temperature field of this configuration. As we can see, that large amount of area shows the blue color that indicates low temperature. Figure 62 compares the mean temperature, changing with time, for different locations of active cooling.

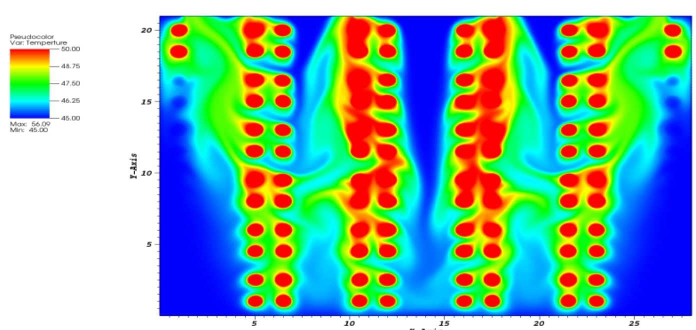

Figure 61: Local temperature for case 2, red and blue colors indicate high and low temperature, respectively.

We have employed our high fidelity code to simulate the temperature rise in the cable corridor under different design and cooling strategies. First, to estimate the worst scenario, we assumed that no forced

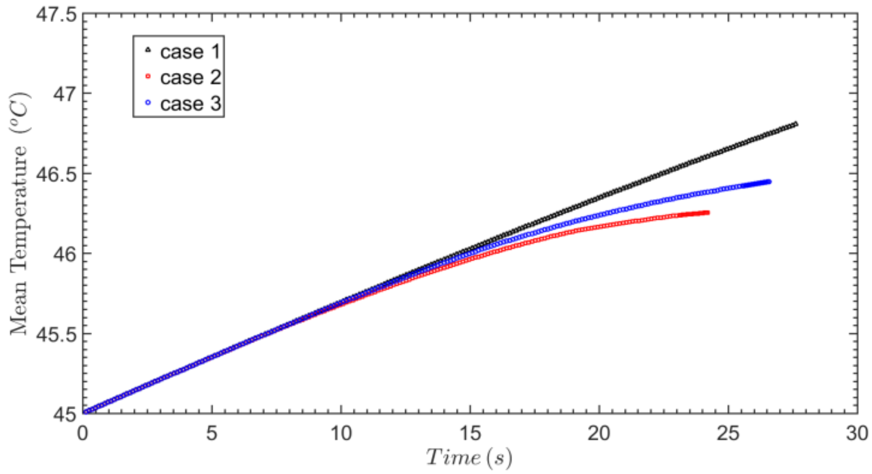

Figure 62: Mean temperature varying with time for three different cases.

cooling was used inside the cable corridor, and the temperature on the bottom surface was kept the same as that of ambient. In the following left figure, we show an instantaneous temperature field at time t=1 hour. We see that due to the buoyancy force (gravity induced), the hot plume (red color) rising from the surface of the cable makes the temperature on the top boundary of the corridor higher. In the right figure, we present the comparison of the maximum temperature of different designs. Here, for the first design, we have 16 pairs of cables; the outer diameter of each cable is 1 inch and the current is 125 A. For the second design, we have 2 pairs of cables with the same total copper area and the same total current; for each cable, the outer diameter is 1.63 inches and the current is 1000 A. We see that for both cases, the temperature can easily rise over 40°C, even if the temperature at the corridor bottom is constant. In this example, the peak temperature for 16 pairs of cables is lower than that for 2 pairs of cables because the 16-pair configuration has a higher surface area for an equivalent conductor cross-sectional area, and thus better heat transfer to the surrounding air.

In ongoing work, we are designing an effective forced convection system to cool the system and maintain the temperature within accepted bounds. We will also develop a simplified computer model that can be used as a design tool that will select the optimum configuration given the number of cables and total current. Hence, we can determine very efficiently the proper insulation or the sudden temperature rise in the case of damaged insulation.

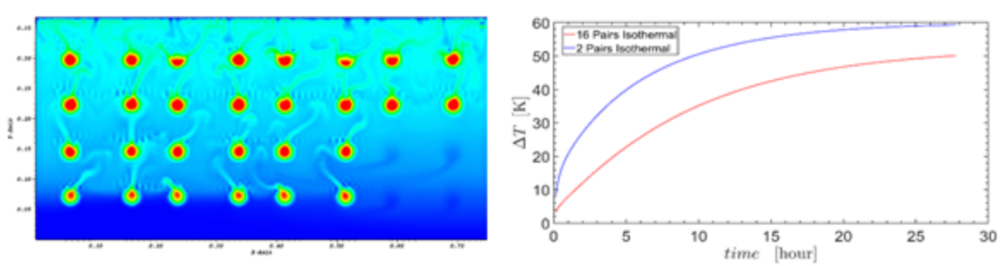

Figure 63: (left) Temperature field of free convection of the 16 pairs of cables, each of which conveys 125 A current, at time 1.0 hour; (right) the maximum temperature in the cable corridor varies with time and cable size; note that for the case of 2 pairs of cables, the current is 1000 A in each cable.

2.2.2 Design considerations for MVDC cables

Technical Objectives

Develop cable plants in future electric ships that are smaller, lighter, and reliable. To achieve this goal, this project will develop the theoretical and experimental data required to assess the construction of existing DC cabling, and to identify opportunities to minimize the size and weight of the cable plant aboard future DC electric ships with operating voltages ranging from 5 kV to 25 kV, for steady-state operation and under pulsed conditions. Both the performance of today's technology and of future emerging materials will be evaluated. This information will be used to develop a process to design a smaller DC cable configuration for future electric ships, meeting or exceeding the Navy's performance requirements with long-term reliability.

Technical Approach

Study laboratory data to determine if it may be possible to reduce the size of the cable plant on future ships, whether that plant is made from flexible cables or bus pipe. These data have been obtained using partial discharge (PD) activity as the key diagnostic tool to assess the condition and performance of the cable samples. This diagnostic method has been chosen because conventional life tests involve long-term, expensive multi-stress tests designed to accelerate aging with results that are often suspect, as it has not been possible to develop an appropriate aging model that provides confidence in the results of the multi-stress tests. Evidence suggests that the insulation failure in a cable is preceded by a partial discharge, except possibly in the case of a severe overvoltage. While there has been significant research into the PD performance in AC systems, similar research in the PD performance of cables under DC power has been very limited.

- Generate the experimental data to assess unequivocally whether better PD cable performance is achieved in the presence of DC power rather than AC power.
- Establish a thorough understanding of this behavior through accompanying modeling and theoretical evaluation.

Progress Statement Summary

A wide selection of commercial cables have been examined to date, including cables with Cross-Linked Polyethylene (XLPE) or Ethylene-Propylene-Rubber (EPR) insulation. PD activity for each cable has been measured from room temperature up to its rated temperature. Data collected to date by monitoring PD activity on these cables subjected to AC or DC excitation in the voltage range of 5-25 kV have shown significantly better performance for each cable with DC power than ac power.

While the experimental work continues, modeling of the PD process under DC and AC power is under way. These experiments and simulations so far raise the interesting potential that a DC cable ship plant can be made with smaller insulation than conventional ac cables, and, thus, be smaller and lighter with no sacrifice in reliability.

Furthermore, the question being examined is to what extent we can confidently use the comparison of AC and DC PD activity to assess cable life, and whether DC cables are inherently less sensitive to primary processes in cable aging than AC cables (electrical, mechanical, and thermal characteristics) [86].

Since the measurements have been taken over the course of several months, some evolution of the experimental set-up and measurement techniques inevitably has occurred during this time. The present day system is much more immune to noise than the original one making the repetition of some experiments necessary.

As an example, Figure 64 shows the current test matrices for two types of cables under test in the period of April-September 2017.

In addition, over this period a focus has been on the continued development of a coupled electric/thermal model of multi-conductor coaxial cable to enable comparison of the performance of such topologies with

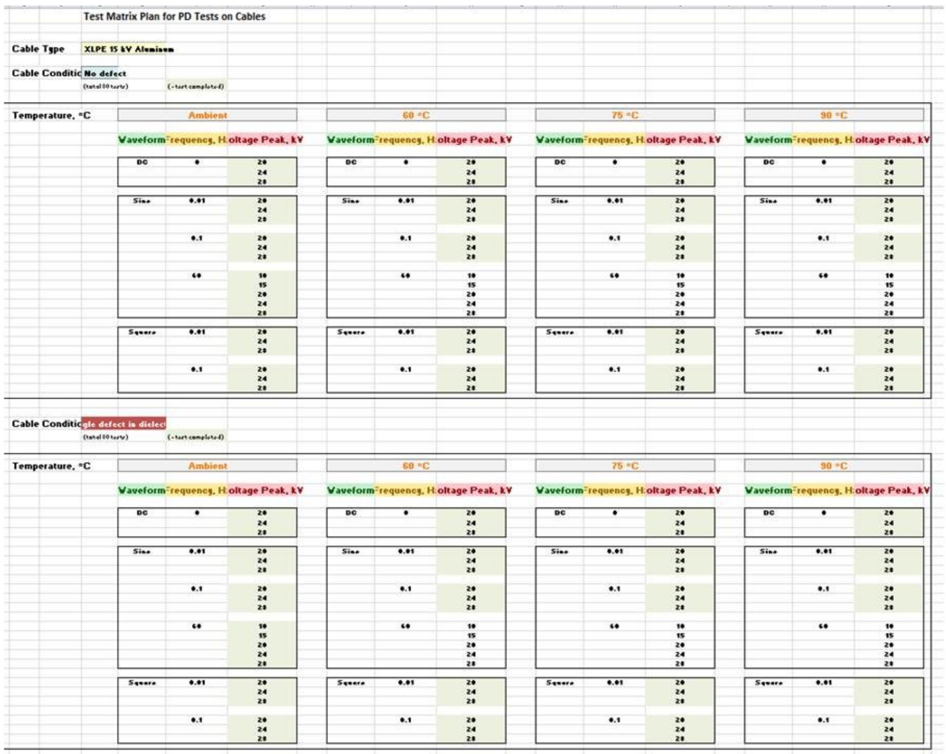

Figure 64: Test matrix for 15 kV XLPE cable, with and without defect; total of 160 tests, 81% completed (shaded).

single conductor coaxial cable. The single conductor models developed under this effort were presented at the 2017 ESRDC conference. In addition, a toolbox is being developed to enable calculation of the external magnetic field resulting from arbitrary cable geometries to be calculated as part of the cable plant optimization/evaluation. To calculate the external field, a 2-D Galerkin-based method of moments approach is being implemented. It is envisioned that the toolbox can be used as part of S3D, so that engineers that apply a first stage design can evaluate the impact that cable and other equipment placement has on electromagnetic fields at an arbitrary distance from the ship.

The measured data set spans a voltage range from 0–30 kV AC and DC, a temperature range from 25° C to 75° C, and encompasses undamaged cables, cables with a defect in the dielectric, and cables with a defect at the dielectric-outer semiconductor interface. Therefore all tests under electrical and thermal stress have been completed for the cables of interest. Incidentally, since the measurements have been taken over the course of several months, some evolution of the experimental set-up and measurement techniques inevitably has occurred during this time. The present day system is much more immune to noise than the original one.

While the experimental work continues, modeling of the PD process under AC and DC power is under way. These experiments and simulations so far raise the interesting potential that a DC cable ship plant can be made with smaller insulation than conventional AC cables, and, thus, be smaller and lighter with no sacrifice in reliability [87].

Furthermore, the question being examined is to what extent we can confidently use the comparison of AC and DC PD activity to assess cable life, and whether DC cables are inherently less sensitive to primary processes in cable aging than AC cables (electrical, mechanical, and thermal characteristics). Experience suggests that the environment initiates voids or delaminations in the insulation and these in turn produce partial discharges. Those discharges lead to premature failure, which raises the possibility of assessing life by determining any unique void initiating situations on the ship and using the wide body of partial discharge information to predict life.

This approach has generated exciting results:

- A company loaned us a second partial discharge measurement system to expand the measurement capability.
- Gian Carlo Montanari, University of Bologna, joined UT to accelerate progress in life assessments. One of his Ph.D. student at Bologna is developing a scaling law to assess the relationship between frequency of the applied field and partial discharges.
- Published a joint paper with the Bologna team, which looks at the effect of inverters on insulation life in cables or rotating machines. The partial discharge patterns change dramatically highlighting why low frequency sine waves may be better than PWM if one wants to minimize insulation size and weight [88].
  - Working with NASA to minimize power electronics in future aircraft.
- Working with Virginia Tech to minimize PD in power electronics.
  - New cooperative agreement with the Army may point to fundamentally new packaging techniques for high voltage power electronics.
- Life depends on processes in the bulk, at interfaces and at junctions and splices; partial discharge pattern recognition can point to the challenges in various designs.
- A preliminary assessment of life models of medium-voltage DC cables with extruded polymeric insulation has been conducted, focusing on electrical and thermal life models.
- To help link with published 60 Hz data, studied the effects of supply frequency between 0.01 Hz and 60 Hz [89].

This is an important applied research problem at the state-of-the art and we are collaborating to use the skills and funding from as many sources as possible to try to get an outstanding solution with the time and funding available.

In addition, over this period a focus has been on the continued development of a coupled electric/thermal model of multi-conductor coaxial cable to enable comparison of the performance of such topologies with single conductor coaxial cable. The single conductor models developed under this effort were presented at the 2017 ESRDC conference. In addition, a toolbox is being developed to enable calculation of the external magnetic field resulting from arbitrary cable geometries to be calculated as part of the cable plant optimization/evaluation. To calculate the external field, a 2-D Galerkin-based method of moments approach is being implemented. It is envisioned that the toolbox can be used as part of S3D, so that engineers that apply a first stage design can evaluate the impact that cable and other equipment placement has on electromagnetic fields at an arbitrary distance from the ship.

Task: Field prediction in cable design/layout

Technical Objectives

Cables play an important role in the design of a power system. The design of DC and AC cables has been considered by numerous researchers [90–92]. To establish the designs, they have traditionally relied on analytical expressions, experiments, or finite element analysis to predict the electromagnetic fields within the dielectric/conductors. DC cable design presents unique challenges due to the fact that space charge can accumulate within the dielectric over time. The space charge accumulation is a function of temperature, electric field, and material properties. Of particular concern is that the space charge leads to electric fields that are sufficient to break down the cable, particularly during transient conditions. A question arises as to whether cables used for ship electrical systems can be optimized to minimize the impact of space charge while also considering objectives of minimal cable mass and loss. A second question arises as to whether single conductor, or multi-conductor geometries are best to achieve these multiple objectives.

In this research, an objective is on the development of a coupled thermal-equivalent and electrical-equivalent circuit model that is general and provides the ability to model electric fields and space charge accumulation in single and multi-conductor DC cables. In contrast to analytical models, the proposed coupled model is more general, allowing for exploration of a wide spectrum of geometries. In addition, it does not rely on the solution of partial differential equations (PDEs), which is used by those that apply FEA or numerical differentiation to estimate fields [90–92]. This enables the solution to be computed rapidly, which eases the burden of population-based design where a large number of candidate evaluations is necessary to explore a design space.

Technical Approach

In the initial year of this research, an approach to model the electric field in cables using an equivalent electric circuit coupled with a thermal equivalent circuit, was derived. The basis of the modeling approach that has been developed is highlighted in Figure 65. Therein one can observe that a dielectric is discretized into a finite number of electrical and thermal equivalent circuits. The electrical resistances represent a volume that current density enters and leaves only at two equipotential surfaces. The resistance of the volume is

$$R = \int \frac{dr}{\sigma(T, E)A}$$

where the conductivity σ is a function of temperature T and electric field E, and r and A are the radial length and cross sectional area. The value of temperature is determined using a thermal equivalent circuit. The nonlinear electric field is determined through the solution of the nonlinear electric circuit. Boundary conditions are imposed to determine volume capacitance. The model has been validated using a number of comparisons with data in literature and finite element analysis. It has also been utilized to facilitate cable designs for an MVDC bus in which the goals are to minimize cable mass/volume/loss subject to ensuring minimal electric field enhancement.

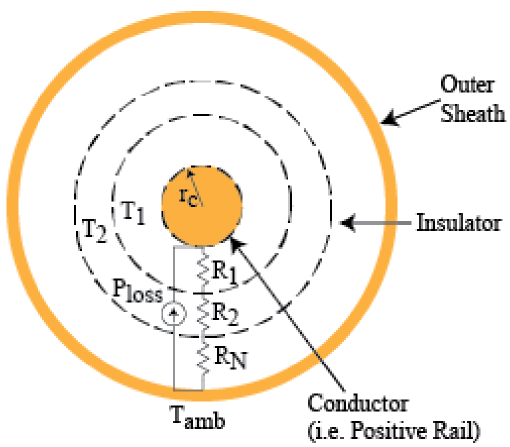

Figure 65: Equivalent circuit to predict electric fields within cable.

Progress Statement Summary

Over the reporting period, focus has been twofold. First, a method to incorporate defect charge into the equivalent circuit models of cables has been developed. Defect charges create the potential for enhanced electric field in the insulator that can lead to breakdown. To incorporate defect charges into the equivalent circuit model, an approach based upon the method of images has been derived. Using this approach, a defect within the dielectric is modeled using equivalent charges placed inside the inner conductor and outside the outer conductor. The charge placement is established to meet the boundary conditions at the insulator/conductor interfaces and is used to establish equivalent voltage sources within the equivalent circuit. The voltage sources are shown in within the equivalent circuit in Figure 66.

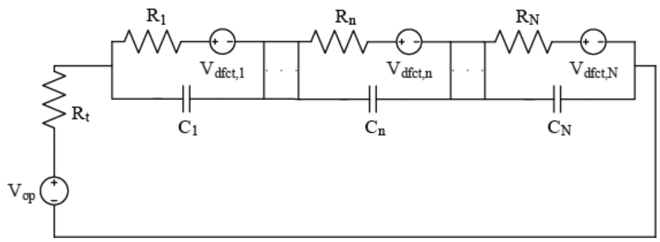

Figure 66: Modified equivalent circuit to include the impact of defect charges in the dielectric.

The defect charges impact the electric field in all three directions (into page, radial, and axial). However, the magnitude of the electric field in such cables is in the radial direction so that only the radial component is included within the model. The method has been validated by comparing the values of the voltage sources with voltage levels between regions of the dielectric that are obtained using finite element analysis (FEA). A representative comparison is shown in Figure 67. Therein it is seen that the voltage predicted using the image charge method matches that of the FEA-based model-reasonably well. The ability to capture the impact of the defect charges enables the team to explore cable optimization in the expected presence of expected defect charge densities that are provided in literature.

A second area of focus is to create an equivalent circuit model of a two-conductor cable that enables design comparison with the single-conductor cable. Toward this effort, a proposed equivalent circuit has been created based upon studying the electric field of two-conductor cables under alternative geometries (distances between conductors, radius, etc.). A representative cable geometry and FEA-based field is shown next to proposed equivalent circuit in in Figure 68. From the figure on the right, one can observe that the dielectric has been discretized into regions (labeled A, B, C, D, E,). For example, Region A represents the area between an inner conductor and the outer conductor. Region C represents the area directly between the inner conductors. Equivalent electric flux tubes have been derived for each of the regions. The electric field predicted by the equivalent circuit model has been compared to FEA prediction for several alternative geometries. A representative comparison is shown in Figure 69. One can observe that the overall behavior of the electric field is predicted reasonably well. There are some differences that are being evaluated, but it is believed that the existing model is suitably accurate to support design studies. Presently, the team is evaluating a thermal equivalent circuit model that enables one to capture the electrical conductivity of the dielectric under different heat loading.

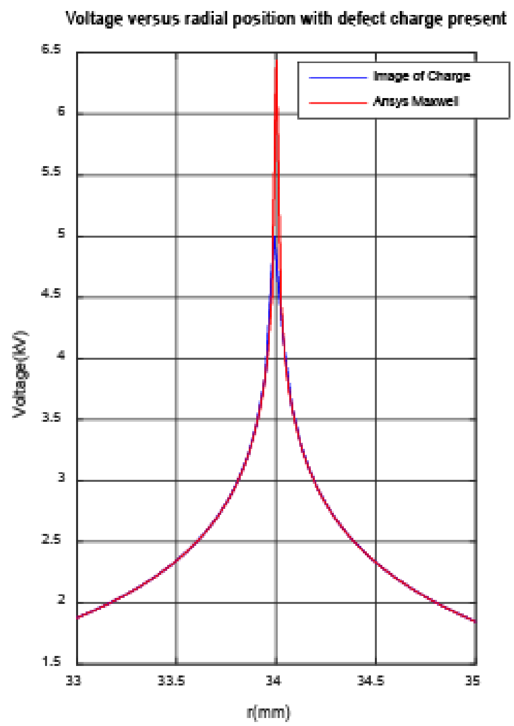

Figure 67: Comparison of equivalent circuit model and FEA in predicting voltage in dielectric in area around defect charge.

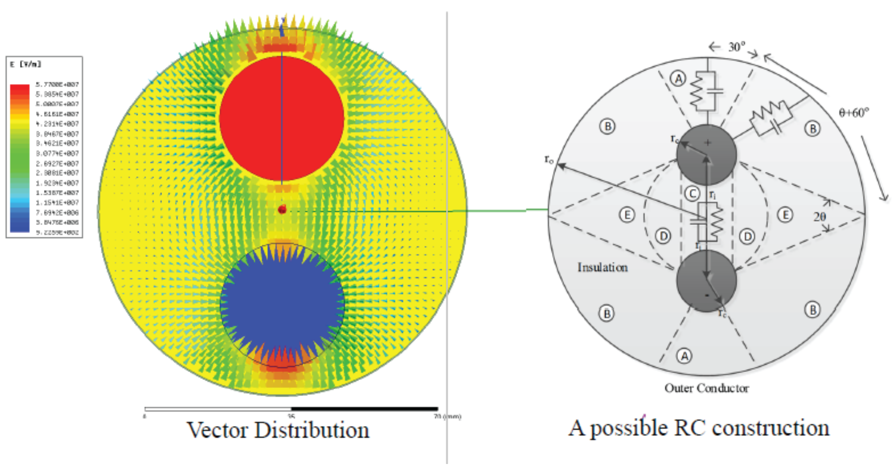

Figure 68: FEA-based evaluation of the electric field of a two-conductor cable (left) and a likely equivalent circuit used to model the dielectric (right).

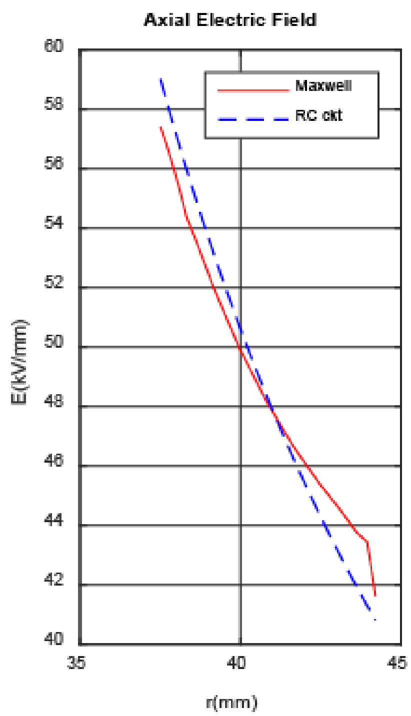

Figure 69: Representative comparison of the radial field between inner conductors in two-conductor cable predicted by FEA and an equivalent circuit.

2.2.3 Develop requirements for power dense superconducting cables for MVDC systems

Technical Objectives

Develop modeling tools for HTS power-distribution cable systems and components that couple electrical and cryogenic thermal characteristics and generate basic data on prototype devices that are developed in various related efforts at CAPS.

Technical Approach

- Develop computationally effective tools and models of HTS power cable system components.
- Develop methods for estimation of the cryogenic cooling requirements of each component.
- Devise design improvements to minimize the cryogenic thermal load to enhance the stability, reliability and efficiency of HTS multiple cable systems.

Progress Statement Summary

Two modeling approaches for HTS cable systems have been undertaken. The Finite Element Methods (FEM) were developed to understand the local temperature gradients and finer details of the roles of various components in the cryogenic thermal behavior of HTS cables. Thermal network models were developed for faster integration of various devices and operational decisions related to various scenarios of system failures and how the failures can be mitigated to support operational needs. Two graduate students and a post-doc researcher contributed to the progress along with the PIs and full-time researchers. The work resulted in three papers that were accepted in 2016 for publication in IEEE Transactions on Applied Superconductivity [93–95].

The efforts of this project for the reporting period were focused on the development of a technique for enhancing the stability and reliability of superconducting cable systems by incorporating a small volume of solid nitrogen in superconducting terminations. Modeling and experimental studies were conducted on solid nitrogen storage methods. Two graduate students and a post-doc researcher contributed to the progress along with the PIs and full-time researchers. The work resulted in three conference presentations and papers that were accepted in 2017 for ESTS 2017 [96, 97] and the IOP Conference Series: Materials Science and Engineering, Advances in Cryogenic Engineering [98].

2.2.4 Develop integrated thermal and electrical power corridor concepts

Task: Models of modular integrated poer corridors

Technical Objectives

Develop flexible and adaptable electric distribution for future load systems. Power distribution is an essential component for the all-electric ship power system. There will be many electric loads distributed all about the ship besides propulsion. Flexible and adaptable electric distribution is essential for future load systems. Furthermore, to avoid the expensive historical model of custom-designed and custom-installed electrical distribution apparatus tailored to the configurations of each ship, a new highly adaptable common concept approach is required. This requirement is achieved with a modular approach that employs factory-assembled modules made and pretested off-ship and installed as essentially complete subsystem units. A reserved-space approach is employed to enable rapid cost-effective installation and to guarantee flexible access for present and future loads throughout the ship.

Conceptually, this approach provides a plug-and-play distribution system to power the entire ship. The core structure is highly modular with a suite of common components. For example, power is carried along the corridors by prearranged supply cables, tap-offs that connect to these supply cables' power protection, power conversion/conditioning, measurement sensing, and in some cases, energy storage units, all within the corridor. The output from the corridor is provided by plug-in connections at pre-assigned locations as well as additional locations that can serve future needs not known/available at the time of ship design. Our prior work on compact self-actuating circuit breakers, the H Breaker [99], is an example of possible protection components that are to be part of the integrated power corridor.

Technical Approach

- Quantify component requirements and complementing technologies for electrical and thermal compatibility.
- Coordinate with Navy and shipyard requirements to enable modular manufacturing.
- Develop design constraints that enable flexible yet cost competitive constructions.
- Establish scaling relations for various power capabilities.

Progress Statement Summary

Our research has focused on key questions of scale: dimensional, thermal and level of power. To sustain a modular approach, it is essential to establish unit sizes that are neither too small, so too many modules are needed, nor too large to be unsuitable for lighter load situations. The work has examined different scenarios for power needs to determine likely required power levels. For example, an integrated power corridor of 20 MW rating is a size that can handle large load needs, but at the same time can be paralleled with other 20 MW corridors to help meet vulnerability needs and higher power ships, such as the 100 MW ESRDC baseline design.

Further evaluations of power corridor arrangements have been carried out including more details concerning the internal layout of various components [100]. Figure 71 depicts a side view of one possible arrangement.

Figure 71 illustrates the possibility of integrating the power cables in a conduit section at the bottom of the corridor, along with circuit protection devices, electronic power conversion for 4 MW, energy storage and space for control sensors and access for heat removal piping. Additionally, there are coupling interface junction box that enables the selection of which power cables are to be connected to which power converters. An example for such a set of cable selection switches is depicted in Figure 72.

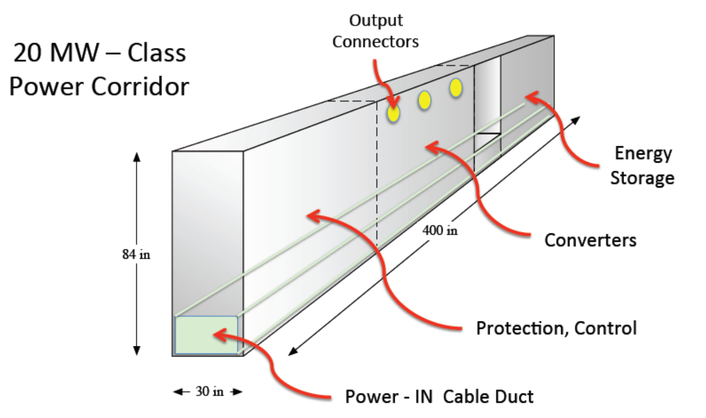

Figure 70: Example: integrated power corridor arrangement.

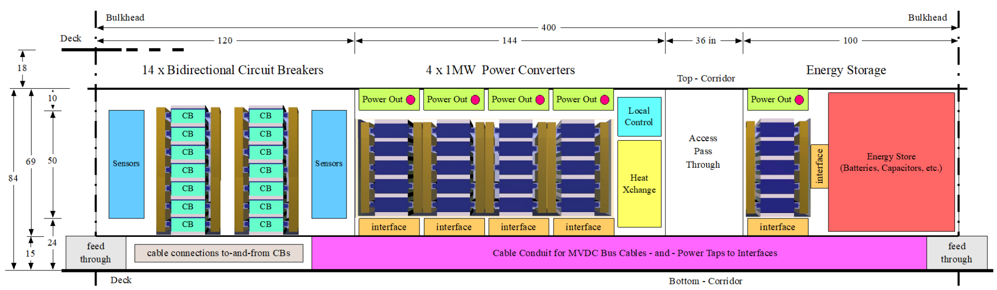

Figure 71: Power corridor interior layout with cables, fault protection, converters, and energy storage.

Hence within each bulkhead region along the length of the power cables a power corridor provides all connection protection and conditioning for loads within that bulkhead region. This is depicted in Figure 73.

To improve survivability there could be multiple power corridors in parallel, but in different locations across the ship. An example arrangement of four corridors of 20 MW each is illustrated in the ship cross-section view of Figure 74.

The length of the corridors would extend over a portion of the length of the ship, essentially where the loads and sources are located. Figure 75 depicts these possible corridor locations for a notional size ship.

Future work will evaluate in more detail the power connections and redundancy for improved survivability. For example, what is the impact of employ a N+1 design rule, meaning if there is a need for N elements to deliver power to any load then the design will incorporate N+1 elements. In this way if there is a single failure there is always immediate full power available to the operating loads.

The goal of this project is to determine the allocation of connections to cables in the corridor such that the load is balanced across cables and the proper number and size of cables are allocated to the power corridor for any given loading scenario.

Two simulation models were created to evaluate and contrast different designs from an operational and a spatial point of view. The results of these models are a load distribution along the Power Corridor's cables and the Power Corridor's geometry generated in a parametric CAD program.

Loads and generation are distributed throughout the ship. The topology of the system is designed so that the main bus can receive input at multiple separated points this way the system can be simplified as a bus bar or single cable system, as represented in Figure 73. The maximum power flow at any section will be less than the total aggregated load demanded and will depend on the arrangement chosen of generation

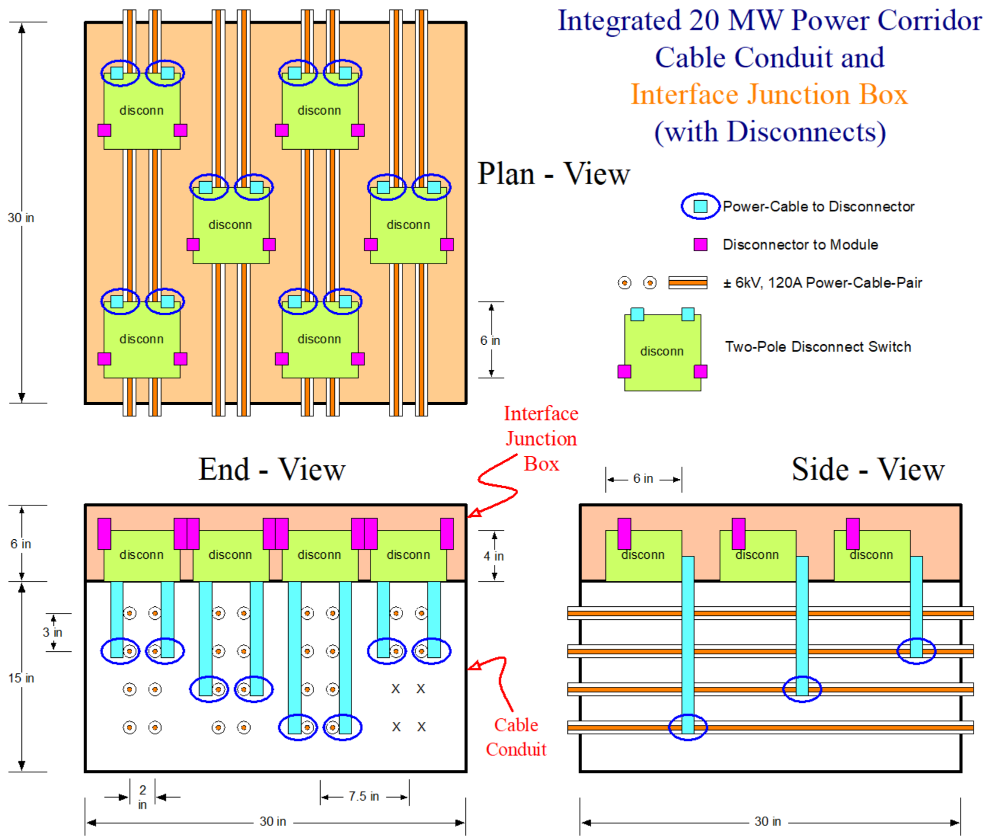

Figure 72: Interface junction box; cables to converters selection.

and load distribution, for each cable in the power corridor. A simple algorithm is applied to determine the maximum expected power flow in any section of the bus.

A second algorithm allocates the loads to the cables more uniformly and efficiently. The mission of this algorithm is to go through the most heavily loaded lines within a corridor, and check if there is equipment that is also connected to other underloaded lines through any other connections that it may be using, then shift some of the load to a more lightly loaded line. Thus, the excess amount of energy is distributed among the available least loaded lines in an iterative process.

The end result of this code is an even distribution of the power demand among all cables or at least the best possible configuration with this purpose in mind. Figure 76 shows the Maximum Expected Power Flow after executing the Balancing Algorithm.

In the next period we plan to collaborate with personnel with shipyard experience to further define key power corridor attributes that enhance construction efficiency, sailor safety, reliable performance and other value added characteristics. Furthermore we plan to explore the impact of energy storage on both the design of the power corridor and the overall power flow in the ship.

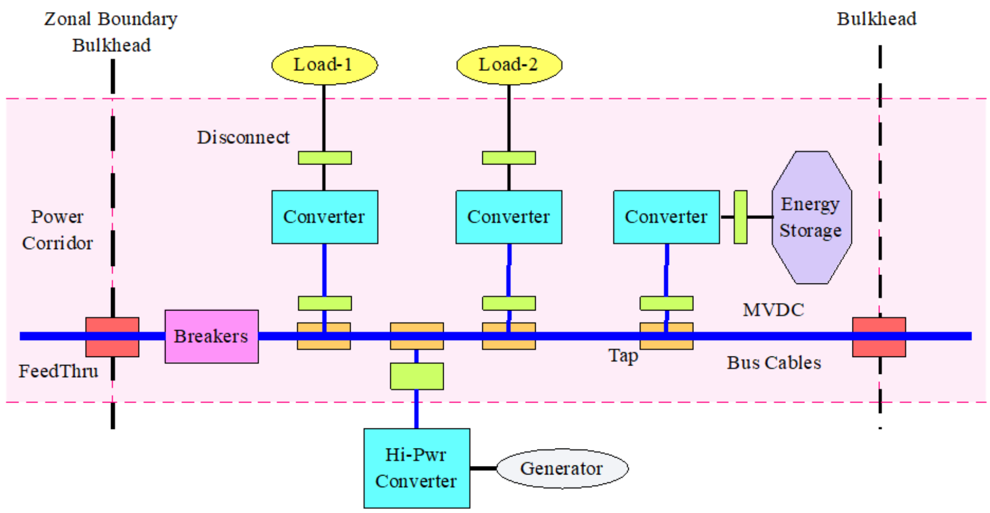

Figure 73: Illustration of connections within a power corridor.

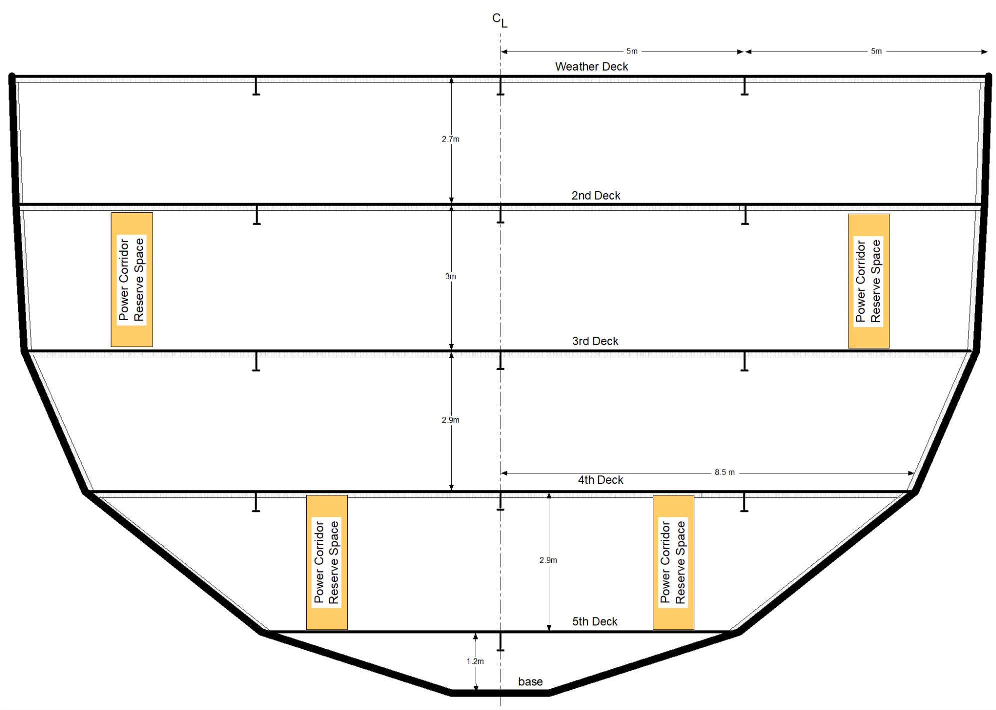

Figure 74: Possible location of four power corridors to improve survivability.

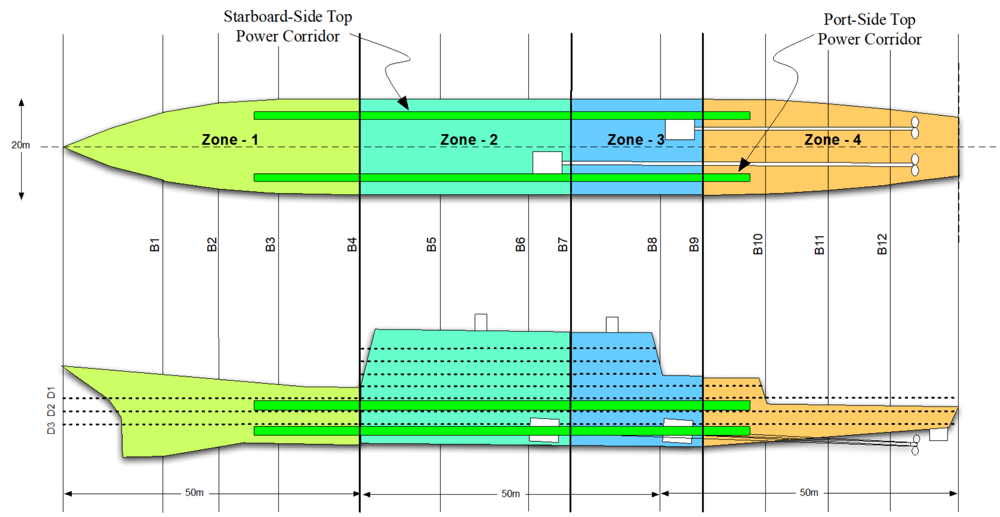

Figure 75: Candidate locations for power corridors on a notional ship.

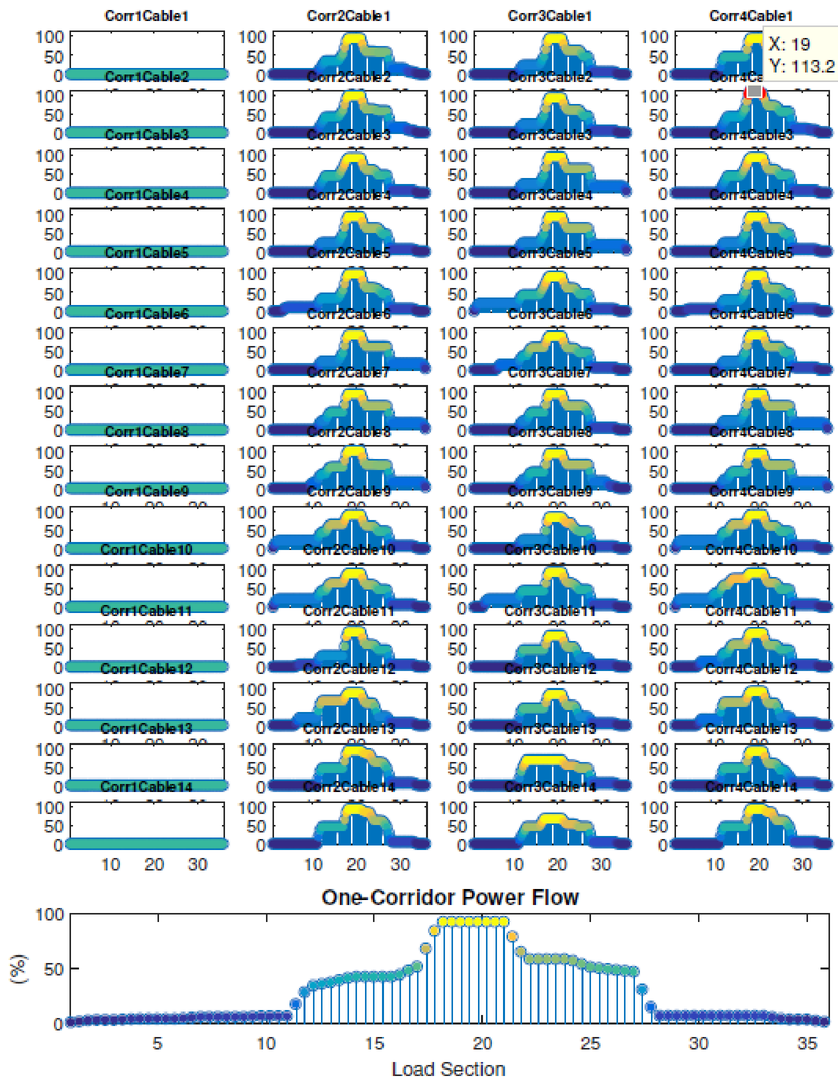

Figure 76: Maximum power flow along each cable in all corridors after performing load balancing algorithms.

Task: Achieve global thermal efficiency of electric ships through realizing timely and localized heating/cooling needs via a thermal bus

Technical Objectives

Design two fluid lines using high-fidelity multi-objective optimization: thermal interface interaction between high temperature line for heating and low temperature line for cooling will be optimized. The temperature of a hot-fluid loop may take advantage of available high energy density thermal energy storage; while the temperature of a cold-fluid loop will be sustained by chillers.

Technical Approach

- Design and build a lab-scale thermal bus.

Progress Statement Summary

A concept diagram of the thermal bus is shown in Figure 77.

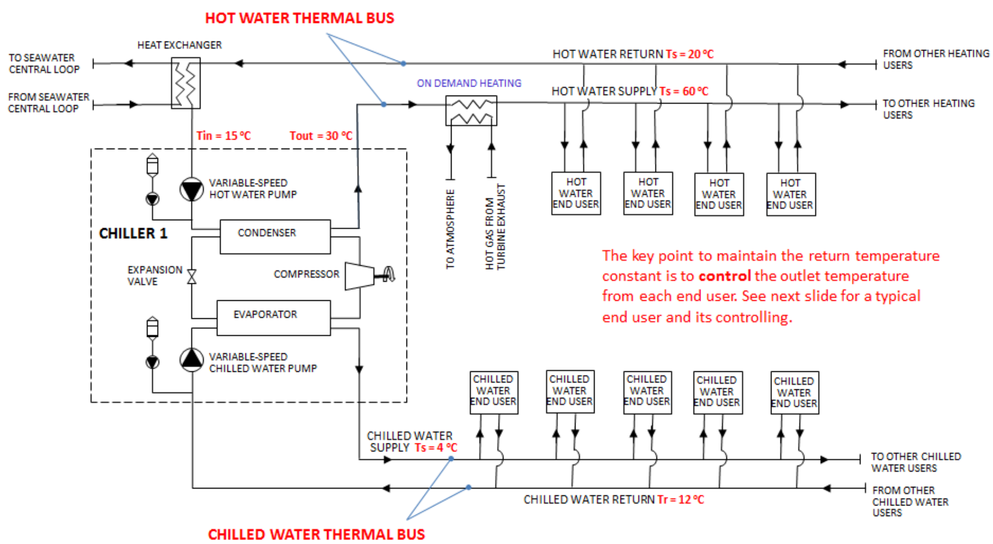

Figure 77: A lab-scale thermal bus and control algorithm.

A two-phase loop has been built, and will be operational within the next one to two months.

Thrust 3: System Management and Control Technologies

Technical Objectives

Develop control algorithms and methods that provide a variety of capabilities and desired features, such as power and energy management, system state monitoring, system stability management, equipment health monitoring, and fault management. The availability of a well-designed and tested system level control approaches is a prerequisite for a successful implementation of the CPES concept on future surface combatants. Recognizing the limitation imposed by communication latency, power system control approaches are focusing on coordinated local control to react to changes on the appropriate time scale. Control approaches are being developed that dynamically incorporate risk and changing priorities using faster, more versatile, and more affordable hardware.

Technical Approach

Conduct research in four major areas:

- Power and energy management.
- Thermal and electrical energy management.
- Fault detection, location, and reconfiguration.
- System-level common mode impact.

Progress Statement Summary

Current work reported herein includes:
3.1.1 Active power and energy management
3.1.2 Develop impedance-based control approaches for multi-converter systems
3.2.1 Develop heterogeneous control strategies for thermal and electrical energy management
3.2.2 Develop piping network configuration
3.2.3 Develop thermal control to improve reliability of PEBB-based converters
3.3.1 Develop resilient sensor systems
3.4.1 Develop fault detection and location (FDL) approaches at different levels of shipboard power system
3.4.2 Develop system-level fault recovery and soft start up methods
3.5.1 Develop methods to model common mode effects and means of integrating pertinent factors to de-risk ship designs
3.5.3 Impedance measurement unit for 4,160 V AC networks
3.6.1 Develop fault tolerant control (FTC) and fault mitigation
3.6.2 Develop fault-triggered reconfiguration solutions

The following projects are planned for future work:
3.3.2 Verification and validation approaches to operating and automation procedures
3.5.2 Active power and energy management

3.1.1 Active power and energy management

Task: Distributed adaptive power management

Technical Objectives

Develop advanced distributed control techniques for the power management layer of the next-generation shipboard power systems. The main requirement for the power management controllers is to regulate the power sharing among distributed resources (DR) and to ensure voltage stability throughout the distribution system.

Conventional droop control can be used to facilitate power sharing among resources in a DC distribution system. However, designing linear controllers such as PI for adjusting the droop parameters requires an accurate model of the system for control design, which cannot be readily derived due to model uncertainties, nonlinear load changes, and plug-and-play phenomena. Therefore, model reference adaptive control (MRAC) is proposed for adjusting the droop parameters in an online fashion to relax the modeling requirements of the system and adjust the control parameters to optimal values as the system operates. This task focuses on the development of MRAC control and their application to fulfill the system objectives via identifying the droop control parameters employed by DR along DC distribution systems.

Technical Approach

The MRAC control algorithm will be utilized for the distributed control algorithm in the power management layer. The step-by-step technical approach is elaborated as follows:

- Develop control architecture for distributed power management of DC distribution systems, proposed in Figure 78.
- Test MRAC algorithms in a notional simulation system to demonstrate controller parameter adaptation when dealing with model uncertainties or plant parameter changes.
- Apply distributed power management to notional system model for management of distributed energy resources.
- Validate control algorithms via experiment in a reduced-scale lab environment.
- Validate control algorithms in real-time simulation medium voltage system with controller hardware-in-the-loop and power hardware-in-the-loop techniques.

Progress Statement Summary

There are two main adaptive control techniques, which are the direct and indirect MRAC. In our previous research, the direct technique has been implemented in simulation and hardware for power management of a two-converter system [101]. To utilize the best of both adaptive techniques, we are currently focusing on the combined MRAC method, which employs both direct and indirect MRAC to improve the transient performance and robustness of ship power systems [102].

So far in the work, the combined MRAC method has been developed and proven stable via Lyapunov analysis. Simulation results on a notional plant validate these results, and show the method's ability to adapt the control parameters in response to varying parameters and plug-n-play conditions. The algorithm has also been applied to a two-converter system to demonstrate the power sharing and bus voltage regulation capabilities of the algorithm in a simulation environment [102]. The future work for this task includes analysis of the scalability and stability of the system in a multi-agent network, and implementation on the reduced-scale lab equipment for experimental testing of the algorithm.

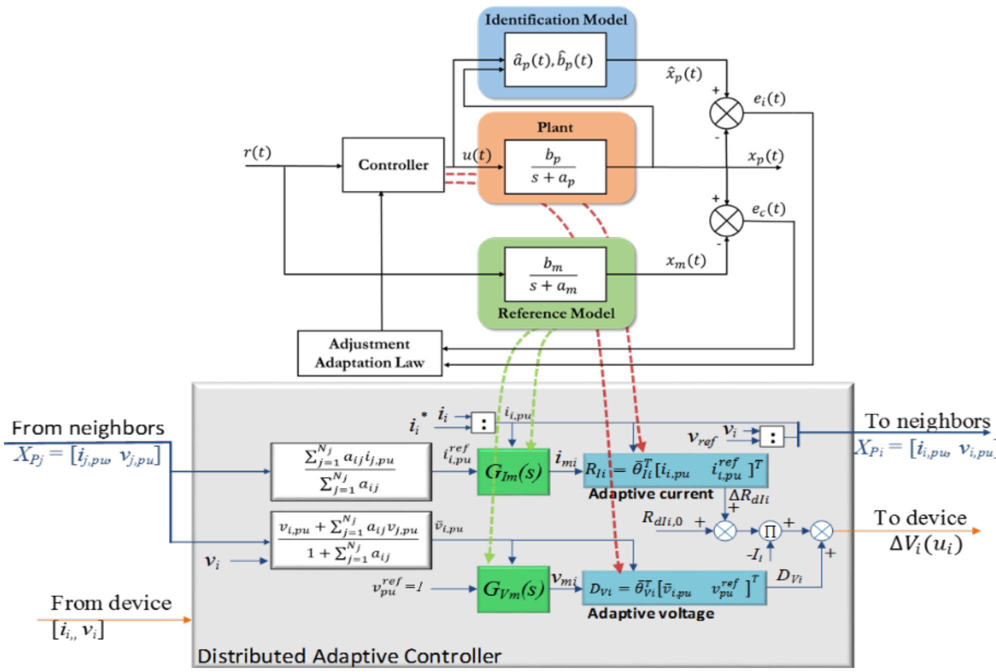

Figure 78: Distributed controller architecture.

Task: Distributed predictive energy management

Technical Objectives

Develop an energy management technique as an integral part of the control strategy developed for electric ships. The energy management layer is to ensure that load demand is met while also ensuring other objectives such as the optimal power flow. Distributed Model Predictive Control (DMPC) can provide an effective way for achieving an energy management scheme capable of coordinating a multitude of sources and loads while also providing resiliency towards any issues that may arise. When applying energy management to a ship power system, the scaling issue of DMPC presents itself. The hundreds, or even thousands, of electrical devices that are on a ship present a difficult task for an energy management scheme to coordinate their power flow effectively and in a timely manner.

DMPC techniques have been shown in a multitude of papers; however, approaching the problem of an effective scaling technique for the energy management in a large power system has yet to be tackled. Using a hierarchal-based DMPC can mitigate the scalability issues relating to the number of variables within the optimization, which correlates to a reduction in computational time, for the energy management [103]. By reducing the number of variables in an optimization, a reduction in computation time can be achieved.

Technical Approach

The hierarchical DMPC approach will be utilized in for the energy management layer. The step-by-step technical approach is elaborated as follows:

- Develop a centralized MPC approach for a reduced-scale ship power system that includes multiple energy storages.
- Develop a DMPC approach and apply it to the reduced-scale ship power system.

- Formulate the energy management problem for a notional ship power system that includes six zones and apply the DMPC technique.
- Devise and apply the hierarchical DMPC for the notional ship power system.
- Demonstrate the hierarchal DMPC utilizing a medium-voltage test system with controller hardware in the loop and power hardware in the loop techniques for the notional ship power system.

Progress Statement Summary

Energy management utilizing a combined heuristic and centralized MPC approach has been completed for reduced scale ship power system with a single energy storage [104]. The same approach has been extended to accommodate multiple energy storages in the reduced scale ship power system [105,106]. Current progress includes the formulation of a centralized MPC approach that does not need the heuristic part. The MPC can potentially take the appropriate action to ensure that load demand is met while attempting to satisfy the cost function objective. Current progress also includes the formulation of the DMPC approach for the reduced scale ship power system with multiple energy storage.

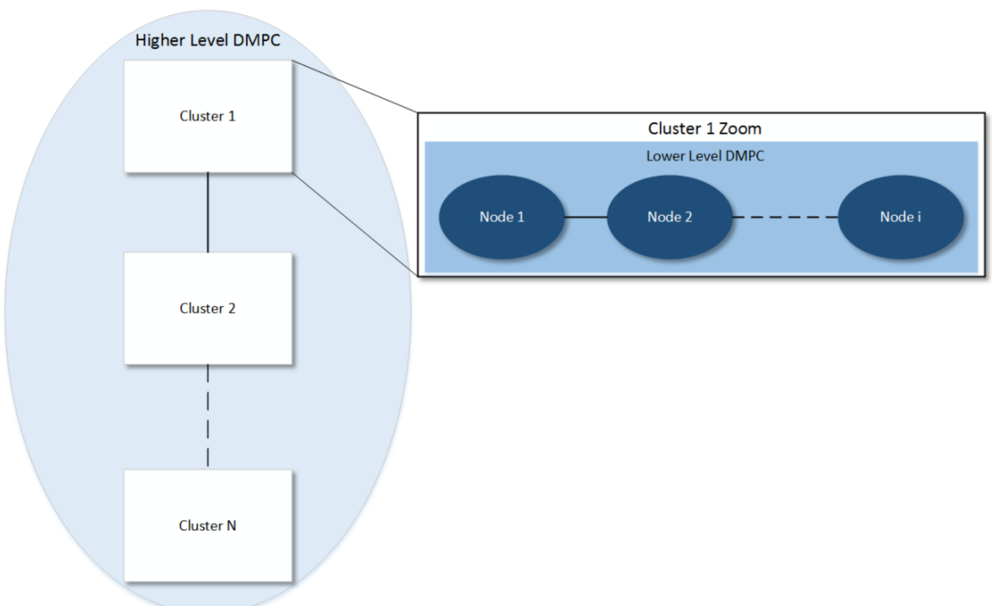

Figure 79: Hierarchical distributed MPC approach.

A centralized MPC has been applied for the entire Energy Management routine; the heuristics have been removed. Current progress includes the formulation of the DMPC approach utilizing a distributed optimization algorithm known as the alternating direction method of multipliers (ADMM) for a reduced scale ship power system with multiple energy storage. The energy management will utilize a distributed framework for the control that combines heuristics and DMPC. The DMPC, using ADMM, will be utilized to ensure the energy storages are charged optimally while the heuristics will ensure that load demand is met by the generators and possibly the energy storages, if needed.

Task: Develop power and energy management architecture

Technical Objectives

Develop a more generalized distributable optimization cost function for application in distributed power system control. This will require expansion of the time scale of operation for the control architecture as compared to that developed in [107] and, therefore, ensure its more general applicability for shipboard power system control. Toward this end, a distributable cost function formulation will be explored with the goal of maximizing power ramp rates by specifying coordination of power electronic converters in conjunction with energy storage systems. The optimization function will be developed to meet the requirements of a test system that consists of generation and energy storage interfaced to the system through power electronic converters.

Technical Approach

- Various system representations and cost function minimization algorithms will be explored to determine which are the most suitable given the zonal and bus level control architectures.
- The hard, real-time constraints will be considered along with relaxation methods of the timing constraints that can be provided by the stored energy in the system.
- This will also require detailed model development of the generator systems and energy storage module control.

Progress Statement Summary

Methods of expansion for the optimization cost function appropriate for energy ramp-rate maximization are currently under investigation.

This work has not been funded this year.

Task: Distributed model-based power management architecture for MVDC shipboard power systems

Technical Objectives

Conduct a performance analysis by comparing centralized and distributed control of global and partitioned MVDC model for two cases of continuous and discrete control inputs. In this work, we first propose a centralized Model Predictive Control (MPC) for a nonlinear Medium-voltage DC (MVDC) Shipboard Power System (SPS). MPC is a representative model-based approach that uses the system model to predict the future output states, and generates an optimal control sequence over the prediction horizon by minimizing an objective function subject to the system and operating constraints. Since the shipboard power system is an independent electric network without any external support, the centralized control structure may provide some limitations under battle mode or when dealing with sudden disturbances and errors due to its complicated framework, (i.e. one system, one controller). Especially, the model-based controllers can be prohibitive if a huge system model is used. In this work, we also propose a distributed control structure for a nonlinear MVDC SPS to develop power management architecture. In this framework, each subsystem is controlled by a model predictive controller using local state variables and parameters, as well as interaction variables from other subsystems shared through a coordinator.

Besides considering the local specifications, constraints, and stability criteria for each subsystem, there is also a convergence stability specification and a coupling constraint for the coordinator. The resulting distributed control structure brings out several significant advantages including a higher robustness and good error tolerance characteristics, higher system flexibility, and less computational complexity, as well as a good overall system performance. Reliability and maintainability could also be improved when compared with centralized controller. To demonstrate the efficiency of the proposed distributed approach, a performance analysis is accomplished by comparing centralized and distributed control of global and partitioned MVDC model for two cases of continuous and discrete control inputs.

Technical Approach

- Develop a Centralized Model Predictive Control of MVDC Shipboard Power System.
    1. Applying a nonlinear MPC approach on MVDC when we have pulsed loads in the system.
        (a) The comparison is accomplished for different cases for MPC, when we have:
            i. No prediction.
            ii. Perfect prediction.
            iii. ARIMA prediction with different delay for MPC controller.
        (b) Accordingly, an improvement factor is defined based on this comparison.
    2. Reconfiguration problem of the MVDC system based on MPC approach when we have constant load power changes (a load power increment or decrement).
        (a) The loads are categorized as vital loads, semi-vital loads, and non-vital loads.
        (b) The main goal is to maximize the power delivered to the loads with respect to power balance and generation limits.
- Develop a distributed control structure for a nonlinear MVDC shipboard power system.
    1. Each subsystem is controlled by a local model-predictive controller.
    2. In the coordinator level, an optimization problem is iteratively solved to update a Lagrange multiplier vector to have a global optimal solution.
    3. The control inputs can be either continuous or discrete by using two different optimization problems for MPC.
- Conduct a performance analysis by comparing a centralized control and a distributed control on the same model and considering different specifications in the MVDC system.
    1. Comparison between centralized control and distributed control.
    2. Comparison based on continuous control inputs and discrete control inputs with different optimization methods.
    3. Comparison based on different horizons.

Progress Statement Summary

Through the evolution of computer and network communication technologies, the distributed control approach offers important advantages over the centralized architecture that enable it to be more applicable to the various real-world problems. In distributed control structure, the centralized problem is decomposed into several local control units that compute their optimization problems in separate processors and communicate efficiently to reach a closed-loop system objective. In this work, for the distributed control purpose, each subsystem is controlled by a local model-predictive controller (MPC). MPC can handle the cost function in any form including nonlinearities or several control objectives, as well as different constraints. The optimization problem for each MPC is solved based on both local measurements, and the latest coordination parameters obtained from coordinator with respect to the subsystem's states and inputs constraints. The Goal Coordination principle is used for interacting information between subsystems. In the coordinator level, an optimization problem is iteratively solved to update Lagrange multiplier vector until the predicted interaction inputs from the local controllers are equal to, or sufficiently close to, the measured interaction inputs, and so global optimal solution is achieved. The maximum coordination error tolerance value ε is defined as a stopping criterion, so, when $\varepsilon \to 0$, the algorithm converges to the optimal solution.

As a case study in the simulation section, the global 37 states nonlinear MVDC model is divided into two subsystems, and the performance analysis of a distributed structure is investigated with comparison to the centralized method for both continuous and discretized control inputs. The model of subsystem one contains the main turbine generator, zonal load 1, zonal load 2, and one electrical propeller. The model of subsystem two includes the auxiliary turbine generator, zonal load 3, zonal load 4, and an energy storage device. The objective of centralized MPC and each local MPC controller in the distributed case is to meet the voltage performance requirement of maintaining the bus voltage in 5000 VDC, with as small as possible changes in the control inputs. The droop gains and the power reference for each generator are defined as control inputs. In the distributed structure, the interaction variables between subsystems are currents of generators, loads, and the energy storage. It is demonstrated that by applying distributed control approach, we have less computational complexity, as well as a good overall performance.

In this reporting period, we continued the previously proposed distributed model-based power management framework development to improve various aspects of the MVDC shipboard power system performance [108]. More specifically, our research focus was on examining and demonstrating if the proposed distributed control paradigm can provide structural and performance-wise advantages over the centralized architecture as in a distributed control structure, the originally centralized problem is expected to be decomposed into several local control units that can be solved in parallel and communicate iteratively to reach a converged, closed-loop system objective. For the distributed control purpose, each subsystem is controlled by a local model-predictive controller (MPC). MPC can handle the cost function in any form including nonlinearities or several control objectives, as well as different constraints. The optimization problem for each MPC is solved based on both local measurements, and the latest coordination parameters obtained from coordinator with respect to the subsystem's states and inputs constraints. The Goal Coordination principle is then used for interacting information between subsystems. In the coordinator level, the Multi-Step Gradient method is employed for updating Lagrange multiplier vector to achieve an optimal solution. The maximum coordination error tolerance value ε is defined as a stopping criterion, which, preferably, needs to be close to zero [109].

As a proof-of-concept, the control design for a 37-state nonlinear MVDC model has been completed in the reporting period. A reduced-order MVDC model has been divided into two subsystems, and a performance analysis has been conducted by comparing centralized control [110,111] and distributed control on the global and partitioned MVDC models for two cases of continuous and discrete control inputs. In the experiment, the objective of the centralized MPC and each local MPC controller in the distributed case is to meet the voltage performance requirement, with minimal changes in the control inputs. The droop gains and the power references for each generator are defined as control inputs. The droop gain control is applied to determine the power sharing between energy sources while the power references determine the desired operating status of the generators onboard. In the distributed structure, the interaction variables between subsystems are currents of generators, loads, and the energy storage. The simulation results obtained from this experiment demonstrated that the proposed distributed control structure has less computational overhead and a good overall performance. This evidence further emphasizes the importance and necessity of adopting distributed structure on the control design to fit the zonal distribution system. This research has been reported in [109] and [111].

Currently, we are working on improvement of the coordination algorithm in the proposed distributed power management architecture for the MVDC ship power system. One of the advanced coordination algorithms that we are using is the Alternating Direction Method of Multipliers (ADMM). We are also working on improving nonlinear optimization algorithms for local MPC controllers to become more efficient dealing with nonlinear models and uncertainties in the model [112]. Moreover, an efficient load prediction will be considered in the distributed power management architecture proposed for the MVDC system.

Current progress includes considering stability analysis in the mathematical formulation of nonlinear centralized MPC by designing terminal state penalty matrix of the terminal cost term in the objective function for the 37-state nonlinear MVDC model previously developed. The setup includes a terminal inequality constraint that forces the states at the end of the finite prediction horizon to lie within a prescribed terminal region. The size of the terminal region depends generally on the nonlinearity of the system to be controlled. Currently, we are working towards the stability analysis and the improvement of coordination algorithm in the proposed distributed power management architecture for the MVDC ship power system. We are also evaluating how vertical and horizontal control techniques can be adopted for operating a multi-zone and multi-level shipboard microgrid as to ensure the effective collaboration among the multiple distributed zones, distributed approaches should allow distributed control decisions to collectively determine the energy allocations within the system as well as the global point of interest.

3.1.2 Develop impedance-based control approaches for multi-converter systems

Task: Develop impedance-based control approaches for multi-converter systems

Technical Objectives

Develop control algorithms and methods that provide power and energy control, system state monitoring and system stability management. The Combat Power and Energy System (CPES) concept is critically dependent on the control systems that manage the ship power and energy under a wide variety of conditions and for different missions.

The all-electric ship power distribution system is enabled by switching power converters. The proper operation of the system requires coordinated controls and knowledge about the system state. Switching converters can be used to probe system impedances by using virtual network analyzer techniques — perturbation is introduced in the switching converter control and the system response provides the desired system impedances. This opens the possibility of real-time state monitoring and control adaptation. Techniques and algorithms will be developed to incorporate these novel capabilities in the CPES distributed control. Additionally, multi-converter systems have multiple control loops and there is a strong possibility of adverse control interactions when a large system is put together. The proposed research activity is to develop a multi-converter control design method that guarantees stability and performance under varying operating and mission conditions.

The research will yield a robust control approach for the CPES multi-converter system based on impedance measurement and control adaptation. The enhanced robustness will ensure proper operation under a variety of operating conditions and scenarios.

Technical Approach

- Use virtual network analyzer techniques to locally probe system impedances using existing converters.
- Develop techniques to measure the overall bus impedance based on multiple converter impedance measurements.
- Use impedance information for system state monitoring and control adaptation.
- Develop control design method that guarantees stability and performance under varying operation and mission conditions.
- Explore various centralized and decentralized control architectures for the CPES multi-converter system.

Progress Statement Summary

The conceptual multi-bus system shown in Figure 80 has been studied. Stability of the overall system can be analyzed based on the individual bus impedances, which consists of the parallel combination of all source and load subsystems seen from each DC bus. The Passivity-based Stability Criterion (PBSC) provides a sufficient condition for stability; if each of the bus impedances are found to be passive at all frequencies, the system is stable. This implies that the Nyquist contour of the bus impedances must lie entirely on the right half plane in the S-domain. This criterion was proved to be effective in analyzing the overall stability. However, it does not provide any information regarding the dynamic performance, and a system satisfying the PBSC might exhibit undesirable oscillations during transients. To overcome this limitation, the Allowable Impedance Region (AIR) has been proposed. This concept is also based on the Nyquist contour of the bus impedances, and it states that if the contour lies completely inside a specified region in the Ss-plane, then the system will exhibit a minimum damping for oscillations.

The AIR was also implemented for the design of a stabilizing controller, leading to a method to calculate the damping impedance required to achieve desired dynamic performance. This damping impedance is then inserted into the system via Positive Feed-Forward control. Analysis of the bus impedances resonance leads to the appropriate PFF implementation on the system. This research effort has been described in [113,114].

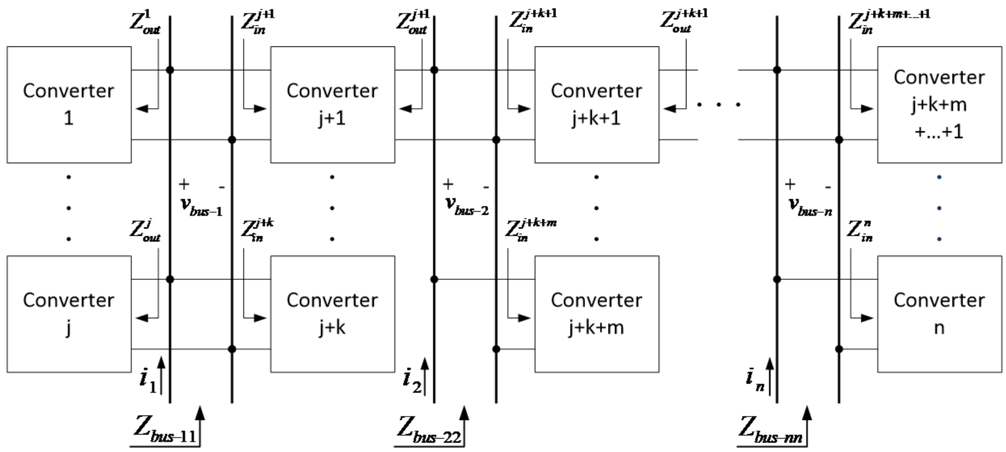

Figure 80: Conceptual multi-bus MVDC system.

Measurement of system impedances is critical for stability analysis and controller design. This is accomplished using online wideband identification techniques. Specifically, small-amplitude Pseudo Random Binary Sequence (PRBS) is used as an approximation to white noise for simultaneous excitation of a broadband set of frequencies. The desired impedances are then extracted through Fourier-based post processing of the measurement results [115]. This principle is shown in Figure 81, for the case of a single source and single load converter.

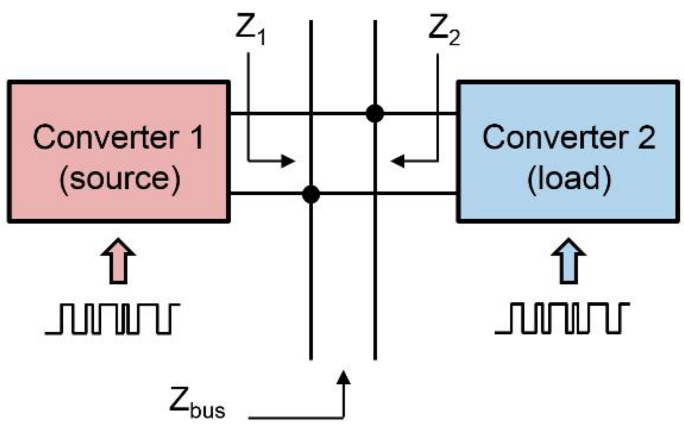

Figure 81: System impedance measurement principle.

In an interconnected system, the mentioned technique can be utilized to obtain the bus impedance by identifying the impedances seen by each converter connected to the bus and combining them together to obtain the overall bus impedance. This requires multiple measurement cycles with converters perturbed one at a time to avoid measurement interference, which makes the overall procedure tedious and time consuming. Additionally, the operating conditions may vary between different measurements, making the overall calculated impedance inaccurate. To overcome such limitations, the possibility of simultaneous measurement of all impedances in a multi-input/multi-output (MIMO) interconnected system is studied. To this end, orthogonal binary sequences are used instead of simple PRBS excitation sequences. Due to orthogonality, the injected sequences excite different frequencies and thus any cross coupling among converters is avoided. Therefore, relying on this method, all the system impedances can be obtained in a single cycle of measurement. This implies that the overall measurement time is significantly reduced. Furthermore, utilizing the proposed MIMO identification technique guarantees no variations in system dynamics between measurements. Therefore, using this method any possible distortion in the system bus impedance measurement is avoided.

We have described the use of impedance-based methods for shipboard DC power distribution in [116]. We have proposed the use of orthogonal pseudo-random binary sequences for bus impedance identification in a DC power distribution system [117, 118]. These sequences are injected into the controls of existing power converters in the system creating a small-amplitude perturbation that can be used to measure the impedance looking out from each converter. Since each sequence excites different frequencies due to orthogonality, all the measurements can be performed at the same time and then the bus impedance is constructed as in 13, where n is the total number of power converters connected to the same bus and $Z_i (i = 1, ..., n)$ is the impedance measured by perturbing the ith converter.

$$Z_{bus} = \frac{1}{n-1}\left(\frac{1}{Z_1} + ... + \frac{1}{Z_n}\right) \tag{13}$$

The proposed technique was implemented in the system depicted in Figure 82. A source buck converter controls the bus voltage and a voltage source inverter feeds a resistive load. This system was constructed in the laboratory using custom designed IGBT-based switching converters. The two perturbation signals are applied at the same time to the control reference of each converter and the impedances Z_{in} and Z_{out} are measured simultaneously. These measurements are shown in Figure 83 (a). The bus impedance is then constructed using equation 13 and is depicted in Figure 83 (b).

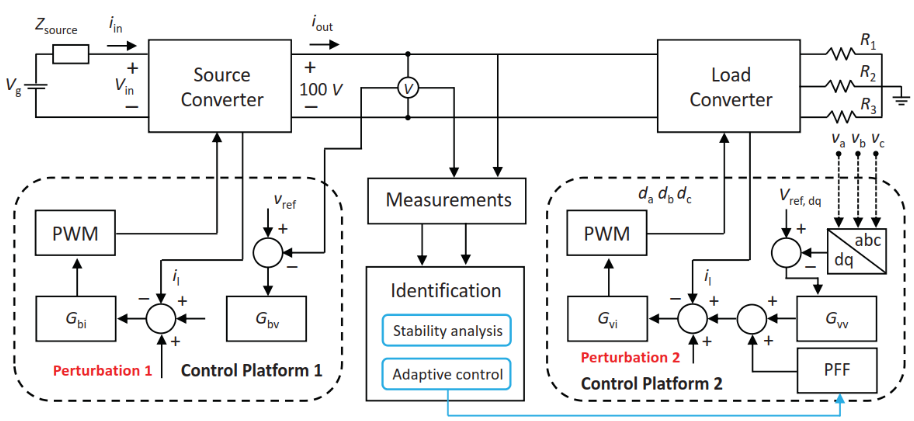

Figure 82: System under test.

Stability of the system was analyzed based on the measured bus impedance using the Passivity Based Stability Criterion (PBSC) and a stabilizing controller was implemented via Positive Feed-Forward control [113, 114]. The controller was designed to satisfy also the Allowable Impedance Region (AIR) criterion to achieve a desired dynamic performance imposing a minimum damping for bus oscillations. Improvement in the transient response after a step change in the load voltage is shown in Figure 84, validating the effectiveness of the controller.

The orthogonal pseudo-random measurement technique can also be applied to three-phase systems [119].

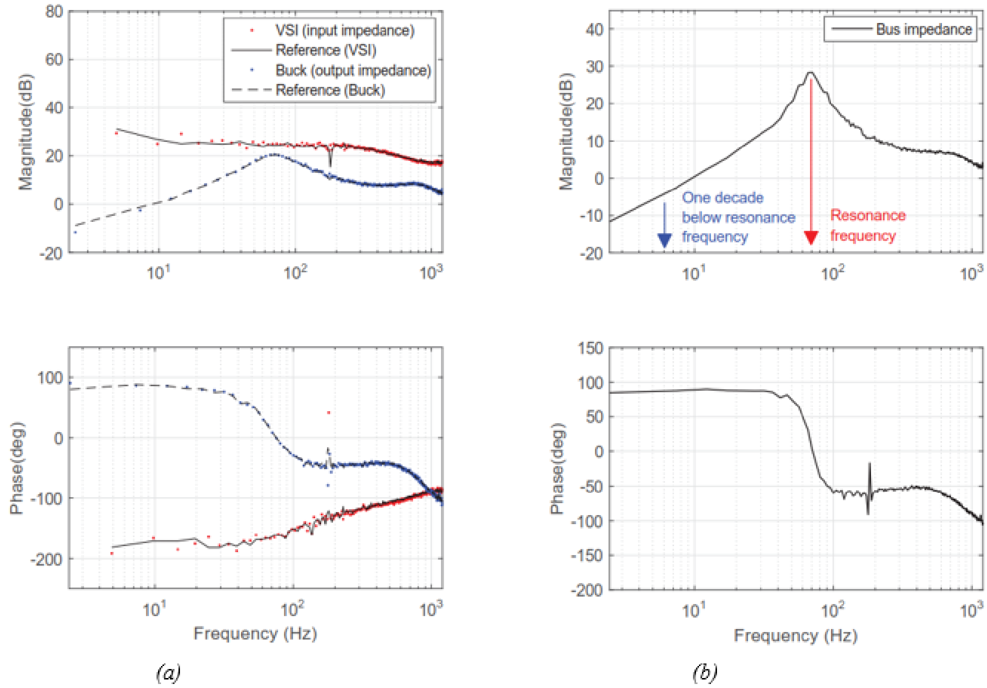

Figure 83: (a) Measured Z_{in} (red) and Z_{out} (blue); (b) bus impedance.

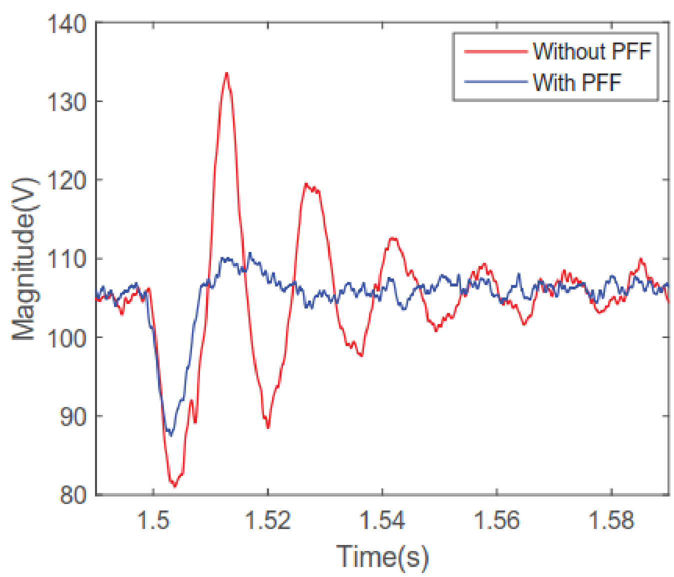

Figure 84: Transient response after a step change in the reference voltage of the load VSI.

3.2.1 Develop heterogeneous control strategies for thermal and electrical energy management

Task: Thermal anticipation

Technical Objectives

Develop thermal control strategies that, through thermal anticipation, prepare the ship's thermal management system to survive events of high cooling demand associated with pulsating loads.

Technical Approach

- Develop accurate modeling of integrated multi-physics phenomena in ship systems that benefit from thermal anticipation (e.g. pulse loads).
- Develop model-based control strategies to maximize system availability under constrained cooling.
- Investigate expansion of thermal management capabilities brought about by thermal anticipation strategies.
- Develop multi-objective optimization of dedicated cooling system control strategies for pulse loads.

Progress Statement Summary

In the context of modeling of integrated multi-physics phenomena in ship systems that benefit from thermal anticipation, a dynamic multi-physics model of a railgun is under development, based on the electromagnetic model presented in [120]. Current progress includes the mathematical formulation of a 2D spatiotemporal thermal model for the rails and cooling channels, which will be coupled to the electromagnetic model and solved to obtain non-uniform current and temperature distributions.

A dynamic multi-physics model of a railgun is under development. The current progress includes the investigation of the effects of heat exchanger design and coolant mass flow rate on railgun cooling performance [120]. As a follow-up work, we are starting to investigate the effects of channel location and thermal anticipation on the thermal management of multi-shot situations.

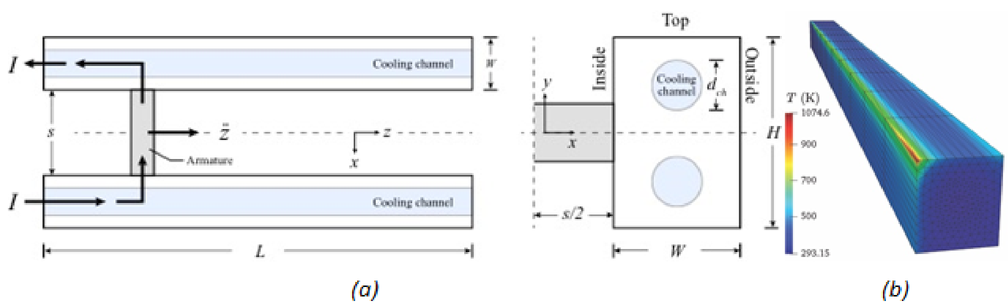

Figure 85: (a) Schematic diagram of a notional railgun where the current path is illustrated by the solid arrow lines; and (b) temperature field after the first shot.

We conducted a study based on a quasi-3D multiphysics model of a notional all-electric ship electromagnetic launcher (EML) and a dynamic parallel-low heat exchanger (PFHX) model to devise effective thermal management strategies for naval EMLs [121]. We deduced the following from our study:

1. Thermal diffusion effectively assists the cooling channel with peak temperature reduction, and its contribution to the determination of optimal channel allocation is non-trivial.
2. Improvement in cooling performance is not always directly proportional to larger heat exchanger size and higher low rateŮincreased low rate and NTU only result in higher pumping power as well as heat exchanger cost and volume without significant improvement in cooling performance beyond the optimal design and operating point.
3. Placing the cooling channel close to the initial hot spot in the rail yields inferior cooling performance at high mass low rate with 10 s of cooling and exacerbates the heat-reversal effect.
4. Optimal cooling channel allocation must therefore base on the given mass low rate and cooling period Ůplacing the channel near the initial hot spot is favorable for lower mass low rates and shorter cooling periods, whereas channels should be placed at the rail center for equidistant heat low from all four corners in the opposite case.

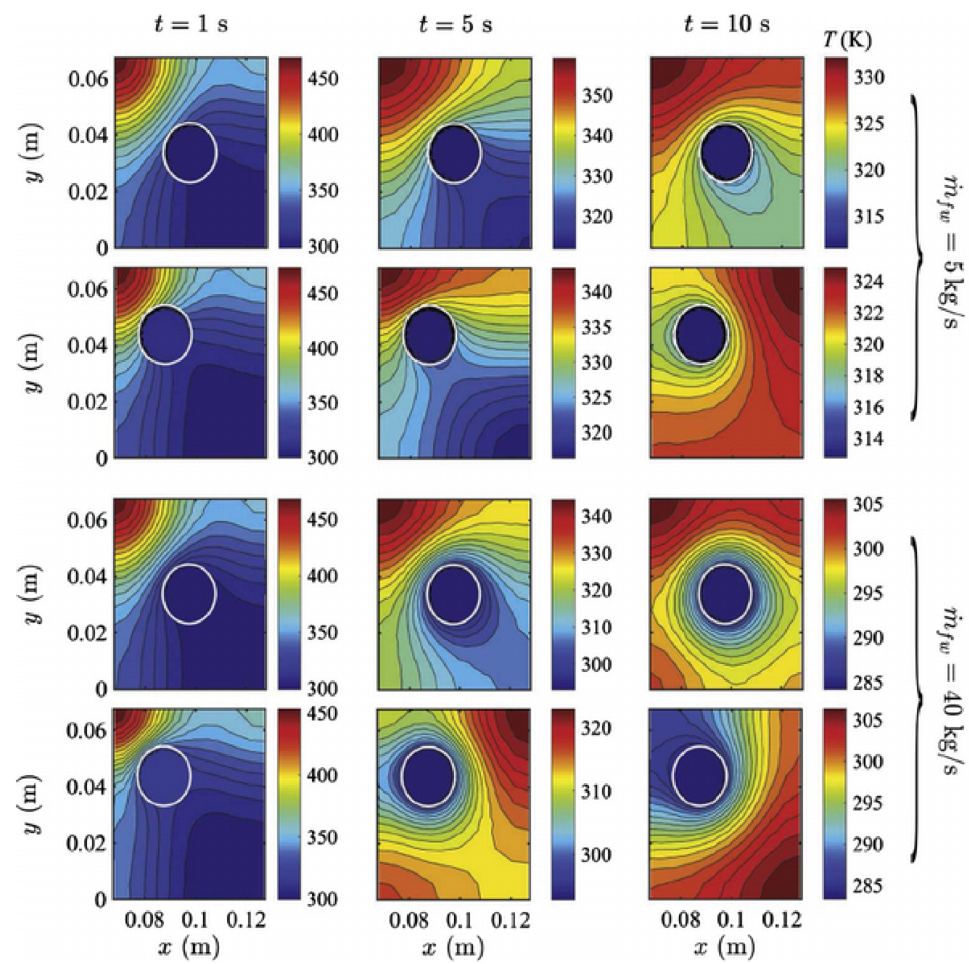

Figure 86: Temperature contours in the rail cross section at z=0 m, as a function of time for different coolant flow rates with centered and eccentric channel allocations.

Task: Thermal management system concepts utilizing common interfaces with generation, mission load, and energy storage devices

Technical Objectives

Develop efficient automation of cooling systems for future ships to ensure efficient and safe operations. Pump and valve automation is important to reduce the risk of machinery/load blowout because of the fast change on ship operating conditions, thereby the fast change in the load heat. The traditional cooling control utilizes the open and close of the valve to control the cooling. It means the valve is open when cooling is needed, and it is off when cooling is not needed. Over this course, the motor of the pump is working all the time and the valve has only two states (ON and OFF). Additionally, flow rate control can be also done through throttling of the regulator. Unnecessary energy is consumed in the above two ways. Control, automation, and optimization enable the cooling system to generate the needed flow rate while saving electricity. In synthesizing the thermal controllers for the cooling system, there are competing performance objectives, such as achieving the desired thermal performance and reducing the power consumed by the cooling system actuators (e.g. pumps and valves), that need to be optimized. Therefore, in this work, we will develop electrothermal control strategies that harmonize both the thermal and electrical aspects in ship power systems.

Technical Approach

Achieve the above management objective by:

- Develop a multi-objective optimization algorithm to determine the water routes that transport cold water from the cooling units to the loads (vital and/or non-vital loads).
- Develop the control strategies and distributed control for pump flow-rate regulation.
- Determine the reconfiguration solution to assure the system reliability in the case of pipe damage or pump/valve failures.
- Develop the optimal control of distributed cooling system for the overall shipboard system (develop an automatic flow control of shipboard chilled water, beneficiating from the ESRDC equipment database for control strategy design and validation).
- Verify the algorithms via real-time simulation, experiments, CHIL, and PHIL.

Progress Statement Summary

The work is under development. Currently, we are focusing on utilizing the sequence based control (SBC) for solving the multi-objective cost function of the systems of power converters. The systems of power converters can be shown in Figure 87.

The cost function that reflects the electro-thermal characteristics can be shown as

$$minJ_{ET} = w_E J_E(s) + w_T J_T(s) \quad s.t.s \in S \tag{14}$$

where i denotes the converter index, n is the total number of converters, s is the switching state of a converter, S is the feasible set of s, w_E is the electrical weight constant, w_T is the thermal weight constant, $J_E(s)$ is the cost function related to the electrical performance, and $J_T(s)$ is the cost function related to the thermal performance.

As a result, the solution of the electro-thermal cost formulation of the proposed SBC will be the optimal switching sequence applied in each converter of the ship power systems. Future work will focus on the development of SBC for the electro-thermal optimization of the ship power systems.

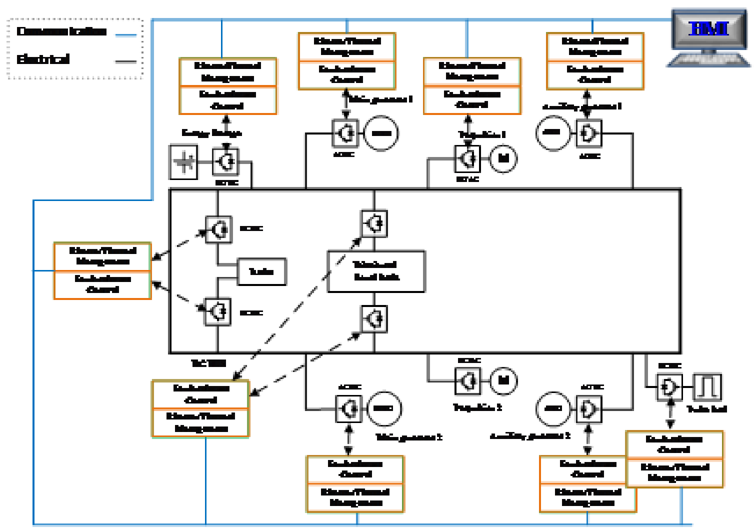

Figure 87: Notional ship system with hierarchical objective.

Task: High fidelity scalable thermal/fluid models are needed to realize precise temperature control and energy efficiency

Technical Objectives

Experimentally validated models will be developed to predict required flow rate and pumping power, particularly under dynamic working conditions.

Technical Approach

To realize this target, a test setup that is capable of enabling and measuring dynamic two-phase transport needs to be established and calibrated.

Progress Statement Summary

A dynamic two-phase transport test rig has been designed, constructed, and calibrated. A set of dynamic two-phase transport tests has been conducted at 10 kHz. Transient temperature, flow rate, pressure drop with synchronous visualization capability will be used to develop dynamic thermal/fluid models.

3.2.2 Develop piping network configuration

Task: Develop piping network configuration and equipment placement implications on thermal management

Technical Objectives

Develop robust, reconfigurable ship piping network configurations that contribute to survivability, load management, and reduced pumping power.

Evaluate implications of equipment placement decisions on ship thermal management. Component temperatures are affected by thermal interactions with surrounding environment and equipment. These complex interactions affect component performance.

Technical Approach

- Develop an algorithm that provides the optimal piping network configuration for a given set of loads (size, location, required cooling, etc.) and operating conditions.
- Implement an algorithm into vemESRDC to account for the energy interactions between the components and their surroundings, and integrate the algorithm into S3D.
- Devise concrete strategies for optimal equipment placement within an all-electric ship as follows:
  1. Develop a model to investigate the mutual thermal interactions between components and their surroundings, and quantize the inefficiency based on the generated entropy.
  2. Find the optimal equipment placement by employing the entropy generation minimization approach.
  3. Experimentally demonstrate the assets of the approach.

Progress Statement Summary

Concrete integration strategies have been devised for the integration of SMCS [122] with vemESRDC [123] to generate the piping network topology according to user-provided ship geometry, equipment locations, and operating conditions. An exergy destruction minimization method for determining different optimal network configurations based on graph theory is being developed. Current studies are focused on determining an objective function that can be defined in terms of energy while appropriately capturing the physics of the network and its topology.

vemESRDC and SCMS have been integrated to generate the piping network topology according to user-provided ship geometry, equipment locations, and operating conditions [124]. Figure 88 depicts the temperature distribution and piping network generated by the integrated tool for a notional all-electric ship. We are currently working on the selection and implementation of an appropriate graphics algorithm to ensure that all pipes are generated within the ship structure characterized by curved surfaces.

A dimensionless model of a notional all-electric ship integrated energy system constituted of three loads (i.e., two pulsating and one fixed), heat exchanger, chilled water unit has been developed. The primary objective of this work is to determine the optimal flow configuration based on entropy generation minimization as a function of mass flow rate distribution and flow configurations (i.e., serial and/or parallel flow). We plan to incorporate concepts from graph theory (see Figure 89 and advanced optimization algorithm (e.g., ant colony optimization) to solve the optimization problem.

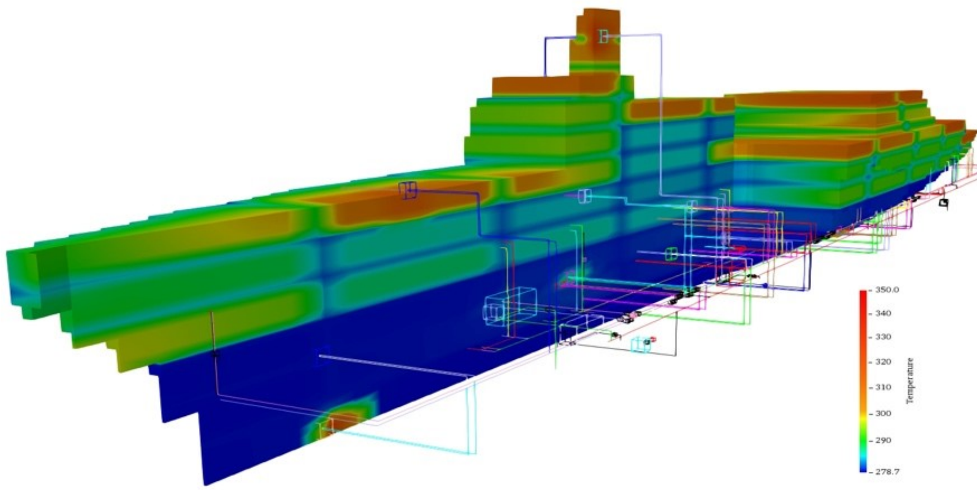

Figure 88: Temperature and piping network distributions in a notional all-electric ship obtained with integrated tool; note that this ship has been partially sliced along the centerline.

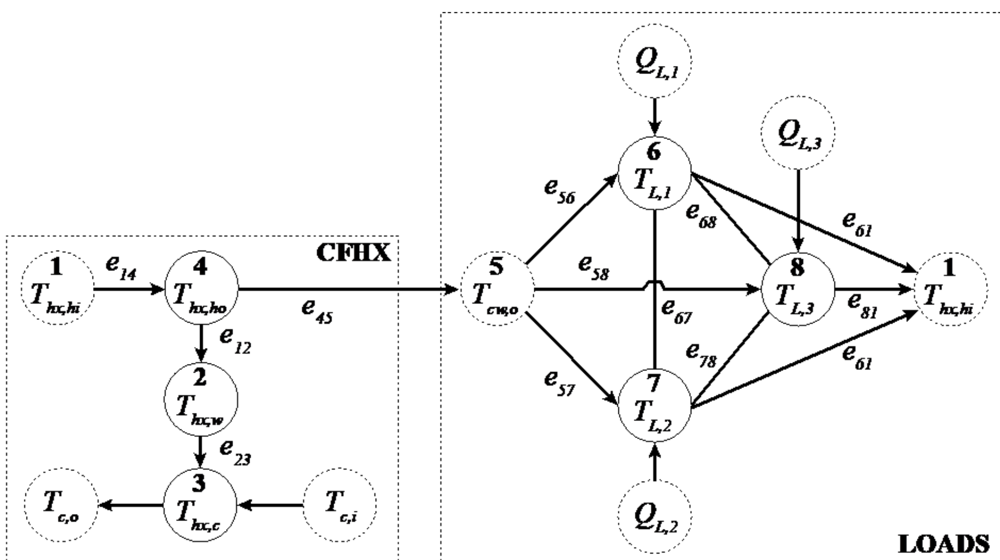

Figure 89: Graph representation of a notional all-electric ship cooling network.

Task: Shipboard integrated cryogenic system development

Technical Objectives

Develop the concepts for a centralized large cryogenic system to serve the cooling needs of various superconducting power devices to achieve system-level efficiency, operational flexibility, and higher efficiency.

The concepts developed identify technology gaps that need to be addressed to facilitate research and development investments focused in the areas of high power density superconducting cables and other machinery for integrated MVDC power systems.

Technical Approach

- Incorporate HTS devices into S3D to enable assessment of system-level benefits on MVDC ships.
- Develop models to study various aspects of integrated cryogenic systems and the benefits of integrating HTS devices with a large centralized cryogenic system.

Progress Statement Summary

Significant progress has been made by the ESRDC team working on the incorporation of HTS components into S3D. Through regular biweekly meetings, practical approaches are being devised to quickly incorporate pertinent attributes of HTS cables into S3D to allow for assessment of system benefits of installing them on future MVDC ships.

CAPS has made progress in developing a system model for studying a set of HTS devices cooled by a centralized cryogenic system. The results will be presented at the ESTS 2017 conference.

The focus for this reporting period was the development of coupled cryogenic thermal and electrical models for transient analysis of superconducting power devices with integrated cryogenic systems. System level benefits of integrating multiple HTS devices and the necessary cryogenic circulation systems in a closed loop configuration are studied. The integrated approach allows system level optimization and enables taking advantages of the tunable power rating of HTS devices. The integrated system also allows directing the cooling power as needed to serve particular mission scenarios and offers significant benefits in ship system design options and operational flexibility. The versatility of the modelling methodology is demonstrated using several case studies involving a system with an HTS generator, an HTS motor, and a power cable. The case studies conducted study show that the hybrid systems minimize the required total cooling power and also give the flexibility in terms of obtaining the most cooling power from cryocoolers. In case of cryogenic system failures, how the two cryogens, GHe and LN2, differ in terms of evolution of temperature was studied.

The effort on incorporating HTS devices into S3D to enable assessment of system level benefits is being performed as part of a collaborative effort among the ESRDC member teams (MIT, USC, FSU, MSU, and UT) with contributions from Georgia Institute of Technology and NSWC Philadelphia. The progress on this effort is included in the report for Projects 5.1.1 and 5.1.2.

We have made significant progress on the effort in developing models to study various aspects of integrated cryogenic systems and the benefits of integrating HTS devices with a large centralized cryogenic system. The development of coupled cryogenic thermal and electrical models for steady state and transient analysis of multiple superconducting power devices with integrated cryogenic systems continued in this reporting period. The idea of cryogenic thermal storage (illustrated in Figure 90) in the form of solid nitrogen (SN2) in superconducting cable terminations was explored (see Figure 91 to enhance resiliency of the power system and to provide enough time to continue operating the cable while contingency plans are activated.

An abstract has been submitted to the 20th International Cryocooler Conference to be held in Burlington, VA during June 18-21, 2018. A paper is under preparation to submit to the proceedings.

A more detailed Finite Element Analysis of superconducting cable terminations with SN2 storage is being developed. The results will be presented at the Applied Superconductivity Conference 2018 to be held in Seattle, WA during October 28-November 3, 2018.

The MS student (Sharath Satyanarayana), who worked on the development of thermal network models has completed his work and started writing his thesis. He is expected to graduate in August 2018.

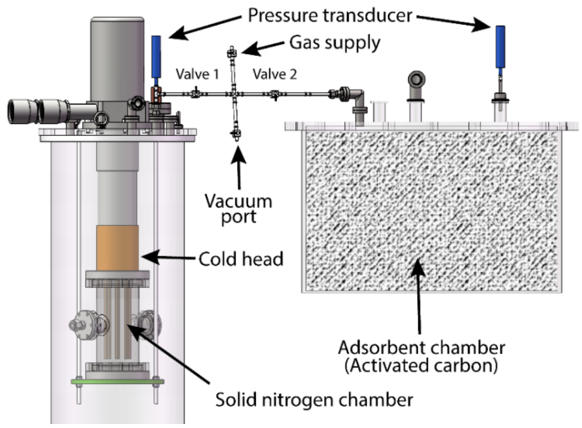

Figure 90: Experimental setup of cryogenic thermal storage system for solid nitrogen.

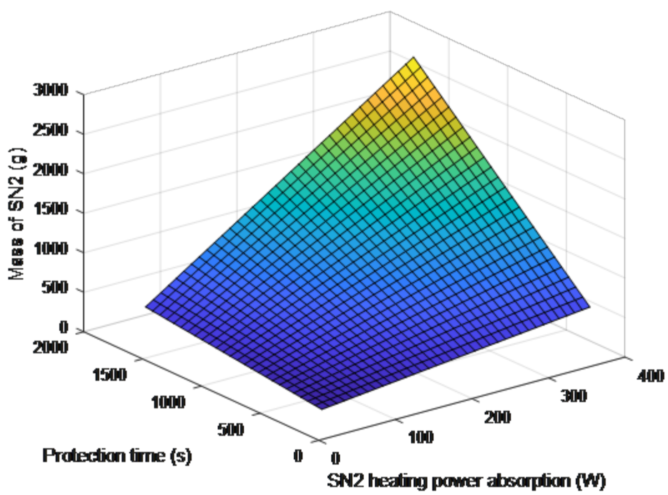

Figure 91: Time allowed for the protection of the HTS system based on given mass and heat absorbed by solid nitrogen.

We developed a dimensionless model for the heat transfer and fluid flow optimization of an HTS superconducting cable. The numerically calculated DC cable heat leak rate under different environmental conditions was initially adjusted and then experimentally validated by direct comparison to actual experimental data. Then, the experimentally validated model was used to perform the DC cable design and operating parameters optimization in order to obtain minimum heat leak rate and pumping power (or total consumed power). By adopting a fixed cable cross sectional area constraint (or total volume for a given length).

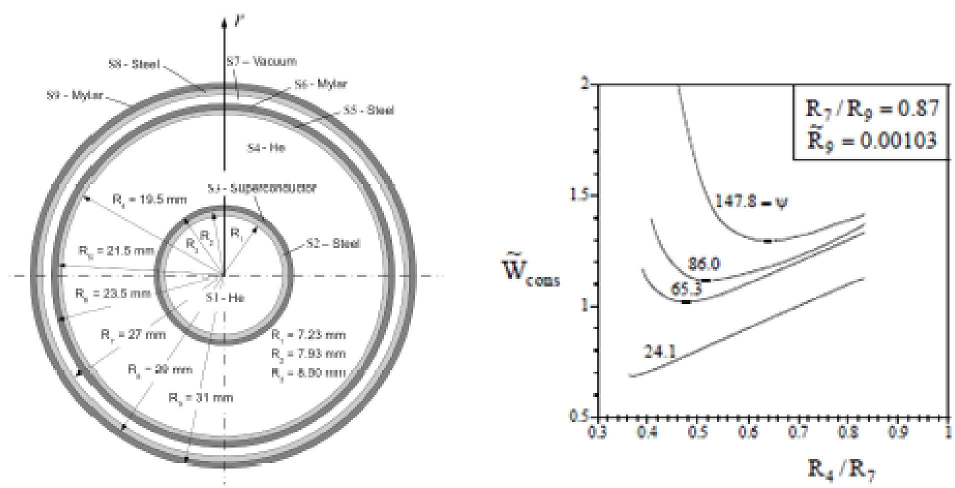

(a) (b)

Figure 92: (a) The superconducting cable cross sectional area layers distribution in the radial direction; (b) the minimization of dimensionless total consumed power with respect to annular to vacuum space ratio for different dimensionless mass flow rates.

3.2.3 Develop thermal control to improve reliability of PEBB-based converters

Task: Develop thermal control to improve reliability of PEBB-based converters

Technical Objectives

Develop thermal control to improve reliability of MMC and MCC-based DC/DC converters.

Improve the thermal management of power electronics converters by control and optimization the heat generation profile.

Technical Approach

- Reduce temperature variation of power electronics devices by controlling the circulating current inside the power converters.
- Modify the control algorithm for capacitor voltage balancing to cope with circulating current injection algorithm as this one will influence the capacitor voltage balancing within and between the arms of a MMC.

Progress Statement Summary

The software tool vemESRDC has been adapted to study the dynamic thermal behavior of an electronic cabinet (PEBB) cooled by two internal fans. The tool has been amended to account for the external air flow interacting with the cabinet that leads to mass and heat transfer with its surrounding.

We conducted a preliminary thermal study of a PEBB and its stack with both forced and natural cooling to assess various cooling strategies and design limits. High fidelity thermal analyses using an immersed boundary method have started with the objective of providing flow and temperature information for configurations that require high resolution. The idea is to employ advanced numerical methods and algorithms to combine high fidelity (sophisticated and time-consuming) models with low-order models (simpler and faster) to explore the design space while retaining acceptable accuracy.

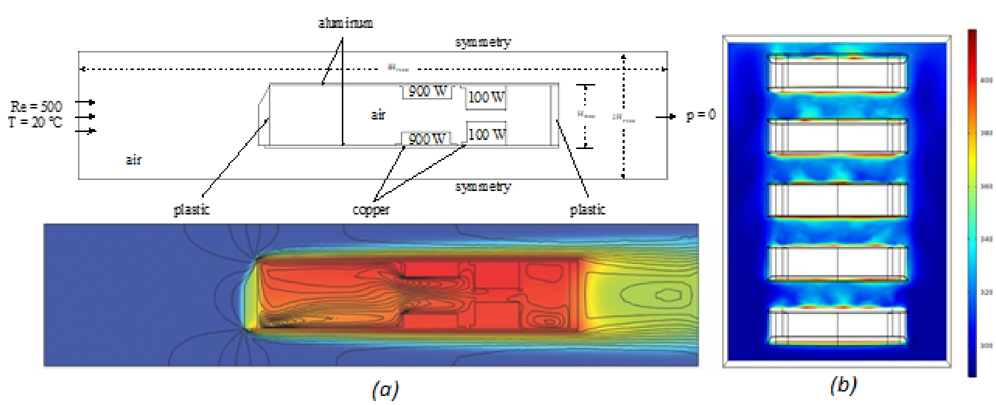

Figure 93: (a) PEBB simulation setup and its temperature field with forced cooling; and (b) temperature field of a PEBB stack enclosed in a cabinet with natural cooling.

A volume element model of a PEBB consisting of a variable thermal load and two fans was developed, and was then validated against the experimental data. The model is currently being used to determine the optimal height of the heat load that maximizes the system thermal conductance.

3.3.1 Develop resilient sensor systems

Task: Continuous state awareness

Technical Objectives

Provide continuous distributed state awareness architecture for the Ship Power System (SPS). As a basic matter, it is necessary to place measurement sensors in the proper points of the electrical system to reach full observability of the entire SPS. If all buses of the system are placed with sensors, the system will be completely observable and there is no need for any further calculations. However, the universal sitting of sensors is barely possible, due to:

1. Cost of sensors and interfaces devices.
2. Deficiency of communication facilities (depending on the resolution of transferring signals).

Generally, in the sensor placement problem, we need to consider different types of scenarios under which the redundancy for physical fail of one or more sensors is crucial. Another important factor is that for the system that is already populated with power measurement devices, it will eventually reduce the number of required sensors for full observability. There is a vast amount of research papers that have addressed such a matter regarding the PMU placement in the AC networks [125,126], but none of them have been applied to the hybrid AC/DC microgrids.

When all the critical buses are covered by the minimum number of sensors and ensured of the full observability of the system, then it is required to place some Control Agents among the sensors on the higher level of measuring system to gather necessary data for different distributed applications. To reach that point, a new metric for supervision of the physical failure on one, or multiple sensors at the same time, has been conducted for this layer, the outcome of which will result in the declaration for maintenance or replacement of damaged sensors. Figure 94 illustrates the proposed architecture for sensor, control agents, and the state awareness layer in the measurement system.

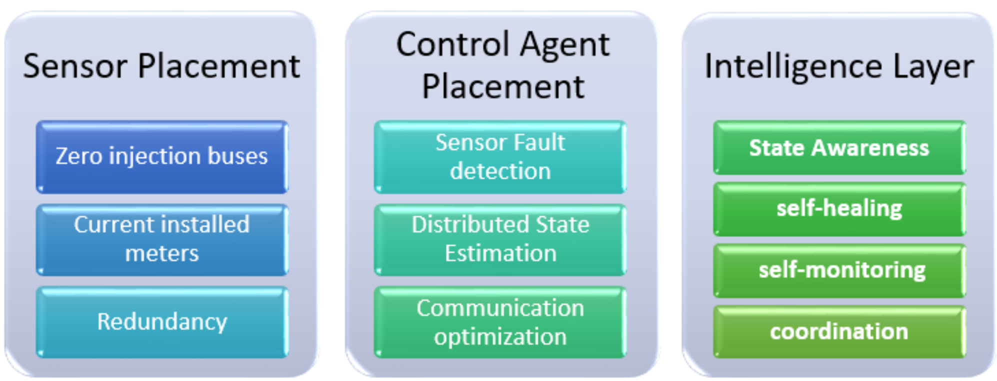

Figure 94: State monitoring and multilayer intelligence system for SPS.

Technical Approach

- Develop a metric for sensor placement in the MVDC SPS with regard to the AC inner loops for full observability and reaching the acceptable redundancy.
- Develop a method for finding the optimal number of, and the best place for, the control agents to minimize the communication infrastructure.

- Develop a new metric for a higher level of data processing from the Control Agent layer to provide Continuous System State Awareness (CSSA).

Progress Statement Summary

Currently, the ECI group is working on optimal sensor placement on the notional MVDC SPS (see Figure 95), proposed by N. Doerry, to find the most suitable places for placing the measurement sensors considering different constraints. Also, along with the sensor placement, we are working on the optimal agent placement based on the candidate sensor places. Figure 96 and Table 4 illustrate some results for the sensor placement.

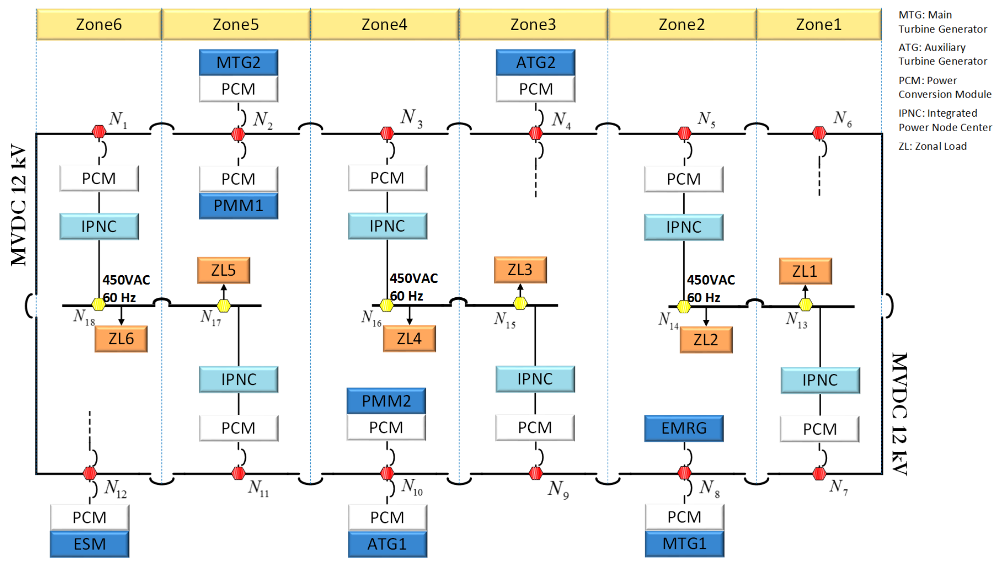

Figure 95: Test system: MVDC ship power system proposed by N. Doerry.

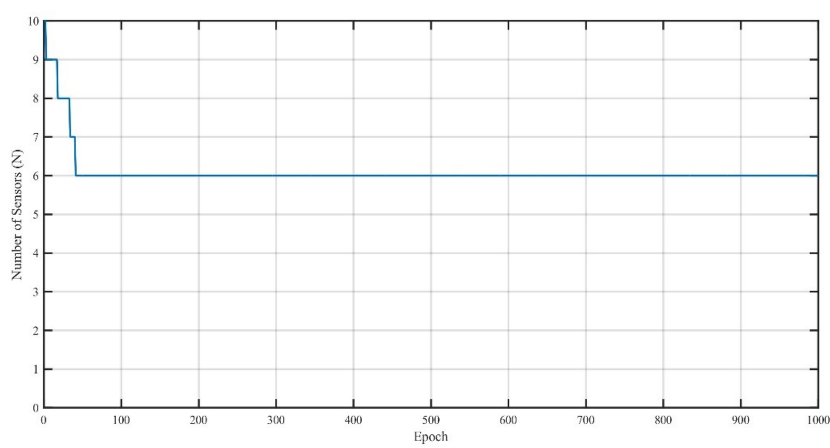

Figure 96: Solver convergence on optimal number of sensors.

Table 4: Optimal amount sensors and candidate places.

Case	Test system	Sensor Quantity
1	18 Bus MVDC Ship Power System	6
	Location of the Sensor for Complete System Observability	
1	1 3 5 7 9 11	

The optimal sensor placement algorithm for allocation of the minimum number of the sensors in the six-zone notional SPS has already been developed and the results of the research [127] were presented at ESTS 2017. The focus of the current research is to implement the real-time complexity measurement (RSM) and real-time stability measurement (RSM) metrics for real-time calculation of the order and disorder in the data collected from all the measurement points. Then, multiple cases with different scenarios incorporating the fault in the power system, fault in the sensor(s), activation of high-ramp rate loads and a few multi-incidents scenarios should be simulated for the purpose of metadata preparation. After all, the processed data can be fed back into the trained machine learning (ML) system for reporting/taking action for the different system incidents. The closed loop implementation of the proposed algorithm is shown in Figure 97.

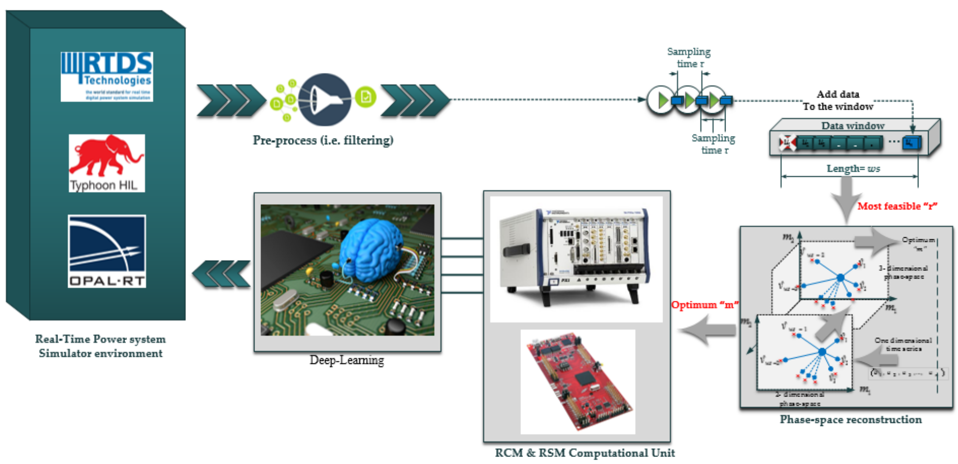

Figure 97: Closed loop implementation of the state awareness architecture.

Task: Stabilization, optimal performance, and learning under information costraints

Technical Objectives

Networked control systems challenge the paradigm of classical control theory that information can be transmitted instantaneously, without loss, and with arbitrary precision. In a fully operational environment, we can expect to have sufficient and timely data from all subsystems. However, faults might compromise sensors at a time when they are most needed. If one opts for a lower-bandwidth emergency sensor network, then we need to evaluate the effect of partial and/or intermittent observations on state estimation and control. We are currently focusing on three directions: (a) optimal data assimilation and sensor scheduling under intermittency or network constraints, (b) modeling and optimization via mean-field game approximations, and (c) optimal scheduling of stochastic networks under service disruptions, and bustiness.

Technical Approach

Develop improved sensor scheduling, we consider a discrete-time linear quadratic Gaussian (LQG) system observed by a finite number of sensors. When queried, a sensor attempts to transmit the measurement to the controller over a noisy network, which intermittently loses the measurement. Further, the network has its own query-dependent stochastic dynamics, allowing for complex congestion models. With only mild assumptions on the system structure, we have derived a wealth of interesting new results:

- A stationary, average-cost optimal policy exists, and under that policy the system is geometrically ergodic.
- The solution of the dynamic programming equation can be effectively approximated by considering a bounded subset of the state space and extending with a known function. The process turns out to be geometrically stable under the calculated policy, and the approximated average cost is also an effective estimate of the optimal value.
- The value iteration algorithm, linking the finite horizon control problem and the average cost ergodic control problem, converges.
- The sub-optimal policies calculated via the value iteration algorithm also induce a geometrically ergodic system, and the induced average cost converges geometrically to the optimal average cost.

A comprehensive set of results can be shown with only basic assumptions for a practical MDP with an infinite state space. Combining these key results, one can find a near-optimal, geometrically stable policy in just a few steps of the value iteration algorithm using a truncated state space.

In mean-field games (MFG) there are three important focus areas:

- Existence and uniqueness of solutions of MFG.
- Long-time behavior of the finite horizon MFG.
- Establishing rigorous connection of N-player games with MFG:
    1. Convergence of a N-player game Nash equilibria to a MFG solution.
    2. Construction of approximate Nash equilibria for the N-player game from a MFG solution.

In the area of stochastic networks under service interruptions and burstiness, we are currently focusing on the study of the diffusion limit approximation of these systems under heavy traffic. This limit takes the form of a multidimensional piecewise Ornstein-Uhlenbeck process with jumps. Specifically, the Itô equations have a piecewise linear drift, and are driven by:

- Either a Brownian motion and a pure-jump Lévy process, or
- A symmetric alpha-stable Lévy process, or
- A combination of the two.

The current focus is on the study of the ergodic properties of these processes, specifically, to identify conditions for sub-exponential and exponential ergodicity.

Progress Statement Summary

There has been substantial activity in all the focus areas. We made a substantial progress in the study of mean-field games in [128]. Summarizing our contributions in this paper, (i) we establish the existence of MFG solutions for a large class of mean-field games, (ii) we prove the convergence of the finite horizon MFG solution to the stationary one, under mild hypotheses, (iii) we study the existence of Nash equilibria for N-player games and prove that they converge to a MFG solution.

Our work on stochastic networks has been focusing on controlled diffusion approximations in the Halfin-Whitt regime. The problem here has two important components: first, design optimal decision rules for the diffusion limit, and second, implement these rules to the pre-limit system by approximation (truncation) and establish near optimality and stability for the original dynamics. A fairly recent work supported by ONR is in [129], where in addition we study the problem of fairness and optimization under load constraints. This is followed by [130], where the difficult problem of asymptotic optimality is addressed for a simple network topology that has been a benchmark in the field. A substantial part of the analytical background for the study of service interruptions and bustiness via jump processes can be found in [131].

We would also like to report some related work in [132–134]. In particular, the paper in [132] has undergone a recent important revision, which substantially strengthens the results.

Additional work on the sensor scheduling problem, ergodicity of Lévy-driven sides, and the problem of asymptotic optimality for general large scale stochastic networks is nearing completion and journal papers are in preparation.

An important piece of work completed is [16], in which study a class of multidimensional piecewise Ornstein-Uhlenbeck processes with jumps, which contains the limit processes arising in multiclass many-server queueing models with bursty arrivals and/or asymptotically negligible service interruptions in the Halfin-Whitt regime as special cases.

In these queueing models, the Ito equations have a piecewise linear drift, and are driven by either (1) a Brownian motion and a pure-jump Lévy process, or (2) an anisotropic Lévy process with independent one-dimensional symmetric-stable components, or (3) an anisotropic Lévy process as in (2) and a pure-jump Lévy process. We also study the class of models driven by a subordinate Brownian motion, which contains an isotropic (or rotationally invariant) stable Lévy process as a special case. The paper concentrates on the study of the ergodic properties of these processes. Specifically, we identify conditions on the parameters in the drift, the Lévy measure and/or covariance function which result in subexponential and/or exponential ergodicity.

In [135] we study infinite-horizon asymptotic average optimality for parallel server network with multiple classes of jobs and multiple server pools in the Halfin-Whitt regime. Three control formulations are considered: 1) minimizing the queueing and idleness cost, 2) minimizing the queueing cost under constraints on idleness at each server pool, and 3) fairly allocating the idle servers among different server pools. For the third problem, we consider a class of bounded-queue, bounded-state (BQBS) stable networks, in which any moment of the state is bounded by that of the queue only (for both the limiting diffusion and diffusion-scaled state processes). We show that the optimal values for the diffusion-scaled state processes converge to the corresponding values of the ergodic control problems for the limiting diffusion. We present a family of state-dependent Markov balanced saturation policies (BSPs) that stabilize the controlled diffusion-scaled state processes. It is shown that under these policies, the diffusion-scaled state process is exponentially ergodic, provided that at least one class of jobs has a positive abandonment rate. We also establish useful moment bounds, and study the ergodic properties of the diffusion-scaled state processes, which play a crucial role in proving the asymptotic optimality.

Another piece of work supported under this task is [136]. In small-cell wireless networks where users are connected to multiple base stations (BSs), it is often advantageous to opportunistically switch off a subset of BSs to minimize energy costs. We consider two types of energy cost: (i) the cost of maintaining a BS in the active state, and (ii) the cost of switching a BS from the active state to inactive state. The problem is to operate the network at the lowest possible energy cost (sum of activation and switching costs) subject to queue stability. In this setting, the traditional approach — a Max-Weight algorithm along with a Lyapunov-based stability argument — does not suffice to show queue stability, essentially due to the temporal co-evolution between channel scheduling and the BS activation decisions induced by the switching cost. Instead, we develop a learning and BS activation algorithm with slow temporal dynamics, and a Max-Weight based channel scheduler that has fast temporal dynamics. We show using convergence of time-inhomogeneous Markov chains, that the co-evolving dynamics of learning, BS activation and queue lengths lead to near optimal average energy costs along with queue stability.

3.3.2 Verification and validation approaches to operating and automation procedures

Task: Verification and validation approaches to operating and automation procedures

Technical Objectives

Relax restrictive, simplified assumptions and a means to combine appropriate problem abstraction levels while maintaining salient ship power system characteristics.

- Means and procedures to formalize descriptions of the ship power system operation with respect to the system management problems
- Approach for automated reconfiguration procedures tested on meaningful system models

Technical Approach

- Develop formalized models for shipboard power systems with respect to the system management layers.
- Evaluate trade-offs between various levels of abstraction to gauge benefits.

Progress Statement Summary

This project will commence in 2018.

3.4.1 Develop fault detection and location (FDL) approaches at different levels of shipboard power system

Task: Algorithm development for fast fault detection, fault location identification and network reconfiguration with or without communication

Technical Objectives

Develop/identify various types of fault detection and location identification methods for MVDC shipboard power systems that can aid in system fault management in a fast and timely manner. Create rules for network reconfiguration that can work with or without communication after the occurrence of a fault or due to change in the SPS network of operation.

Technical Approach

- Identify and develop different fault identification methods that can operate on a zonal SPS with bi-directional power flow, current limited PGMs, non-linear, stochastic loads.
- Utilize notional zonal MVDC shipboard power system model that can aid in testing of fault algorithms.
- Perform rigorous testing of developed/identified algorithms under various SPS conditions to verify satisfactory operation of fault detection and location identification.
- Analyze network reconfiguration options and deduce best operational methodology for reconfiguration after occurrence of fault.
- Study DC arc fault characteristics to aid in the development of better/faster fault detection algorithms utilizing our readily available 5 MW converter system, which consists of four 1 MW current-limiting MMCs.

Progress Statement Summary

FSU tested and demonstrated megawatt-scale high-speed fault clearing and power restoration utilizing their 5 MW MVDC testbed. Overall, FSU was able to achieve a much faster sequence (from $\tilde{8}0$ ms down to $\tilde{1}9$ ms) than previously achieved thanks to improvements made to the controls. The experiment was also conducted at higher voltage and power (from 2 kV to 5 kV at the same current levels) than the previous tests conducted. A summary of the work was published [137] and is explained in detail. By further improving the controls and speeding up their response as well as adding another control layer to account for fault currents, we expect even faster fault clearing and power restoration sequences to be achieved.

Task: MVDC system protection

Technical Objectives

Develop practical fault detection and location algorithms for line-to-line and line-to-shield faults, and demonstrate technological solutions on testbeds for fault management of the MVDC system. Battle damages may cause serious short-circuit faults in Navy ship power systems. Medium Voltage Direct Current (MVDC) shipboard power system is a tightly coupled microgrid. After a short-circuit fault happens, the fault current increases very fast due to the low fault resistance and inductance. The fault current limiter in converters may quickly limit the converter current to a low level, but the discharge current of output filter may still generate a high peak current. In addition, the fault current limiter restricts the current to a constant value in a steady state, which makes the fault location and coordination very challenging in a DC system. How to quickly and reliably detect, locate, and isolate a short-circuit fault is a great challenge in MVDC system.

The objective of this work is to develop practical fault detection and location algorithms for line-to-line and line-to-shield faults, and demonstrate technological solutions on testbeds for fault management of the MVDC system. The research will explore the dynamic characteristics of the MVDC system under different fault scenarios, investigate the implications of the system configurations on fault detection, isolation, and mitigation, and develop algorithmic solutions to address the issues of MVDC system protection.

Technical Approach

- Develop appropriate system protection approach for MVDC shipboard power system.
    1. Study the MVDC transient behaviors under various fault scenarios.
    2. Design appropriate fault detection, location, and coordination approach for MVDC system.
- Create prototype protection algorithms on embedded control system.
- Control hardware-in-the-loop (CHIL) tests for the developed protection algorithm.
    1. Simulate a suitable MVDC system in real-time digital simulator for fault emulation.
    2. Configure the interface between embedded control system and the real-time simulator.
    3. Perform CHIL tests for the developed protection solution.

Progress Statement Summary

UT-CEM team has worked closely with ISSAC Corp. on the MVDC protection topic under a NAVSEA SBIR project entitled 'Medium Voltage Direct Current (MVDC) Fault Detection, Localization, and Isolation (DLI).' The research team has conducted a comprehensive literature survey on the DC distribution system protection. The advantages and limitations of each existing protection method have been studied and compared. Various fault isolation solutions for DC system are also studied. Team researcher has worked on a line impedance-based DC protection algorithm development for general DC systems [31, 138]. The developed approach has potential to be used in MVDC ship system. The next step would focus on developing a simplified modeling approach to estimate fault current behaviors in a MVDC system based on the proposed approach in [139, 140]. In addition, a detailed transient model for MVDC system will be implemented in the real-time digital simulator for algorithm tests.

During May-September 2017, researchers at UT-CEM developed various MVDC protection solutions. The first protection solution is fault current limitation (FCL) for power generation modules (PGMs) and differential protection for a main dc bus in a sub-scale MVDC system [33]. Numerical simulation was performed to validate the feasibility of the proposed approach. Sensitivity analysis was performed to test the impact of the fault resistance on the dynamic behavior of fault current in the MVDC system. The fault current limitation capability of PGMs has been tested in the numerical environment and hardware-in-the-loop (HIL) simulation environment. In addition, the practical design issue has been evaluated to help determine the most appropriate current threshold for fault detection in the differential protection zone. This approach will be first tested on a 30 kW converter unit with necessary downstream circuit and devices as an initial hardware test.

In addition, the research team explores general protection approaches for AC-DC rectifiers which may be used in PGMs. Various power converter topologies were explored to study the feasibility of implementing FCL functions. Conventional two-level voltage source converters (VSCs) handle dc faults by turning-off all IGBTs in order to prevent device damage. The fault current of a two-level VSC and a Half Bridge Modular Multi-level Converter (HB MMC) after the IGBT turning-offs cannot be blocked by converter switches. The anti-parallel diodes will form a fault current path for dc faults. To protect this type of power converters, fault current bypassing technologies are explored [141]. In order to allow power converter bypassing relatively high fault current for certain period of time, the power electronics devices in converters need to be oversized which may increase the cost and complexity of the system. Existing fault current limiting converters include thyristor rectifiers, DC-DC buck converters, Full Bridge Modular Multi-level Converters (FBMMCs), and Clamp double Modular Multi-level Converters (CDMMCs). Numerical simulation for VSC fault current bypassing approach has been conducted in $MATLAB$/SimPowerSystem. The study results suggested that additional thyristors are required to bypass the fault current.

To support the dc protection test, a simplified MVDC network is being implemented in the Opal-RT and NI PXIe FPGA simulator. Some preliminary model effort for a PGM unit has been performed. The HIL test for the dc protection approach is being conducted.

In addition to low impedance pole-to-pole faults, the high impedance pole-to-ground faults need also to be considered in the MVDC distribution protection design as pointed out in [142]. High impedance faults may be caused by insulation degradation, dirt accumulation on an insulator, and a broken conductor falling to the ground [143]. The fault current path is usually not clearly established and a permanent fault may be delayed or even not happen at all. Even though the high impedance fault current level is small, the fault may exist in the power circuit long enough to cause fire or even more serious subsequent faults. Due to the high resistance of ground faults, the fault current is usually small and it is difficult to reliably separate such ground faults from normal system changes. Existing overcurrent method could not be reliably used to detect the high impedance ground faults. The measured common-mode current may be used to detect the high impedance ground fault. However, as suggested in [144], the normal capacitive leakage current value may be comparable to the ground fault current caused by a high impedance ground fault.

CEM researchers reviewed the high impedance dc fault detections. Three types of approaches to detect high impedance ground faults have been proposed in literature. The first approach is based on the differential current measurement in each protection zone [145] and [146]. Once a high resistance ground fault happens, the current sensor will observe a capacitive spike current. In addition, there may be a difference between measured positive-pole-to-ground voltage and negative-pole-to-ground voltage. The measured voltage difference could be used to declare a ground fault in the circuit. In each protection zone, the capacitive current directions from two zonal boundary current sensors will be compared. If the capacitive current direction is the same, it is an external fault; otherwise, it is an internal fault. In [147], capacitor-based voltage transient compensator circuits are proposed to connect to the positive and negative poles. The voltage transient compensators are used to provide high sensitive leakage current detection by introducing capacitive currents during ground faults.

The second type of approach is based on the frequency spectrum signature of the measured electrical signals to separate high impedance ground faults from other normal system changes [144, 147]. Fast Fourier transform is usually performed on the measured electrical signals to obtain frequency spectra. During high resistance ground faults, some unique features would exist in the frequency spectra. These unique features would be used to differentiate ground faults from other system changes. This approach requires that the algorithm has self-learning mechanism to train itself to differentiate the unhealthy conditions and healthy conditions. Machine learning and artificial intelligence would play an important role in this type of applications. Off-line time domain simulation results of the power circuits would also be very helpful to train the ground fault detection algorithm.

The third approach is based on the midpoint-to-ground voltage measurement [148, 149]. The voltage between a middle point of the dc network and a ground potential is measured to detect a high resistance ground fault. If the measured midpoint-to-ground voltage includes a dc bias and the dc bias is higher than a predefined threshold, a high resistance ground fault is detected; otherwise, there is no dc ground fault.

Additional modeling and simulation as well as experimental tests will be conducted to explore the most suitable high impedance fault detection and location approach for MVDC distribution systems.

From October 2017 to April 2018, the UT-CEM research team has tested the proposed local measurement-based fault localization method in both a control-HIL simulation environment and a LVDC hardware circuit. The differential protection approach was also tested in the LVDC hardware circuit. The simulation and test results have been summarized in [150]. The research team is transferring the tested control and protection platform to a MVDC hardware circuit with a MW-level converter and MV cables. The developed fault detection and localization approach will be tested using the MVDC test platform.

Task: Efficient event and intrusion detection systems for shipboard power systems

Technical Objectives

In this work, we consider failures that can occur to the shipboard system as a result of a cyber-security attack. Cyber-attacks on power systems can create N-k contingencies which are even more critical compared to a single or double component failure. Coordinated attacks on multiple components have ability to disrupt electrical power to a critical level. Current practices in power systems design do not consider cybersecurity requirements; and the monitoring and control practice do not consider the potential cyber borne contingencies and disturbances. Hence, there is a need to incorporate advanced event and intrusion detection systems in power systems to enhance situational awareness for efficient power system operation. In addition, the tool must be able to identify the event location as fast as possible to avert chain failure and isolate the affected part of the system to ensure system stability and reliability.

To this end, the first part of this work aims at developing effective intrusion detection system that can identify attacks. The second part aims at developing an automated protection techniques based on model-based control techniques, such as model-predictive control. For the first part, we will investigate effective feature selection techniques to enhance the overall accuracy and reduce false positive rate of the Event and Intrusion Detection System (EIDS). Every time an optimal set of attributes for a particular scenario is obtained from the feature selection method, these features will be fed into the data processing units and then fed into the detection algorithm to evaluate the classification performance. This procedure will be repeated until the best classification performance is obtained. The following techniques for feature selection will be investigated: 1) Brute force method, 2) Correlation based feature selection (CFS), 3) Mutual information based feature selection, and 4) State Tracking and Extraction Method (STEM). To evaluate the feature selection methods and develop EIDS, we will use two detection algorithms based on machine learning techniques. Non-Nested Generalized Algorithm (NNGE) is suitable for offline analysis. However, with little modification, it can be used in real-time. For real-time application, a data stream mining algorithm based on Hoeffding Tree will be used.

Technical Approach

- Determine the critical attributes for establishing high detection accuracy EIDS.
    1. Review correlation-based feature selection methods.
    2. Select candidate features.
- Process attack data using STEM algorithm and extract common paths associated with specific system behaviors.
    1. Apply STEM algorithms to process cyber-attack data.
    2. Formalize output datasets.
- Establish an offline EIDS and ensure a 95% (or higher) detection accuracy and a 1% (or lower) false positive rate.
    1. Evaluate candidate machine learning algorithms (either NNGE or HAT).
- Develop the optimal heuristics for feature selection based on the evaluation of the machine learning algorithm from item 3.
    1. Select the best candidate methods and features for heuristics.
    2. Summarize the year-one research results and submit a technical report.
- Implement EIDS for electric ship power system.

1. Create power system model and scenarios in PSSE and select candidate system model.
2. Model attack scenarios.
3. Simulate scenarios and generate datasets.

Progress Statement Summary

With the awareness that the structural and programming vulnerabilities could be potentially exploited by the attackers to intrude the supervisory control and data acquisition (SCADA) system and power/energy management system (EMS/PMS), in this report period, we re-evaluated the proposed technical approach and determined a design strategy that focuses on modeling the impacts of cyber-attacks on both the information flow within the communication channel and the performance of the control-related management functionalities, evaluating the vulnerabilities of the SCADA/EMS for shipboard power system against malicious activities and cyber-attacks, and enhancing the overall reliability and resilience of the Naval warships equipped with advanced information and communication technology (ICT). More specifically, we have developed a design flow that takes advantage of the event and intrusion detection systems (EIDS), so we can accurately identify whether the detected cyber-attacks, modeled by a modified Bayesian attach graph model, can result in wide-spread disruptions of electric power supplies and quantitatively investigate the cyber-security of onboard SCADA/EMS systems. A mean-time-to-compromise (MTTC) model is planned to be developed as well as the mean-time-to-repair (MTTR) model of cyber components to estimate the frequency of attacks on the targeted system components and the resulted probabilities of successful cyber-attacks. Then, from the control perspective, model-based strategies will be developed based the cyber failure probabilities to counter potential cyber-threats and thus enhance the reliability of the generic cyber-physical shipboard power system. The originally proposed Task: Efficient event and intrusion detection systems for shipboard power systems Technical Objectives and Technical Approach, as well as the anticipated results are expected to be partially updated during the next reporting period.

With the employment of sensors, advanced computation systems, and communication network, the traditional Shipboard Power System (SPS) has turned into a multi-dimensional, heterogeneous complex Cyber-physical Shipboard Power System (CPSPS) that incorporates the new abilities of real-time temporal and spatial sensing, dynamic control, as well as multi-way flow information service. The control of CPSPS needs to be treated as a unified combination of problems where regulations and control decision are dependent on both the control heuristics and cyber-integrity. This indicates that the vulnerability of the communication systems for all-electric ships needs to be carefully evaluated and integrated into the control design to assure cyber-resiliency.

Realizing the technical challenges for the control solution to incorporate the distributed structure and the highly stochastic and unpredictable character of the latest MVDC architecture, a novel 'Web-of-Grids' (WoG) framework is proposed in the reporting period as an incorporation of task-oriented mechanism to simultaneously co-operate the distributed and integrated CPSPS. In the context of CPSPS, each electrical zone can be considered a cyber-physically integrated grid as it contains the 'buffer' mechanism to store energy and cyber-information, 'router/hub/switch' infrastructure and 'routing' algorithms to control energy and information flows, as well as 'protocol' to regulate cyber and physical operations. The proposed WoG concept fully explores the interdependencies among zones with physical interconnectivity (e.g., shared energy resources) within the SPS and the cyber interconnectivity (e.g., collaborative load management) between the zones (grids) as each of the zones involved in the SPS can be separately considered as systems that are both administratively and operationally self-governing while seamlessly integrated to accomplish a system mission collaboratively. Realizing that cyber faults/failures and attacks perhaps can never be completely prevented and eliminated, we are developing a new CPSPS paradigm to evaluate and analyze cyber events that could adversely impact the performance of the control system. The vulnerabilities of the sensing devices, communication channel and actuators are systematically modeled in the control algorithm design to provide insights for the controller to be more adaptive, preventive, reliable and resilient in face of cyber system errors and attacks.

3.4.2 Develop system-level fault recovery and soft start up methods

Task: DC zonal converter fault recovery and soft startup

Technical Objectives

Solve the inrush current and instability issues during fault recovery period, and thereby achieve the soft start up for the DC zonal converters. Previous study shows that modular multilevel converter (MMC) based DC zonal converters have the ability of limiting current at MVDC bus short circuit fault condition [151]. During MVDC fault protection period, the DC zonal converter will continue to provide energy to the load. The energy stored in the capacitors will be discharged to around 60%-70% of the nominal value. Therefore, during startup, there will be a large inrush current which can trigger the converter overcurrent protection or cause stability issues.

Technical Approach

- Design a control strategy that coordinates the LVDC side converter and MVDC side converter, and achieves the following two targets:
  1. Maintain LVDC side voltage within acceptable range.
  2. Limit MVDC side current by preventing the converter entering uncontrolled rectifier mode.
- Derive the value of passive elements to meet the energy storage requirement of proposed control strategy.
- Design the control parameters to meet the dynamic requirement of proposed control strategy.
- Verify the proposed control in simulation.

Progress Statement Summary

The ESRDC power electronics group has proposed a control strategy for the MMC-based zonal converter that coordinates the LVDC side converter and MVDC side converter [152]. The proposed control strategy has been compared with conventional input series-output parallel (ISOP) based solution.

The fault recovery and soft start up of MVDC side is more challenge than those of LVDC side if the zonal converter provide Uninterruptible Power Supply (UPS) function during the fault condition. In this scenario, energy stored in the capacitors will be discharged to around 60%-70% of the nominal value, resulting in a large inrush current during recovery which can trigger the converter overcurrent protection or cause stability issues. Our research is to solve the inrush current and instability issues during fault recovery period, and thereby achieve the soft recovery for the dc zonal converters.

The MVDC side fault scenario is shown in Figure 98. After fault occurs, the inrush current from dc capacitors can be effectively limited by turning off power switches due to the absence of bus capacitors on the MVDC side of the zonal dc-dc converter based on MMC topology. It should be noted that though the MVDC bus voltage drops to zero, the built-in energy storage of proposed converter can implement UPS function to continue to provide power to LVDC loads and the cell capacitor within the converter is not discharged completely. Therefore the fault of MVDC side is completely isolated from the LVDC zonal loads. The proposed iM2DC converter topology is shown in Figure 99 where no capacitors located on the dc bus side and the internal cell capacitors (C and C') can operates as energy storage units during fault. The HVS and LVS of iM2DC converter can be treated as two relatively independent converters, which facilitate the fault isolation capability. The control strategy of HVS is shown in Figure 100. As can be seen in Figure 100 (a), the transformer voltage va', vb' and vc' are controlled by the HVS voltage command. The fault current limiting mechanism shown in Figure 100 (b) contains two key factors: upper limit of dc current reference as current limiter and dc bus voltage feedforward control to actively lower bus voltage during fault

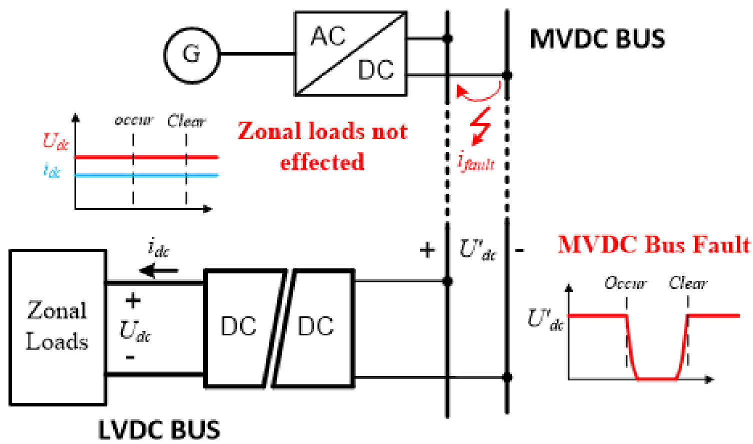

Figure 98: The zonal dc-dc converter under MVDC side fault scenario.

in order to reduce fault current from the source. Meanwhile, the ac side transformer voltage will not be effected, and thus LVDC zonal loads will not see the fault. However, during this bus de-energizing period, the cell capacitors of the HVS will keep on discharging to feed the LVDC loads. Once the fault is cleared and MVDC bus voltage starts to recovery, the converter soft-recovery will begin automatically using the power provided by the MVDC bus. The HVS converter may operate in slight over-load mode due to the additional power requirement for cell capacitor re-charging in this recovery period. So the MVDC dc current should be controlled carefully to avoid triggering overcurrent protection. This can be achieved by setting the upper limit of dc current reference lower than overcurrent protection threshold. The dc voltage feedforward control also will contribute the dc current limiting.

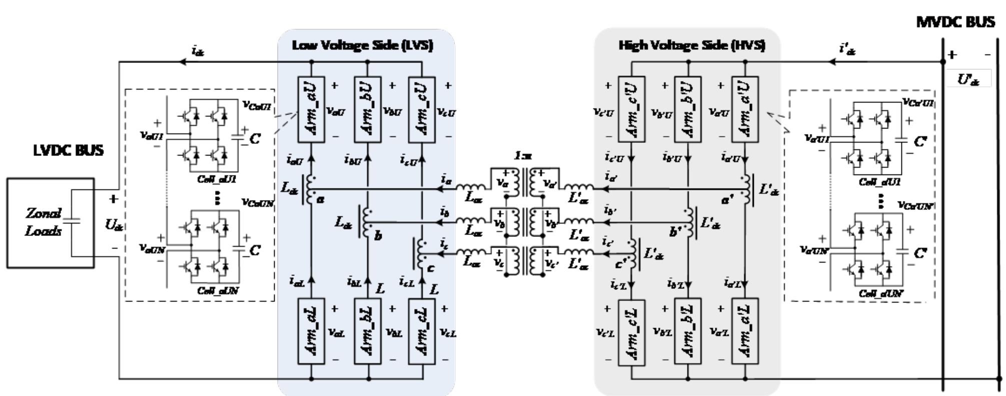

Figure 99: iM2DC topology formed by LVS MMC and HVS MMC.

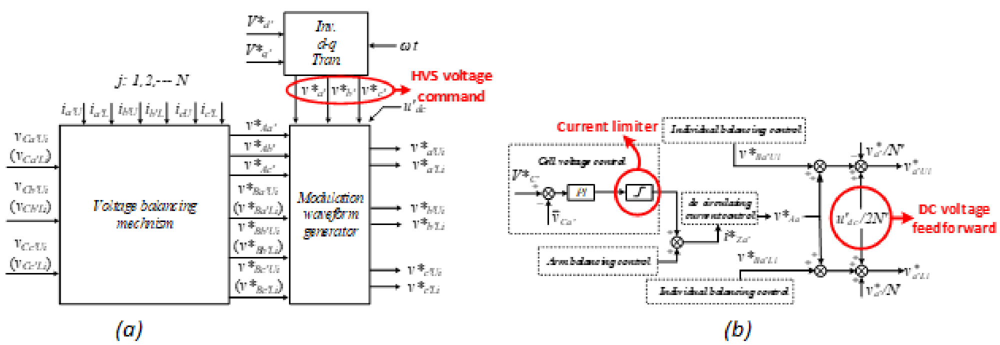

Figure 100: Control block diagram of HVS MMC; (a) control diagram, and (b) proposed control mechanisms to limit the fault current.

3.5.1 Develop methods to model common mode effects and means of integrating pertinent factors to de-risk ship designs

Task: Predicting effects from common mode couplings on ship designs based on circuit topologies

Technical Objectives

Model common-mode (CM) coupling effects in a computationally effective way, where those models can be used for early and mid-stage design studies. Current research will utilize techniques developed by Purdue [153, 154], on MW-scale equipment located at FSU-CAPS. Efforts to characterize and model this equipment will further help to set up PHIL-based ship design topologies to validate and verify system simulations. This task will produce validated methods and models to predict effects from CM couplings on ship designs, and link to Thrust 5 to validate system CM coupling effects with hardware.

Technical Approach

- Further the emphasis on S-parameters to characterize CM voltage sources in MW-scale equipment at CAPS, such as a single PEBB from the IMU, DC VVS, MMC converters.
- Model the common-mode equivalent circuit of the above-mentioned MW-scale equipment to verify and compare with mixed-mode detailed models.

Progress Statement Summary

FSU effort on this task is ongoing [155, 156].

Task: Predicting effects from common mode couplings on ship designs based on circuit topologies

Technical Objectives

Model common-mode (CM) currents and voltages in the ship electrical system and develop techniques for predicting impacts of parasitic components on ship designs.

Wide-bandgap (WBG) devices enable wide bandwidth control and will potentially reduce the size of passive components (i.e. inductors, capacitors). Although enabling, they also introduce secondary issues such as CM currents through the ship's hull, which will produce interference with other systems (i.e. cathodic protection and degaussing), and negatively influence a ship's electromagnetic signature.

Accurately predicting the CM currents is necessary due to the introduction of WBG power electronics. A significant contribution of ESRDC was the derivation of CM equivalent circuits to predict CM current in ship systems [153, 154].

Technical Approach

- Develop computationally effective modeling of CM coupling effects for use in early and mid-stage design studies.
- Predict effects from CM couplings on ship designs based on geometries.
- Predict and model accurate CM currents and voltages at frequencies above 1 MHz.
- Develop techniques of predicting the parasitic components of ship electrical systems based on the geometric and material layouts from S3D.

Progress Statement Summary

The ESRDC grounding group has focused on measurement and characterization of MW-scale equipment to better understand CM operational characteristics. Current progress includes an application of the CM equivalent circuit approach described in [153] to the recently developed Notional Two-Zone MVDC ship power system from [157]. Additional progress was obtained in addressing the challenge of computing CM currents and voltages in the time domain with band-limited frequency domain models, such as S-parameters, of ship structures including parasitics. A novel wavelet-based transformation was shown to allow missing frequency domain model data to be successfully extrapolated [158].

A hypothetical model of pathways for CM currents to be conducted to through the ship's hull from isolated undergrounded systems such as PEBB has been developed. This model focuses on capacitively coupled pathways through the parasitic capacitance associated with multi-chip power module baseplates and the individual semiconductor die packaged within the modules. This model identifies multiple independent paths which result in complex interactions of the multiple terminals of devices found in a three-phase inverter for example. This complexity is further compounded when multiple power conversion systems are considered which may be co-located within a single power conditioning cabinet.

To advance toward a theoretical model for CM current pathways experimental data is required. In an effort to reduce the complexity of the system as well as enable a metrologically sound approach a test platform has been constructed and brought on-line. This experimental tool includes a purpose built multi-phase inverter core incorporating three half bridge SiC MOSFET power modules capable of operating at an input voltage of up to 1000 VDC and theoretical power output in excess of 50 kW. Purpose built line impedance stabilization networks (LISN) have been constructed which are capable of operating at the specified voltage rating of the inverter. To generate baseline data for model validation no output filtering of the inverter phases has been included. As a consequence the LISN devices applied to the inverter output legs must be capable of thermally managing power dissipation imposed by the inverter output node switching between the DC bus voltage and the local ground reference potential at frequencies exceeding 100 kHz. The inverter and LISNs are all situated on single copper sheet suspended on a large high dielectric substrate. The copper sheet is galvanically isolated from all ground potentials as well as the inverter core. Common-mode currents can be directly measured through the measurement terminals of the LISNs. A high level schematic of the test platform is shown in Figure 101. This figure simplifies the model by illustrating a single half-bridge inverter. Capacitively coupled CM current pathways are shown in red as CUS, CALS and CLS.

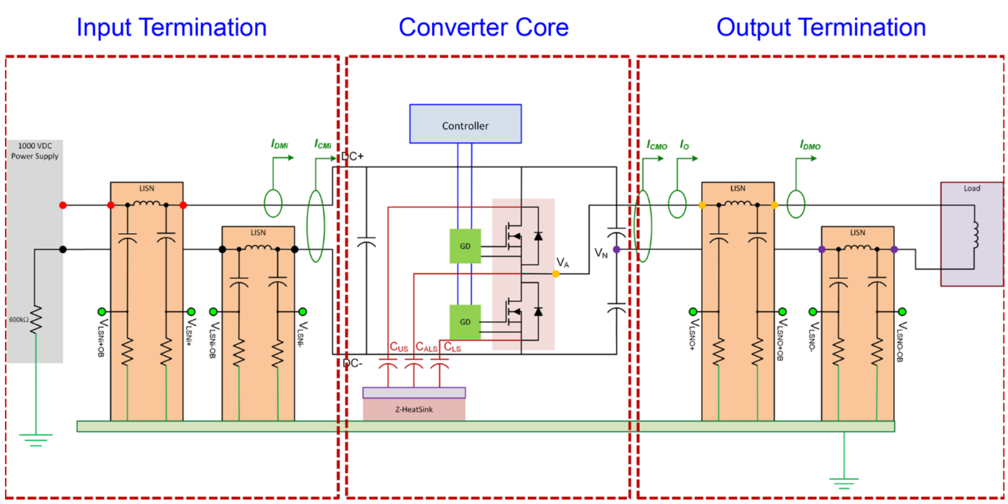

Figure 101: Simplified schematic of the CM current model validation test circuit.

The test platform is presently operational. Data has been collected from this operational system and is being analyzed. Future investigations will focus on validation of metrology, impact of switching frequency, and a comparative study using Si IGBT power modules.

Aspects of this work have been detailed in [159]. MSU organized and conducted a series of discussions with the Aerospace Systems Design Laboratory at the Georgia Institute of Technology. These discussions also included collaborators from non-ESRDC institutions supported separately by ONR on this effort from the University of Alabama, the University of Wisconsin – Milwaukee, and the University of North Carolina – Charlotte. These discussions sought mutual understanding of the work in shipboard EMI related topics being investigated at each institution.

Task: Minimizing common mode coupling in WGB-based P&E system

Technical Objectives

Validate the common-mode equivalent circuit (CMEC) model of complex power systems [153,154], using Purdue's reduced-scale naval DC microgrid (PDCM) that consists of a generator/active rectifier coupled to an inverter/propulsion drive through an electrically long DC bus. Both the active rectifier and inverter utilize Si-based switching devices. In addition, a second focus was on the validation of the approach on a system of the size and complexity of a Naval power system. A final objective is to utilize the CMEC to consider the impact that wide-bandgap (WBG) devices would have on the CM behavior of the future Naval power systems.

Technical Approach

A CMEC of a portion of Purdue's PDCM has been created using the approach outlined in [154]. To illustrate how this is performed,

- A mixed mode model (including parasitics) is first derived as shown in the upper portion of Figure 102.
- Subsequently, the CMEC transformation is applied to represent the CM behavior of the mixed mode model. The transformation results in the model of the form shown in the lower circuit of Figure 102. One notes that the CMEC shown is represented in the frequency domain, where parasitics are represented using impedances.
- There are no power electronic devices in the CMEC. Rather, the switching of the power electronics is represented using equivalent voltage sources.
- Once the CMEC is expressed, measurements are used to characterize each of the impedances and the voltage sources.

For the voltage sources, an important differentiator of the ESRDC approach is that CM voltage is not defined relative to ground. Rather, it is defined relative to a user-specified point that enables easy measurement and analysis. In the case of the Purdue testbed, that lower rail of the active rectifier and the lower rail of the inverter were used as the CM voltage reference points.

Progress Statement Summary

Progress was made on validating the CMEC approach first in the Purdue testbed. Details and the results were prepared and published in [154]. An example of the results, which are important since they enable one to assess the influence of WBG devices, is shown in Figure 103. These are the equivalent CM impedances that are observed when viewing the system from the rectifier and inverter. Once can see that the CMEC accurately predicts the impedances obtained from measurement.

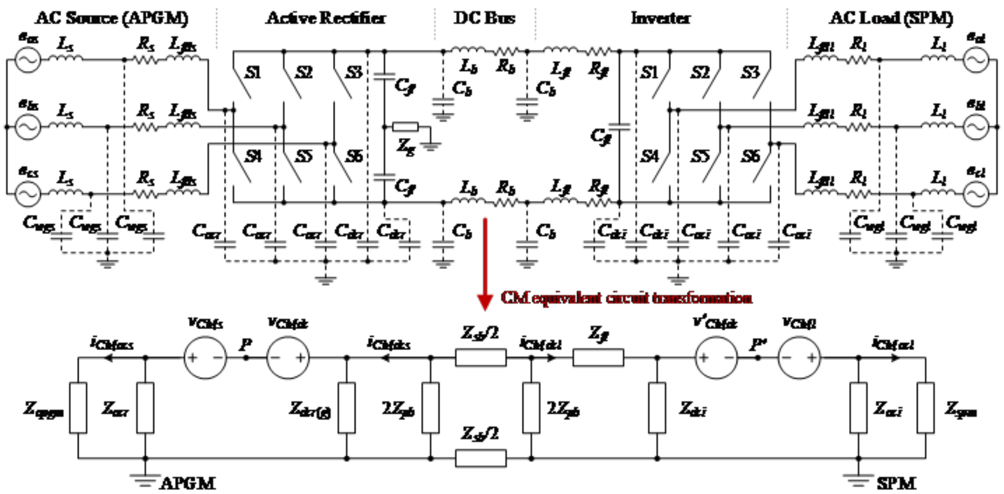

Figure 102: Detailed DM/CM model of Purdue DC microgrid (upper circuit) and its CM equivalent circuit (lower circuit).

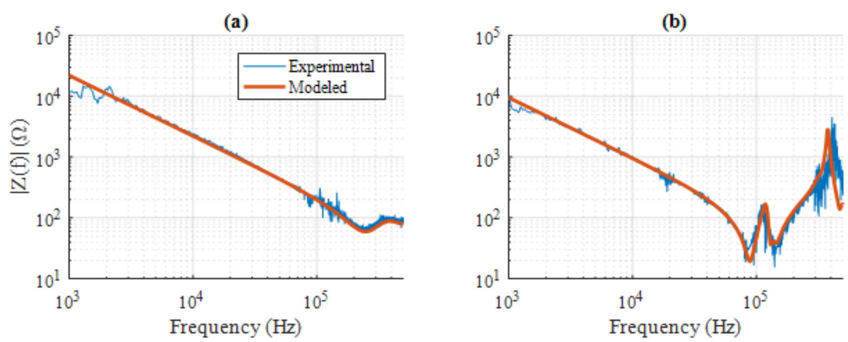

Figure 103: Measured and modeled equivalent impedance seen by the (a) active rectifier, and (b) inverter in the Purdue DC microgrid.

Figure 103 clearly indicates system-level resonances in the CM at approximately 100 kHz. These resonances are expected to be problematic as WBG-based converters enable switching frequencies approaching and surpassing 100 kHz. Indeed, we have derived the CM voltage expected in the active rectifier and inverter assuming the switching frequency of the converters is increased from 10 to 100 kHz and edge rates are likewise scaled up by a factor of 10. The resulting voltages were placed in the CMEC, as shown in Figure 104 (a). The predicted CM current is shown in Figure 104 along with those measured in the existing testbed. Quantitatively speaking, the computed signal power of CM current from 1 to 500 kHz increases roughly tenfold throughout the entire system. This is significant and would likely result in a loss of operation of the system due to electromagnetic interference with other circuits and systems. Details of the impedance characterization and the impact of WBG devices are available in [160].

In addition to the Purdue testbed, an attempt was made to validate the CMEC approach on a Navy Hybrid Electric Drive. Specifically, a CMEC of the HEV at LBES was created. ESRDC researchers traveled to the HEV manufacturer and worked with Nate Spivey (and others) to measure each of the impedances of the circuit. A method of solving the CMEC of the HEV was derived and provided to the Navy. At first pass, it appears that the model is capturing measured phenomenon. Validation is ongoing.

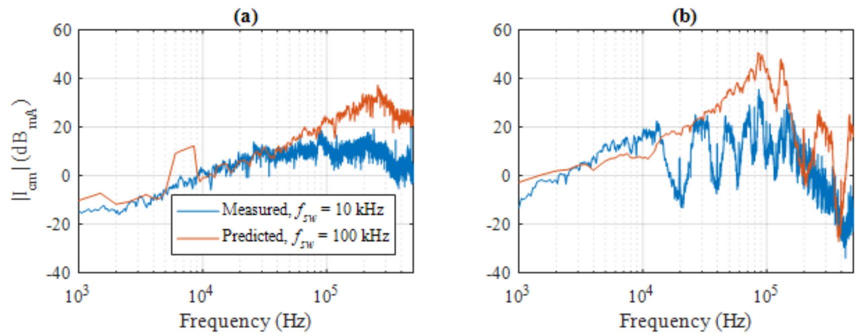

Figure 104: Predicted CM current through the (a) source (APGM), and (b) load (SPM) for a switching frequency of 100 kHz, compared to the CM current measured at a switching frequency of 10 kHz.

Figure 104 clearly indicates system-level resonances in the CM at approximately 100 kHz. These resonances are expected to be problematic as WBG-based converters enable switching frequencies approaching and surpassing 100 kHz. Over this period of performance, the models have been utilized to further analyze the impacts that WBG devices have on the overall CM current. Details of the impedance characterization and the impact of WBG devices was prepared [160] and presented at ESTS 2017. Among the analysis performed was an evaluation of the CM current at the APGM and SPM as the switching frequency of the respective converters was increased from 10 kHz to 40 kHz and 80 kHz, as well as the influence of keeping the same 10 kHz switching frequency while adjusting the edge rates of on/off transitions to match those of WBG devices. The bandpower of the CM current is shown as a function of frequency in Figure 105.

From the results, it is interesting to note that over the frequencies up to 1 MHz, the influence of the edge rate is relatively minor. This is due to the fact that the edge rates have relatively little impact on the CM voltages in the areas of the resonances (around 100 kHz). In addition, one can observe that increasing the switching frequency does result in an increase in CM current band power. This is due to the fact that the CM impedances of the APGM and SPM decrease from 10 kHz to 100 kHz and indeed have resonances at frequencies where CM voltage harmonics are present. This points to a potential need to have converters designed in such a way that the switching frequencies can be adjusted in situ as CM impedances of the system become known. In addition to the Purdue testbed, an attempt is being made to validate the CMEC approach on a Navy Hybrid Electric Drive. Specifically, a CMEC of the HEV at LBES was created. ESRDC are working with Nate Spivey (and others) to obtain some data to validate the model. At first pass, it appears that the model is capturing measured phenomenon.

Over the reporting period, a focus has been on further application and validation of the method. Specifically, a goal is to derive and validate models of the entire PDCM. A diagram of the full PDCM is shown in Figure 106. As shown, the testbed contains the APGM and SPM highlighted previously. It also consists of Isolating Converter Modules (ICMs) and Inverter Modules (InMs) that feed three DC zones.

To establish a CMEC of the ICM/InMs, a mixed mode circuit was first derived. The circuit is shown in Figure 107. As shown, the ICM consists of an input DC-AC converter, isolating transformer, and diode rectifier. There is a filter on its output stage prior to the DC bus. The InM is a traditional 6-switch DC-AC converter that serves an RLC AC load that is adjustable. Parasitic capacitances are placed within the figure of the circuit to represent parasitic coupling paths. A commercial power supply is shown, which has been utilized to provide the DC voltage for operating the circuits. Within the laboratory, there is a dedicated ground for the room that is tied to building structure ground. This is referred to as the power structure ground in Figure 106. The power electronics circuit is placed within metal enclosures and there is a 120 V feed to each rack from the room power. The ground of this 120 V supply is connected to the metal enclosure and heatsinks of the power electronic circuits. In theory, this chassis and the structure ground should be at the same potential. However, in practice due to long ground cable runs through different paths, if has been found that these are not at the same potential. Rather, there is an impedance between the two grounds.

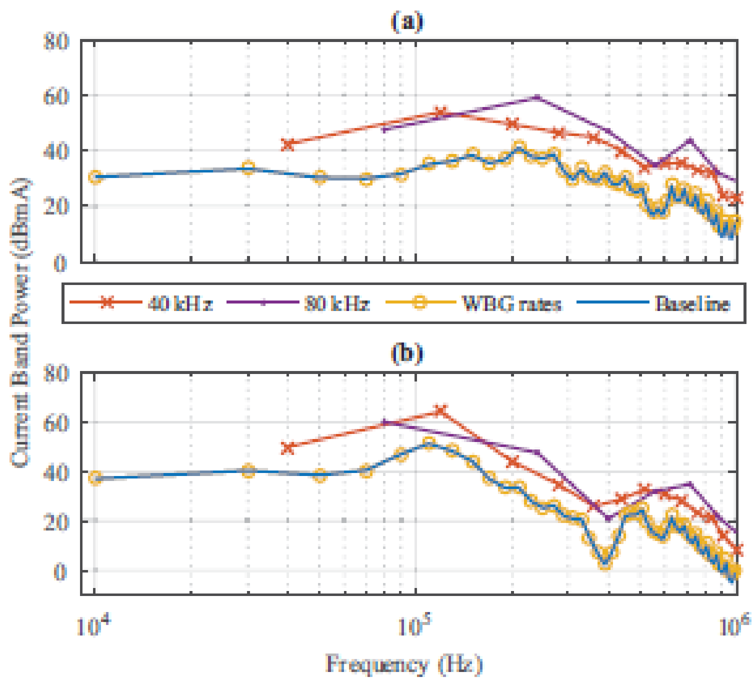

Figure 105: Predicted CM current through the (a) source (APGM), and (b) load (SPM) under WBG-based frequencies and edgerates compared to the CM current measured at a switching frequency of 10 kHz.

As a result, within Figure 107 there is an impedance placed between the two grounds. This impedance has been measured using an impedance analyzer.

The CMEC of the circuit is shown in Figure 108. Within the figure the rectangles represent CM impedances that were measured in hardware. A few details are of note. First, the CM impedances of the ICM at its input were measured both with respect to the structure ground and the chassis ground. The impedances of the power electronic modules (IGBT and diode) where each measured with respect to the heat sink, which is tied to the chassis ground. Similarly, the input impedance of the InM and the load were measured with respect to the chassis ground. This was due to the fact that the structure ground is not directly tied to the InM.

The CM voltage sources of both the ICM and InM were both characterized through hardware measurement. Once the parameters of the CMEC were characterized, the CM current within the system was simulated and also measured in the laboratory. A comparison of the measured and simulated CM current as a function of frequency is shown in Figure 109. The top plot is the CM current at the input to the ICM from the power supply side. The bottom plot is the CM current into the InM from the ICM. Comparing measured and simulated currents, it is clear that the model predicts the measured behavior well over a majority of the frequency range, which extends to roughly 4 MHz. There are some differences between measured and simulated waveforms, particularly between 200-500 kHz. It is possible that this may be due to an asymmetry in the circuit that is not being considered. The source of the error remains under investigation. Nonetheless, overall we are pleased with the results so far. Presently, measurements are being taken on the cables throughout the testbed. In addition, a method to utilize Thevenin-based concepts to characterize components is being evaluated.

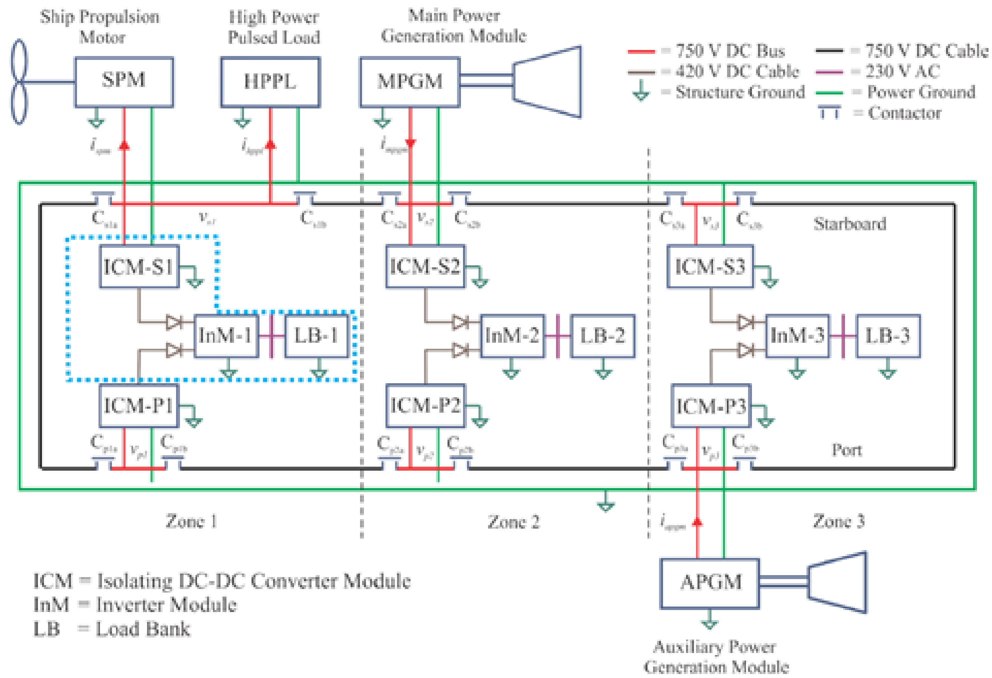

Figure 106: Purdue PDCM.

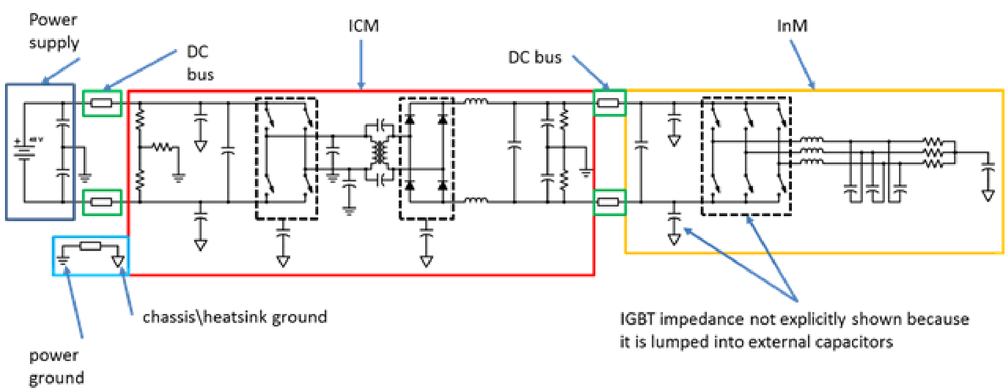

Figure 107: Detailed DM/CM model of Purdue PDCM isolated converter module (ICM) and inverter module (InM) CM equivalent circuit.

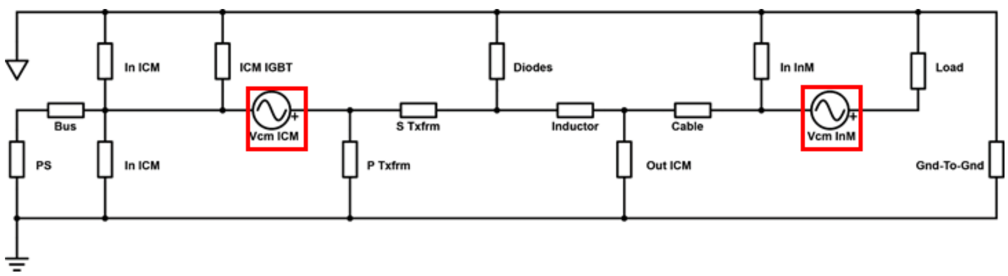

Figure 108: CM equivalent circuit of Purdue PDCM isolated converter module (ICM) and inverter module (InM).

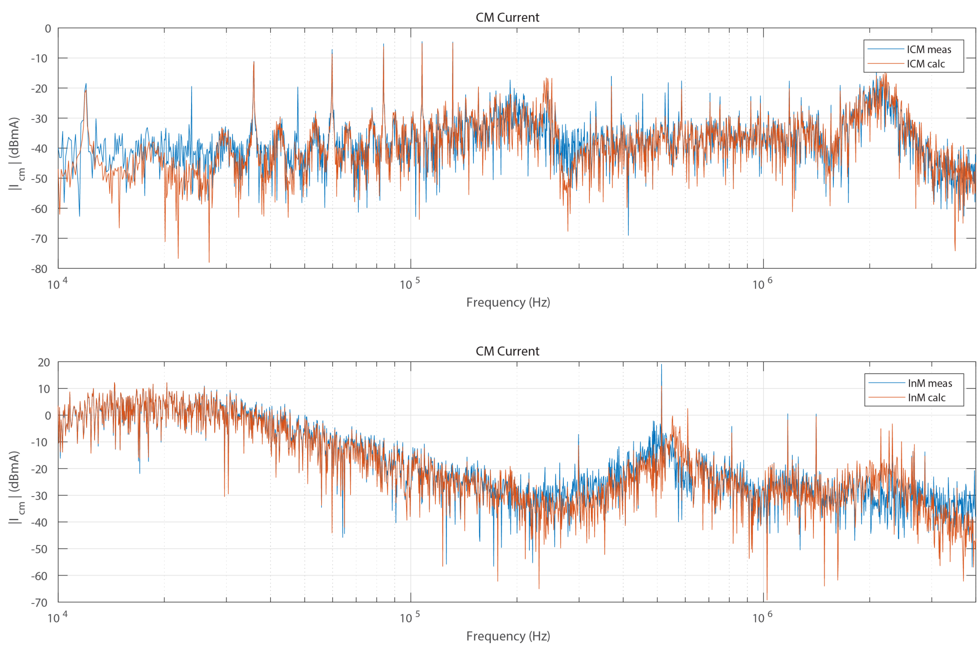

Figure 109: Simulated versus measured CM current at the input to the ICM (top) and InM (bottom).

Task: Real time ground fault localization

Technical Objectives

Determine autonomously the location of line to ground faults in a DC zonal electrical distribution system (DCZEDS) in real time.

Traditional methods of localizing a line to ground fault involve expensive sensors or highly involved human interaction with meters and manual measurements. An autonomous approach has been devised using multi-resolution analysis (MRA) on a single signal in the system to observe its frequency component changes in energy as the ground fault occurs. The major changes can be extracted and ran through a classifier algorithm to determine where the fault occurs based on the frequency changes in the signal. This project focuses on identifying and applying classification algorithms to determine ground fault locality in real time from the features extracted using MRA on the signal.

Technical Approach

The step-by-step technical approach is elaborated as follows:

- Generate large amounts of data from a power system model with different line to ground faults applied throughout the model for the purpose of classification.
- Develop classifier algorithms for determining ground fault locality.
- Evaluate the success rate of chosen classifiers in non-real time, then compare performances.
- Validate classification algorithm performance using real-time simulation system.

Progress Statement Summary

Since the original research classifies fault locality based on features of energy levels in a signal [161], there's an implicit pattern associated to fault location in a system. A two-layer feed forward neural network was chosen as one of the classification algorithms to investigate due to neural network's being strong tools for pattern recognition problems.

For proof of concept, *MATLAB*'s neural network tools were used to classify the data after it has been generated, to validate the ability to sort the data in the first place. A small amount of data was generated and tested, the confusion matrices shown in Figure 110. The important takeaway is that the neural network did not sort the data out correctly to any significant level of accuracy, as indicated by the blue square in the bottom right of each matrix. The conclusion was that there were not enough signals to train the network (only sixteen were used in that experiment).

Currently, significantly more data is being generated and tested. Another step in improving accuracy is providing less general data to the neural network, in order to have more unique samples overall. Previously, ten energy levels were given to the neural network for all signals; however, there is much overlap between the signal energy levels across select frequency ranges which can confuse the neural network. Therefore, if only a specific range of energy levels per frequency band are supplied, the neural network may have more accurate output. Other classification algorithms need to be investigated as well.

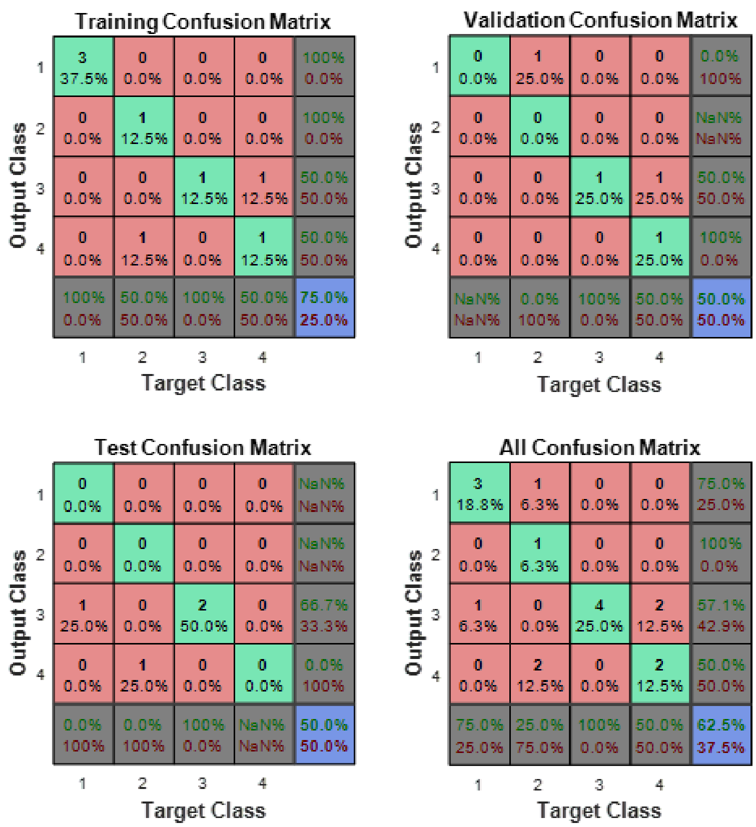

Figure 110: Confusion matrices.

3.5.2 Active power and energy management

Planned future work

3.5.3 Impedance measurement unit for 4,160 V AC networks

Technical Objectives

The objective of this project is performance improvement of the Impedance Measurement Unit (IMU) prototype for 4,160 V AC networks built using 10 kV SiC devices [162–164]. The developed IMU is capable of characterizing in-situ impedances of medium-voltage shipboard power systems (both MVAC and MVDC) in the frequency range from 0.1 Hz to 1 kHz, necessary for system stability assessment. It features Power Electronics Building Block (dubbed PEBB 6000) modular concepts developed using remarkably powerful 10 kV SiC MOSFET modules, and can significantly aid design of the advanced Navy shipboard platforms with contemporary all-electric architecture.

The IMU had been designed, built, and tested in CPES labs under the ONR project award N000141310157 that was completed in the fourth quarter of 2014. After completion, IMU was tested at the medium voltage DC lab at CAPS (FSU), achieving full functionality at 2.8 kV [165]. Operation at 4.16 kV has not been accomplished due to significant negative impact of high-frequency common-mode currents.

This task will perform an upgrade and redesign of the existent PEBB 6000 units used in the medium voltage IMU built at Virginia Tech, which for now has been limited to operate at 2.5 kV AC due to electromagnetic compatibility (EMC) problems resulting from the fast switching of its 10 kV SiC MOSFET power modules. This upgrade will effectively enable the IMU to handle 5 kV DC bus under hard switching, making possible the impedance measurements and stability assessment of 4,160 V AC networks and 6 kV SC in both shunt and series connection modes. Specifically, this task will conduct the PEBB 6000 redesign work at Virginia Tech, and conduct the medium voltage testing and stability assessment at CAPS. The key challenges are: 1) EMC of PEBB 6000 units in the 4,160 V AC IMU, which result from the fast switching (>30 V/ns) of the 10 kV SiC MOSFET devices used, and the large capacitance to ground (>500 pF) of the corresponding power modules; and 2) the IMU perturbation of the medium voltage AC (4,160 V) and DC (6 kV) networks in order to measure impedances.

Technical Approach

Detailed testing of one PEBB 6000 beta-prototype unit will be performed in order to analyze high-frequency common-mode current propagation, and develop efficient methods to mitigate this impact. PEBB 6000 will be partially redesigned to accommodate engineering solutions for improved operation under hard-switching conditions. A systematic EMI study will be performed in order to understand common mode current coupling paths and methods to mitigate their effects before performing hardware improvement of the IMU.

Progress Statement Summary

A systematic EMI propagation study has been in progress for the IMU unit shown in Figure 111. Before expanding the analysis to three PEBBs (whole IMU converter), the study focuses on one PEBB only as marked on Figure 112. Three important factors have been considered in the analysis: the noise source, the coupling channel (propagation path), and the receptor. Although conducted and radiated EMI may both simultaneously exist, the EMI study was initially simplified by putting all the local controllers far away from the power circuit, temporarily eliminating radiated EMI from the study (the noise source is far enough from the receptor). Figure 112 illustrates possible Common-Mode (CM) noise propagation paths for each PEBB from the IMU after such simplification. As illustrated on this figure, the ground network and associated interconnection impedances between different reference points (planes) have a significant impact on the CM propagation paths [166–168].

The CM noise analysis was further performed within a spectrum of interest up to several tens of megahertz using the balanced Wheatstone bridge. Additionally, possible conductive CM coupling parts have been identified by analyzing complete IMU and individual PEBBs and their interconnection. Detailed structure of the PEBB used for that purpose is shown in Figure 113 and Figure 114.

Figure 111: PEBB-based medium voltage impedance measurement unit (IMU).

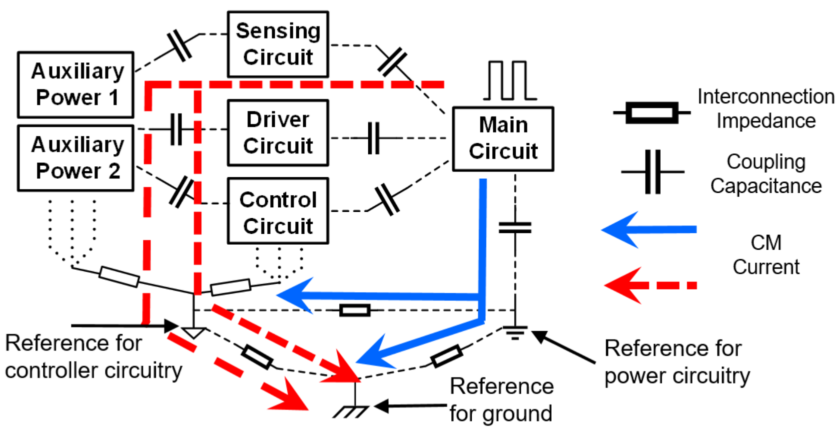

Figure 112: Possible conducted EMI propagation paths.

Critical coupling paths between the control box and main power stage are estimated, and shown in Figure 115, with estimated range of coupling capacitances.

In order to perform any meaningful measurement of CM currents, a proper choice of the current probe is critical. Hence, in order to determine the best possible probe choice, a test setup using 1.7 kV SiC MOSFET half-bridge modules was built. Various tests have been performed and it was found that High Frequency Current Transformer (HFCT) among other options (Rogowski current probe, Hall effect sensor, and isolated voltage probe) gives the best results in the range from 1 MHz to minimum 30 MHz. This probe will be used to measure numerous high frequency CM current paths inside the PEBB 6000 beta prototype in the coming months.

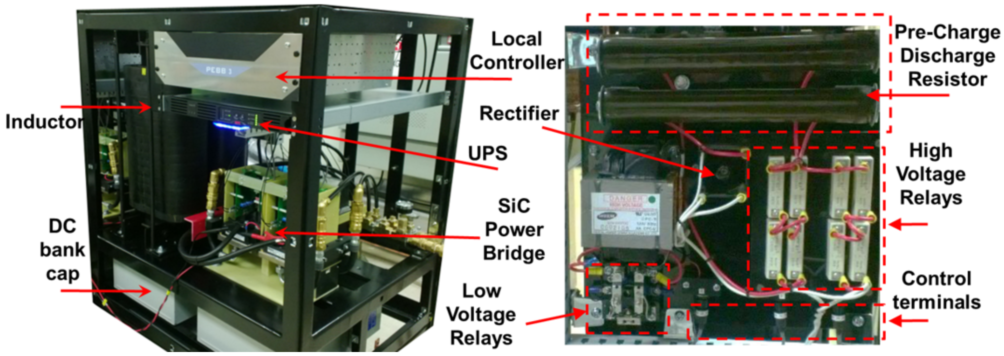

Figure 113: PEBB 6000 beta prototype.

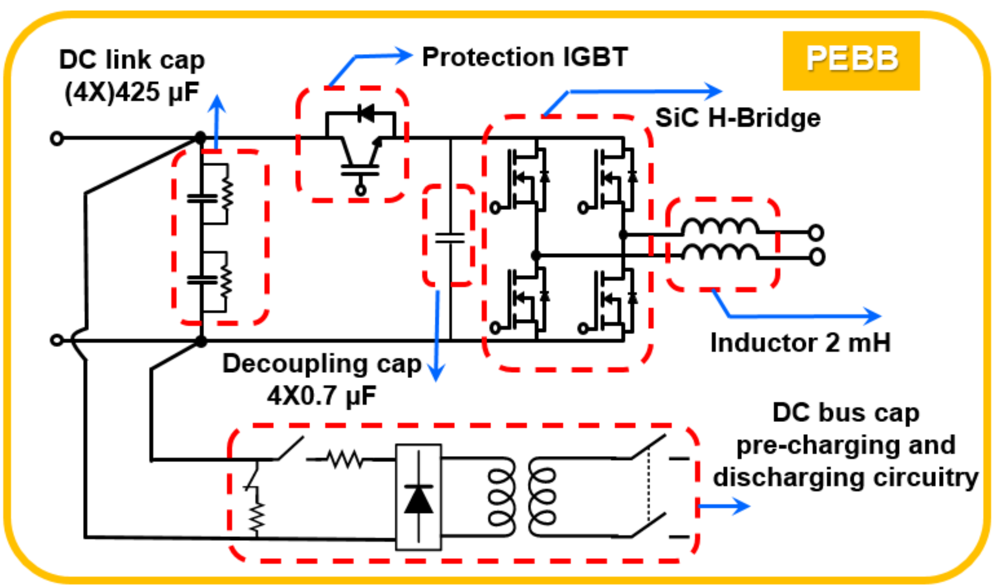

Figure 114: PEBB 6000 internal schematic.

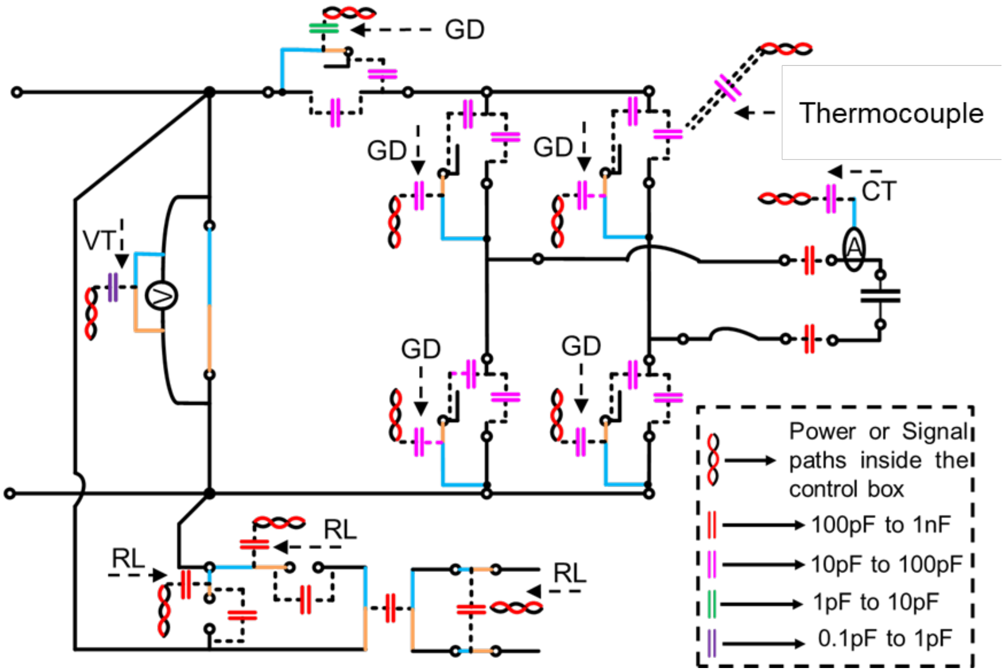

Figure 115: Circuit showing coupling paths between the control box and the PEBB power stage.

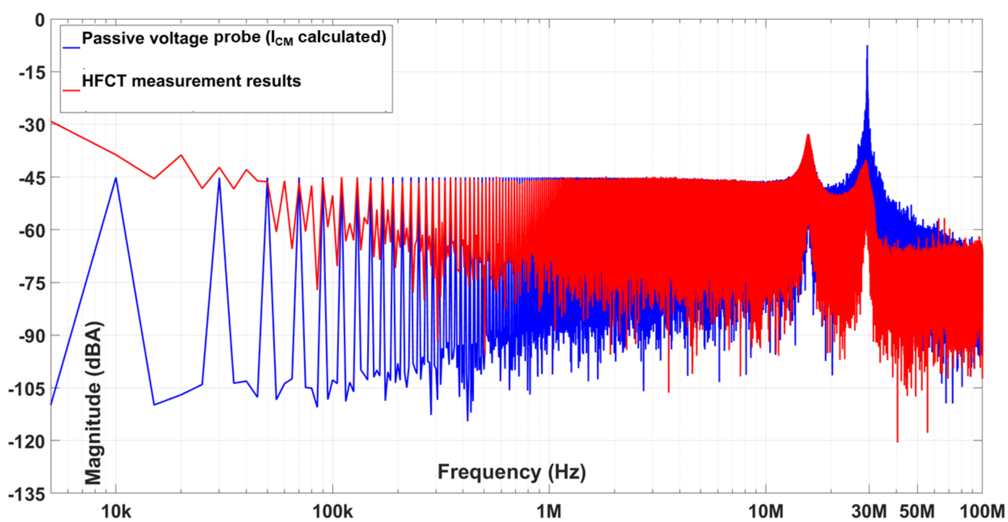

Figure 116: Comparison of CM current measurement at the switching node by using HFCT and passive voltage probe.

3.6.1 Develop fault tolerant control (FTC) and fault mitigation

Task: Fault tolerance control based on sequence-based control

Technical Objectives

Enhance the control resiliency at the power conversion level by directly controlling the switching devices of a single power converter and an interconnected system of power converters. The effect of faults and fault accommodation technique based on sequence-based control (SBC) on ship power system services and functions will be conducted.

In sequence-based control, the behavior of the system based on the system model and specific assumptions is projected in a finite prediction horizon. The assessments on the predicted system behavior are then conducted to detect the optimal sequence of events to be applied to the system [169].

In converter control point of view, the switching sequence determines the output voltage, the thermal characteristics, and FTC capability of power converters. The conventional control methods, such as PWM or hysteresis, are fixed in the thermal characteristics and cannot bear with the switching faults. A subset of SBC, the model-predictive control using a finite control set (FCS-MPC), is utilized in [170] to control an inverter. However, the only prediction horizon utilized in FCS-MPC does not contain enough information to reflect the system behavior and dynamics. Moreover, the constraints in voltages and currents in this approach are not considered in the optimization process. Therefore, the extended SBC is investigated in this research for distributed coordination control of ship systems, where the sequences are projected in multiple horizons, which yield the system performance.

The main issue of the SBC is on its computational burden since the total number of trajectories increases exponentially as the prediction horizon increases. Figure 117 illustrates the SBC concepts for a multilevel converter system. Thus, to facilitate the research, we will develop an algorithm to look at the minimum set of sequences for real-time implementation capability, and apply the developed algorithm for distributed coordination of multi-converter ship power systems.

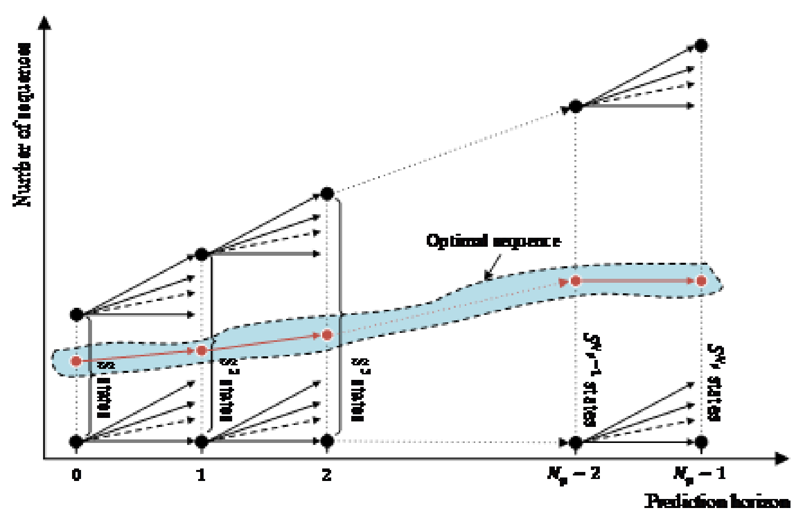

Figure 117: Sequence based control for multilevel converters.

Technical Approach

To realize the FTC based on SBC the following must be applied:

- Develop a control method to directly control the power converter switches.
- Determine the level of decentralization to identify the necessity of distributed control vs. decentralized control.
- Develop reconfiguration schemes for the system to satisfy the desired objectives such as minimal loss, maximum energy availability, and other mission requirements.
- Develop dynamic load shedding strategies to fulfill the energy requirements in different operation modes.
- Evaluate the algorithms via real-time simulation, experiments, and hardware-in-the-loop (HIL) methods.

Progress Statement Summary

Progress has been made on utilizing one SBC control type (predictive control) in [169] for power control in an islanded DC microgrid and [170] for a low-voltage ride through for PV grid-connected systems. The current work will extend the algorithms proposed in [169,170] for the SBC realization in FTC control in ship power systems.

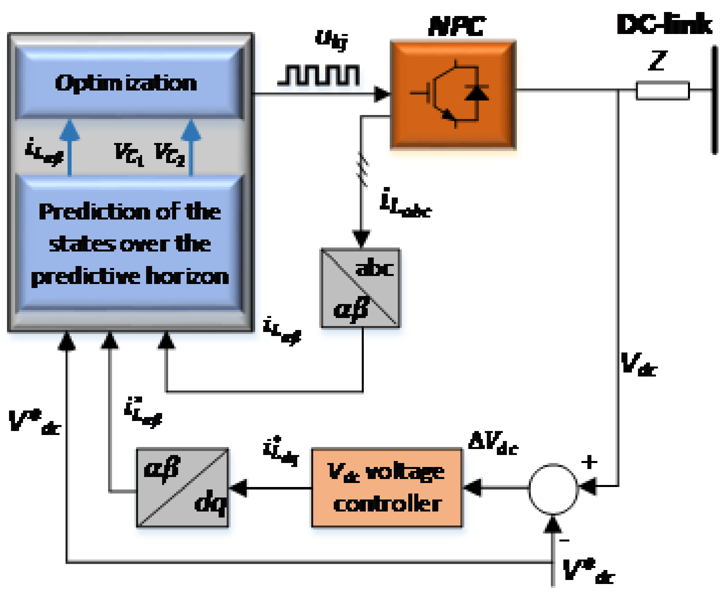

Figure 118: SBC scheme for NPC converter.

The SBC for FTC has been developed for the neutral point-clamped converter (NPC), as shown in Figure 118. Initial results for the FTC capability of the SBC algorithm are shown in Figure 119 and Figure 120. In this case, an NPC with the parameters shown in Table 5 is taken into account. There were two tests performed for the fault occurrence in the upper most IGBT of phase A(S_{21}) at 0.5 s. The first test utilized PI control with the PWM modulation technique (Figure 119). The second test utilized SBC control (Figure 120). Results indicate that the NPC with the PI control fails to respond to the output voltage command at 0.5 s as the DC voltage and AC input currents proceed to instability. In contrast to the PI control, the SBC was able to regulate the DC output voltage close to the reference value with stable AC input currents. Hence, the SBC technique represents a more promising result in comparison to the conventional

PI control method under a fault condition. Our next step is to extend the research to the multi-converter systems.

Table 5: System parameters.

E_m	Amplitude of the line voltage	50 V
ω	Line frequency	377 rad/s
R	Line resistance	0.2 Ω
L	Line inductance	0.804 mH
C	DC bus capacitor	380 μF
R_L	Load resistor	100 Ω
V_{OC}	Output DC	120 V
$S1$ *and* S	Bidirectional switches	$k = a, b, c$

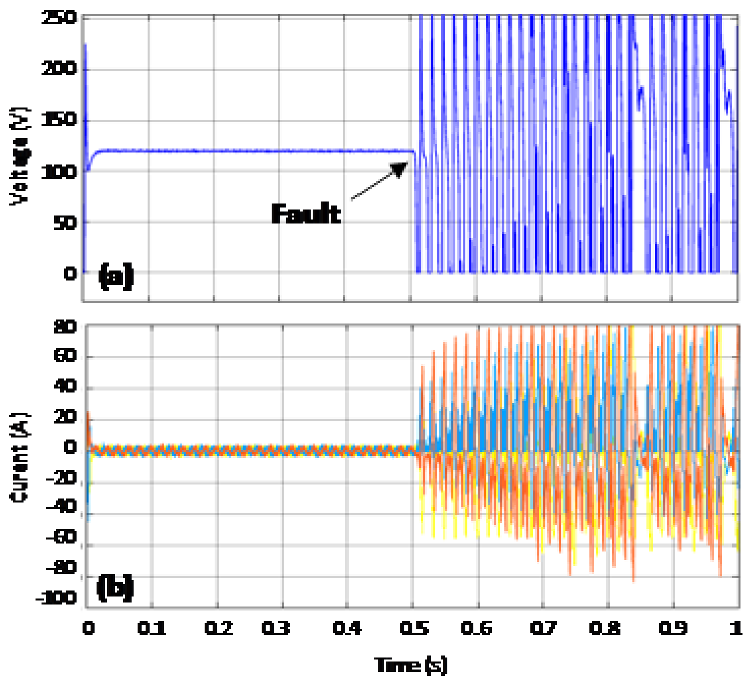

Figure 119: System responses under PI control; (a) DC output voltage, (b) AC input currents.

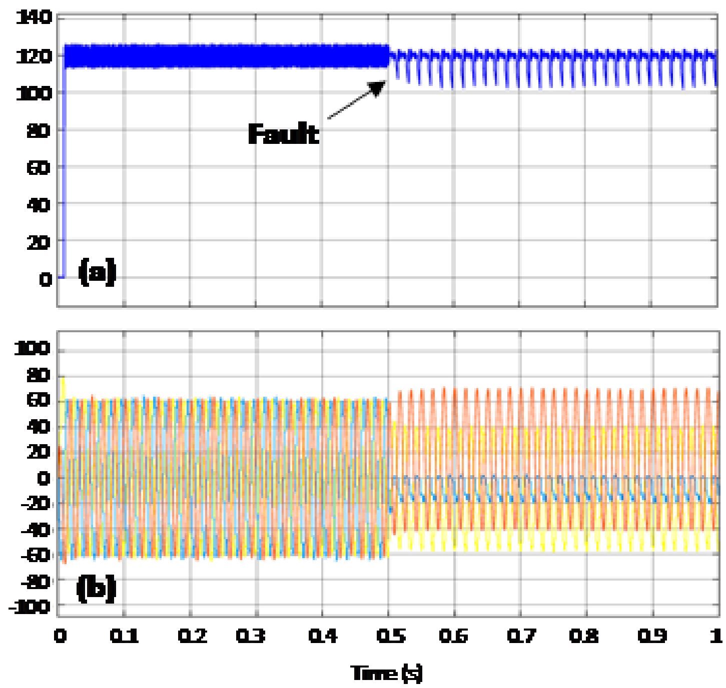

Figure 120: System responses under SBC; (a) DC output voltage, (b) AC input currents.

Task: Toward fault adaptive power system in electric ship

Technical Objectives

Develop novel and effective approaches to deal with different types of faults that may occur in the Shipboard Power System (SPS).

The (SPS) plays a major role in the next-generation Navy fleets. With the increasing power demand from propulsion loads, ship service loads, weaponry systems, and mission systems, a stable and reliable SPS is critical to support different aspects of ship operation and becomes the technology enabler to improve ship economy, efficiency, reliability, and survivability. In SPS, a minor fault can result in destructive consequences, so fault-tolerance becomes an imperative consideration during the early-design step of the SPS. A fault-management system can be employed to increase the capability of the SPS to continue the proper service in the presence of faults. The primary objective of an onboard fault management system is to monitor the current operating status of the electrical power systems, identify the fault at an early stage, take appropriate actions to minimize the effects of the fault, and enable reliable, safe, and robust restoration. This research work aims to introduce novel and effective approaches to deal with different types of faults that may occur in the SPS. An appropriate design of fault mitigation techniques becomes fundamental for the design and analysis of SPS. The main objectives of these techniques are to minimize the effects of the fault and maintain the system performance close to normal conditions.

Technical Approach

- Develop an intelligent real-time reconfiguration algorithm through an optimization technique implemented inside the Runtime environment of RSCAD software in the RTDS.

- Employ a Simulated Annealing (SA) optimization technique, which have advantages over other meta-heuristic methods to solve the reconfiguration problem in the real time.
- Propose a novel approach to mitigate the effects of the unsymmetrical transient faults in the MVDC SPS by employing STATCOM on the AC load side of the SPS.
- Utilize an improved Genetic Algorithm (FGA) to find optimal STATCOMs controller parameters in MVDC SPS to minimize the effects of the faults.

Progress Statement Summary

In this work, we address various fault types within the context of MVDC SPS and their effects on the system performance, these include:

1. Transient faults, including:
    (a) Single line to ground on the AC load (including Load and Generator side).
    (b) Double line to ground on the AC load (including Load and Generator side).
    (c) Three phase to ground on the AC load (including Load and Generator side).
2. Permanent faults, including:
    (a) Loss of Main generator due to fault.
    (b) Loss of Auxiliary generator due to fault.
    (c) DC faults on DC side of the system.

To handle the permanent faults in SPS, a real-time Simulated Annealing (SA)-based reconfiguration technique is designed and implemented in the Real-Time Digital Simulator (RTDS) [171]. To validate the proposed approach, two MVDC SPS models, including four and six zonal loads, respectively, are used to simulate several fault scenarios. The simulation results demonstrate the effectiveness of the proposed reconfiguration approach to deal with different fault scenarios.

Moreover, a solution to minimize the effects of the asymmetrical transient faults in the MVDC SPS that employs a Static Synchronous Compensator (STATCOM) in the AC load side of the SPS [172] has been proposed. An improved Genetic Algorithm (FGA) is also introduced for optimal design of the STATCOM. The underlying optimization problem is to identify the STATCOM controller parameters using the FGA optimization technique. The performance of the proposed FGA-based controller design is compared with the GA-based STATCOM design under different operating conditions and faults. The optimal design of the controller with a FGA optimization approach provides an acceptable post-disturbance and post-fault performance to recover the system to its normal situation.

In this reporting period, in order to deal with the reconfiguration problem during the fault situations in MVDC SPS, we continued the previous research effort in designing and testing of a real-time Simulated Annealing (SA)-based reconfiguration technique on the Real-Time Digital Simulator (RTDS) to quickly restore the power supply to the affected parts of the SPS and reconfigure the system to improve its reliability and ensure safe and satisfactory operation of the system after the occurrence of faults. We have completed the validation of the proposed approach based on two MVDC SPS models including four and six zonal loads under several fault scenarios. The simulation results obtained during this report period have demonstrated the effectiveness of the proposed approach to reconfigure the system under different fault situations in the real-time operation of the SPS. The mathematical model of the reconfiguration is also solved in the GAMS optimization software to verify the results from the real-time RTDS-based reconfiguration design. The results of this work are reported in [171].

Another accomplishment we have made is the investigation of the application of combined Static Synchronous Compensator (STATCOM)-Super Conducting Fault Current Limiter (SFCL) on the AC load side of the SPS to improve the stability of the system during transient faults. Performance of the Fluid Genetic Algorithm (FGA) which was previously proposed has been verified in solving the multi-objective optimization problem by successfully identifying the STATCOM controller parameters. We have also considered various types of short-circuit faults to obtain the optimal impedance of the SFCL. The performance of the proposed scheme to minimize the effect of faults has been confirmed through time-domain simulations with *MATLAB*/SIMULINK platform. As envisioned in our previous research statement, the proposed technique is now experimentally proven to produce improved post-disturbance and post-fault transient response and effectively restore the system to its normal situation. The outcome of this research effort is reported in [172].

In this reporting period, we are working on stochastic and robust control for operating a resilient shipboard microgrid. Physical events such as faults and failures are coupled with cyber-events, which is covered in Task: Efficient event and intrusion detection systems for shipboard power systems, to deliver a unified control strategy to prevent events that may severely disturb the stability of the system and cause significant frequency and voltage oscillation. We focused on deriving a Web-of-Grid based uncertainty handling mechanism. We have developed an innovative unified stochastic and robust optimization model to take advantage of both stochastic and robust optimization approaches. The proposed approach can provide control decisions that can lead to a minimum expected cost function while ensuring the system robustness with the consideration of physical faults, high-power loads that requires a very high amount of power in a very short period of time, as well as the highly uncertain, unpredictable and non-exhaustive nature of the environment the warships. We are currently working on finalizing the proposed approach and demonstrating that it could expand the stability margin under stressed conditions given the limited generation capacity and slow-reacting dynamics of onboard generators.

3.6.2 Develop fault-triggered reconfiguration solutions

Task: Optimized reconfiguration of shipboard power systems

Technical Objectives

Develop an infrastructure (e.g. algorithms, architecture) to reconfigure the SPS with the objectives of isolating faulty section(s), reestablish operation of healthy sections, and reach an optimal state as measured by performance metrics. After detection and isolation of a fault, reconfiguration of the SPS may result in improved performance (e.g. probability of mission success); however, the best possible reconfiguration option is often dynamic and based on criteria including: SPS mission load requirements, available system resources, and energy storage systems.

Technical Approach

- Develop a useful definition of 'optimal' list criteria that helps define situation-dependent optimality and means-to-rank configurations. A graph representation of SPS will be developed and used for reasoning about possible configurations (e.g. paths to get power to the loads). The substantial existing work mainly concerns issues such as unit commitment and fuel-cost optimized dispatch orders but does not directly apply to the SPS needs with respect to varying load priorities and heavily resource constraint power and energy distribution.
- Expand automated enumeration and testing of fault scenarios on a real-time power system simulation using SPS model to the newly envisioned MVDC system architecture, and build on modeling and simulation efforts of supporting projects under Thrust 1. To help evaluate solution options, both offline and real-time testbeds will be implemented. While the offline approach supports evaluation of many large-scale solution spaces, evaluation, and benchmarking of the real-time counterpart allows for identifying possible issues with respect to timing and resource sharing.

Progress Statement Summary

A means to derive the graph representation of a shipboard power system has been developed using a notional two-zone ship board system [157]. Progress has been made towards automated generation of a graph from the source code of the model, but is not fully complete. The automated generation work includes a parser written in *Python* for RTDS .dft files.

A controller hardware-in-the-loop (CHIL) setup with a surrogate platform (including hardware) has been interfaced to the RTDS installation at CAPS, and an initial fault detection and isolation architecture (including a prototype) has been developed [173, 174]. There has been regular collaboration with the design team developing the RTDS model. Results of the collaboration include interfaces and modular design built into the model to provide sufficient flexibility for eventual CHIL experiments.

There has been regular participation in the Time Domain Electric System Model Working Group (TDESMWG) under Project 1.4.4 and collaboration with the team developing the RTDS model implementation.

Progress has been made integrating reconfiguration used as part of fault management into a real-time simulation environment. The integration was performed in collaboration with Project 1.3.3. This integration helped to further refine and develop real-time simulation interfaces for reconfiguration development and evaluation.

Work on designing a distributed version of an existing centralized reconfiguration algorithm specifically targeted for fault management is being done. A consensus-based approach is being investigated where multiple nodes perform current differential-based detection and compute reconfiguration options in parallel.

The fault detection and isolation architecture has been implemented and demonstrated with a CHIL setup leveraging a surrogate hardware platform interfaced to a simplified one-zone digital real-time simulation.

A lack of scalability with the offline analysis of the previously developed fault detection solution was discovered when migrating the previously developed solution to a larger two-zone real-time simulation model. The offline analysis is used to determine the set of available measurements that can be used for detecting faults. When running the fault detection on the two-zone model, the offline analysis consumed a much more significant time (∼4 hours) than the simpler one-zone model, which completed in seconds. After a close inspection of the algorithm, it was determined that the algorithm had an exponential computation complexity for the number of disconnect switches in the system.

An improved solution was developed to overcome the lack of scalability, which has near linear computational complexity with respect to the number of disconnect switches. Figure 121 illustrates the graph representations of the one and two-zone [157] notional ship systems. Table 6 provides the difference in computation time for the two solutions.

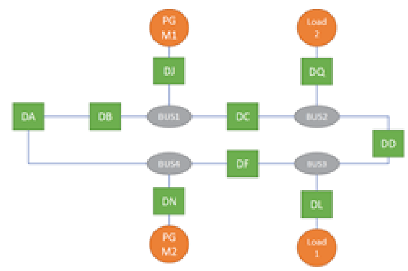

One-Zone Model

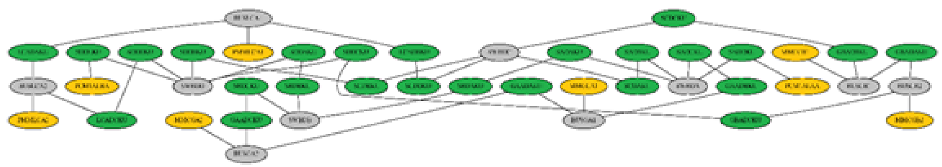

Two-Zone Model

Figure 121: Graph representations of the one and two-zone notional ship system models.

Table 6: Measured computation time (typical desktop computer).

	Simplified One-Zone	Notional Two-Zone	Notional Four-Zone (expected)
Initial Algorithm	150 ms	3 hours	> 100 years
Improved Algorithm	0.3 ms	0.8 ms	5 ms

This page intentionally left blank

Thrust 4: Developing New Design Functionalities

Technical Objectives

Enhance the ESRDC's S3D research and development platform while also transferring relevant technologies to the Navy. It will preserve the Navy's investment in S3D as an agile rapid tool development testbed, and ultimately will enable Navy engineers to more quickly develop better and more capable ships. The S3D incorporates data exchange capabilities that support collaborative and concurrent engineering design methodologies. It comprises a suite of tools that includes, a dedicated tool that enables users to better depict power interconnects (cables, bus bars). Such functionality within S3D makes use of spatial information that adds reliability and confidence to early-stage design of a ship's power system. The ESRDC tools were developed in and utilize design data that adheres to relevant IEEE standards and the best practices of naval shipyards.

Technical Approach

Conduct research in seven major areas:

1. System engineering guidelines for electric ship design.
2. Controls.
3. Time domain simulation.
4. Automated SBD.
5. Distributed system design and analysis.
6. LEAPS/FOCUS ontology compliance.
7. Traceability and documentation of electric ship design.

Progress Statement Summary

Current work reported herein includes:
4.1.1 Enhance the DGT to encompass systems engineering, SBD, and shipboard equipment scaling rules
4.1.2 Develop multi-scale thermal models and management strategies
4.1.3 Improve the fidelity of mechanical system representation within S3D
4.2.1 Evaluate the performance of power system device behavioral models in S3D
4.2.2 Experimentation of early stage controls for shipboard system design in S3D
4.2.3 Validate control design as well as compatibility with other systems
4.3.1 Dynamic linking of external time domain simulation programs with S3D
4.3.2 Evaluation of time domain thermal simulation capabilities and integration with S3D
4.4.1 Explore methods to integrate HPC capability with S3D
4.5.1 Evaluate the performance of distributed system designs in S3D including V&V
4.5.2 Implementation of templates-based design in S3D including utilization of established equipment-scaling laws
4.5.3 Integration with S3D to provide optimized design (based on volume and weight) of thermal system
4.6.1 Develop unified and compatible ontologies between S3D and prevalent Navy ship design tools
4.8.1 Adapt technologies developed in S3D to the Navy

The following projects are planned for future work:
4.4.2 S3D exercises to test automated SBD
4.6.2 Integration of scalable high speed machine models into S3D

4.7.1 Investigation of feasible methods to enable automatic, traceable, and updatable documentation
4.7.2 Develop customer end data management and transferability

4.1.1 Enhance the DGT to encompass systems engineering, SBD, and shipboard equipment scaling rules

Technical Objectives

Expand the design capabilities by:

- Enhancing the design guidance tool (DGT) to readily leverage the larger body of ship design knowledge that exists within research journals, military specification documents, as well as Navy and industry standard practices, both when making decisions at design time and when performing assessments of an existing design.
- Expanding the capabilities in S3D by incorporating set-based design (SBD) and risk analysis capabilities. Additional capabilities such as the development of components that utilize scaling laws, an assessment of overall accuracy, and other user supporting features will be included in the DGT. Supporting documentation will be an added outcome of this project.

Technical Approach

Initially the focus will be on the development of algorithms and methods capable of analyzing human-entered queries and finding strong correlations between these queries and the larger corpus of design guidance and research documentation. Tools and processes will be developed to enable the corpus to be periodically updated, and also purged of dated information. Design rules and guidelines must be codified, and violations within a design should be made detectable and possibly enforceable. This requires the development of tools that allow such rules to be entered into S3D and permit the user to specify how a design can be generically checked to ensure the rule is not violated.

Work done in Project 1.1.1 will help to guide the implementation efforts for this project by advancing the knowledge gained by benchmarking the MMC-based system through the rigorous tasks [175,176] summarized as follows:

- Expert knowledge elicitation — This first step in gathering subject-specific data forms the input to the house of quality (HOQ). Surveys aimed at power electronics experts to obtain information that sheds light on the various MMC-related design aspects will be used.
  - Implementation plan — Utilize sophisticated data mining techniques (response-tagging being one) to build a comprehensive repository that links expert knowledge regarding relevant shipboard systems with early-stage ship design requirements.
- HOQ — Data from the customer (in this case, naval shipboard compatibility guidelines from IEEE and MIL standards, etc.) and subject matter experts obtained from step 1 form the inputs. HOQ combines the customer needs with technical aspects to help rank and filter pertinent engineering characteristics (EC).
  - Implementation plan — Incorporate a ranking system derived from the design database to help focus on pertinent design factors or considerations for a particular system or subsystem.
- Taguchi method (TM) — Highlighted EC from the HOQ form a basis to build a Taguchi orthogonal array. This process helps us better understand the various combinations of design factors and their interactive impacts on the desired output, and to eventually obtain the most optimal or 'robust' design.
  - Implementation plan — Develop representative code to automatically build a Taguchi table with decision making to narrow down the most feasible designs that fulfill certain user-defined criteria, such as those based on a particular mission profile.

Progress Statement Summary

A prototype of the decision support tool has been developed and integrated into the S3D design environment. Users can query the corpus using a natural language expression. The search process utilizes an algorithm developed by FSU to determine relevant keywords within the query and correlates these with all uploaded journals and military specification documents. The initial exercising of the tool identified a need for several new features and enhancements to the existing capabilities.

Additional work focuses on developing a process that utilizes surveys, HOQ and TM to narrow down the designs for an MMC-based system. This work is ongoing outside of S3D and future efforts will deliver *MATLAB* code that demonstrates the application of the proposed step-wise methodology. This work will utilize outcomes from related research done in the appendix of reports. Originally proposed sub-thrust 4.1 project 'Scaling laws for modular scalable design for CPES and its application in S3D' is now consolidated into Project 4.5.2 and reported separately.

Work described in [7, 177, 178] focuses on the development of potential tools for designing a Modular Multilevel Converter (MMC). The investigated tools and methodologies aid in better identification and exploration of the design domain to develop pertinent metrics. Some identified techniques including quality function deployment (QFD), Taguchi method (TM), and full factorial method (FFM) are detailed in [8,178].

A tool for sizing MMCs has been developed in *MATLAB* and *Excel* environments. This tool can perform the design cycles governed by TM and FFM. The outcomes of the tool are metrics such as power density, reliability, etc., along with scaling relations that exist between different design parameters and outcomes. Currently, this tool is in the process of being integrated into S3D. Current work focuses on developing a similar study with line commuted converters such as a Thyristor Controlled Rectifier (TCR). A comparative analysis between MMC and TCR from the perspective of power density can aid in choosing the right converter topology for power generation modules on all-electric ships.

Integration of additionally developed tools mentioned herein into S3D will take place under Project 4.3.1, with further development of component scaling laws under Project 4.5.2.

The research team updated algorithms for the scalable motor and generator models in S3D. The new model is similar to the earlier version, except that it now reports tip speed and also has a provision for a free aspect ratio.

Previous efforts to develop a set-based design methodology [9] were extended to include the reliability metric for Modular Multilevel Converters (MMC). The addition of this metric along with the power density metric aid in providing a full picture of the design outcomes [179]. Some of the technical strategies for the developed methodology are as follows:

- Formulating Reliability Value Metric (RVM): MMC converters components such as IGBTs, submodule (SM) capacitors, thyristors, inductors, etc., contribute to overall converter reliability. A brief literature review on the context suggests that IGBTs and capacitors are the most vulnerable components in terms of reliability in MMCs [179]. However, according to the methodology developed in [178], the number of IGBTs in a SM is fixed for being full bridge, but capacitors can be of different voltage rating and capacitance to fulfill the requirements. Hence the focus is made on arranging capacitors of different ratings and using well-established equations for determination of RVM. Following previous design steps [9], a full factorial analysis was performed using a signal-to-noise ratio (SNR) based evaluation to narrow down the sets. Eventually a choice can be made by identifying the most dominant design factors from the outcomes. A comparison study between RVM and the power density metric was carried on to establish a tradeoff which can help the designer obtain a comprehensive view of the design.
- Incorporation of Similar Converter Topologies: Apart from MMCs, Thyristor Controlled Rectifier (TCR) can be another option for the power generation module of electric ship. Based on the harmonic requirements structure of a TCR they can be either 6, 12, 18, or 24 pulse. However, better performance comes with the cost of bulky transformers which increases the size and weight of the overall system. To evaluate these facts, a study is being performed to develop similar methodologies as derived in [178], but for sizing a TCR. Well- established equations along with some defined design rules are being

applied for sizing components such as damping capacitors, resistors, valve reactors, grading resistors and capacitors, smoothing reactors, and DC side filters. A comparison study with an MMC is planned in terms of system power density, which will benefit in selecting a system to fit the requirements.

A rigorous design exercise was performed to develop the RVM for an MMC converter. The addition of RVM with the power density metric establishes certain tradeoffs in the design domain where the user can select to pursue the design in a way which meets the criteria. The full factorial design tool developed to perform the study is fully automated and can readily be integrated into S3D. Current work is focused on developing a similar tool for sizing a TCR which is expected to make the options for the design tool more robust and flexible for the designer.

4.1.2 Develop multi-scale thermal models and management strategies

Technical Objectives

Develop a multiscale thermal management approach (i.e. modeling and simulation methodologies) to derive a dimensionless model that relates cooling systems and thermal loads to geometric and operational parameters. Work will also be done to simulate and experimentally validate the models using components of different scales. Relevant mechanical and machinery system requirements driven by electrical and thermal system designs, as well as equipment placement, will be captured. In addition, scaling relationships will be developed to determine the required size and weight of these thermal subsystems.

Technical Approach

- Develop an integrated thermal management approach that captures the integration of multi-scale thermal management solutions.
- Develop dimensionless models that relate cooling systems and thermal loads to geometric and operational parameters.
- Develop scaling laws for ship thermal systems.
- Simulate and experimentally validate models using components of different scales.
- Develop a guideline to be used as a reference in conjunction with Navy rules in S3D.

Progress Statement Summary

A novel dimensionless mathematical model of a vapor compression cycle has been developed based on the effectiveness-NTU method. The model allows the visualization of temperature distributions in the heat exchangers (e.g. condenser and evaporator), as well as the fraction of the total heat exchanger area occupied by each refrigerant phase. The model validation and integration with system-level thermal management design tools have started.

The mathematical model of a vapor compression cycle [123] was used to study the effects of pressure ratio on the refrigeration system performance by computing the second law efficiency, coefficient of performance, and refrigeration load. The work has been done dimensionless and it is therefore extensible to other design configurations.

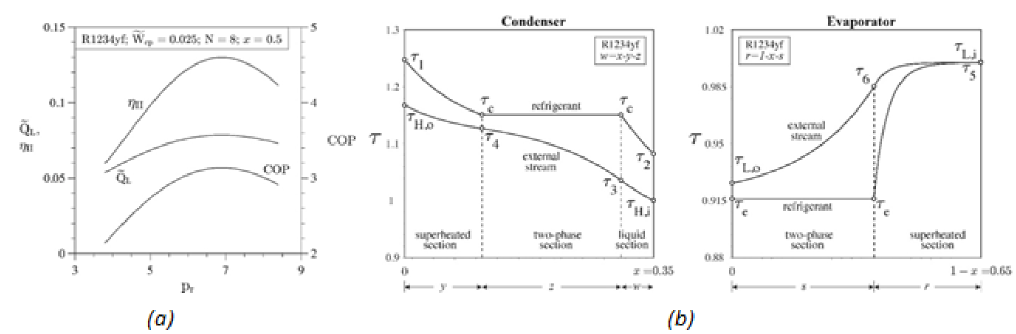

Figure 122: The effects of (a) pressure ratio on system performance; and (b) total heat transfer area allocation on the match between the temperature distributions of the two streams in the condenser and in the evaporator.

We optimized the internal structure (heat exchanger areas) of a dynamic vapor compression refrigeration system for maximum global system performance described by the coefficient of performance (COP), refrigeration rate, second law efficiency, and pull-down time. The numerical optimization was subjected to fixed system heat transfer surface, and the relative sizes of condenser and evaporator were selected optimally via parametric sweeps. Optimization results demonstrated the existence of distinct optimal area allocation for each objective function considered herein while higher evaporator to condenser global heat transfer ratio was preferred in all cases. Maximum COP was achieved, for instance, with smaller evaporator area than maximum second law efficiency that yielded shorter pull-down time and lower refrigerated space temperature in exchange for slightly higher compressor power and total exergy destruction. In summary, this work provides insights into the selection of an optimal refrigeration system design based on its dynamic responses and physical implications [180].

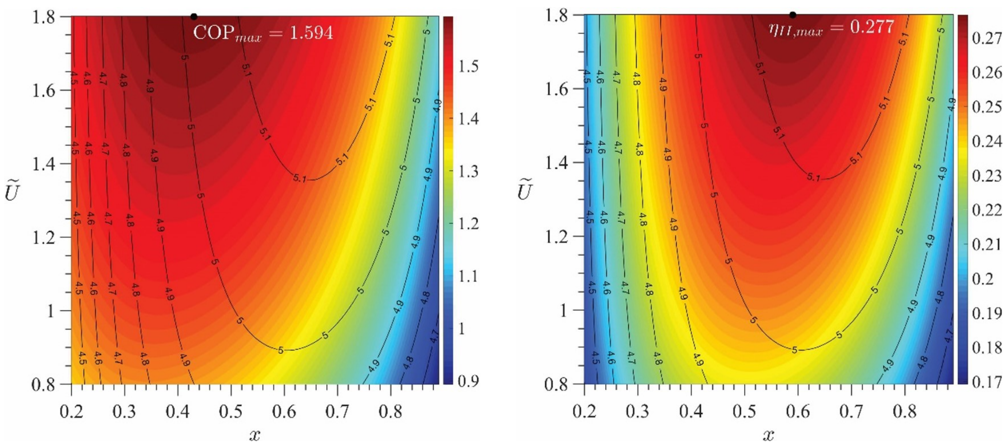

Figure 123: Variations in (left) COP and (right) second law efficiency along with constant cooling rate curves as functions of heat exchanger area and overall heat transfer coefficient fractions.

4.1.3 Improve the fidelity of mechanical system representation within S3D

Technical Objectives

Expand the design capabilities by developing methodologies for characterizing the performance of and assessing the arrangement of critical mechanical systems on board the ship. Relevant mechanical and machinery system requirements driven by electrical and thermal system designs, as well as equipment placement, will be captured. In addition, scaling relationships will be developed to determine the required size and weight of these mechanical subsystems.

Technical Approach

- Capture relevant elements of Mil-Std-3045, 'Design Criteria Standard for U.S. Navy Surface Ship Machinery Arrangements.' Important elements will include vital component locations and interconnections as well as gas turbine engine intake and uptake systems. Intake and uptake systems are an important consideration because of the large physical volume they represent.
- Explore methods for automating the sizing of select mechanical and auxiliary systems including fuel and lubrication systems, seawater service systems, and others.

Progress Statement Summary

Preliminary intake specifications for a variety of common gas turbine prime movers have been captured. These specifications will drive a number of calculations including mass flow rate, volumetric airflow, component cross-sectional areas, and duct element pressure drops. These calculations and other relationships defined in Mil-Std-3045 are being distilled for incorporation into the S3D tool.

This project will continue when FY18 funds become available.

4.2.1 Evaluate the performance of power system device behavioral models in S3D

Technical Objectives

Develop tools that help the user capture and inject controls into the S3D conceptual designs.

Proper evaluation of competing ship designs within the S3D environment is time consuming and error prone as the user must manually establish an appropriate and optimal operating point for each operational state for which the ship is to be analyzed. Methods and tools that reduce the time required to establish an optimal plant alignment and that automatically and intelligently handle unanticipated simulation events, such as damage scenarios, faults, energy or fuel constraints, etc., must be developed.

The research efforts under sub-thrust 1.3 and Project 4.2.2 will help formulate the concrete implementation plans for this project. The research conducted in Project 4.2.2 will help to determine the requirements and feature set for a control layer to be integrated into S3D.

Technical Approach

There are several possible forms by which to capture controls at the conceptual design stage.

- Create a design tool that allows the user to develop a control system that integrates with other schematic design tools within S3D.
- Create a set of optimization algorithms and tools that work in conjunction with user-supplied constraints and enable the system under study to provide reasonable responses to various simulation events that occur during co-simulation.

As research progresses in the associated sub-thrust and projects, the approach for this project will become more narrowly focused.

Progress Statement Summary

This project will not start until the controls layer has been formally defined along with a set of software requirements by which it can be implemented.

For the automation of batch S3D runs, MSU has had several conference calls and email exchanges with both USC and Georgia Tech in order to be able to assist in running parameter sweeps, tradespace exploration, or SBD. MSU is working with Georgia Tech and USC in defining and initializing parameter sweeps to run. MSU is working with USC to design a GUI, targeting fall of 2018. Proper design of this automation on the front end will enable more adaptability to HPC platforms or multi-core desktops for smaller runs.

4.2.2 Experimentation of early stage controls for shipboard system design in S3D

Technical Objectives

Develop algorithms and methods that help reduce the time required to properly and fairly perform an analysis of alternatives across designs, as well as permit S3D to operate in a more scalable mode with the potential to evaluate thousands of ship designs within a suite of mission scenarios.

Proper evaluation of competing ship designs within the S3D environment is time consuming and error prone as the user must manually establish an appropriate and optimal operating point for each operational state for which the ship is to be analyzed. Methods and tools that reduce the time required to establish an optimal plant alignment and that automatically and intelligently handle unanticipated simulation events such as damage scenarios, faults, energy or fuel constraints, etc. must be developed.

The research efforts under sub-thrust 1.3 will help formulate the concrete implementation plans for this project. The research conducted in sub-thrust 1.3 will help determine what types of surrogate controls should be included as part of the early-stage ship design process and how these should be integrated into S3D. Once the research and methodology stats become more mature, it will be incorporated into the S3D environment.

Technical Approach

- Develop optimization algorithms and tools that permit the user to supply weighted objective functions that can be applied generally to all ship designs; the initial development will focus on working with a simplified version of the ESRDC 10kT baseline design.
- Automatically determine which gas turbines should be powered and how the load should be split across all generators in order to achieve the minimum fuel consumption rate given the operational state of the ship as a whole.

Once this initial problem has been solved and a generalized framework has been formulated, additional capabilities will be added to the tool eventually allowing S3D to be utilized in a more autonomous mode.

Building upon the successful implementation of the cable calculator within S3D, MSU has proposed to assist USC in the development of a user input interface for establishing parameters and initial conditions for various mission profile studies.

Progress Statement Summary

The ESRDC held a meeting in February 2017 in conjunction with a conference on controls. The purpose of this meeting was to start a dialogue about the level of control that should be captured within the S3D environment, as well as what information should be captured. The initial meeting helped answer some of these questions, but will require further investigation before we are ready to start implementation. The results of the research effort under sub-thrust 1.3 will feed into the implementation effort in this project. The MSU and USC teams will engage periodically to determine the automation implementation. This project is currently on schedule.

The USC and MSU teams participated in an August 2017 ONR conference on controls. MSU has identified a potential framework for developing a user input interface for establishing parameters and initial conditions for the automation of various mission profile studies. MSU and USC will collaborate to implement the interface.

4.2.3 Validate control design as well as compatibility with other systems

Technical Objectives

Build a lab-scale thermal bus, develop an associated control algorithm, and characterize the thermal bus.

Technical Approach

- Validate the thermal/fluid models and associated control algorithm experimentally, using the lab-scale thermal bus as shown in Task: Achieve global thermal efficiency of electric ships through realizing timely and localized heating/cooling needs via a thermal bus.

Progress Statement Summary

A new two-phase loop with an integrated control system is being built. Two flowmeters have been ordered and will be installed in the near future. Once installation is completed the two-phase loop will be operational.

4.3.1 Dynamic linking of external time domain simulation programs with S3D

Technical Objectives

Increase the analysis time resolution within S3D by transitioning from a time series of algebraically defined mission operating points to a set of coupled differential algebraic equations. With increased time resolution the S3D environment will help expedite and automate the exploration of a design, and will provide feedback mechanisms in order to update and improve the fidelity of conceptual models. Ultimately, S3D will support faster than real-time mission-level simulation with dynamic system models that will help ship design teams provide transformational solutions to complex problems, integrate new features and capabilities, and de-risk these complex solutions at the earliest possible time.

Sub-thrust 1.4 investigates the theoretical aspects of this topic and will provide input into the implementation of these capabilities within the S3D environment. A prototype will be constructed in order to help the development team gain insight into the unanswered questions and topics that require further research and investigation. Collaboration with the team investigating sub-thrust 1.4 will provide answers to these and other questions.

Technical Approach

- Generate automatic migration of a conceptual design to one or more external simulation tools.
- Develop new algorithms and a new type of solver that integrates directly with S3D which may reduce the time required to perform a time-domain simulation.
- Develop a model library tool that will enable equipment, captured in the conceptual design, to be mapped to models within specific simulation tools and environments; this would include capturing appropriate parameterization of such models in order to represent the equipment with a high degree of accuracy.
- Develop a separate tool that will be responsible for the creation of tool-specific schematics including model parameters and connectivity, in order to provide the time domain analyses.
- Develop a post processing tool to interpret the results of the simulation and push information gleaned from the time-domain simulation back into the conceptual design where appropriate.

The fundamental idea of the proposed approach is to combine Quantized State Systems (QSS) with orthogonal decomposition (e.g. Dynamic Phasor (DP)) to represent the system of interest. The system model will be defined as a set of coupled Discrete Event System Specification (DEVS) models. While traditional DEVS models are coupled using a signal flow approach (implying causality), in the proposed approach component models will be coupled to satisfy energy conservation laws (non-causally) by adopting the Latency Insertion Method. Changing the quantization size of the QSS approach will allow the method to adapt a single model to different levels of detail, while the approximation order of the DP representation will allow the method to adapt a single model for analysis while using different time scales. The DEVS approach will also allow using the solver embedded in S3D to work as coordinator for the interface to domain-specific tools.

Progress Statement Summary

Progress on this project has been made in two separate research areas: (1) the development of a prototype mechanism to migrate a conceptual model from S3D to an external time-domain simulation tool; (2) initial work on a time-domain simulation tool that will be integrated directly within S3D.

A prototype of the model library and schematic generation tools were developed in order to gain deeper insight into the problem space and formalize the research questions that need to be answered in order to provide time-domain simulation capability within the S3D environment. The prototype loaded a simple conceptual design from S3D and utilized the model library tool to provide appropriately parameterized models. For this exercise, the Simulink simulation environment was utilized as it is quite commonly used by the engineering community. The schematic generation tool created a schematic in Simulink and performed a basic simulation. These efforts and results are documented in [181].

A preliminary solver was developed in VTB and tested with a micro-grid model [182]. Work is now proceeding with the creation of needed models and a demonstration test case. The demonstration reference scenario has been created in S3D and it is a simplified version of the 100 MW 100 kton design, a simplified scenario has been created to reduce the number of models that have to be created for this first demonstration but electrical, thermal and mechanical domain models have been included to show the benefit of the proposed approach when very different dynamic behaviours co-exist in the same model. Completed models include a generic power electronics converter (can be used as a DC-DC, DC-AC, and AC-DC converter), a synchronous machine, and a propeller.

The research team also began a theoretical analysis of the error-quantum relation in QSS integration, this step is critical to ensure execution speed and accuracy. The relationship between simulation error and quantum value in QSS has been investigate both for linear and nonlinear systems. A method is defined to make the quantum proportional to the value of the integrated variable, which is a significant advantage over traditional fixed quantum selection because it allows obtaining a relative error control. The method is based on a logarithmic quantization and its boundedness has only been proven for linear time invariant system, but even if not formally demonstrated the applicability to non-linear cases has been tested. To really be able to use the QSS approach as an integration method for multi-physics simulation in support of design applications, it is necessary to develop a method for proper selection of relative error accuracy for each variable in the system. The major challenge in this context is to develop a method that can actually be applied in a simulation tool. Many accuracy and stability analyses for simulation methods are based on eigenvalues or Lyapunov function calculation. While the results obtained with those analyses are of significant interest from a theoretical point of view, they are of little or no utility in practical cases due to the difficulties of calculating those quantities. One possible candidate may be the utilization of the concept of signal activity.

Additionally, a prototype of the model library and schematic generation tools were presented at ESTS 2017 [181]. Example code and data was created to permit developers to export and examine nodal connectivity and parameterization for input to external tools. The S3D application programming interface (API) was improved to allow analysis of design across disciplines and to perform mission analysis through the API.

As a precursor to the linking of S3D with additional external time domain simulation tools, two external design tools (non real-time) developed by the ESRDC are being linked with S3D using existing S3D functionalities. This effort aims to link external tools used for distributed energy storage allocation and power converter sizing (see description of this tool in Project 4.1.1 update) with the S3D design environment.

Using the prototype solver previously developed, the performance of the developed method is being assessed using two test cases. As a first test case, an artificial system consisting of 65 states is being used. This test case will demonstrate the fundamental integration characteristics and compare the performance of several integration methods that fit quantized integration of stiff systems. The second test case is a ship system composed of three zones. A block diagram representation of the system is shown in Figure 124. The model is composed of six PCMs, three zonal loads, two PGMs, and two PMMs. Low dynamic order models of each component have been developed and each model is being parameterized. The developed models include electrical, thermal, and mechanical dynamics. With this test case the purpose is to demonstrate how the developed solver can be applied to analyze a long-duration mission scenario while also providing sufficient detail to resolve the dynamics involved in a fast-acting electrical event, such as a short circuit.

A journal publication is in preparation that will include the theoretical formalization of the developed approach as well as an analysis of the achieved performance using the two test cases that were recently developed.

Effort is underway to link a stand-alone external toolset for analysis of distributed energy storage [26], developed by the ESRDC, with the S3D design environment. The framework leverages available tools for

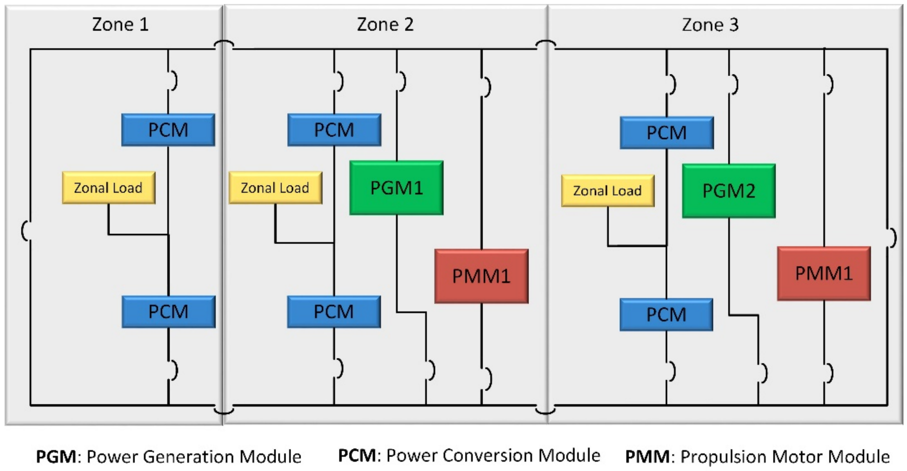

Figure 124: Ship system test case.

graph-based power flow solutions along with metrics such as operability to assess performance of an energy storage system. Specifically, during periods of power-constrained engagement, the typical approaches used for energy storage management may not result in maximum system operability. This effort seeks to provide S3D designers with analysis tools that can determine the optimal performance of a given distributed energy storage system during the early stages of design. Work to this point has involved the review of a technical report [183] regarding the framework for analysis of distributed energy storage, and scrutiny of the MATLAB source code underpinning this work. This code provides a determination of optimal operability after constraining the overall system with a power discharge limit. The toolset provides both graph-based and time-based power flow solutions. Particular focus was concentrated on code for an example case which represents a system comprised of a generator, centralized energy storage module, and dedicated energy storage modules each coupled with a load. Depending on the use of stored energy in each case, the generated power and energy versus time plots clearly show differences in system operability throughout the scenario. The immediate next phase in this effort involves using the previously developed MATLAB toolset to run additional simulated scenarios in order to develop the knowledge and experience necessary to dynamically link the distributed energy storage analysis toolset with S3D.

4.3.2 Evaluation of time domain thermal simulation capabilities and integration with S3D

Technical Objectives

Take ESRDC-developed ship system-level thermal management time-domain tools and integrate them into the S3D design environment.

Technical Approach

- Make improvements to a thermal simulation tool that could provide greater insight into the thermal dynamics of surface combatants.
- Devise and assess physics-based synchronization strategies that allow the use of time-domain thermal simulations in S3D; addressing numerical stability and accuracy while keeping the rapid prototyping goals of S3D in mind.
- Identify the information required to conduct the thermal time-domain analysis, manage such information within S3D (and similar tools), analyze and manage the data derived from the time-domain simulations.

Progress Statement Summary

Improvements were made to a time-domain thermal simulation tool. The user interface of vemESRDC has been enhanced for improved accessibility by S3D users, permitting them to explore various thermal system configurations and run test cases with ease. Moreover, the tool has been equipped with an implicit numerical method (i.e. Backward Differentiation Formula) suitable for solving stiff system of nonlinear differential equations [123]. In addition, the templates for vemESRDC input files have been prepared to be implemented into S3D for an enhanced interaction between them.

Further improvements were made to a time-domain thermal simulation tool, adding the capability of generating piping networks that serve the thermal loads. The information required to conduct thermal time domain analysis has been incorporated as templates for vemESRDC input files. The next step is for the S3D team to implement those templates into their data exporting features.

The research team met with the S3D development team and discussed the implementation of input file templates for vemESRDC into S3D, and a linkage between S3D and vemESRDC that would provide the ability to do seamless updates to vemESRDC. The implementation of those are pending.

4.4.1 Explore methods to integrate HPC capability with S3D

Technical Objectives

Develop a tool that helps the user define the type of capabilities desired, the set of mission loads, any constraints or goals, such as range, speed of the ship, etc., while requiring a minimum of user inputs.

S3D needs to be capable of both automatically generating concepts from a minimal set of user-supplied inputs and also be able to evaluate thousands of these concepts quickly in order to permit the rapid and full exploration of a concept space. Both of these capabilities will allow the Navy to explore a wide range of potential candidate ship designs and help determine which ones are likely to produce feasible solutions.

We will develop a tool that helps the user define the type of capabilities desired, the set of mission loads, any constraints or goals, such as range, speed of the ship, etc., while requiring a minimum of user inputs. Another tool will be developed that allows engineers to specify designs in a generalized manner via patterns or templates. The distributed systems work in Project 4.5.1 will feed directly into this project. The design process, using patterns or templates, will create a large number of candidate designs, likely thousands or tens of thousands.

In order to expedite the analysis of this large set of designs, a process must be defined and code implemented that will enable the analyses to be performed within an HPC environment. We will apply the many years of experience gained with the CREATE program in developing ground vehicle power-train models capable of running on an HPC platform, to the set-based design of ship systems. We have delivered and had their power-train federate run successfully in conjunction with other federates to complete ground vehicle simulations in an HPC environment [184].

Technical Approach

The generalized process for the creation of large sets of potential variant designs given minimal user input is as follows:

- High-level user requirements are captured.
- Patterns and templates are established and saved to a repository.
- A schematic generation tool uses the user-supplied requirements and sets of patterns and templates in order to produce many potential designs that meet the initial criteria.
- Distributed systems (piping, cabling, etc.) are automatically routed.
- Automatic evaluation of the set of potential designs is conducted.

Progress Statement Summary

This project has dependencies on some outputs from sub-thrust 4.5 and sub-thrust 1.1 and is awaiting these before significant advances can be made.

Specifically to this project, MSU and USC held several teleconferences and meetings to determine the direction of the project. Major ongoing progress includes the following:

- Exploring the use of MSU HPC clusters for running large numbers of jobs for a Set-Based Design approach using an arbitrary C++ object aiming for 1000s of clones, running concurrently.
- Launching multiple jobs through MPI (Message Passing Interface), shell scripts, etc. (currently on 128 processors, with more to come).
- Investigating different inputs to processes (files, command-line, etc.).
- Organizing and analyzing the output of arbitrary C++ code.

Once the MSU implementation of the arbitrary C++ code has yielded results, then MSU will implement the C code that USC provided to MSU as a more advanced test. MSU and USC will continue to collaborate to achieve the end goal of S3D C++ code that is capable of running in an HPC environment [185].

Specific to this project, MSU and USC held several teleconferences and meetings, along with the S3D Design team and Georgia Tech, to help determine specific needs and direction of the project.

The MSU team has continued exploring the use of MSU HPC clusters for running large numbers of jobs for a SBD approach using arbitrary C++ objects aiming for 1000 s of clones, running concurrently. Multiple tasks have been launched through an MPI (Message Passing Interface) program and the results are listed as follows for different MSU HPC clusters:

- 128 on Raptor (4ppn, now decommissioned, so transferred to Talon/Shadow), 192 on Talon (12ppn), 200 on Shadow (20ppn).
- Higher queue limits requires MSU's HPC board approval.
- Each MPI process can create a new folder for its output, change into that folder, then run the program. This is necessary if the program being run has fixed (compiled-in) filenames.

The MSU team has also made progress launching multiple non-MPI processes through shell scripts via secure shell client. The team ran multiple copies of a powertrain simulation with different input files. This could be easily used on a non-HPC linux server or desktop for smaller jobs. Different inputs to the processes have been investigated as far as using files, command-line arguments, etc. The plan is to compare start-up times and ease of use for the MPI-based and non-MPI-based methods to select the most appropriate method.

4.4.2 S3D exercises to test automated SBD

Technical Objectives

Perform V&V of SBD exercises within the S3D environment. These exercises will test the machinery model, automated SBD model development, and early-stage controls. This project is dependent on inputs from sub-thrusts 1.1 and 4.5, and is expected to start in FY18.

Technical Approach

N/A

Progress Statement Summary

This project has dependencies on some outputs from sub-thrust 4.5 and sub-thrust 1.1, and is awaiting these before the project can begin.

4.5.1 Evaluate the performance of distributed system designs in S3D including V&V

Technical Objectives

Reduce the time required to create the design and perform the analysis of ship systems within S3D while increasing the fidelity and confidence in the design. Currently, there are three efforts in this arena: automated system layout, improved cooling system design and analysis, and equipment scaling for templates.

The design and layout of the distributed systems for a ship is a tedious and time consuming process. These systems should not be overlooked, even in the conceptual design phase, as they have significant implications on the design of the ship and are necessary in order to achieve a high level of confidence in the final product. This project seeks to reduce the time required to develop the distributed systems and their arrangement while increasing the fidelity of the ship design as a whole. Transient analysis of cooling systems, equipment, and spaces has been implemented in related forms under recent ESRDC efforts. The continuation of this work addresses conversion of the code to C++ for the future integration with the Navy's LEAPS data repository.

Technical Approach

- The design of distribution systems generally follows well-defined rules or patterns. One way to reduce the burden of designing distribution systems is to identify and leverage these patterns so as to create these systems in an automated way. A tool must be developed that allows engineers to specify designs, or parts of a design, in a generic form via a pattern or template. A design captured as a pattern or template is one that is somewhat malleable in that the specific components utilized can be modified or parametrized so as to accommodate a design in a specific context. This approach requires that the components themselves be scalable. Therefore, the development of a scalable model library will also be necessary.
- The Software vemESRDC is a physics-based software tool that evaluates temperature and humidity effects of equipment operating in a shipboard environment. SMCS is a physics-based software tool that analyzes the flow rate and temperature of cooling water in shipboard piping systems. The integrated product of the two provides for the dynamic analysis of cooling systems and the resultant temperatures and humidity in shipboard spaces.

Progress Statement Summary

- Several meetings have been conducted with ESRDC and NSWC in order to establish the requirements and functionality, and provide definition for the concept of patterns and templates. The design for patterns and templates has been captured in a software requirements document [186]. The process is not yet complete, but has been progressing and will continue to evolve throughout the 2017 calendar year. Once the requirements and definition are mature and agreed upon by all parties, the implementation of this part of the tool set will begin. A software implementation of a templating methodology is found in ESRDC Project 1.1.1.
- The SMCS developed by MIT [122] is currently being translated from *MATLAB* to C++ for its integration with vemESRDC [123], which was developed in *FORTRAN* by FSU. These tools have been tested individually in order to identify the variables to be shared when integrating. A quasi-transient integration approach has been proposed, wherein vemESRDC solves for transient thermal solutions using small time steps at which SMCS provides steady-state fluid pressure and temperature distributions in the piping network accordingly.

- Various thermal/fluid models have been developed in S3D, namely HVAC models, a zonal freshwater cooling system, chilled water system, etc. Those models/subsystems are composed of various thermal/fluid components (pumps, pipes, valves, HEXs, chillers, etc.). A structure to realize a seamless integration has been drafted as shown in Figure 125.

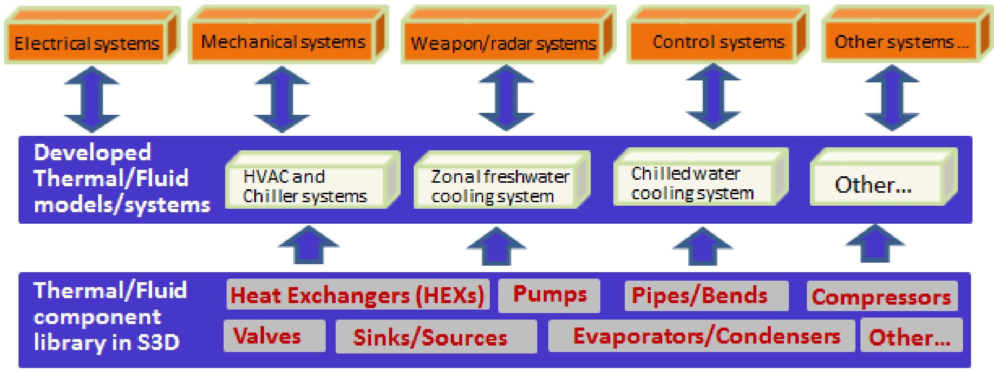

Figure 125: The SMC vemESRDC integration, discussed in the previous report is reported in [123]; future work includes developments to guarantee the confinement of the piping structure within the ship hull.

A new capability that provides enhanced freedom to create compartments of difference sizes in all Cartesian directions has been incorporated into vemESRDC. This new capability will allow us to, for example, model power corridors that cross sections of decks but do not necessarily extent the whole zone length (all illustrated in Figure 126).

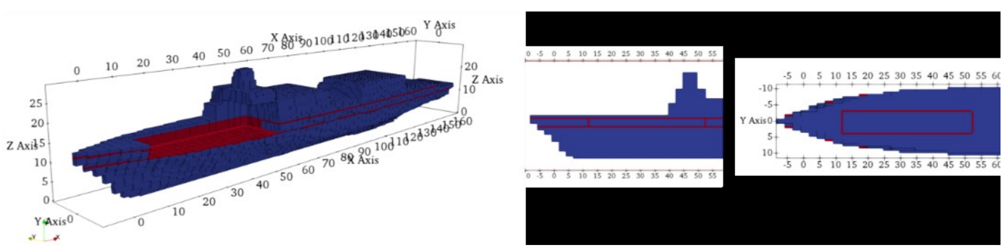

Figure 126: Variations in (left) COP and (right) second law efficiency along with constant cooling rate curves as functions of heat exchanger area and overall heat transfer coefficient fractions.

4.5.2 Implementation of templates-based design in S3D including utilization of established equipment-scaling laws

Technical Objectives

Implement previously developed scaling laws and template generation functionalities via S3D-based experimentation. The major outcomes will be establishment in accurate, reliable, and traceable scaling laws for power and thermal equipment using varied design guidelines, as well as performance evaluation of ship designs using templates. Research performed in Projects 1.1.1 and 1.2.2 will form the basis of the implementation plans in this project.

Technical Approach

The previous work, at present bench-marked using the MMC-based system, will be expanded to other shipboard systems of interest to apply pertinent scaling laws for power equipment.

Progress Statement Summary

At present, no work has been performed. However, a report on the supporting work being performed in Projects 1.1.1 and 1.2.2 can be found in this semi-annual report under Thrust 1.

A set-based design exercise has been performed to design an MMC converter. In addition, an MMC sizing tool has been developed and coded in *MATLAB* and *Microsoft Excel* environments. This tool can perform set-based design for modular multilevel converters where the main focus is to design a power dense converter within the given specification. Additionally, scaling relations between different systems and converter parameters can be derived from the tool. This feature can aid the early stage ship designer in S3D. Current work focuses on investigating other converter topologies along with other components such as isolating switches, energy storage modules, etc., and eventually perform set-based design exercises for MVDC breaker-less architectures for all-electric ships.

Additionally, the S3D development team continues to participate in discussions with the Thrust 1 team that is exploring early stage control methods to ensure that the level of detail is compatible with and sufficient for S3D power flow analysis.

4.5.3 Integration with S3D to provide optimized design (based on volume and weight) of thermal system

Technical Objectives

Develop proper interfaces to enable smooth data flows in S3D.

Technical Approach

- Integrate with electrical systems; namely power generation, conversion, and distribution systems.
- Integrate with mechanical systems; including gas turbines, gear boxes, bearings, etc.
- Integrate with weapons/radar systems which need instantaneous cooling.
- Integrate with control systems for the thermal plants, such as in the case of emergency zonal isolation.
- Integrate with other systems in S3D that require thermal management.

Progress Statement Summary

A structure to realize a seamless integration has been drafted and will be refined.

4.6.1 Develop unified and compatible ontologies between S3D and prevalent Navy ship design tools

Technical Objectives

Provide deeper analysis of ship designs and allow for greater confidence in early-stage designs. To permit this, the S3D design environment must easily target detailed, time-domain, discipline-specific simulation platforms. In order to provide the data necessary to conduct analysis in these time-domain simulation environments, the S3D underlying data store will be extended to include additional details about the models in the equipment library. The underlying ontology for the equipment library will be upgraded as is born out through research activities and experimentation.

Technical Approach

- Define the nature and types of data that must be captured about the equipment in order for these devices to be adequately represented by the detailed time-domain models.
- Develop a unified ontology-compliant equipment library and data sets to support all of the analysis required during the design development cycle (DDC).
- Continually improve equipment database and associated parametric information; S3D will require an equally up-to-date designer support framework that is able to give state-of-the-art and expert-validated information at various stages of the DDC.

It is likely that an iterative process is required to fully capture the needed data, especially as additional simulation tools are added to the process and as various forms of the detailed time-domain model are required to answer specific engineering concerns.

Progress Statement Summary

An initial prototype tool was developed to port a simple S3D conceptual model into Simulink for time-domain analysis based on work performed under sub-thrust 4.3. This work led to better understanding of some of the attributes that need to be captured and helped start the process of formalizing a data structure that would be sufficient. This work will pick up momentum in subsequent years as the work under sub-thrust 4.3 and sub-thrust 1.4 matures.

Moving from S3D v1.2 to v2.0, the system component data was revised to adhere to FOCUS ontology. S3D v2.0 is now fully FOCUS compatible with LEAPS components.

4.6.2 Integration of scalable high speed machine models into S3D

Technical Objectives

Develop methods to generalize equipment scaling, and appropriate user interfaces for defining scaling across disciplines. Generalized scaling methods will permit development of a standard ontology for the scalable equipment, and therefore, a smoother transition to Navy design tools.

Technical Approach

- Equipment scaling methods are being developed for equipment in other categories such as heat exchangers, power converters, etc.
- Evaluate the scaling methods produced from this research that span a range of disciplines and determine how to best generalize, and then implement these as a set of S3D models.
- Develop prototype UIs and evaluate these in the context of designs and eventually within templates and patterns.

Progress Statement Summary

This project is dependent upon development of equipment scaling algorithms in several other projects. Significant work on this project is not expected until FY18.

4.7.1 Investigation of feasible methods to enable automatic, traceable, and updatable documentation

Technical Objectives

Ensure that the software and other products of the ESRDC research activities are documented in order to facilitate the transfer of knowledge to the Navy. Of foremost concern is the documentation of the models and solvers that are used within the S3D environment. Project 4.7.1 focuses on the formalization of the documentation process, and tools to help automate the documentation will expedite the transfer of knowledge from the research community to the practitioners. Development of best practices for documenting models will help lead to formal processes for the verification and validation of these models within the S3D environment, as well as with external simulation and design tools.

Technical Approach

- Develop a tool to help model developers produce adequate documentation and reduce, as much as possible, the documentation burden on the model developer.
- Develop recommendations for model documentation standards that will be applied to existing documentation and incorporated into any tool that is developed; the model documentation process will also benefit from feedback from both industry and the Navy.

Progress Statement Summary

This project supports all other sub-thrusts in that as algorithms, models, and tools mature, documentation of these items will begin. This project is expected to begin in FY18.

4.7.2 Develop customer end data management and transferability

Technical Objectives

Ensure that the software and other products of ESRDC research activities are documented in order to facilitate the transfer of knowledge to the Navy. Of foremost concern is the documentation of the models and solvers that are used within the S3D environment. Project 4.7.2 will develop methods to permit the Navy to better incorporate, leverage, and utilize the research conducted by the ESRDC, documentation and traceability mechanisms must be developed and incorporated into the research and development process. Development of best practices for documenting models will help lead to formal processes for the verification and validation of these models within the S3D environment, as well as with external simulation and design tools.

Technical Approach

- Develop and formalize a process for verification and validation of models that will be applied to and incorporated into the documentation where appropriate.
- Auditing of the models for compliance will also be incorporated into the tool set.
- Beyond model documentation, any algorithms or tools created for the S3D design environment will also be documented.

Progress Statement Summary

This project is expected to begin in FY18.

4.8.1 Adapt technologies developed in S3D to the Navy

Technical Objectives

Define and achieve the speedy and efficient transition of S3D to Navy use.

The Navy has expressed a desire to use the S3D design environment on pending Navy design work and is actively seeking transition of the research to the Navy. To bring about this transition, S3D must be integrated with current Navy design tools and the Navy data repository, and the code base must be ported to C++. Further, the functionality of S3D and the equipment library included within S3D must be guided by the Navy's needs.

Technical Approach

- Adopt common core systems that can be shared between the ESRDC and Navy communities such as the underlying models, solvers, and simulation framework.
- Maximize the value of S3D as the preferred agile rapid development testbed for design tools and methodologies, as well as the preferred vehicle for speedy transition of new technologies to the Navy.
- Develop a version of S3D that is fully integrated with Navy design tools.

Progress Statement Summary

Progress during this reporting period includes:

- Delivery of the Software Architecture Document version 2. This document provides a comprehensive architectural overview of the system, treating architectural, use-case, logical, data, and quality aspects of the transitioned product.
- Delivery of the Data Dictionary Update 2, which delineates the views and properties required to fully describe the data associated with each specified type of component for integration with the Navy's data repository, LEAPS, and the product meta-model, FOCUS.
- Organizing, conducting and reporting of the S3D/LEAPS Integration Sprint Meeting, February 15, 2017. The main topic was laying the groundwork for incorporating controls into early-stage design, involving representatives across academia and the government well beyond ESRDC and the core S3D Navy team.
- The ESRDC has been actively engaged in the porting of C# code to C++. This also includes becoming the primary development team for the implementation of S3D v2.0. The 2.0 version of S3D will be fully integrated with LEAPS and coded entirely in C++. This effort is significant in scope and will likely be a continuing effort for some time.
- Organized, conducted and reported two program reviews with U.S. Navy personnel on June 6, 2017 and September 28, 2017. Discussed progress during sprint period and plan for upcoming sprint.
- Concentration during this period included usability features, greatly improving interface and FOCUS compliance.
- Released an alpha version of S3D version 2.0 in June 2017. After the release, conducted extensive testing and upgraded user experience and FOCUS compliance.
- Continued porting of C# code to C++. Code development is tracked in Sprint backlog tracking system. Navy personnel have access to this system.

- Developed documentation for new models and updated existing documentation to any reflect changes to existing models.

- Implemented automated build and compile system that compiles all code across all supported operating systems and generates error reports. This process will support development of automated installer generation.

- Completed version 2 of the FOCUS Data Dictionary.

- Began development of a publicly available website to provide: S3D installer, S3D development roadmap, change log, model library, ESRDC research documents, etc.

- Paper presented at ESTS 2017 detailing progress in this area [187].

Organized, conducted and reported on the January 24, 2018 S3D/LEAPS Integration Sprint Meeting at USC. The Sprint meeting included a review of what coding was achieved in the previous sprint and what is planned for the next sprint, and discussion of future items including software architecture planning and pending functionality from ESRDC. The ESRDC continues porting of C# code to C++. S3D v2.0 was released. Version 2.0 is fully integrated with LEAPS. Currently, the User Interface and system building portion is coded entirely in C++, whereas the simulation engine is coded in C#. Progress is on track to convert the simulation engine to C++ with a target release date of September 2018. Daily builds are now posted to the S3D website, so that the latest code is available for use and testing. New models were created including: 3 and 4-way pipes with integrated valves, and a high-temperature superconducting motor. Additionally, the model of the chiller was changed to better reflect actual performance.

Significant progress has been made on the S3D framework development:

- Implementation of a new file structure for entities that separates visual information (icon) from metadata information about ports. Ultimately, this should speed up loading times once we switch to framework simulation.

- Creation of base classes for the implementing the solvers/system that dynamically loads any available solvers. This will be useful for developers of third-party solvers for S3D.

- Implementation of port types and info for powerflow and fluid solvers. Solver implementation has not yet begun.

- Implementation of a prototype mapping between equipment and simulation models using the new system. The prototype was developed as a step towards enabling migration of S3D designs to other industry standard tools. Testing of prototype has not yet begun.

- Implementation of a prototype for aggregate equipment types. This will enable future capability that will permit the creation of equipment that is an aggregate of other equipment e.g. create a genset equipment type by aggregating a generator and a turbine equipment types.

- Began initial implementation of some graph objects that will be available as math utilities to be consumed outside the framework.

Significant progress has been made on the S3D GUI including:

- For the equipment library tool, finished support for viewing the standard distribution library, capability to create custom libraries stored per user, and ability to add/edit/delete equipment types and specify their attributes/attribute values.

- Prototyped user experience for aggregation of equipment types.

- In support of framework integration, incorporated new features and changes to the framework into tools, and provided feedback and testing on software design of the framework.

We began working with NSWC Carderock and Philadelphia divisions to define a LEAPS example application to guide future developers trying to use the LEAPS Framework. For this we provided mockups of desired functionality for example application, created and incorporated a LEAPS Example Application (shell only) into our build environment and worked with Adam Tucker (Philadelphia) to give him access to the S3D source code. We began porting C# simulation entity development tool to C++, and completed an initial layout of the Entity Designer tool. We ported an existing S3D polygon model to NURBS format as proof of concept for integrating with Navy design tool graphics format. We began documenting Framework code using Doxygen, and created a public Wiki to host documentation for tools, models, and solvers on the S3D website.

This page intentionally left blank

Thrust 5: System Level Experimentation

Technical Objectives

Support design exercises to demonstrate enhancement of S3D's design capability through a full DDC of an existing ship or facility. Regular activities such as these are likely to provide substantial V&V and show promise for the Navy to adopt S3D as a tool for design of future vessels. Almost all of the technologies developed within proposed scope, with the exception of the S3D specific sub-thrusts, will be assessed via reduced scale testing. This testing will typically be at the kilowatt to megawatt power scale and will frequently incorporate hardware-in-the-loop technology. This thrust will explore the full functionality, including system-level control, of the emerging MVDC system protection paradigms such as the breaker-less approach. This thrust will also focus on exploring experimentally the effect of various control strategies to maximize the system performance.

Technical Approach

Conduct research in four major areas:

- S3D design capability.
- Power dense component performance.
- MVDC system protection.
- System level control.

Progress Statement Summary

Current work reported herein includes:

The following projects are planned for future work:

5.1.1 Superconducting shipboard power and energy architecture study for next-generation surface combatant (SuPEr ship study)

Technical Objectives

Perform a ship design exercise with the following goals:

- Quantify the benefits of superconducting systems integration including electrical distribution, propulsion, generation, energy storage, and degaussing on overall ship synthesis.
- Develop an implementation of the Technology Identification, Evaluation and Selection (TIES) methodology specific to S3D to enable response surface exploration of ship design study results.
- Expand the capabilities of S3D to include high-temperature superconducting (HTS) equipment.

Technical Approach

- Use the S3D design environment to design and evaluate a baseline conventional ship and several variants including advanced conventional technologies and high-temperature superconducting technologies.
- Use multiple novel integration concepts that shall be considered, including an integrated cryogenic cooling network, in addition to distributed, but otherwise isolated, cryogenic system dedicated to an individual superconducting component.
- Compare superconducting integrated concepts against an equivalently capable, non-superconducting shipboard design.

Progress Statement Summary

The design team has been formed and several initial meetings have been held. A regular conference call schedule has been implemented. Progress to date includes the following:

- Outline of the project to include delineation of baseline ship requirements, HTS equipment to be modeled and evaluated, expected effects of HTS technology to inform metrics development, and evaluations for implementation of the TIES methodology.
- Production of the baseline model in ASSET, transfer of pertinent data to S3D, and the beginning of establishing connected systems within S3D.
- Discussions of HTS component modeling and the initial draft of an HTS cable model in S3D.

The design team continues meeting bi-weekly. Major progress includes the following:

- Established a matrix of planned study options for development of the TIES methodology.
- Established a conventional baseline ship design and one variant; working mission scenario alignment toward simulation and finalizing the models.
- Created S3D models of HTS cable, HTS cable termination, cryo transfer line, cryocooler, and cryofan; also created specialized degaussing cable models.

Several papers and a tutorial were presented at ESTS 2017 detailing progress in this area [96, 188, 189].

The design team finalized HTS ship design variant 1, which replaces conventional power cables with HTS cables. The initial design of variant 1 led to productive discussion of the use of HTS power cables, location and sizing of terminations, and selection of conventional cables to be replaced. This led to the design of additional variants within the power cable variant family, based on different choices regarding the selection of power cables to replace and the number and topology of cryo chillers selected.

In order to expand the number of designs explored in the HTS study we migrated the baseline and variant 1 designs to the S3D v2.0 application. This will allow us to more readily vary component parameters to explore the designs using a range of component technologies. Additionally, the v2.0 designs can be used with the GA Tech TIES tools.

In the process of migrating the designs we tested and refined the LEAPS database merge tool developed by MIT under Task: Implementation of templates for semi-automated design of ship systems. The electrical and piping designs were developed separately and successfully merged using the tool.

Additionally, the process of developing the designs provided the opportunity to test S3D v2.0 on a scale not attempted before. The GUI was found to be much more responsive than S3D v0. A few bugs were identified, and are in the process of being corrected.

The use of S3D in the HTS project was presented at the Annual Naval Superconductivity Program Review hosted by the Naval HTS Applications Team at NSWCPD and held in the Philadelphia Navy Yard from April 11-12. The ESRDC presentations at the review described the study objectives, the technology analysis process, and some details of ESRDC-related HTS research, thus exposing the wider NSWCPD and HTS technical communities to the capabilities of S3D.

5.1.2 Superconducting shipboard power and energy architecture study for next-generation surface combatant (SuPEr ship study)

The originally proposed Projects 5.1.1 (Support and validate S3D capabilities for existing designs) and 5.1.2 (Perform S3D exercises involving future designs) have been superseded by Project 5.1.1 Superconducting shipboard power and energy architecture study for next-generation surface combatant (SuPEr ship study) which combines the efforts of the two originally proposed projects. Reporting for this combined current effort is available in the Project 5.1.1 semi-annual report.

5.2.1 Thermal control to improve reliability of MMC and MMC-based DC/DC converters

Technical Objectives

Utilize the extra control freedom and control bandwidth of the MMC-based converter during normal operation, to reduce the thermal stress of the semiconductor devices in the converter, so that the reliability of MMC-based converters can be improved.

Modular multilevel converters (MMC) and MMC-based DC/DC converters have extra control freedoms that can be designed to provide advanced functions including fault current limiting, fast startup/fault recovery, and active power filling, etc. [51, 52, 152]. Usually these advanced functions are only needed in a short period of time. In most operation times, these functions are not required and thereby the extra control freedoms are redundant.

Technical Approach

- Modeling in electrical domain: derivation of a detailed mathematical model for MMC-based converters, to explore and quantify the control freedom and control bandwidth of the converter.
- Modeling in thermal domain: derivation of the relationship between electrical power consumption and the thermal stress of a semiconductor device.
- Developed control and modulation strategy than can reduce the electrical power fluctuation on semiconductor devices.
- Verify the developed control method in CHIL simulation.

Progress Statement Summary

We have been focused on characterization of different types of MMC-based DC/DC converters, including a proposed current-fed modular multilevel dual active bridge (M2DAB) converter [190], a proposed voltage-fed M2DAB [191], and a two-stage DC/DC converter based on conventional MMC topology [51]. Current progress includes the mathematical modeling and offline simulation of the three topologies. The next step will be simulation verification of the mathematical model and detailed circuit model.

5.3.1 Experiment with fault mitigation approaches

Task: Breakerless generator fault demonstration

Planned future work

Task: MMC converters and fault management demonstration

Planned future work

5.3.2 Experimental verification of DC zonal converter fault performance using CAPS/MVDC test bed

Technical Objectives

Utilize the CAPS/MVDC lab facility to verify the MMDAB fault performance experimentally in an efficient and practical way to operate the MMDAB topology with higher AC operation frequency.

A modular multilevel DC/DC converter (MMDAB) based on a modular multilevel converter (MMC) was proposed in previous research [152]. With the fault protection and ride-through capability, MMDAB can be applied as the DC zonal converter in the shipboard breakerless MVDC system. The MMDAB hardware prototyping will be very costly and time-consuming due to its high ratings.

The CAPS MVDC lab has been equipped with four MMCs delivering 210A at 0$\tilde{6}$ kV individually that also features hardware-in-the-loop capability [192], which provides an approach for the experimental verification of MMDAB fault performance. However, this setup is targeted for MMC converters with comparatively low switching frequency and AC port frequency (50/60 Hz). To apply it for MMDAB featuring much higher switching and AC port frequency (10 kHz) will face the following challenges: First, the sampling frequency of current controller corresponding to a low control bandwidth is not sufficient for MMDAB requiring a higher control bandwidth; Moreover, the communication protocol between different control levels in the controller hardware is not fast enough to support the data transmission in a high speed control system required by the high operation frequency. In addition, the implementation of the medium frequency transformer interfacing two MMCs in MMDAB is challenging.

Technical Approach

- Implement CHIL simulation of fault ride-through capability and fault recovery of DC zonal converter on CAPS/MMC testbed with 60 Hz operation.
- Implement CHIL simulation of fault ride-through capability and fault recovery of DC zonal converter on CAPS/MMC testbed up to 200 Hz operation.
- Investigate the possibility of PHIL experiments of 60 Hz operation.

Progress Statement Summary

Current progress includes implementing the MMDAB control strategy that is modified from the embedded basic converter control in the commercial control hardware, and developing a real-time simulation model of MMDAB. The CHIL simulation has been conducted with 200 Hz operation frequency. Even with such a compromise, the main fault functionality and operation of proposed MMDAB technology could be validated. The results shown in Figure 127 verify the fault current limiting capability of proposed MMDAB. It shows that when the bus voltage drops to zero under fault conditions, the converter can maintain operation and provide stable DC current limited at any desired level rather than tripping.

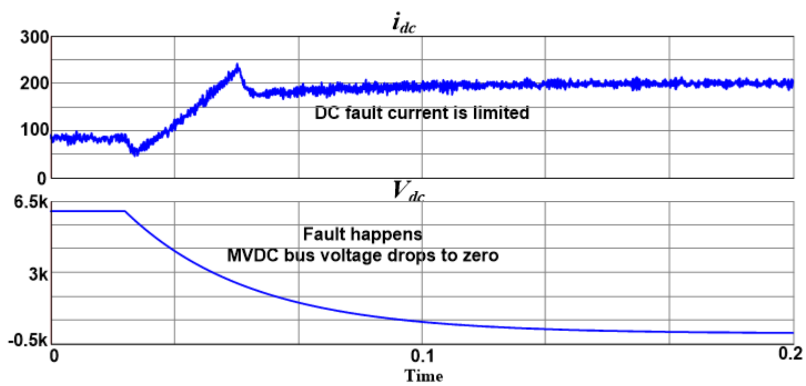

Figure 127: CHIL results of MMDAB fault performance.

5.4.1 HIL testing of energy storage management using fuzzy logic

Technical Objectives

Validate the operations of the designed Fuzzy Logic (FL)-based energy storage management (ESM) system through controller hardware-in-the-loop (CHIL)-based testing. This project is focused on developing a real-time simulation model of the medium voltage direct current (MVDC) shipboard power system in a real-time simulator (Opal-RT), and implementing the ESM system in a controller such as a field-programmable gate array (FPGA) board.

Technical Approach

With the objectives of implementing a CHIL testing setup, the following steps are taken:

- All of the loads (propulsion loads, pulsed load, radar load, and ship service loads), generation sources (main AC gas turbine-based generator and auxiliary AC gas turbine-based generator), modular multilevel converters (MMC), energy storage (battery and supercapacitor), and dual active bridge (DAB) bi-directional DC/DC converters are modeled in four different subsystems and are run on four different cores of the real-time simulator (Opal-RT) [193–195].
- The Xilinx System Generator (XSG) library is used to model the FL-based ESM system; the RT-XSG is capable of compiling the model of the ESM system and generates VHDL (VHSIC Hardware Description Language) code and FPGA bit streams file.
- A Virtex-7 FPGA VC707 board (OP7020) and a Virtex-7 FPGA VC707 board (OP5607) are used to perform the CHIL.
- Both FPGA boards are connected to the real-time simulator (Opal-RT) through fiber optic cable (PCIe cable).
- For power sharing among multiple energy storage devices, two power sharing strategies (SOC based, FL-based) are designed.
- Later, the SOC-based power sharing strategy is incorporated with an FL-based ESM system and both systems are implemented on Virtex-7 FPGA VC707 board (OP7020) and CHIL-based experiments are being conducted.

Progress Statement Summary

- Developed a real-time simulation model in Opal-RT of an integrated power system structure of 5kV MVDC shipboard power system with gas turbine-based generators, modular multilevel converters (MMC), propulsion load, battery, supercapacitor, dual active bridge (DAB) converters, ship service load, pulsed load, and radar load.
- The designed FL-based ESM system is added with the MVDC shipboard power system to control the operation of the energy storage (battery and supercapacitor) and incorporated with the real-time simulation model.
- The ESM system is under implementation in FPGA and some initial CHIL-based experiments are conducted.
- Additional experiments are expected to be completed in the future.
- The designed FL-based ESM system was implemented on FPGA to validate the operation of the energy storage (battery and supercapacitor), and CHIL-based experiments have been conducted [194, 195].

- To have a proper comparison between the real-time and offline simulation method, the offline simulation has been modified. The SOC based power-sharing strategy has been implemented with the FL-based ESM system in FPGA and initial CHIL testing is being conducted.

- The project needs a little more work to make it complete. However, no progress has been made in this six months due to insufficient funding. If funding is available, it is expected to be finished with a publication as an outcome.

5.4.2 Exploration of scaling system experiments to validate active power management concepts

Planned future work

5.4.3 HIL testing of controls and fault protection in reduced scale ADM setup with pulsed loads

Technical Objectives

As the Navy adds high power pulsed systems to ships, validated test results are needed to show that the system control is appropriate for stressful operation. The test bed at UT has demonstrated the successful firing of an electromagnetic gun from a two-zone MW power system and 0.5 MW scale load and source transfers. Much additional work needs to be done to identify critical control schemes and potential power system failure modes.

This effort will provide the Navy with a higher degree of confidence on the performance of integrated power systems to operate reliably with the incorporation of pulsed systems. The resulting information can be integrated into standards and specifications for future ships.

Technical Approach

To support development of various MVDC controls and fault protection solutions, UT-CEM researchers will exercise the recently enhanced dc test-bed at the MW power level. An incremental approach will be used with increasing levels of either power or complexity to build up to the final sub-scale ADM setup. These steps will include modeling and simulation, controller hardware in the loop testing (HIL), subscale testing using a Semikron 30 kW power converter, single source fault testing, two source fault testing, two source fault testing with reconfigurable grid (power nodes), and then two source fault testing with reconfigurable grid and multiple loads (final ADM fault test setup) at larger power scales. The objective test bed will include pulsed loads.

The first protection solution to be tested is a fault current limiter (FCL) for power generation modules (PGMs) and differential protection for a main dc bus in a sub-scale MVDC system [33]. The second protection solution is local measurement-based impedance protection approach. The algorithm has been developed and evaluated in HIL simulation environment for short-circuit dc faults [152]. The next step work is to test the impedance protection approach offline using the captured fault voltage and current signals from the dc test bed. Once the research team gains enough confidence, the online test will be conducted to demonstrate the performance of the protection approach.

Progress Statement Summary

- The controller has been migrated to and tested with the RTS system. The next step will be to commission the 30 kW DC-DC test bed for testing of the controller and fault protections algorithms.
- A simplified MVDC network has been implemented in the Opal-RT and NI FPGA simulator. Some preliminary model effort for a PGM unit has been performed. The HIL test for the dc protection approach is underway.
- Numerical simulation of the FCL approach was performed to validate feasibility including a sensitivity analysis to test the impact of the fault resistance on the dynamic behavior of fault current in the MVDC system. The FCL capability of PGMs has been tested in the numerical environment and hardware-in-the-loop (HIL) simulation environment. In addition, the practical design issue has been evaluated to help determine the most appropriate current threshold for fault detection in the differential protection zone.
- The local measurement-based protection approach has been studied to ensure it could be used in the demonstration dc test bed. The HIL test results suggested that the impedance protection can detect and locate a short-circuit fault in one millisecond with acceptable accuracy.

List of Figures

List of Tables

This page intentionally left blank

References

[1] P. Perdikaris, D. Venturi, and G. E. Karniadakis. Multi-fidelity information fusion algorithms for high-dimensional systems and massive data sets. *SIAM J. Sci. Comput.*, 38(4):B521–B538, 2016.

[2] P. Perdikaris, M. Raissi, A. Damianou, N. D. Lawrence, and G. E. Karniadakis. Nonlinear information fusion algorithms for data-efficient multi-fidelity modeling. In *Proc. R. Soc. A*, volume 473:2198, page 20160751. The Royal Society, 2017.

[3] H. Babaee, P. Perdikaris, C. Chryssostomidis, and G. E. Karniadakis. Multi-fidelity modeling of mixed convection based on experimental correlations and numerical simulations. *J. Fluid. Mech.*, 809:895–917, 2016.

[4] L. Bonfiglio, P. Perdikaris, S. Brizzolara, and G. E. Karniadakis. A multi-fidelity framework for investigating the performance of super-cavitating hydrofoils under uncertain flow conditions. *AIAA Non-Deterministic Approaches*, 2017.

[5] T. Sauer, J. A. Yorke, and M. Casdagli. Embedology. *Journal of Statistical Physics*, 65(3):579–616, May 1991.

[6] L. Seungjoon, G E. Karniadakis, and I. Kebrekidis. Linking gaussian process regression with data-driven manifold embeddings for robust nonlinear information fusion. In *SIAM Conference on Uncertainty Quantification*, Garden Grove, CA, USA, April 2018.

[7] R. R. Soman et al. Investigation of product development tools to aid naval shipboard power systems design. In *IEEE Electric Ship Technologies Symposium (ESTS)*, pages 466–470, Arlington, VA, USA, August 2017.

[8] T. A. Toshon et al. Set-based design for naval shipboard power systems using pertinent metrics from product development tools. In *IEEE Electric Ship Technologies Symposium (ESTS)*, pages 164–169, Arlington, VA, USA, August 2017.

[9] R. R. Soman et al. Exploration and investigation of appropriate tools to facilitate set-based design. In *ASNE Design Sciences Series: Set-Based Design*, Washington, DC, USA, September 2017.

[10] J. Chalfant and C. Chryssostomidis. Application of templates to early-stage ship design. In *IEEE Electric Ship Technologies Symposium (ESTS)*, pages 111–117, Arlington, VA, USA, August 2017.

[11] J. Chalfant, C. Chryssostomidis, D. Snyder, M. A. Parsons, and A. Brown. Graph theory applications in FOCUS-compliant ship designs. In *IEEE Electric Ship Technologies Symposium (ESTS)*, pages 471–477, Arlington, VA, USA, August 2017.

[12] A. Arapostathis and A. Biswas. Infinite horizon risk-sensitive control of diffusions without any blanket stability assumptions. *Stochastic Processes and their Applications*, 128(5):1485–1524, May 2018.

[13] A. Arapostathis, A. Biswas, and S. Saha. Strict monotonicity of principle eigenvalues of elliptic operators and risk-sensitive control. *ArXiv e-prints*, April 2017.

[14] A. Arapostathis, V. S. Borkar, and K. S. Kumar. Risk-sensitive control and an abstract Collatz-Wielandt formula. *Journal of Theoretical Probability*, 29(4):1458–1484, 2016.

[15] A. Arapostathis, A. Biswas, and D. Ganguly. Some Louiville-type results for eigenfunctions of elliptic operators. *ArXiv e-prints*, August 2017.

[16] A. Arapostathis, G. Pang, and N. Sandri. Ergodicity of Lèvy-driven SDEs arising from multiclass many-server queues. *ArXiv e-prints*, July 2017.

[17] A. Arapostathis, L. Caffarelli, G. Pang, and Y. Zheng. Ergodic control of a class of jump diffusions with finite Lévy measures and rough kernels. *ArXiv e-prints*, January 2018.

[18] S. Krishnasamy, A. Arapostathis, R. Johari, and S. Shakkottai. On learning the $c\mu$ rule: single and multiserver settings. *ArXiv e-prints*, February 2018.

[19] A. Arapostathis. A counterexample to a nonlinear version of the Krein-Rutman theorem by R. Mahadevan. *ArXiv e-prints*, February 2018.

[20] R. Mahadevan. A note on a non-linear Krein-Rutman theorem. *Nonlinear Analysis*, 67(11):3084–3090, December 2007.

[21] N. Doerry. Naval power systems: Integrated power systems for the continuity of the electrical power supply. *IEEE Electrification Magazine*, 3(2):12–21, June 2015.

[22] J. Salmeron, K. Wood, and R. Baldick. Worst-case interdiction analysis of large-scale electric power grids. *IEEE Transactions on Power Systems*, 24(1):96–104, February 2009.

[23] S. Jothibasu and S. Sanosa. New electric shipboard topologies for high resiliency. *IEEE Transactions on Power Systems*, 33(3):2975–2983, May 2018.

[24] D. J. Singer, N. Doerry, and M. E. Buckley. What is set-based design? *ASNE Naval Engineers Journal*, 121(4):31–43, 2009.

[25] H. L. Ginn, E. Santi, B. Langland, A. Ferraro, S. Arrua, and H. Abdollahi. Incorporation of control systems in early stage conceptual ship designs. In *IEEE Electric Ship Technologies Symposium (ESTS)*, pages 1–8, Arlington, VA, USA, August 2017.

[26] J. Langston, M. Stanovich, K. Schoder, and M. Steurer. Distributed energy storage allocation algorithm for early stage design. In *IEEE Electric Ship Technologies Symposium (ESTS)*, pages 345–351, Arlington, VA, USA, August 2017.

[27] M. Bosworth et al. Dual power hardware-in-the-loop simulation of energy storage systems for shipboard applications. In *ASNE Advanced Machinery Technology Symposium (AMTS)*, Philadelphia, PA, USA, March 2018.

[28] IEEE Guide for Control Architecture for High Power Electronics (1 MW and Greater) Used in Electric Power Transmission and Distribution Systems. In *IEEE Std 1676-2010*, pages 1-47, February 2011.

[29] The Linux Foundation. NetEm, wiki.linuxfoundation.org/networking/netem.

[30] C. S. Edrington et al. Demonstration and evaluation of large-scale distributed control for integrated power and energy MVDC systems on ships. In *ASNE Advanced Machinery Technology Symposium (AMTS)*, Philadelphia, PA, USA, March 2018.

[31] X. Feng, L. Qi, and J. Pan. A novel fault location method and algorithm for DC distribution protection. *IEEE Transactions on Industry Applications*, 53(3):1834–1840, May-June 2017.

[32] X. Feng, L. Qi, and J. Pan. A novel fault locaiton method and algorithm for DC distribution protection. In *Industry Applications Society Annual Meeting*, Portland, OR, USA, 2016.

[33] S. Strank et al. Experimental test bed to de-risk the navy advanced development model. In *IEEE Electric Ship Technologies Symposium (ESTS)*, pages 352–358, Arlington, VA, USA, August 2017.

[34] X. Feng, A. Shekhar, F. Yang, R. Hebner, and P. Bauer. Comparison of hierarchical control and distributed control for microgrid. *Electric Power Components and Systems*, 45(10):1043–1056, July 2017.

[35] X. Feng. Security-Based Power and Energy Management for Mission Critical Energy Systems, chapter in *Intelligent Power Grid of Tomorrow: Modeling, Planning, Control, and Operation*.

[36] E. Doroudchi, J. Kyyra, X. Feng, S. Strank, and R. E. Hebner. Hardware-in-the-loop test for real-time economic control of a DC microgrid. In *International Conference on Power Electronics, Machines and Drives*, Liverpool, UK, April 2018.

[37] J. Langston, K. Schoder, M. Steurer, F. Fleming, and M. Kmiecik. Medium voltage impedance measurements on a MW scale power conversion module using PHIL simulation. In *ASNE Advanced Machinery Technology Symposium (AMTS)*, Philadelphia, PA, USA, March 2018.

[38] G. Chauncey, J. Langston, K. Schoder, T. Szymanski, and M. Steurer. Impedance measurement techniques for PHIL simulation experiments in noisy environments. In *ASNE Technology, Systems & Ships (TSS)*, Washington, DC, USA, June 2018.

[39] Z. Cai, M. Yu, M. Steurer, and J. Ng. A new grouping protocol for smart grids. *IEEE Transactions on Smart Grid*, October 2017.

[40] X. Liu. *A centralized fault management approach for the protection of smart grids.* PhD thesis, Florida State University, 2015.

[41] ESRDC Team. RTDS Implementation of notional four zone MVDC shipboard power system, February 2018.

[42] IEEE P2004 Standards Working Group. Hardware-in-the-loop (HIL) simulation based testing of electric power apparatus and controls, 2017.

[43] M. Stanovich et al. General-purpose data recording. In *North American RTDS Applications & Technology Conference*, Winnipeg, Canada, May 2017.

[44] K. Schoder et al. Evaluation framework for power and energy management shipboard distribution controls. In *IEEE Electric Ship Technologies Symposium (ESTS)*, pages 388–393, Arlington, VA, USA, August 2017.

[45] K. Schoder et al. Evaluation framework for power and energy management shipboard distribution controls. In *ONR Controls Workshop*, Philadelphia, PA, USA, August 2017.

[46] M. Stanovich et al. ONR controls workshop presentation: ESRDC controls evaluation framework – models, load profiles, evaluation metrics, partitioning, March 2018.

[47] Notes from ONR controls workshop presentation: ESRDC controls evaluation framework – models, load profiles, evaluation metrics, partitioning, March 2018.

[48] M. Stanovich et al. Implementation and baseline characterization of a heterogeneous controller hardware-in-the-loop simulation platforms. In *ASNE Advanced Machinery Technology Symposium (AMTS)*, Philadelphia, PA, USA, March 2018.

[49] ONR DURIP Award N0001414410198. An open-source distributed control platform for HIL-based testing and demonstration of advanced power systems.

[50] H. Ravindra et al. Dynamic real time simulation models of notional zonal medium voltage DC shipboard power system for controls evaluation. In *ASNE Advanced Machinery Technology Symposium (AMTS)*, Philadelphia, PA, USA, March 2018.

[51] R. Mo, R. Li, and H. Li. Isolated modular multilevel (IMM) DC/DC converter with energy storage and active filter function for shipboard MVDC system applications. In *IEEE Electric Ship Technologies Symposium (ESTS)*, pages 113–117, Alexandria, VA, USA, June 2015.

[52] R. Mo and H. Li. Hybrid energy system with active filter function for shipboard MVDC system applications based on isolated modular multilevel DC/DC converter. *IEEE Journal of Emerging and Selected Topics in Power Electronics*, 5(1):79–87, March 2017.

[53] J. Wang, Z. Shen, R. Burgos, and D. Boroyevich. Integrated switch current sensor for shortcircuit protection and current control of 1.7-kV SiC MOSFET modules. In *IEEE Energy Conversion Congress and Exposition (ECCE)*, Milwaukee, WI, USA, September 2016.

[54] J. Wang, R. Burgos, and D. Boroyevich. Power-cell switching-cycle capacitor voltage control for the modular multilevel converters. In *International Power Electronics Conference (IPEC-Hiroshima 2014 - ECCE ASIA)*, pages 944–950, Hiroshima, Japan, May 2014.

[55] J. H. Guo. *Distributed, modular, open control architecture for power conversion systems*. PhD thesis, Virginia Polytechnic Institute and State University, 2005.

[56] T. Laakkonen, T. Itkonen, J. Luukko, and J. Ahola. Time-stamping-based synchronization of power electronics build block systems. In *IEEE Industrial Electronics Society (IECON)*, pages 925–930, Porto, Portugal, November 2009.

[57] C. L. Toh and L. E. Norum. A high speed control network synchronization jitter evaluation for embedded monitoring and control in modular multilevel converter. In *IEEE Grenoble Conference*, Grenoble, France, June 2013.

[58] P. D. Burlacu, L. Mathe, and R. Teodorescu. Synchronization of the distributed PWM carrier waves for modular multilevel converters. In *International Conference on Optimization of Electrical and Electronic Equipment (OPTIM)*, pages 553–559, Bran, Romania, May 2014.

[59] C. Carstensen, R. Christen, H. Vollenweider, R. Stark, and J. Biela. A converter control field bus protocol for power electronic systems with a synchronization accuracy of ±5ns. In *Power Electronics and Applications (EPE'15 ECCE-Europe)*, Geneva, Switzerland, September 2015.

[60] T. Wlostowski. Precise time and frequency transfer in a white rabbit network. Master's thesis, Warsaw University of Technology, 2011.

[61] I. Milosavljevic. Power electronics system comunications. Master's thesis, Virginia Polytechnic Institute and State University, 1999.

[62] G. Francis. A synchronous distributed digital control architecture for high power converters. Master's thesis, Virginia Polytechnic Institute and State University, 2004.

[63] S. Debnath, J. Qin, B. Bahrani, M. Saeedifard, and P. Barbosa. Operation, control, and applications of the modular multilevel converter: a review. *IEEE Transactions on Power Electronics*, 30(1):37–53, January 2015.

[64] R. Sahu and S. D. Sudhoff. High-speed simulation of modular multilevel converters for optimization based design. In *IEEE Electric Ship Technologies Symposium (ESTS)*, pages 134–141, Arlington, VA, USA, August 2017.

[65] D. Gerada et al. High-speed electrical machines: technologies, trends, and developments. *IEEE Transactions on Industrial Electronics*, 61(6):2946–2959, June 2014.

[66] R. R. Moghaddam. High-speed operation of electrical machines, a review on technology, benefits and challenges. In *IEEE Energy Conversion Congress and Exposition (ECCE)*, pages 5539–5546, Pittsburgh, PA, USA, September 2014.

[67] F. Zhang, G. Du, T. Wang, G. Liu, and W. Cao. Rotor retaining sleeve design for a 1.12-MW high-speed PM machine. *IEEE Transactions on Industry Applications*, 51(5):3675–3685, October 2015.

[68] A. Damiano, A. Floris, G. Fois, M. Porru, and A. Serpi. Modeling and design of PM retention sleeves for high-speed PM synchronous machines. In *Electric Drives Production Conference (EDPC)*, pages 118–125, Nuremberg, Germany, November 2016.

[69] A. Borisavljevic, H. Polinder, and J. A. Fereira. Enclosure design for a high-speed permanent magnet rotor. In *IET International Conference on Power Electronics, Machines and Drives (PEMD)*, Brighton, UK, April 2010.

[70] V. S. Duppalli and S. Sudhoff. Computationally efficient leakage inductance calculation for a high-frequency core-type transformer. In *IEEE Electric Ship Technologies Symposium (ESTS)*, pages 635–642, Arlington, VA, USA, August 2017.

[71] K. Ahsanullah, R. Dutta, and M. Rahman. Review of PM generator designs for direct-drive with turbines. In *Australasian Universities Power Engineering Conference (AUPEC)*, Bali, Indonesia, September 2012.

[72] A. Wang, Y. Jia, and W. Soong. Comparison of five topologies for an interior permanent-magnet machine for a hybrid electric vehicle. *IEEE Transactions on Magnetics*, 41(10):3606–3609, October 2011.

[73] R. Lin and S. Sudhoff. A hybrid model to calculate air gap flux density for a V-shape interior permanent magnet machine. In *IEEE Power and Energy Conference at Illinois (PECI)*, Urbana, IL, USA, February 2016.

[74] R. Lin, S. Sudhoff, and C. Krousgrill. Analytical method to compute bridge stressed in V-shape IPMs. *IET Electric Power Applications*, March 2018.

[75] D. V. Ragone. Review of battery systems for electrically powered vehicles. In *Mid-Year Meeting of the Society of Automotive Engineers*, Detroit, MI, USA, May 1968.

[76] K. R. Davey and R. E. Hebner. A fundamental look at energy storage focusing primarily on flywheels and superconducting energy storage. In *Electric Energy Storage Applications and Technologies (EESAT)*, pages 17–18, San Francisco, California, USA, October 2003.

[77] T. Christen and M. W. Carlen. Theory of Ragone plots. *Journal of Power Sources*, 91:210–216, March 2010.

[78] R. E. Hebner. Energy storage on future electric ships. In *Electric Ship Research and Development Consortium*. ESRDC, 2014.

[79] R. E. Hebner et al. Dynamic load and storage integration. *Proceedings of the IEEE*, 103(12):2344–2354, December 2015.

[80] H. Lund et al. Energy storage and smart energy systems. *International Journal of Sustainable Energy Planning and Management*, 11:3–14, 2016.

[81] R. Cammack, M. Frey, and R. Robson. *Hydrogen as a Fuel: Learning from Nature*, CRC Press, 2015.

[82] A. L. Gattozzi et al. Power system and energy storage models for laser integration on naval platforms. In *IEEE Electric Ship Technologies Symposium (ESTS)*, pages 173–180, Alexandria, VA, USA, June 2015.

[83] S. Sabihuddin, A. E. Kiprakis, and M. Mueller. A numerical and graphical review of energy storage technologies. *Energies*, 8(1):172–216, January 2015.

[84] X. Luo, M. R. Maxey, and G. E. Karniadakis. Smoothed profile method for particulate flows: error analysis and simulations. *Journal of Computational Physics*, 228(5):1750–1769, 2009.

[85] H. Babaee. Conjugate heat transfer with spectral/hp element method, MIT Sea Grant technical report, 2015.

[86] R. E. Hebner, A. L. Gatozzi, and S. D. Pekarek. Performance assurance for DC cables for electric ships. In *IEEE Electric Ship Technologies Symposium (ESTS)*, pages 343–348, Alexandria, VA, USA, June 2015.

[87] A. Shekhar et al. Impact of DC voltage enhancement on partial discharges in medium voltage cables – an empirical study with defects at semicon-insulation interface. *Energies*, 10(12):1–18, November 2017.

[88] G. G. Montanari, P. Seri, and R. Hebner. Type of supply waveform, partial discharge behavior and life of rotating machine insulation systems. In *IEEE International Power Modulator and High Voltage Conference (IPMHVC)*, Jackson, WY, USA, June 2018.

[89] X. Feng et al. Cable commissioning and diagnostic tests: the effect of voltage supply frequency on partial discharge behavior. In *International Conference on the Properties and Applications of Dielectric Materials (ICPADM)*, Xi'an, China, May 2018.

[90] C. C. Reddy and T. S. Ramu. On the computation of electric field and temperature distribution in HVDC cable insulation. *IEEE Transactions on Dielectrics and Electrical Insulation*, 13(6):1236–1244, December 2006.

[91] R. Bodega. *Space charge accumulation in polymeric high voltage DC cable systems*. PhD thesis, Delft University of Technology, 2006.

[92] R. Liu, T. Takada, and N. Takasu. Pulsed electroacoustic method for measurement of space charge distribution in power cables under both DC and AC electric fields. *Journal of Physics D: Applied Physics*, 26(6):986–993, February 1993.

[93] N. Suttell et al. Three-dimensional finite-element analysis of terminations for gaseous-helium-cooled high-temperature superconducting power cables. *IEEE Transactions on Applied Superconductivity*, 26(4), June 2016.

[94] L. Graber, J. G. Kim, C. H. Kim, and S. V. Pamidi. Thermal network model for HTS cable systems and components cooled by helium gas. *IEEE Transactions on Applied Superconductivity*, 26(4), June 2016.

[95] Z. Zhang et al. Current distribution investigation of a laboratory-scale coaxial two-HTS-layer DC prototype cable. *IEEE Transactions on Applied Superconductivity*, 26(4), June 2016.

[96] S. Satyanarayana, S. V. Pamidi, L. Graber, J. G. Kim, and C. H. Kim. Modeling methodology for analysis of shipboard power systems with multiple superconducting devices. In *IEEE Electric Ship Technologies Symposium (ESTS)*, pages 280–284, Arlington, VA, USA, August 2017.

[97] P. Cheetham, C. H. Kim, L. Graber, and S. Pamidi. Practical considerations for the design of superconducting gas-insulated transmission line for shipboard applications. In *IEEE Electric Ship Technologies Symposium (ESTS)*, pages 292–298, Arlington, VA, USA, August 2017.

[98] N. Suttell et al. Investigation of solid nitrogen for cryogenic thermal storage in superconducting cable terminations for enhanced resiliency. In *Materials Science and Engineering, Advances in Cryogenic Engineering*. IOP Conference Series, 2017.

[99] P. Prempraneerach, C. Cooke, and C. Chryssostomidis. Transient analysis for H-bridge type DC circuit breaker. In *IEEE Transportation Electrification Conference and Expo (ITEC)*, pages 401–406, Chicago, IL, USA, June 2017.

[100] C. M. Cooke, C. Chryssostomidis, and J. Chalfant. Modular integrated power corridor. In *IEEE Electric Ship Technologies Symposium (ESTS)*, pages 91–95, Arlington, VA, USA, August 2017.

[101] T. Vu et al. Robust adaptive droop control for DC microgrids. *Electric Power Systems Research*, 146:95–106, May 2017.

[102] D. Perkins, T. Vu, H. Vahedi, D. Gonsoulni, and C. S. Edrington. Distributed power management for DC distribution system with model uncertainties. In *IEEE Electric Ship Technologies Symposium (ESTS)*, pages 534–538, Arlington, VA, USA, August 2017.

[103] B. T. Stewart, J. B. Rawlings, and S. J. Wright. Hierarchical cooperative distributed model predictive control. In *Proceedings of the 2010 American Control Conference*, pages 3963–3968, Baltimore, MD, USA, June-July 2010.

[104] T. Vu, D. Gonsoulin, F. Diaz, T. El-Mezyani, and C. S. Edrington. Predictive control for energy management in ship power systems under high-power ramp rate loads. *IEEE Transactions on Energy Conversion*, 32(2):788–797, June 2017.

[105] D. E. Gonsoulin et al. Centralized MPC for multiple energy storage in ship power systems. In *IEEE Industrial Electronics Society (IECON)*, pages 6777–6782, Beijing, China, October-November 2017.

[106] D. E. Gonsoulin et al. Coordinating multiple energy storages using MPC for ship power systems. In *IEEE Electric Ship Technologies Symposium (ESTS)*, pages 551–556, Arlington, VA, USA, August 2017.

[107] M. R. Hossain and H. Ginn. Real-time distributed coordination of power electronic converters in a DC shipboard distribution system. *IEEE Transactions on Energy Conversion*, 99:19–26, 2017.

[108] N. Zohrabi, J. Shi, and S. Abdelwahed. An overview of design specifications and requirements for the MVDC shipboard power system. submitted to The International Journal of Electrical Power & Energy Systems, 2018.

[109] N. Zohrabi and S. Abdelwahed. On the application of distributed control structure for medium-voltage DC shipboard power system. In *IEEE Conference on Control Technology and Applications (CCTA)*, pages 1201–1206, Kohala Coast, HI, USA, August 2017.

[110] N. Zohrabi, S. Abdelwahed, and J. Shi. Reconfiguration of MVDC shipboard power systems: a model predictive control approach. In *IEEE Electric Ship Technologies Symposium (ESTS)*, pages 253–258, Arlington, VA, USA, August 2017.

[111] N. Zohrabi, H. Zakeri, and S. Abdelwahed. Efficient load management in electric ships: a model predictive control approach. submitted to IEEE Conference on Decision and Control (CDC), 2018.

[112] N. Zohrabi and S. Abdelwahed. Distributed model predictive control for MVDC shipboard power system management. in preparation.

[113] J. Siegers, S. Arrua, and E. Santi. Stabilizing controller design for multi-bus MVDC distribution systems using a passivity based stability criterion and positive feed-forward control. *IEEE Journal of Emerging and Selected Topics in Power Electronics – Special Issue on Emerging Electric Ship MVDC Power Technology*, 5(1):14–27, March 2017.

[114] J. Siegers, S. Arua, and E. Santi. Allowable bus impedance region for MVDC distribution systems and stabilizing controller design using positive feed-forward control. In *IEEE Energy Conversion Congress and Exposition (ECCE)*, Milwaukee, WI, USA, September 2016.

[115] A. Riccobono et al. Online wideband identification of three-phase AC power grid impedances using an existing grid-tied power electronic inverter. In *IEEE Workshop on Control and Modeling for Power Electronics (COMPEL)*, Trondheim, Norway, June 2016.

[116] A. Riccobono et al. Stability of shipboard DC power distribution – online impedance-based systems methods. *Electrification Magazine*, September 2017.

[117] T. Roinila, H. Abdollahi, S. Arrua, and E. Santi. Online measurement of bus impedance of interconnected power electronics systems: applying orthogonal sequences. In *IEEE Energy Conversion Congress and Exposition (ECCE)*, pages 5783–5788, Cincinnati, OH, USA, October 2017.

[118] T. Roinila, H. Abdollahi, S. Arrua, and E. Santi. MIMO identification techniques in online measurement of bus impedance of interconnected power-electronics systems. In *IEEE Electric Ship Technologies Symposium (ESTS)*, pages 316–321, Arlington, VA, USA, August 2017.

[119] T. Roinila, T. Messo, and E. Santi. MIMO-identification techniques for rapid impedance-based stability assessment of three-phase systems in DQ domain. *IEEE Transactions on Power Electronics*, 33(5):4015–4022, May 2018.

[120] A. N. Smith, R. L. Ellis, J. S. Bernardes, and A. E. Zielinski. Thermal management and resistive rail heating of a large-scale naval electromagnetic launcher. In *Symposium on Electromagnetic Launch Technology*, pages 116–121, Snowbird, UT, USA, May 2004.

[121] S. Yang, M. B. Chagas, and J. C. Ordonez. Thermal managemnt of a notional all-electric ship electromagnetic launcher. *Energy Conversion and Management*, 157:339–350, February 2018.

[122] A. B. Sanfiorenzo. Cooling system design tool for rapid development and analysis of chilled water systems aboard US Navy surface ships. Master's thesis, Massachusetts Institute of Technology, 2013.

[123] S. Yang, J. C. Ordonez, J. V. C. Vargas, J. Chalfant, and C. Chryssostomidis. Mathematical formulation and demonstration of a dynamic system-level ship thermal management tool. *Advances in Engineering Software*, 100:1–18, June 2016.

[124] S. Yang, J. C. Ordonez, J. V. C. Vargas, J. Chalfant, and C. Chryssostomidis. System-level ship thermal management tool for dynamic thermal and piping network analyses in early-design stages. In *IEEE Electric Ship Technologies Symposium (ESTS)*, pages 501–507, Arlington, VA, USA, August 2017.

[125] S. Chakrabarti, E. Kyriakids, and D. G. Eliades. Placement of synchronized measurements for power system observability. *IEEE Transactions on Power Delivery*, 24(1):12–19, January 2009.

[126] N. Doerry and J. Amy. MVDC shipboard power system considerations for electromagnetic railguns. In *Electromagnetic Railgun Workshop*, Laurel, MD, USA, September 2015. DoD.

[127] H. Vahedi, D. Perkins, D. Gonsoulin, T. Vu, and C. S. Edrington. Optimal sensor placement for MVDC ship power system. In *IEEE Elecric Ship Technologies Symposium (ESTS)*, pages 207–211, Arlington, VA, USA, August 2017.

[128] A. Arapostathis, A. Biswas, and J. Carroll. On solutions of mean field games with Ergodic cost. *Journal de Mathématiques Pures et Appliquées*, 107(2):205–251, October 2015.

[129] A. Arapostathis and G. Pang. Ergodic diffusion control of multiclass multi-pool networks in the Halin-Whitt regime. *Annals of Applied Probability*, 26(5):3110–3153, August 2015.

[130] A. Arapostathis and G. Pang. Infinite horizon average optimality of the N-network under Ergodic criteria. *Mathematics of Operaions Research*, September 2016.

[131] A. Arapostathis an A. Biswas and L. Cafarelli. The Dirichlet problem for stable-like operators and related probabilistic representations. *Communications in Partial Differential Equations*, 41(9):1472–1511, June 2016.

[132] A. Arapostathis, A. Biswas, and V. S. Borkar. Controlled equilibrium selection in stochastically perturbed dynamics. *Annals of Probability*, April 2017.

[133] A. Arapostathis. Some new results on sample path optimality in Ergodic control of diffusions. *IEEE Transactions on Automatic Control*, 62(10):5351–5356, October 2017.

[134] A. Arapostathis and V. S. Borkar. A correction to 'a relative value iteration algorithm for nondegenerate controlled diffusions'. *SIAM Journal on Control and Optimization*, May 2017.

[135] A. Arapostathis and G. Pang. Infinite horizon asymptotic average optimality for large-scale parallel server networks. *ArXiv e-prints*, January 2018.

[136] S. Krishnasamy, P. T. Akhil, A. Arapostathis, S. Shakkottai, and R. Sundaresan. Augmenting max-weight with explicit learning fo wireless scheduling with switching costs. In *IEEE Conference on Computer Communications (INFOCOM)*, Atlanta, GA, USA, May 2017.

[137] D. Soto, M. Sloderbeck, H. Ravindra, and M. Steurer. Advances to megawatt scale demonstrations of high speed fault clearing and power restoration in breakerless MVDC shipboard power systems. In *IEEE Electric Ship Technologies Symposium (ESTS)*, pages 312–315, Arlington, VA, USA, August 2017.

[138] X. Feng, L. Qi, and J. Pan. Fault inductance based protection for DC distribution systems. In *International Conference on Development in Power System Protection (DPSP)*, Edinburgh, UK, March 2016.

[139] IEC 61660-1. Short-circuit currents in d.c. auxiliary installations in power plants and substations, part 1: calculation of short-cicuit currents, 1997.

[140] X. Feng, L. Qi, and Z. Wang. Estimation of short circuit currents in mesh DC networks. In *IEEE PES General Meeting*, National Harbor, MD, USA, 2014.

[141] L. Qi, J. Pan, X. Huang, and X. Feng. Solid-state fault current limiting for DC distribution protection. In *IEEE Electric Ship Technologies Symposium (ESTS)*, pages 187–191, Arlington, VA, USA, August 2017.

[142] J. V. Amy and N. H. Doerry. MVDC grounding and common mode current control. In *IEEE Electric Ship Technologies Symposium (ESTS)*, pages 64–70, Arlington, VA, USA, August 2017.

[143] D. Russell. High impedance fault detection apparatus and method, US Patent 4466071A, 1984.

[144] Mirafzal. Technique for high-impedance ground fault detection at the common DC bus of multi-axis drives, US Patent 7751993B2, 2010.

[145] S. Lazarovich, R. Dangeti, S. Keshri, I. Rusan, and S. K. Chaudhary. Ground fault detection and location in an ungrounded or floating DC electrical system, US Patent 7969696B2, 2011.

[146] Y. C. Liu and J. K. Huang. DC power supply insulation fault detection circuit, US Patent 8559142B2, 2013.

[147] M. Agamy, A. Elasser, A. W. Galbraith, and M. H. Todorovic. Method for locating ground faults and insulation degradation condition in energy conversion systems, US Patent Application 2014/0176151A1, 2014.

[148] L. Wei et al. System for detection of a ground fault in high resistance ground network, US Patent Application 2012/0086458A1, 2012.

[149] J. Gaughan. DC ground fault detecting apparatus with an auto-null circuit and method, US Patent 5530363A, 1996.

[150] X. Feng et al. Converter-based DC distribution system protection. submitted to IEEE IAS Annual Meeting, 2018.

[151] R. Xie, R. Mo, Y. Shi, and H. Li. Comparative study of the DC-DC power conversion module based on dual active bridge converter and modular multilevel converter for shipboard MVDC system. In *IEEE Electric Ship Technologies Symposium (ESTS)*, pages 36–43, Arlington, VA, USA, August 2017.

[152] R. Xie, Y. Shi, and H. Li. Modular multilevel DAB (M2DAB) converter for shipboard MVDC sytem with fault protection and ride-through capability. In *IEEE Electric Ship Technologies Symposium (ESTS)*, pages 427–432, Alexandria, VA, USA, June 2015.

[153] A. D. Brovont and S. D. Pekarek. Equivalent circuits for common-mode analysis of naval power systems. In *IEEE Electric Ship Technologies Symposium (ESTS)*, pages 245–250, Alexandria, VA, USA, June 2015.

[154] A. D. Brovong and S. D. Pekarek. Derivation and application of equivalent circuits to model common-mode current in microgrids. *IEEE Journal of Emerging and Selected Topics in Power Electronics*, 5(1):297–308, March 2017.

[155] M. Bosworth, H. Ravindra, M. Steurer, and S. D. Pekarek. Common-mode equivalent modeling of a notional two-zone MVDC ship power system. In *IEEE Electric Ship Technologies Symposium (ESTS)*, pages 79–83, Arlington, VA, USA, August 2017.

[156] M. Bosworth, J. Langston, and M. Steurer. Considering effects of parasitic coupling to ground in a switching power amplifier. In *IEEE International Midwest Symposium on Circuits and Systems (MWSCAS)*, pages 472–474, Boston, MA, USA, August 2017.

[157] H. Ravindra, M. Stanovich, and M. Steurer. Documentation for a notional two zone medium voltage DC shipboard power system model implemented on the RTDS, December 2016.

[158] M. Rahmani, M. Mazzola, and S. Yarahmadian. Computation of time-domain impulse-response from band-limited ship power distribution models using wavelet transformation. In *IEEE Electric Ship Technologies Symposium (ESTS)*, pages 322–326, Arlington, VA, USA, August 2017.

[159] A. Lemmon et al. Methodology for characterization of common-mode conducted electromagnetic emissions in wide-band-gap converters for ungrounded shipboard applications. *IEEE Journal of Emerging and Selected Topics in Power Electronics*, 6(1):300–314, March 2018.

[160] A. D. Brovont and S. D. Pekarek. Impact of switching frequency and edge rates on common-mode current in MVDC microgrids. In *IEEE Electric Ship Technologies Symposium (ESTS)*, pages 16–24, Arlington, VA, USA, August 2017.

[161] Y. Pan. *Noise pattern analysis based ground fault location approach for ungrounded electrical distribution systems*. PhD thesis, Florida State University, 2009.

[162] I. Cvetkovic et al. Modular scalable medium-voltage impedance measurement unit using 10 kV SiC MOSFET PEBBs. In *IEEE Electric Ship Technologies Symposium (ESTS)*, pages 326–331, Alexandria, VA, USA, June 2015.

[163] Z. Shen et al. Design of a modular and scalable small-signal dq impedance measurement unit for grid applications utilizing 10 kV SiC MOSFET PEBBs. In *European Conference on Power Electronics and Applications (EPE'15 ECCE-Europe)*, Geneva, Switzerland, September 2015.

[164] M. Jakšić et al. Medium-voltage impedance measurements unit for assessing the system stability of electric ships. *IEEE Transactions on Energy Conversion*, 32(2):829–841, April 2017.

[165] F. Bogdan et al. Test environment for a novel medium voltage impedance measurement unit. In *IEEE Electric Ship Technologies Symposium (ESTS)*, pages 99–103, Alexandria, VA, USA, June 2015.

[166] Z. Zhang and C. M. Johnson. Suppression of electromagnetic interference using screening and shielding techniques within the switching cells. In *IEEE International Workshop On Integrated Power Packaging (IWIPP)*, Delft, Netherlands, April 2017.

[167] V. S. Nguyen, L. Kerachev, P. Lefranc, and J. C. Crebier. Characterization and analysis of an innovative gate driver and power supplies architecture for HF power devices with high dv/dt. *IEEE Transactions on Power Electronics*, 32(8):6079–6090, August 2017.

[168] H. Chen and D. Divan. High speed switching issues of high power rated silicon-carbide devices and the mitigation methods. In *IEEE Energy Conversion Congress and Exposition (ECCE)*, pages 2254–2260, Montreal, Canada, September 2015.

[169] T. V. Vu, S. Paran, F. Diaz, T. E. Meyzani, and C. S. Edrington. Model predictive control for power control in islanded DC microgrids. In *IEEE Industrial Electronics Society (IECON)*, pages 1610–1615, Yokohama, Japan, November 2015.

[170] F. Diaz-Franco, T. Vu, T. El Mezyani, and C. S. Edrington. Low-voltage ride-through for PV systems using model predictive control approach. In *North American Power Symposium (NAPS)*, Denver, CO, USA, September 2016.

[171] M. Babaei, R. Jafari-Marandi, and S. Abdelwahed. Real-time implementation of MVDC shipboard power system reconfiguration. In *IEEE Electric Ship Technologies Symposium (ESTS)*, pages 514–519, Arlington, VA, USA, August 2017.

[172] M. Babaei, R. Jafari-Marandi, S. Abdelwahed, and B. Smith. Application of STATCOM for MVDC shipboard power system. In *IEEE Electric Ship Technologies Symposium (ESTS)*, pages 142–147, Arlington, VA, USA, August 2017.

[173] C. Diendorfer. Graph traversal-based fault management for medium voltage DC shipboard power systems. Master's thesis, University of Applied Sciences, Austria, 2016.

[174] C. Diendorfer et al. Graph traversal-based automation of fault detection, location, and recovery on MVDC shipboard power systems. In *IEEE International Conference on DC Microgrids (ICDCM)*, pages 119–124, Nuremburg, Germany, June 2017.

[175] R. M. Cuzner et al. Approach to scalable model development for Navy shipboard compatible modular multilevel converters. *IEEE Journal of Emerging and Selected Topics in Power Electronics*, 5(1):28–39, March 2017.

[176] R. Soman et al. Size and weight computation of MVDC power equipment in architectures developed using the smart ship systems design environment. *IEEE Journal of Emerging and Selected Topics in Power Electronics*, 5(1):40–50, March 2017.

[177] R Soman et al. Contribution of heat sinks to overall size of modular multilevel converters. In *ASNE Intelligent Ships Symposium*, Philadelphia, PA, USA, May 2017.

[178] T. Toshon et al. Component level decomposition approach to develop selection metrics for shipboard power converter systems. In *ASNE Intelligent Ships Symposium*, Philadelphia, PA, USA, May 2017.

[179] R. R. Soman, T. A. Toshon, M. O. Faruque, and M. Steurer. Reliability metric influenced full factorial design evaluation. In *ASNE Advanced Machinery Technology Symposium (AMTS)*, Philadelphia, PA, USA, March 2018.

[180] S. Yang and J. C. Ordonez. Integrative thermodynamic optimization of a vapor compression refrigeration system based on dynamic system responses. *Applied Thermal Engineering*, 135:493–503, May 2018.

[181] B. Langland, R. A. Leonard, H. Pais, and R. A. Dougal. Automatic synthesis of detailed designs from early-stage conceptual designs. In *IEEE Electric Ship Technologies Symposium (ESTS)*, pages 126–133, Arlington, VA, USA, August 2017.

[182] A. Benigni, M. Brown, R. A. Leonard, and R. A. Dougal. QDEVS natural coupled simulation of a microgrid. In *IEEE Industrial Electronics Society (IECON)*, pages 5014–5019, Yokohama, Japan, November 2015.

[183] J. Langston, K. Schoder, M. Stanovich, M. Andrus, and M. Steurer. Framework for analysis of distributed energy storage, version 2.0, ESRDC technical report, October 2016.

[184] T. Haupt et al. Powertrain analysis and computational environment (PACE) for multi-physics simulations using high performance computing. In *SAE World Congress and Exhibition*, April 2016.

[185] M. S. Mazzola, T. Haupt, G. Henle, A. Card, and J. Shi. Co-simulation of electric ship power and control systems using high performance computing. In *IEEE Electric Ship Technologies Symposium (ESTS)*, pages 25–29, Arlington, VA, USA, August 2017.

[186] D. Rigterink et al. Smart ship systems design (S3D) software architecture document, version 2.0, December 2016.

[187] J. Chalfant et al. Smart Ship System Design (S3D) integration with the leading edge architecture for prototyping systems (LEAPS). In *IEEE Electric Ship Technologies Symposium (ESTS)*, pages 104–110, Arlington, VA, USA, August 2017.

[188] R. Smart et al. High temperature superconducting technology for future all-electric ships. In *IEEE Electric Ship Technologies Symposium (ESTS)*, pages 96–103, Arlington, VA, USA, August 2017.

[189] S. Pamidi and L. Graber. High temperature superconducting technology for future all-electric ships. In *IEEE Electric Ship Technologies Symposium (ESTS)*, pages 134–141, Arlington, VA, USA, August 2017.

[190] Y. Shi, R. Li, and H. Li. Modular multilevel dual active bridge DC-DC converter with ZVS and fast DC fault recovery for battery energy storage systems. In *IEEE Applied Power Electronics Conference and Exposition (APEC)*, pages 1675–1681, Long Beach, CA, USA, March 2016.

[191] Y. Shi and H. Li. A novel modular dual-active-bridge (MDAB) dc-dc converter with dc fault ride-through capability for battery energy storage systems. In *IEEE Energy Conversion Congress and Exposition (ECCE)*, Milwaukee, WI, USA, September 2016.

[192] M. Steurer et al. Multifunctional megawatt scale medium voltage DC test bed based on modular multilevel converter (MMC) technology. In *International Conference on Electrical Systems for Aircraft, Railway, Ship Propulsion and Road Vehicles (ESARS)*, Aachen, Germany, March 2015.

[193] M. M. S. Khan, M. O. Faruque, and A. Newaz. Fuzzy logic based energy storage management system for MVDC power system of all electric ship. *IEEE Transactions on Energy Conversion*, 32(2):789–809, June 2017.

[194] M. M. S. Khan. Fuzzy logic based energy storage management system for MVDC power system of the all-electric ship. Master's thesis, Florida State University, 2017.

[195] M. M. S. Khan and M. O. Faruque. Energy storage management for MVDC power system of all electric ship under different load conditions. In *IEEE Electric Ship Technologies Symposium (ESTS)*, pages 192–199, Arlington, VA, USA, August 2017.